

AMERICAN UNIVERSITY OF BEIRUT

RELIABILITY OF SPATIALLY VARIABLE UNDRAINED
SLOPES

by
GHINA ALI FAOUR

A thesis
submitted in partial fulfillment of the requirements
for the degree of Master of Engineering
to the Department of Civil and Environmental Engineering
of the Faculty of Engineering and Architecture
at the American University of Beirut

Beirut, Lebanon
September 2014

AMERICAN UNIVERSITY OF BEIRUT

RELIABILITY OF SPATIALLY VARIABLE UNDRAINED
SLOPES

by
GHINA ALI FAOUR

Approved by:



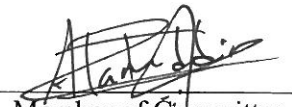
Dr. Shadi Najjar, Associate Professor
Civil and Environmental Engineering

Advisor



Dr. Salah Sadek, Professor
Civil and Environmental Engineering

Member of Committee



Dr. Ibrahim Alameddine, Assistant Professor
Civil and Environmental Engineering

Member of Committee

Date of thesis defense: September 2, 2014

AMERICAN UNIVERSITY OF BEIRUT

THESIS, DISSERTATION, PROJECT RELEASE FORM

Student Name: Faour Ghina ALi
Last First Middle

Master's Thesis Master's Project Doctoral Dissertation

I authorize the American University of Beirut to: (a) reproduce hard or electronic copies of my thesis, dissertation, or project; (b) include such copies in the archives and digital repositories of the University; and (c) make freely available such copies to third parties for research or educational purposes.

I authorize the American University of Beirut, **three years after the date of submitting my thesis, dissertation, or project**, to: (a) reproduce hard or electronic copies of it; (b) include such copies in the archives and digital repositories of the University; and (c) make freely available such copies to third parties for research or educational purposes.

Ghina Faour 25/9/2014
Signature Date

DEDICATION

To my late father Ali Faour, I miss him every day.

His words of inspiration and encouragement
in pursuit of excellence, still linger on.

ACKNOWLEDGMENTS

I would like to sincerely thank my advisor, Dr. Shadi Najjar for his cordiality, guidance, and support throughout the work of this research. It was a remarkable experience to work with him. I will forever be grateful for his role in making me what I am today. I would also like to thank the rest of my thesis committee: Dr. Salah Sadek and Dr. Ibrahim Alameddine for their encouragement and insightful comments.

Throughout my studies over the years, I have surrounded by friends who provided me with continuous support and encouragement, I would like to thank them all and wish them the best of luck.

Finally, I would like to thank my family for their enduring kindness, care and support.

AN ABSTRACT OF THE THESIS OF

Ghina Ali Faour for Master of Engineering
Major: Geotechnical Engineering

Title: Reliability of Spatially Variable Undrained Slopes

Conventionally, the stability of a soil slope is evaluated by adopting a deterministic approach that is based on a target global factor of safety that is calculated either through limit equilibrium methods or through numerical analyses. Slope stability analysis is a branch of geotechnical engineering that is highly amenable to uncertainties. Spatial variability and model uncertainty are considered the major sources of geotechnical uncertainties.

To account for such uncertainties in slope stability problems, numerous steps have been undertaken in recent years to adopt a probabilistic stability analysis that considers the uncertainties of soil properties in a systematic manner. However, there is currently an inconsistency in the evaluation of the spatial uncertainty and no accounting of the model uncertainty in the analysis.

The primary objective of this thesis is to provide slope stability investigators with a robust reliability analysis that takes into consideration the combined uncertainty of spatial variability and model uncertainty. To achieve this objective, a thorough investigation is conducted to evaluate the model uncertainty of common slope stability models (ex. Bishop, Ordinary Method of Slices, Janbu, and Spencer) by assembling and analyzing a database of historical failures of slopes. The database is also used to investigate the possibility of a lower-bound factor of safety for undrained slopes and its impact on the reliability of slopes. The model uncertainty and the uncertainty due to spatial variability are then combined within a reliability-based design framework to recommend design factors of safety that would result in acceptable probabilities of failure for undrained slopes.

CONTENTS

ACKNOWLEDGEMENTS.....	v
ABSTRACT.....	vi
LIST OF ILLUSTRATIONS.....	xii
LIST OF TABLES.....	xx

Chapter

1. INTRODUCTION.....	1
1.1. Background	1
1.2. Objective and Approach of Research.....	4
1.3. Thesis Organization	6
2. LITERATURE REVIEW.....	7
2.1. Introduction.....	7
2.2. Application of Reliability Based Design to Slope Stability Problems	7
2.3. Studies Involving LEM with Random Field Theory.....	11
2.3.1. Li and Lumb (1987)	11
2.3.2. Christian et al. (1994)	12
2.3.3. Malkawi et al. (2000).....	13
2.3.4. El- Ramly et al. (2002).....	14
2.3.5. Low (2003).....	15
2.3.6. Babu and Mukesh (2004).....	16
2.3.7. Cho (2007).....	16
2.3.8. Cho (2010).....	17

2.3.9. Wang et al. (2011).....	18
2.4. Studies Involving FEM with Random Field Theory	19
2.4.1. Griffiths and Fenton (2000).....	20
2.4.2. Griffiths and Fenton (2004).....	21
2.4.3. Griffiths et al. (2009).....	22
2.4.4. Griffiths et al. (2010).....	23
2.4.5. Jha and Ching (2013).....	24
2.5. Studies Involving Probabilistic Slope Stability Analyses Based on Search to Find the Minimum Reliability Index.....	25
2.5.1. Hassan and Wolff (1999).....	26
2.5.2. Bhattacharya et al. (2003).....	27
2.5.3. Xue and Gavin (2007).....	27
2.5.4. Deng and Luna (2013).....	28
2.6. Studies Involving System Reliability Analysis.....	29
2.6.1. Chowdhury and Xu (1995).....	26
2.6.2. Hong and Roh (2008).....	31
2.6.3. Huang et al. (2013).....	32
2.6.4. Zhang et al. (2013).....	32
3. DATABASE COLLECTION.....	34
3.1. Introduction.....	34
3.2. Database Collection.....	35
3.2.1. Slide at Nettet	38
3.2.2. Slide at PresterØdbakken.....	41
3.2.3. Slide at Âs	43
3.2.4. Slide at Skjeggerod	45
3.2.5. Slide at Tjernsmyr.....	48
3.2.6. Slide at Aulielva	50
3.2.7. Slide at Falknstein	52
3.2.8. Slide at Jalsberg.....	54
3.2.9. Slide at Saint- Alban	57
3.2.10. Slide at Narbonne	60
3.2.11. Slide at Lanester	62

3.2.12. Slide at Cubzac les-Ponts	65
3.2.13. Slide at Lodalen 1	67
3.2.14. Slide at Lodalen 2.....	69
3.2.15. Slide at Lodaln 3	70
3.2.16. Slide at Rio de janeiro	70
3.2.17. Slide at New Liskeard	73
3.2.18. Slide at Bangkok A	75
3.2.19. Slide at Drammen V	78
3.2.20. Slide at Drammen VI.....	79
3.2.21. Slide at Drammen VII	80
3.2.22. Slide at Pornic.....	81
3.2.23. Slide at Saint-Andre.....	83
3.2.24. Slide at South of France.....	85
3.2.25. Slide at NBR Development.....	86
3.2.26. Slide at Portsmouth.....	89
3.2.27. Slide at Kameda.....	90
3.2.28. Slide at Khor Al-Zubair	94
3.2.29. Slide at Lian-Yun-Gang	96
3.2.30. Slide at Congress Street	97
3.2.31. Slide at Daikoku-Cho Dike	100
3.2.32. Slide at Cuyahoga AA	102
3.2.33. Slide at King's Lynn	104
3.2.34. Slide at Muar	106
3.2.35. Slide at North Ridge Dam	107
3.2.36. Slide at Seven Sisters Dike.....	110
3.2.37. Slide at Shellmouth Dam Test Fill.....	111
3.2.38. Slide at Juban	113
3.2.39. Slide at Bradwell	115
3.2.40. Slide at Genesee	117
3.2.41. Slide at Precambrian	118
3.2.42. Slide at Scrapsgate	120
3.2.43. Slide at Scottsdale.....	123
3.2.44. Slide at Iwai	124
3.2.45. Slide at Fair Haven.....	126
3.2.46. Slide at Boston Marine Excavation	128
3.2.47. Slide at Desert View Drive	130
3.2.48. Slide at Siburua	132
3.2.49. Slide at Tianshenqiao	134
3.2.50. Slide at San Francisco Bay	136
3.2.51. Slide at Carsington	138
3.2.52. Slide at Atchafalaya	140

4. QUANTIFICATION OF MODEL UNCERTAINTY AND INVESTIGATION OF THE PRESENCE OF LOWER-BOUND FACTORS OF FACTORS OF SAFETY	150
4.1. Introduction.....	150
4.2. Quantification of Model Uncertainty	151
4.2.1. The Importance of Quantification of Model Uncertainty...	151
4.2.2. Mean, COV, and Distribution Type of Model Uncertainty	151
4.2.2.1. Evaluation of the Statistical Parameters of the Model Uncertainty.....	152
4.2.2.2. Probability Distribution of λ	158
4.3. Evidence of a Lower-Bound Factor of Safety of Slopes.....	160
4.4. Summary	164
5. IMPACT OF SPATIAL VARIABILITY IN THE UNDRAINED SHEAR STRENGTH ON THE FACTOR OF SAFETY OF UNDRAINED SLOPES	150
5.1. Introduction.....	165
5.2. Characterization of Soils	166
5.2.1. Coefficient of Variation.....	166
5.2.2. Scale of Fluctuation.....	166
5.3. Brief Summary of Work Done by Jha and Ching (2013).....	167
5.4. Method for Combining Uncertainties.....	172
6. COMBINATION OF BOTH MODEL UNCERTAINTY AND SPATIAL VARIABILITY	175
6.1. Introduction.....	175
6.2. Conventional Probability Distributions for Factors of Safety.....	175
6.2.1. Normal Distribution.....	175

6.2.2. Log-normal Distribution.....	177
6.3. Distribution Types Adopted in the Analysis.....	179
6.4. Estimation of the Statistical Parameters of the Factor of Safety.....	180
6.5. Summary.....	180
7. RECOMMENDATION OF DESIGN FACTORS OF SAFETY FOR UNDRAINED SLOPES.....	182
7.1. Introduction.....	182
7.2. Reliability – Based Design of Undrained Slopes.....	182
7.2.1. Effect of Coefficient of Variation and Scale of... Fluctuation of Undrained Shear Strength on the... Probability of Failure.....	183
7.2.2. Effect of Lower-Bound Factor of Safety on the... Probability of Failure.....	191
7.2.3. Recommendation for the Factors of Safety of Undrained Slopes.....	196
7.2.3.1. Acceptable Probability of Failure.....	202
7.2.3.2. Design Graphs for Factors of Safety of ... Slopes.....	204
7.3. Summary.....	212
8. CONCLUSIONS AND RECOMMENDATIONS	213
8.1. Introduction.....	213
8.2. Summary of Findings.....	213
8.2. Design Steps.....	218
8.2.1. Estimation of the Probability of Failure of Undrained... Slopes.....	218
8.2.2. Estimation of the Design Factors of Safety of Undrained Slopes.....	219
REFERENCES.....	220

ILLUSTRATIONS

Figure		Page
3.1.	Borehole Profile at Nettet (Flaate and Preber 1974).....	39
3.2.	Critical Slip Surface (Flaate and Preber 1974).....	40
3.3.	Critical Slip Surface using SLIDE Software.....	40
3.4.	Borehole Profile at Presterødbakken (Flaate and Preber 1974).....	42
3.5.	Critical Slip Surface at Presterødbakken (Flaate and Preber 1974).....	42
3.6.	Critical Slip Surface Using SLIDE.....	43
3.7.	Borehole Profile at Âs in Norway (Flaate and Preber 1974).....	44
3.8.	Critical Slip Surface at Âs in Norway (Flaate and Preber 1974).....	44
3.9.	Critical Slip Surface using SLIDE.....	45
3.10.	View of the Slide Occurred at Skjeggerod in Norway (Flaate and Preber 1974).....	45
3.11.	Borehole Profile at Skjeggerod in Norway (Flaate and Preber 1974)..	46
3.12.	Critical Slip Surface at Skjeggerod (Flaate and Preber 1974).....	47
3.13.	Critical Slip Surface using SLIDE.....	47

3.14.	Borehole Profile at Tjernsmyr (Flaate and Preber 1974).....	48
3.15.	Critical Slip Surface at Tjernsmyr (Flaate and Preber 1974).....	49
3.16.	Critical Slip Surface at Tjernsmyr (Flaate and Preber 1974).....	49
3.17.	Slide at Aulielva (Flaate and Preber 1974).....	50
3.18.	Borehole Profile at Aulielva (Flaate and Preber 1974).....	51
3.19.	Critical Slip Surface at Aulielva (Flaate and Preber 1974).....	51
3.20.	Critical Slip Surface using SLIDE.....	52
3.21.	Borehole Profile at Falkenstein (Flaate and Preber 1974).....	53
3.22.	Critical Slip Surface at Falkenstein (Flaate and Preber 1974).....	53
3.23.	Critical Slip Surface Using SLIDE	54
3.24.	Borehole Profile at Jalsberg (Flaate and Preber 1974).....	55
3.25.	Critical Slip Surface at Jalsberg (Flaate and Preber 1974).....	56
3.26.	Critical Slip Surface using SLIDE.....	56
3.27.	Soil Profile at Saint-Alban (LA Rochelle et al. 1982).....	58
3.28.	Cross- section of the Saint-Alban embankment (LA Rochelle et al. 1982).....	59
3.29.	Critical Slip Surface Using SLIDE.....	59
3.30.	Soil Profile at Narbonne (LARochelle et al. 1982).....	60
3.31.	Cross-section of the Narbonne embankment (LA Rochelle et al. 1982).....	61
3.32.	Critical Slip Surface using SLIDE.....	62
3.33.	Soil Profile at Lanester (LA Rochelle et al. 1982).....	63
3.34.	View of the Lanester embankment after Failure (LA Rochelle et al. 1982).....	63

3.35.	Cross-section of the Lanester embankment ((LA Rochelle et al. 1982).	64
3.36.	Critical Slip Surface using SLIDE.....	64
3.37.	View of the Cubzac embankment after failure (LA Rochelle et al. 1982.....	65
3.38.	Soil Profile at Cubzac- les-Ponts (LA Rochelle et al. 1982).....	66
3.39.	Cross-Section of the Cubzac embankment (LARochelle et al. 1982)..	66
3.40.	Critical Slip Surface using SLIDE.....	67
3.41.	Boring Profile at Lodalen (Sevaldson 1956).....	68
3.42.	Actual and Critical Slip Surfaces at Lodalen (Sevaldson 1956).....	68
3.43.	Critical Slip Surface using SLIDE at Lodalen 1.....	69
3.44.	Results of Total Stress Analysis using Slide Software at Lodalen 2...	70
3.45.	Results of Total Stress Analysis using Slide Software at Lodalen 3...	70
3.46.	Summary of Geotechnical Properties, Rio de Janeiro Soft Gray Clay (Ramalho-Ortigão et al. 1983).....	71
3.47.	Results of Total Stress Stability Analysis (Ramalho-Ortigão et al. 1983).....	72
3.48.	Results of Total Stress Stability Analysis using SLIDE software.....	73
3.49.	Undrained shear strengths used in total stress stability analyses (Lacasse et al.1977).....	74
3.50.	LEASE-I critical failure arcs at New Liskeard (Lacasse et al. 1977)...	74
3.51.	SLIDE critical failure arc at New Liskeard.....	75
3.52.	Geotechnical Profile at Bangkok site (Eide and Holmberg 1972).....	75
3.53.	Critical Slip Surface (Eide and Holmberg 1972).....	77
3.54.	Critical Slip Surface using SLIDE software.....	77

3.55.	Soil Properties at Drammen (Kjærnsli and Simons (1962)).....	78
3.56.	Critical Slip Surface (Kjærnsli and Simons 1962).....	79
3.57.	Critical Slip Surface Using SLIDE at Drammen V.....	79
3.58.	Critical Slip Surface using SLIDE software at Drammen VI.....	80
3.59.	Critical Slip Surface using SLIDE software at Drammen VII.....	81
3.60.	Embankment Failure at Pornic (Pilot 1972).....	81
3.61.	Embankment Failure at Saint-Andre (Pilot 1972).....	84
3.62.	Embankment Failure at Saint-Andre using SLIDE.....	84
3.63.	Embankment Failure at South of France (Pilot 1972).....	85
3.64.	Critical Slip Surface at South of France using SLIDE.....	86
3.65.	Stratigraphy and Geotechnical Characteristics of the foundation Soil at NBR Development (Dascal et al. 1972).....	87
3.66.	Results of the total stress stability analysis at NBR Development in France (Dascal et al. 1972).....	88
3.67.	Critical Slip Surface using SLIDE.....	88
3.68.	Soil Profile, Index Properties and Field Vane Strengths at... Portsmouth in USA (Ladd 1972).....	89
3.69.	Results of Total Stress Analysis (Ladd 1972).....	90
3.70.	Critical Slip Surface using SLIDE.....	90
3.71.	Soil conditions at Kameda site (Hanzawa et al. 1994).....	91
3.72.	Undrained Shear Strength at Kameda Site (Hanzawa et al. 1994).....	92
3.73.	Circular Slip Surface (Hanzawa et al. 1994).....	93
3.74.	Circular Slip Surface using SLIDE.....	93
3.75.	Soil Properties at Khor Al-Zubair Site (Hanzawa 1983).....	94

3.76.	Circular Slip Surface at Khor Al-Zubair Site (Hanzawa 1983).....	95
3.77.	Embankment Failure at Khor-Al-Zubair using SLIDE.....	95
3.78.	The Index and the Mechanical Properties of the Subsoil (Chai et al. 2002).....	96
3.79.	Failure Surfaces from Field Observations and in Slip Circle Analysis (Chai et al. 2002).....	97
3.80.	Failure Surface using SLIDE.....	97
3.81.	Compressive Strength and Water- Content at Congress Street (Ireland 1954).....	98
3.82.	Total Stress Stability Calculations (Ireland 1954).....	99
3.83.	Critical Slip Surface using SLIDE.....	100
3.84.	Undrained Shear Strength at Daikoku (Kishida et al. 1983).....	101
3.85.	Circular Slip Surface at Daikoku Site (Kishida et al. 1983).....	101
3.86.	Total Stress Stability Analysis using SLIDE.....	102
3.87.	Soil Properties and Critical Slip Surface at Cuyahoga AA site (Wu et al. 1975).....	103
3.88.	Critical Slip Surface using SLIDE.....	103
3.89.	Soil Properties at King's Lynn (Wilkes et al. 1972).....	104
3.90.	Observed and calculated Slip Surface (Wilkes et al. 1972).....	105
3.91.	Critical Slip Surface using SLIDE.....	105
3.92.	Variation of Soil Properties with Depth (Indraratna et al. 1992).....	106
3.93.	Critical Slip Surface at Muar using SLIDE.....	107
3.94.	Stability Analyses, North Ridge Dam (Rivard et al. 1978).....	109
3.95.	Stability Analyses, SLIDE software.....	109

3.96.	Stability Analyses, Seven Sisters Dike (Rivard et al. 1978).....	111
3.97.	Stability Analyses using SLIDE for Seven Sisters Dike.....	111
3.98.	Stability Analyses using SLIDE for Shellmouth Test Fill Dam.....	113
3.99.	Schematic Model used in the analysis (Zhang et al. 2005).....	114
3.100	Critical Slip Surface using SLIDE.....	114
3.101.	Properties of London Clay at Bradwell (Skempton and LaRochelle 1965).....	115
3.102.	Cross Section of Excavated Slope at Bradwell (Skempton and LaRochelle 1965).....	116
3.103.	Critical Slip Surface at Bradwell using SLIDE.....	116
3.104.	Stratigraphy and Engineering Properties of the soil at Genesee (Been et al. 1986).....	117
3.105.	Slope Geometry at Genesee (Been et al. 1986).....	118
3.106.	Critical Slip Surface at Genesee using SLIDE.....	118
3.107.	Soil Profile at Precambrian (Dascal et al. 1975).....	119
3.108.	Total Stress Analysis (Dascal et al. 1975).....	120
3.109.	Stability Analysis at Precambrian using SLIDE.....	120
3.110.	Shear Strength Values at Scrapsgate (Golder et al. 1954).....	121
3.111.	Stability Analysis at Scrapsgate (Golder et al. 1954).....	122
3.112.	Stability Analysis using SLIDE.....	122
3.113.	Soil Properties at Scottsdale (Parry 1968).....	123
3.114.	Critical Slip Surface using SLIDE.....	124
3.115.	Soil Properties of Organic Clay (Shogaki et al. 2008).....	124
3.116.	Soil Properties of Clay1 & Clay2 (Shogaki et al. 2008).....	125

3.117.	Soil Properties of Clay1 & Clay2 (Shogaki et al. 2008).....	126
3.118.	Critical Slip Surface using SLIDE.....	126
3.119.	Stability Analyses (Haupt and Olson 1972).....	127
3.120.	Critical Slip Surface using SLIDE.....	128
3.121.	Undrained Shear Strength using Field Vane (McGinn et al. 1993).....	129
3.122.	Stability Analyses (McGinn et al. 1993).....	129
3.123.	Stability Analyses using SLIDE.....	130
3.124.	Critical Slip Surface at Desert View Drive (Day 1996).....	131
3.125.	Critical Slip Surface using SLIDE.....	131
3.126.	Total Stress Analysis at Siburua (Wolfskill et al. 1967).....	133
3.127.	Stability Analyses using SLIDE.....	133
3.128.	Geological Profile at Tianshenqiao (Chen and Shoe 1988).....	135
3.129.	Critical Slip Surface using SLIDE.....	135
3.130.	Undrained Shear Strength using Field Vane Tests (Duncan and Buchignani 1973).....	136
3.131.	Slope Geometry at San Fransisco (Duncan and Buchignani 1973).....	137
3.132.	Critical Slip Surface using SLIDE.....	137
3.133.	Profile at Carsington Dam (Skempton and Coats 1985).....	139
3.134.	Critical Slip Surface using SLIDE.....	139
3.135.	Soil Properties at Atchafalaya Levees (Kaufman et al.1967).....	140
3.136.	Geometry and Soil conditions at Atchafalaya Site (Kaufman et al. 1967).....	141
3.137.	Critical Slip Surface using SLIDE.....	141

4.1.	Values of the ratio of measured to predicted factor of safety for the 52 case histories.....	155
4.2.	Values of the model uncertainties for the 52 cases (Shear strength corrected to UU).....	156
4.3.	Actual and Theoretical best-fit CDFs for the model uncertainty (λ)...	159
4.4.	Relation between sensitivity and liquidity index.....	161
4.5.	Evidence of a lower-bound factor of safety of 52 slope failure cases..	162
4.6.	Comparison of measured, predicted, and lower-bound factor of safety of 52 slope failures.....	163
4.7.	Predicted Lower-Bound Factors of Safety Excluding Cases with Highly Sensitive Soils.....	164
5.1.	Determination of vertical scale of fluctuation(Jha and Ching 2013)...	168
5.2.	Relationship between $(FS_d - \mu_{FS})/ FS_d$ and V (Jha and Ching 2013)	169
5.3.	Relationship between V_{FS}/V and $(V, \delta z /L_f, \delta x/ \delta z)$ (Jha and Ching 2013).....	171
5.4.	Relationship between actual V_{FS}/V and V_{FS}/V estimated by Equation 2.....	172
6.1.	Normal Probability Distribution.....	176
6.2.	Lognormal Probability Distribution.....	178
6.3.	Probability density function of truncated lognormal.....	179
7.1.	Variation of P_f with V and $\delta z /L_f$ for $FS =1.5$ & $FS = 1.7$	185
7.2.	Variation of P_f with V and $\delta z /L\phi$ for $FS =2$ & $FS = 2.25$	186
7.3.	Variation of P_f with V and $\delta z /L_f$ for $FS =2.5$ & $FS = 2.75$	187
7.4.	Variation of P_f with V and $\delta z /L_f$ for $FS =1.5$ by considering spatial variability only.....	190
7.5.	Variation of P_f with V and Sensitivity for $\delta z /L_f = 0.1$, $FS =1.5$ & $FS=1.7$	192

7.6.	Variation of P_f with V and Sensitivity for $\delta z / L_f = 0.1$, $FS = 2.00$ & $FS = 2.25$	193
7.7.	Variation of P_f with V and Sensitivity for $\delta z / L_f = 0.1$, $FS = 2.50$ & $FS = 2.75$	194
7.8.	Recommended factor of safety needed to accomplish a target P_f for different sensitivities for $V = 0.1$ & $V = 0.2$ and $\delta z / L_f = 0.1$	197
7.9.	Recommended factor of safety needed to accomplish a target P_f for different sensitivities for $V = 0.3$ & $V = 0.4$ and $\delta z / L_f = 0.1$	198
7.10.	Recommended factor of safety needed to accomplish a target P_f for different sensitivities for $V = 0.5$ and $\delta z / L_f = 0.1$	199
7.11.	Recommended factor of safety needed to accomplish a target P_f for different sensitivities for $V = 0.1$ and $V = 0.2$ and $\delta z / L_f = 0.2$	200
7.12.	Recommended factor of safety needed to accomplish a target P_f for different sensitivities for $V = 0.3$ and $V = 0.4$ and $\delta z / L_f = 0.2$	201
7.13.	Recommended factor of safety needed to accomplish a target P_f for different sensitivities for $V = 0.5$ and $\delta z / L_f = 0.2$	202
7.14.	Recommended factors of safety for different coefficients of variation for probabilities of failure of 0.001 & 0.005 for slopes with ratio $\delta z / L_f = 0.1$	205
7.15.	Recommended factors of safety for different coefficients of variation to achieve probabilities of failure of 0.01 & 0.05 for slopes with ratio $\delta z / L_f = 0.1$	206
7.16.	Recommended factors of safety for different coefficients of variation to achieve probability of failure of 0.1 for slopes with ratio $\delta z / L_f = 0.1$	207
7.17.	Recommended factors of safety for different coefficients of variation to achieve probability of failure of 0.001 and 0.005 for slopes with ratio $\delta z / L_f = 0.2$	208
7.18.	Recommended factors of safety for different coefficients of variation to achieve probabilities of failure of 0.01 & 0.05 for slopes with ratio of $\delta z / L_f = 0.2$	209

7.19. Recommended factors of safety for different coefficients of variation to achieve probabilities of failure of 0.1 for slopes with ratio $\delta z/ L_f = 0.2$ 210

TABLES

Table		Page
3.1.	Database of undrained slope failure cases.....	36
3.2.	Soil properties adopted for the analyses of the 52 cases.....	142
3.3.	Main soil characteristics of soils at Saint- Andre in France (Pilot 1972).....	83
3.4.	Soil properties of highly plastic clay North Ridge Dam (Rivard et al. 1978).....	108
3.5.	Soil properties of highly plastic clay, Seven Sisters Dike.....	110
3.6.	Stability analyses, Shellmouth Dam test fill.....	112
3.7.	Geotechnical soil parameters used in the stability analysis for Tianshenqiao (Chen and Shoe 1988).....	134
3.8.	Soil stratification at Carsington Dam (Skempton and Coats 1985).....	138
4.1.	Predicted and lower-bound factors of safety for the slopes in Database	154
4.2.	Statistical parameters of λ for the four LEM models.....	155
4.3.	Statistical parameters of the model uncertainty (after shear strength correction).....	157

4.4.	Statistical parameters of the model uncertainty (after removing the sensitive cases).....	158
6.1.	Estimation of λ and ζ of the factor of safety.....	181
7.1.	Acceptable probability of failure of slopes (Santamarina et al. 1992)...	203
7.2.	Recommended factors of safety for different acceptable probability of failure for $V = 0.1$ & $\delta z/L_f = 0.1$	210
7.3.	Recommended factors of safety for different acceptable probability of failure for $V = 0.3$ & $\delta z/L_f = 0.1$	211
7.4.	Recommended factors of safety for different acceptable probability of failure for $V = 0.5$ & $\delta z/L_f = 0.1$	211
7.5.	Recommended factors of safety for different acceptable probability of failure for $V = 0.1$ & $\delta z/L_f = 0.2$	211
7.6.	Recommended factors of safety for different acceptable probability of failure for $V = 0.3$ & $\delta z/L_f = 0.2$	212
7.7.	Recommended factors of safety for different acceptable probability of failure for $V = 0.5$ & $\delta z/L_f = 0.2$	212

CHAPTER 1

INTRODUCTION

1.1 Background

Traditionally, the stability of a clay slope is evaluated by adopting a deterministic approach that is based on a global factor of safety obtained either through limit equilibrium approaches or through numerical analyses. Slope stability analysis is a branch of geotechnical engineering that is highly amenable to uncertainties. To account for the different sources of uncertainties and reduce the risk of slope failures, common practice involves the use of factors of safety that are generally greater than 1.5 (Terzaghi and Peck 1948). Schweiger et al. (2001) reports that the deterministic approach is simple and straightforward but does not lead to a realistic mathematical treatment of the uncertainties involved in the models and parameters affecting the design of slopes. Li and Lumb (1987) recognized that the factor of safety is not a consistent measure of risk since slopes with the same safety factor value may exhibit different risk levels depending on the variability of the soil properties. Accordingly, to account for such variability, numerous studies have been undertaken in recent years to adopt a probabilistic approach for slope stability analysis that deals with the uncertainties of soil properties in a systematic and explicit manner. This probabilistic analysis can facilitate the development of new perspectives concerning risk and reliability of slopes that are outside the scope of conventional deterministic models.

Reliability analysis of slope stability has attracted considerable research attention in the past few decades. Almost all probabilistic methods described in the literature have at some point been applied to slope stability problems. In general, the probabilistic procedures differ in assumptions, limitations, capability to handle complex problems, and mathematical complexity. In the last few decades, some research efforts have targeted analyzing the effect of spatial variability in the soil properties on the stability of slopes in the framework of a reliability analysis. Li and Lumb (1987), Christian et al. (1994), Malkawi et al.(2000), El- Ramly et al. (2002), Low (2003), Babu and Mukesh (2004), Cho (2007), Cho (2010), and Wang et al. (2011) have targeted analyzing the effect of spatial variability by using limit equilibrium methods with random field theory. The above studies differ in both the deterministic and probabilistic methods used in the analysis and also in the way spatial variability is defined. Malkawi et al. (2000) and Low (2003) studied the effect of spatial variability by varying the coefficient of variation of soil properties. On the other hand, Li and Lumb (1987), El- Ramly et al. (2002), Cho (2007), and Wang et al. (2011) used random fields with an isotropic correlation structure for defining spatial variability. Conversely, Babu and Mukesh (2004) found that random fields with an anisotropic correlation structure should be utilized since soil properties could exhibit a significant degree of anisotropy.

All the above studies have combined the limit equilibrium method (LEM) with random field theory. However, the inherent nature of LEM is that it leads to a critical failure surface which could be non-circular in 2-D analysis and the influence of the random field is only taken into account along the one-dimensional failure line. Thus, to overcome this limitation, Griffiths and Fenton (2000), Griffiths and Fenton (2004),

Griffiths et al. (2009), Griffiths et al. (2010) and Jha and Ching (2013) pursued a more rigorous method of probabilistic slope stability analysis in which nonlinear finite-element methods are combined with random field generation techniques. This approach is currently referred to in the literature as the Random Finite Element Method (RFEM). The approach captures the effect of soil spatial variability and fully accounts for spatial correlation and averaging. It is also a powerful slope stability analysis tool that does not require priori assumptions related to the shape or location of the failure mechanism.

Griffiths (2000) studied the effect of the scale of fluctuation and the coefficient of variation of soil properties. Griffiths (2004) performed a comparison between the simple and advanced probabilistic approach to study the effect of spatial variability and local averaging on the probability of failure of slope. Moreover, Griffiths (2009) built on the work done by Griffiths (2004) and studied the effect of the inclination angle of the slope on the probability of failure. Additionally, Griffiths (2010) performed a comparison between limit equilibrium methods and the random finite element method to indicate the importance and superiority of the RFEM in the stability of slopes.

In a recent study, Jha and Ching (2013) performed a robust and rigorous probabilistic slope stability analysis using the Random Finite Element Method to study the effect of slope geometry, mean and coefficient of variation of the soil parameters, and the scale of fluctuation on the probability of failure of undrained slopes. The authors conducted the study by collecting a database for 34 real undrained engineered slope cases. The paper was aimed at quantifying the effect of spatial variability in the undrained shear strength of clays on the probability of failure of the slopes. An advanced model of

spatial variability that takes into account vertical and horizontal spatial variability was adopted. The vertical scale of fluctuation in the undrained shear strength was back-calculated for each case in the database using the simplified method presented in Phoon and Kulhawy (1999). The horizontal scale of fluctuation in the undrained shear strength was assumed due to the lack of soil data (boreholes) needed to quantify the lateral spatial variability. One of the major contributions of the study is a relationship between the mean and the coefficient of variation of the factor of safety from one hand and the slope geometry, mean and the coefficient of variation of the soil properties, and the scale of fluctuation in the undrained shear strength from the other hand.

It should be noted that the majority of the published work that is related to reliability-based design of slopes targets the issue of spatial variability and its effect on the calculated reliability of the slope. Regarding the evaluation of model uncertainty, only Malkawi et al. (2000) estimated the model uncertainty by comparing the performance of the limit equilibrium methods with the Spencer's method that is considered the most accurate and rigorous. There are no published studies that aim at characterizing the model uncertainty of available slope stability methods with published case histories of failed slopes.

1.2 Objective and approach of research

The primary objective of this thesis is to provide slope stability investigators with a robust reliability-based design procedure that takes into consideration the combined uncertainty of spatial variability and model uncertainty. The main goal is to provide

designers with a systematic and defensible approach for estimating the probability of failure of slopes. The main backbone of the proposed study is a simplified and realistic reliability-based design approach for estimating the probability of failure of slopes by incorporating the effects of model uncertainty and spatial variability in the probability distribution of the factor of safety of the slope. What differentiates this tool from other tools available in the literature is the incorporation of the model uncertainty in the slope probabilistic analysis. The previous reliability studies found that it is difficult to have historical observations to compare with results of slope stability methods. Thus, they don't take into account the model uncertainty. However, in this study an effort is made to collect a database that includes historical observations of failed slopes which will allow for the estimation of the model uncertainty of commonly used slope stability prediction models. The second objective of the study is to investigate the existence of a physical lower-bound factor of safety of the slope, which if incorporated in the modeling of the probability distribution of the factor of safety, could provide a more realistic quantification of reliability and a more rational basis for design.

These goals will be achieved through the following tasks:

1. Conduct an expanded literature review on slope stability and reliability-based design of slopes.
2. Collect a database that includes historical failure observations of real slopes.
3. Use the collected database to investigate the existence of a lower-bound factor of safety for a given slope and to quantify the model uncertainty of the limit equilibrium methods used for slope stability analyses.

4. Investigate the impact of spatial variability in the undrained shear strength on the factor of safety of undrained slopes.
5. Combine both the model and the spatial uncertainties to evaluate the statistical parameters of the factor of safety of an undrained slope.
6. Propose a reliability-based design framework to recommend design factors of safety that would result in acceptable probabilities of failure for undrained slopes.

1.3 Organization of thesis

In chapter 2, a literature review of some of the recent works done in this field will be addressed. The literature review targets studies that include historical failure cases of undrained slopes. It also targets studies where reliability-based design concepts were employed in the analysis of slope stability. In chapter 3, a database of failure historical observations of undrained slopes is assembled. In chapter 4, the collected database is used to analyze biases and uncertainties in current models for predicting the factor of safety of slopes. Moreover, the database is used to investigate the presence of the lower-bound factor of safety. In chapter 5, the work done by Jha and Ching (2013) is used to investigate the impact of spatial variability in the undrained shear strength on the factor of safety of undrained slopes. Both model uncertainty and spatial variability are combined in chapter 6 to evaluate the statistical parameters of the factor of safety of undrained slopes. Finally, a reliability-based design framework is proposed to recommend design factors of safety that would result in acceptable probabilities of failure for undrained slopes in chapter 7. Conclusions and contributions of this research are presented in chapter 8.

CHAPTER 2

LITERATURE REVIEW

2.1 Introduction

Conventionally, the stability of a soil slope is evaluated by adopting a deterministic approach that is based on a global factor of safety that is generally evaluated either through limit equilibrium approaches or through numerical analyses. The input to these slope stability analyses include deterministic soil parameters that are assigned to the different soil layers. Normally, the selection of design input soil parameters to be used in the slope stability analyses is based on local experience and engineering judgment and is most of the time on the conservative side (Schweiger et al. 2001).

To cater for the different sources of uncertainties in the input parameters and in the predictive models, global factors of safety that generally exceed 1.5 are generally adopted in slope stability analyses to ensure safety (Terzaghi and Peck 1948). Schweiger et al. (2001) indicated that the deterministic approach is simple and straightforward but does not give realistic and mathematical treatment to the uncertainties involved in the input soil parameters. Moreover, Li and Lumb (1987) recognized that the factor of safety is not a consistent measure of risk since slopes with the same safety factor value may exhibit different risk levels depending on the variability of the soil properties.

Accordingly, to account for such variability, numerous studies have been undertaken in recent years to adopt a probabilistic stability analysis that deals with the uncertainties of

soil properties in a systematic manner. This probabilistic analysis can facilitate the development of new perspectives concerning risk and reliability that are outside the scope of conventional deterministic models. According to Kulhawy (1996), a reliability analysis is the consistent evaluation of design risk using probability theories, and reliability-based design is any design approach that uses reliability analyses.

2.2 Application of reliability based design to slope stability problems

Slope stability analysis is a branch of geotechnical engineering that is highly amenable to probabilistic treatment. Almost all of the probabilistic methods described in the literature have at some point been applied to slope stability problems. Reliability analysis of slope stability has attracted considerable research attention in the past few decades.

The reliability of slopes is frequently measured by a “reliability index,” β , or a failure probability, P_f , which is defined as the probability that the minimum factor of safety (FS) is less than unity (i.e., $P_f = P(\text{FS} < 1)$). The “reliability index,” β is evaluated as $\beta = -\Phi^{-1}(P_f)$ where $\Phi^{-1}()$ is the inverse of the standard normal cumulative distribution function. Various methods have been proposed to estimate β and (or) P_f . The earliest studies appeared in the 1970’s [e.g. Wu and Kraft (1970); Cornell (1971); Matsuo and Kuroda (1974); Alonso(1976); Tang et al. (1976); and Vanmarcke (1977)] and have continued steadily [e.g., D’Andrea and Sangrey (1982); Chowdhury and Tang (1987); Li and Lumb (1987); Oka and Wu (1990) ;Mostyn and Li (1993); Lacasse (1994); Christian et al. (1994);Chowdhury and Xu (1995); Wolff (1996); Christian (1996); Lacasse and

Nadim (1996); Low (1996); Low and Tang (1997a,b); Low et al.(1998); Hassan and Wolff (1999);Malkawi and Abdulla (2000); Whitman(2000); Duncan (2000); El-Ramly et al. (2002); Low (2003); Baecher and Cristian (2003); Bhattacharya et al. (2003); Griffiths and Fenton (2004); Babu and Mukesh (2004); Xu and Low(2006); Low et al. (2007); Cho (2007); Griffiths et al. (2007); Shinoda (2007); Xue and Gavin (2007); Hong and Roh (2008); Srivastava and Babu (2008); Griffiths et al .(2009); Cho (2010); Griffiths et al. (2010); Wang et al. (2010); Kasama and Zen (2011); Christian et al. (2013); Huang et al. (2013); Zhang et al.(2013); Deng and Luna (2013); Jha and Ching (2013)].

The above studies differ in the probabilistic procedures for slope stability analysis. In general, the probabilistic procedures differ in assumptions, limitations, capability to handle complex problems, and mathematical complexity. These probabilistic methods are divided into two main categories: (1) approximate methods (traditional methods) i.e. the First Order Reliability Method (FORM), the First Order Second Moment Method (FOSM), the Point Estimate Method (PEM), and the Monte Carlo Simulations Method (MCSM) which are generally used in conjunction with Limit Equilibrium Slope Stability methods and (2) more advanced methods that use the Random Finite Element Method. The approximate methods make simplifying assumptions that limit their application to specific classes of problems. Some studies use very simple slope models such as the Ordinary Method of Slices (Tang et al. 1976), while others deal only with frictionless soils (Vanmarcke 1977 and Matsuo and Kuroda 1974). Moreover, many studies restrict their analyses to a circular slip surface (Vanmarcke 1977 and Alonso 1976). Another limitation of these approximate methods is the inability of

these methods to provide any information about the shape of the probability distribution function where these methods can allow the estimation of the mean and the variance of the factor of safety only. Finally, the major limitation of these methods is the ignorance of the spatial variability of soil properties.

Spatial variability is considered one of the major sources of geotechnical variability in slope stability. Geotechnical variability is a complex attribute that results from many sources of uncertainties. Spry et al. (1988), Orchant et al. (1988), Filippas et al. (1988), Kulhawy et al. (1992), Christian et al. (1994), Phoon et al. (1995) and Phoon et al. (1999) investigated geotechnical variability. Both Christian et al. (1994) and Phoon et al. (1999) illustrated that the uncertainties in soil properties are comprised from two sources: scatter in the data and systematic error in the estimate of the properties. Scatter in the data is due to the real spatial variability within the profile and due to random testing errors or noise. However, systematic error is due to the statistical error in the mean value of the property that results from the limited number of tests performed and the bias in the measurement.

Lacasse and Nadim (1996) stated that variability is attributed to factors such as variations in mineralogical composition, conditions during deposition, stress history, and physical and mechanical decomposition processes. To model the spatial variability in problems involving slope stability, statistical parameters such as the mean and the variance of the soil properties must be estimated. However, these statistical parameters are one point statistical parameters and cannot capture the features of the spatial correlation structure of the soil (El-Ramly et al. 2002). Spatial variations of soil properties can be effectively described by their correlation structure within the framework

of random fields (Vanmarcke 1983). To describe this correlation structure, an autocorrelation distance is defined which is the distance within which soil properties show a strong correlation. A large autocorrelation distance value implies that the soil property is highly correlated over a large spatial extent, resulting in a smooth variation within the soil profile. On the other hand, a small value indicates that the fluctuation of the soil property is large (Cho 2010). Some studies in the literature assume isotropic correlation structure. In contrast, other studies assume anisotropic correlation, when the investigators recognized that the correlations in the vertical direction tend to have much shorter distances than those in the horizontal direction.

Below is a summary of the research studies which targeted the probabilistic slope stability analysis taking into consideration spatial variability.

2.3 Studies involving LEM with random field theory

In spite of the fact that most traditional limit equilibrium methods (LEMs) do not consider spatial variability, some investigators investigated the impact of spatial variability of soil properties for slopes by combining the LEM with random field theory. The theory of random fields (Varmarcke 1977a, 1977b, 1983) is a common approach for modeling the spatial variability of soil properties. It is also the basis of probabilistic slope analysis methodology.

2.3.1 Li and Lumb (1987)

Li and Lumb (1987) conducted one of the earliest probabilistic slope stability analyses that combines LEM with random field theory. The approach presented in the

study adopted the Morgenstern and Price method (1965) which is commonly accepted as one of the accurate and rigorous methods for slope stability analysis that incorporates the general slip surface. Li and Lumb adopted the First Order Second Moment Method (FOSM) with some new developments of the technique for analyzing the reliability of slopes. These developments revolved around defining the reliability index by Hasofer and Lind (1974) which is considered an invariant risk measure in which all equivalent formats of the performance function yield the same reliability index. Spatial variability was taken into account in Li and Lumb study by defining an isotropic correlation structure. The authors found from their analysis that the probability of failure of the slope is sensitive to the scale of fluctuation, and recommended that the reliability analyst must pay more attention to the estimation of the scale of fluctuation. The assumption of perfect correlation in soil properties was found to lead to an overestimation of the probability of failure. Nevertheless, Li and Lumb showed that the locations of the deterministic critical slip surface and the surface with minimum reliability index are very close to each other. Thus, the authors recommended the use of the deterministic critical slip surface as an initial trial surface for the general search for the critical slip surface with minimum reliability index.

2.3.2 Christian et al. (1994)

Christian et al. (1994) conducted a probabilistic analysis using the First Order Second Moment Method (FOSM) to evaluate the reliability index of slopes. The authors illustrated the approach by the analysis of a well-known case history (James Bay

Embankments). The construction of the dyke followed three scenarios. The first two alternatives were the construction of the embankment in a single stage either to a height of 6 or 12m. The second alternative was the multi stage construction. Spatial variability in addition to systematic and model errors were all taken into consideration in the analysis. In contrast, errors due to bias were not considered in the analysis due to the difficulty in determining the magnitude of the errors. Local averaging was considered in the analysis. Bishop's method was conducted to evaluate the factor of safety for the dyke for the first two alternatives. Conversely, the stability analysis for the multistage construction alternative was done by Morgenstern Price Method. The results showed that there are difficulties in identifying both the autocorrelation distance and bias. Bias is considered a significant contributor to the overall uncertainty; however, in general it is ignored from the analysis. Hence, the authors recommended that the engineers should be careful when they rely on their judgment to establish the bias contribution.

2.3.3 Malkawi et al. (2000)

Malkawi et al. (2000) investigated the effect of deterministic models [Bishop, Ordinary Method of Slices (OMS), Janbu, and Spencer] and probabilistic models [First Order Second Moment Method (FOSM) and Monte Carlo Simulation Method (MCSM)] on the reliability of homogenous and layered slopes. The authors included the spatial variability into their analysis and studied the effect of uncertainty of each soil property on the calculated factor of safety by varying the coefficient of variation of the soil properties. Furthermore, they conducted a sensitivity analysis to investigate the effect of the seed

random number generator and the sample size of soil properties needed for Monte Carlo Simulation on the reliability index of slopes. They ended up with the following results: In case of homogenous slopes, both OMS and Bishop result in the same reliability index regardless of the reliability method used. Conversely, Janbu and Spencer models exhibit some differences. The FOSM slightly overestimates the reliability index in the case of Janbu's model, whereas the MCSM overestimates the reliability index in the case of Spencer's model. For the case of layered slopes, only Spencer's model results in a slight variation between FOSM and MCSM. The authors also concluded that β isn't sensitive to the selected random number generator. In contrast, it is sensitive to the sample size of soil properties where greater than 700 samples are needed in the analysis. Consequently, they found that FOSM requires fewer calculations and computing time compared to MCSM. However, with the help of computers in data handling and speed, MCSM proved to be powerful and effective method for probabilistic reliability analysis.

In spite of the fact that Malkawi et al. (2000) combined LEM with Random Field Theory to take spatial variability into consideration, they neglected spatial correlation from in their analysis.

2.3.4 El-Ramly et al. (2002)

El- Ramly et al. (2002) conducted a practical probabilistic slope stability analysis based on Monte Carlo Simulation by developing a simple spreadsheet using the well-known software Microsoft Excel 97 and @Risk. The analysis is illustrated by analyzing

the dykes of the James Bay hydroelectric project. The authors modeled the geometry, soil properties, stratigraphy, and slip surface in an excel spreadsheet. The Bishop method is used for the determination of the deterministic factor of safety. The uncertainties in input parameters are modeled statistically by representative probability distributions. The variances of the soil parameters are evaluated using judgment; moreover, the bias in the vane measurements is adjusted by Bjerrum's correction factor which also is considered uncertain in the analysis. The spatial variability of soil parameters was characterized by an isotropic autocorrelation distance assuming exponential autocovariance functions. Finally, the authors investigated the efficiency of the analysis by comparing the results obtained by those obtained using First Order Second Moment Method (FOSM).

The authors concluded that the reliability of a design could be significantly reduced by the use of empirical factors and correlations and this is proven by the sensitivity analysis undertaken to study the impact of the uncertainty of Bjerrum's coefficient on the reliability of the slope. Additionally, they deduced that ignoring spatial variability of soil properties and assuming perfect correlation can significantly overestimate the probability of failure of slopes.

2.3.5 Low (2003)

Low (2003) implemented Spencer's method both deterministically and probabilistically in a spreadsheet platform. The author accomplished the search of the noncircular failure surface by using Spencer's method involving spatially correlated

normal and lognormal variates. Then, he extended the use of the deterministic approach to the probabilistic analysis (FOSM) in order to calculate the Hasofer-Lind reliability index simply without involving complex concepts (eigenvalues, eigenvectors...). Both the probabilities of failures and probability density functions obtained showed a good agreement with those obtained by the Monte Carlo Simulation method.

2.3.6 Babu and Mukesh (2004)

Babu and Mukesh (2004) investigated the effect of spatial variation of soil strength on slope reliability for a simple cohesive soil slope. They defined the geometry, stratigraphy, and soil parameters of the slope. Moreover, they assumed an isotropic correlation structure. The authors calculated the factor of safety using Bishop's method. Next, they calculated the probability of failure of the slope by using the First Order Second Moment Method. After that, they repeated the same procedure stated above but by assuming an anisotropic correlation structure by defining both vertical and horizontal correlation distances. The authors concluded that not only the coefficient of variation of soil parameters and the correlation distance can affect the probability of failure of the slope, but also the mean factor of safety can affect the probability of failure. Additionally, the authors found that there is a significant need to include an anisotropic correlation structure in the probabilistic slope stability analysis. Performing reliability analysis by assuming that the correlation distance is the same in both horizontal and vertical directions leads to an overestimation of probability of failure of slopes.

2.3.7 Cho (2007)

Cho (2007) conducted a probabilistic slope stability analysis through a numerical procedure based on Monte Carlo Simulation (MCS) that considers the spatial variability of the soil properties based on local averaging. Hassan and Wolff (1999) concluded that the deterministic critical failure surface is not necessarily the failure surface with the highest probability of failure. For the sake of that, Cho (2007) adopted the First Order Reliability Method (FORM) to determine the critical probabilistic failure surface. Moreover, the author used both FORM to identify the input parameters that have the greatest impact on the failure probability and Spencer's method to calculate the reliability index. The author concluded that the searched critical probabilistic surface showed somewhat different locations from the critical deterministic surface. Furthermore, the probability of failure decreases with a decrease in the scale of fluctuation and vice versa. In addition to that, he deduced that the assumption of the isotropic field is conservative and the sensitivity of the unit weight is relatively small compared to those of cohesion and the angle of the internal friction. Finally, Cho (2007) found that in the case of small scale of fluctuation, a low probability of failure is obtained. Hence, more realizations are needed to conduct MCSM.

2.3.8 Cho (2010)

All the above case studies used the traditional LEM combined with the random field theory to calculate the probability of failure by taking spatial variability into

consideration. This traditional analysis considers the influence of the random field along the predetermined critical surface. Cho (2010) proposed his method by using the Karhunen – Loeve Expansion Method that is independent of the division of slices in the sliding mass in order to be able to calculate the shear strength at any location along the trial slip surface. The author considered the strength reduction method in the calculation of Bishop’s factor of safety. Conversely, he based his probabilistic analysis that accounts for the spatial variability on a search algorithm that can find the surface with the minimum reliability index. The author illustrated his approach by analyzing a one layered slope twice. One time with $\phi = 0$ slope and the other with the c- ϕ slope.

Cho (2010) deduced that in the case of $\phi = 0$ slope the critical failure surface identified by search algorithm always gives smaller factor of safety compared to that obtained from fixed critical surface. In contrast, the probability of failure that comprises all potential failure surfaces is greater than that obtained from the fixed critical surface and the relative difference between the two probabilities decreases when the autocorrelation distance increases. In contrary, for c- ϕ slope, there is no significant difference between probability of failure obtained from fixed critical surface and that obtained from the search algorithm methodology. However, the negative correlation between C and ϕ has a significant effect on the variance of the shear strength. This latter affects the probability of failure significantly.

2.3.9 Wang et al. (2011)

Wang et al. (2011) conducted a probabilistic slope stability analysis based on MCS by using Simulation Subset in order to improve the efficiency and resolution of the

MCS. The analysis was implemented using a spreadsheet package that was used to explore the effect of spatial variability on the probability of failure of slopes. The methodology is illustrated through applying it to a cohesive slope and the deterministic factor of safety was calculated using the Ordinary Method of Slices. The results were validated by comparing the results with those obtained from other reliability methods. Wang et al. (2011) modeled the undrained shear strength by a lognormal random field and by an isotropic correlation structure using an exponential auto covariance function. The authors found that if the spatial variability is ignored, the probability of failure is significantly overestimated particularly when the effective correlation length is smaller than the slope height. Moreover, they concluded that the variance of the factor of safety is overestimated when the spatial variability is ignored. This variance overestimation may result in either over conservative or under conservative estimation of the probability of failure where if the marginal factor of safety ($FS=1$) occurs at the lower tail of the factor of safety probability distribution, an overestimation of probability of failure occurs. However, if the marginal factor of safety ($FS =1$) is located at the center or approaches the upper tail of the factor of safety probability distribution, an underestimation of probability of failure occurs. Further, they deduced that it is appropriate to use only one given slip surface in the analysis i.e. FOSM or MCS when the spatial variability is ignored. In contrast, when the spatial variability is considered, the critical slip surface varies spatially. Thus, the critical probabilistic surface should be investigated by conducting a search algorithm method to get the surface with the minimum reliability.

2.4 Studies involving fem with random field theory

All the above studies have combined the limit equilibrium method (LEM) with random field theory. However, the inherent nature of LEM is that it leads to a critical failure surface, which in 2-D analysis appears as a line which could be non-circular and the influence of the random field is only taken into account along the line and is therefore one-dimensional. Thus, to overcome this limitation, some investigators pursued a more rigorous method of probabilistic geotechnical analysis in which nonlinear finite- element methods are combined with random field generation techniques. This method is called Random Finite Element Method (RFEM). It captures the effect of soil spatial variability well where it fully accounts for spatial correlation and averaging. It is also a powerful slope stability analysis tool that does not require priori assumptions related to the shape or location of the failure mechanism. The following studies presented the probabilistic slope stability analysis based on Random Finite Element Method.

2.4.1 Griffiths and Fenton (2000)

Griffiths and Fenton (2000) conducted a Random Finite Element probabilistic analysis highlighting the influence of the spatial correlation length on the probability of failure of the slope. Furthermore, the authors performed a parametric study to investigate the effect of the scale of fluctuation and coefficient of variation of the shear strength on the stability of the slope. Griffiths and Fenton illustrated the analysis by analyzing an undrained clay slope. The authors concluded that the probability of failure increases as

the coefficient of variation of the undrained shear strength increases. Also they found that for low values of the coefficient of variation ($0 < COV < 0.5$), the probability of failure increases as the ratio of the correlation length to the slope height increases. On the contrary, for high values of the coefficient of variation, the probability of failure decreases with the increase in the ratio of the correlation length to the slope height. Thus, perfect correlation overestimates the probability of failure for low values of the coefficient of variation and for slopes with high factor of safety ($FS > 1.4$); however, it underestimates the probability of failure for high values of the coefficient of variation and for slopes with low factor of safety ($FS < 1.40$).

2.4.2 Griffiths and Fenton (2004)

In this study the authors performed probabilistic slope stability analysis based on both simple and advanced methods. In the simple approach, the authors treated the undrained shear strength of the cohesive slope as a simple random variable and both spatial correlation and local averaging are ignored. The probability of failure in this simple methodology was estimated as the probability that the shear strength would fall below a critical value based on a log-normal probability distribution. The results of the simple study indicated that the probability of failure increases with the decrease in the factor of safety. If the factor of safety is greater than one ($FS > 1$), the probability of failure increases as the coefficient of variation increases also. However, for $FS < 1$, lower values of coefficient of variation tend to give higher values of probability of failure. Moreover, the results of the simple approach contradicted the practical one; this approach

led to a high probability of failure with mean factor of safety = 1.47; however, practical experience showed that slopes with FS=1.47 rarely fail. To overcome this problem, the authors proposed two factorization methods that used to reduce the mean value of the undrained shear strength. Hence, an increase in the strength reduction factor reduces the probability of failure to an acceptable value. Additionally, the authors conducted a RFEM to model the slope more realistically. The analysis took into account both spatial correlation and local averaging. By comparing the results of the simplified probabilistic analysis and the advanced one, the authors found that the simplified analysis in which perfect correlation is assumed can lead to unconservative estimates of the probability of failure and this contradicted all the previous findings of other investigators.

2.4.3 Griffiths et al. (2009)

Griffiths et al. (2009) studied the advantage of Random Finite Element Method (RFEM) over the traditional probabilistic method (FORM or MCS). The study aimed at investigating the influence of the spatial correlation length, local averaging and the coefficient of variation of the strength parameters on the probability of failure of the slope. The authors found that for a given value of the spatial correlation, there is a critical value of the coefficient of variation of the strength parameters. Thus, if perfect correlation is considered, the traditional methods lead to an underestimation of the probability of failure if the coefficient of variation of the strength parameters exceeds the critical value. This critical value is influenced by slope inclination, mean factor of safety, and

correlation between strength parameters. Its value is lower for steeper slopes with low factor of safety than less steep slopes with higher factor of safety.

The authors concluded from their analysis using FORM that for a given value of the coefficient of variation of the undrained shear strength, the probability of failure increases with the decrease in the factor of safety and for the same value of the factor of safety, the increase in the coefficient of variation of the undrained shear strength leads to an increase also in the probability of failure. However, for the same value of the factor of safety, there is no effect of the slope inclination on the probability of failure. Using RFEM, the authors varied the coefficient of variation and the correlation length of the undrained shear strength in order to study the effects of these descriptors on the probability of failure of the slope. Then, they compare the probability of failure obtained by FORM with that obtained from RFEM. The authors deduced that ignoring spatial variability underestimates the probability of failure for high coefficient of variation of the undrained shear strength and vice versa. Furthermore, the authors deduced that the effect of spatial variability on steeper slopes is more than that on flatter ones, but the probability of failure of a steeper slope is higher than that of flatter ones when RFEM is used. When they studied the effect of the mean factor of safety on the analysis, they found that for low coefficient of variation of the undrained shear strength, the effect of spatial variability on slopes of low factor of safety is higher than that of slopes of higher factor of safety.

2.4.4 Griffiths et al. (2010)

In this study the probabilistic slope stability methods in the literature were reviewed in order to investigate their efficiency in modeling spatial variability of soil

properties correctly. Griffiths et al. (2010) found that Point Estimate Method (PEM), First Order Second Moment Method (FOSM), First Order Reliability Method (FORM), and Monte Carlo Simulations are all used with the combination of Limit Equilibrium Method (LEM) for studying the reliability of slopes. The authors performed the analysis by analyzing a hypothetical slope that has already been analyzed by other authors. The authors showed that LEM combined with 1D random field can give lower probabilities of failure than the RFEM and this is due to the fact that RFEM doesn't require a priori assumptions related to the shape or location of the failure mechanism and also the failure mechanism has more freedom to find the weakest path through the random soil, which is in contrast to the LEM approach, where the failure surface location is fixed before the random field can be accounted for.

2.4.5 Jha and Ching (2013)

Jha and Ching (2013) performed a probabilistic slope stability analysis using the advanced method (Random Finite Element Method). The authors conducted the study by collecting a database for 34 real undrained engineered slope cases. The paper aimed at studying the effect of slope geometry, mean and coefficient of variation of the soil parameters, and the scale of fluctuation on the probability of failure. Jha and Ching (2013) started their analysis by performing a deterministic slope stability analysis for each case to get the nominal factor of safety. In this deterministic analysis, the authors transformed the undrained shear strength to the mobilized one and also they used the strength reduction method to evaluate the factor of safety. Using the RFEM approach, the

authors characterized the undrained shear strength of each layer by a random variable with a mean, coefficient of variation and lognormal distribution. Moreover, spatial variability was taken into account by defining both vertical and horizontal scales of fluctuation. The vertical scale of fluctuation was calculated for each case using Phoon and Kulhawy (1999) approach; however, the horizontal scale of fluctuation was assumed because it can't be calculated.

The results of the analysis indicated that statistical parameters of the factor of safety (μ and COV) depend on the coefficient of variation of the undrained shear strength, scales of fluctuation, and the slope geometry. The authors incorporated the effect of the slope geometry through the length of the failure surface as obtained from the deterministic analysis. The authors' analysis showed that the mean factor of safety is always less than the deterministic factor of safety. This reduction in the mean doesn't depend on the vertical and the horizontal scale of fluctuation; however, it depends on the coefficient of variation of the undrained shear strength. The reduction in the mean is more pronounced when the coefficient of variation of the random field is large. Additionally, the authors found that the coefficient of variation of the factor of safety is always less than the coefficient of variation of the random field. This variance reduction is more pronounced when the coefficient of variation of the random field is large and when the ratio of the vertical scale of fluctuation to the length of the failure surface is small. Furthermore, the authors reported that the ratio of the horizontal scale of fluctuation to the vertical one has a minor effect on the mean and the coefficient of variation of the factor of safety. Finally, the authors proposed a simplified equation to calculate the

probability of failure for the undrained engineered slopes that have a spatially variable shear strengths.

2.5 Studies involving probabilistic slope stability analyses based on search to find the minimum reliability index

The majority of the studies that conducted either LEM with Random Field or Random Finite Element Method (RFEM) consider the deterministic critical failure surface as the surface of the minimum reliability index. Hassan and Wolff (1999) illustrated that the surface of the minimum factor of safety isn't necessary the surface that has the minimum reliability index. Thus, some investigators [Hassan and Wolff (1999), Bhattacharya et al. (2003), Xue and Gavin (2007) and Deng and Luna (2013)] performed new methodologies to search for the critical probabilistic surface. The following section illustrates the work done by these investigators.

2.5.1 Hassan and Wolff (1999)

Hassan and Wolff (1999) proposed a simple and effective method for locating the critical probabilistic surface. The authors provided an algorithm to search for the surface of the minimum reliability index using existing deterministic slope stability computer programs by making a moderate number of multiple runs. Hassan and Wolff applied offset- values of each of the random variables while keeping the remaining parameters at their mean values, so they obtained different surfaces with different factors of safety.

Among these surfaces, the one that has the minimum factor of safety is considered the critical probabilistic surface. The authors obtained three values of reliability index; β_{FS} that corresponds to the critical deterministic surface, and β_f which is the reliability index of the floating surface. The floating reliability index was used by the authors as an indicator to check if there is a surface that has a reliability index lower than that obtained using the deterministic analysis. Furthermore, the authors obtained β_{min} that corresponds to the critical probabilistic surface.

After the application of the technique on case studies (Cannon Dam and Bois Brule Levee), Hassan and Wolff found that their technique can yield an accurate estimation of the reliability index. The authors concluded that both the type of the embankment (layered or homogenous) and the coefficient of variation of soil parameters have a significant effect on the difference between β_{FS} and β_{min} . For homogenous slopes with small coefficient of variation of soil parameters, both the deterministic and the probabilistic surfaces are close together. Conversely, for stratified slopes and in the case of high coefficient of variation, considering the critical deterministic surface as the critical probabilistic surface that has minimum reliability index leads to unconservative probabilities of failure.

2.5.2 Bhattacharya et al. (2003)

Bhattacharya et al. (2003) presented a numerical procedure for locating the surface with minimum reliability index by using a formulation similar to that used to search for the deterministic critical failure surface. The authors developed a computer

program that is an extended version of a deterministic slope program. This program used Spencer's method as a deterministic analysis and the Mean First Order Second Method (MFOSM) as a probabilistic analysis and the Monte Carlo Simulation Method (MCSM) to search for the critical slip surface. Moreover, this program doesn't make any priori assumption regarding the geometry of the slip surface where it can handle any complex slope geometry and layering. Bhattacharya et al. found that the search of the critical probabilistic surface is not different from that of the critical deterministic surface in which the procedure adopted is the same as that used for finding the critical deterministic slip surface with an additional step for the calculation of the reliability index.

2.5.3 Xue and Gavin (2007)

Xue and Gavin proposed a new method for probabilistic slope stability analysis. The new approach solved the reliability problem by using a genetic algorithm approach, which simultaneously locates the critical slip surface and calculates its reliability index. The authors used Bishop's method as a deterministic slope stability method. Furthermore, they illustrated the methodology by analyzing a hypothetical slope which was already studied by Hassan and Wolff (1999). The proposed approach performed well in comparison to FOSM and MCSM where it gave a reliability index close to that obtained by FOSM and MCSM. Conversely, the method has some drawbacks especially due to the implementation of Bishop's method only and due to the assumption that the variables are independent.

2.5.4 Deng and Luna (2013)

Deng and Luna (2013) investigated the effect of soil strength parameters on the probability of failure of the slope for both the deterministic slip surface and the probabilistic slip surface. They conducted a probabilistic slope stability analysis based on First Order Reliability Method (FORM) and Mean First Order Second Moment Method (MFOSM). FORM method was used to search for the surface with the minimum reliability index. Moreover, they used the Ordinary Method of Slices to calculate the deterministic factor of safety of the slope. Furthermore, the authors studied the effect of the distribution type on the reliability index of the slope. The authors found that compared to FORM, MFOSM tends to provide a relatively higher reliability index; however, the difference is too small. Hence, it can be used for the analysis. Moreover, they found that the user should select an appropriate distribution for random variables in probabilistic analysis. The use of lognormal distribution can result on 6% - 10% reliability index higher than that obtained using the normal distribution. Further, they concluded that cohesion is considered the most significant parameter that influences the probability of failure.

2.6 Studies involving system reliability analysis

For a structural or geotechnical system with several components, the overall reliability will depend not only on the reliabilities of the individual components but also on other factors including the correlations between different components or elements of

the system (Chowdhury and Xu 1995). Despite the fact that slope stability problems include many potential slip surfaces each of which has a finite probability of failure associated with it, the majority of the probabilistic slope stability studies are based on a predetermined slip surface. Some studies consider that the critical deterministic failure surface can be considered the surface with the highest probability of failure. Other studies use the critical deterministic failure surface as a trial surface to find the critical probabilistic failure surface. In fact, as a soil slope may have many potential slip surfaces, the failure probability of a slope may be larger than that of sliding along any single slip surface (Cornell 1967). For the sake of that, many investigators found that the slope reliability problem may be better solved in the framework of system reliability.

Chowdhury and Xu (1995) stated that there are three scenarios for the calculation of the system reliability. First scenario, one may simplify the problem by considering it as a simple series system; in this case failure occurs if any element of the system fails. Second scenario, considering the problem as a parallel system; in this case the failure of one element of the system leads to further loading of other elements and consequent decrease in reliability but the system doesn't fail unless all elements fail. The final scenario is a combination of both series and parallel systems. These scenarios are not justified where the series system can lead to a high failure probabilities; in contrast, parallel system can lead to a low failure probabilities. Hence, investigators proposed the approximation of the results by considering the upper and lower bounds of the probability of failure.

The following studies illustrated the use of system reliability for the probabilistic slope stability analysis.

2.6.1 Chowdhury and Xu (1995)

Chowdhury and Xu (1995) performed a system reliability analysis to calculate the upper and lower bounds within a probabilistic framework. The methodology is based in the concept of the limit equilibrium method where Bishop's method is used for the calculation of the deterministic critical surface that is used later for the comparison with the lower and the upper bounds of the system. The authors adopted two equations for the lower and the upper bounds of the probability of failure. The authors concluded from their study that the difference between the system probability of failure and that of the critical one is the correlation coefficients between the surfaces. The difference between the upper and the lower bounds increases as the coefficient of variation of the random variables increases. Furthermore, the difference between the upper bound and the probability of failure associated with the critical surface also increases as the coefficient of variation of the random variables increases.

The authors illustrated the analysis by analyzing two slopes; homogenous and layered slopes. Chowdhury and Xu (1995) deduced that, in the case of homogenous slopes, the correlation between the elements of the system is high. Thus, the probability of failure along different slip surfaces is highly correlated. Therefore, the upper bound of the probability of failure is highly correlated. Hence, the upper bound of the probability of failure is very close to the probability of failure of the critical slip surface. Conversely, for the layered slopes, the correlation is small. Hence, the upper bound probability of failure is greater than that of the critical surface. Finally, the authors found that the value of the upper bound probability of failure depends on the coefficient of variation of the

random variable. For low values of the coefficient of variation, the upper bound isn't high and vice-versa.

2.6.2 Hong and Roh (2008)

Hong and Roh (2008) performed a slope reliability analysis based on the generalized method of slices as a deterministic analysis and on First Order Reliability Method as a probabilistic analysis. The authors chose the generalized method of slices due to its efficiency in modeling slopes with complex geometries. In contrast, the choice of FORM as a probabilistic analysis is based on its effectiveness in overcoming the probability distribution tail sensitive problem. The authors considered the slope as a series system where the failure of any slip surface means failure for all the slope. They dealt with system reliability by defining a limit state function by getting the minimum of the ratio of the shear strength to the mobilized shear strength. Moreover, the study aimed at studying the effect of distribution type and the spatial variability on the probability of failure. The authors concluded that the probability of failure increases with the increase in the coefficient of variation of the random variable and as the probability of failure becomes larger, it is less sensitive to the distribution type. Further, the assumption that the soil properties in a soil layer are fully correlated leads to overestimation of the probability of failure.

2.6.3 Huang et al. (2013)

Huang et al. (2013) conducted three types of analyses; deterministic analyses to investigate the failure regions, probabilistic analyses using Monte Carlo Simulation to investigate the probability density function of the factor of safety and finally RFEM was performed to investigate the influence of spatial variability on the probability of failure of the slope. The authors illustrated the analysis by analyzing a hypothetical slope analyzed by other investigators Ching et al. (2009) and Low et al. (2011). They dealt with reliability problem as a system problem where all potential slip surfaces are considered . The results showed that the probability of failure obtained by FEM is higher than that obtained by LEM and the probability of failure decreases with increasing spatial correlation length.

2.6.4 Zhang et al. (2013)

Zhang et al. (2013) extended the work done by Hassan and Wolff (1999) to get a practical tool for evaluating the system reliability of a soil slope based on computer codes for deterministic slope stability analysis. Moreover, the authors adopted an equation that can be used by the user to get bounds of the system reliability. Zhang et al. (2013) illustrated the effect of the distribution type on the probability of failure. The authors recommended the use of the method for slopes with relatively simple geometry; however, the extended method is less accurate for complex slope geometries. The authors deduced that it is better to use the lognormal distribution for the factor of safety when the

coefficient of variation of the factor of safety is greater than about 30% due to larger uncertainty associated with the basic uncertain variables. Furthermore, they used the Hassan and Wolff method to judge if the system effect in slope reliability analysis is obvious or not. They found that the system effect is less obvious if the probability of failure of the most critical slip surface is greater than those based on other representative slip surfaces. In this case the system probability of failure is governed by the probability of failure of the most critical slip surface.

Regardless of the difficulty in estimating the system probability of failure, Zhang et al. (2013) recommended that its bounds can be estimated based on the probability of failure of the most critical slip surface using a simple equation.

CHAPTER 3

DATABASE COLLECTION

3.1 Introduction

Conventionally, the stability of a soil slope is evaluated by adopting a deterministic approach that is based on a target global factor of safety that is calculated either through limit equilibrium methods or through numerical analyses. Both LEM and FE slope stability models that are used to predict the factor of safety of a slope may not be totally accurate, in the sense that the calculated factor of safety may deviate from the actual factor of safety. The most effective approach that can be used for the evaluation of this deviation is to rely on actual failure cases when they exist. Despite this, actual well-documented failure cases for slopes are rare, especially due to the fact that slopes are typically built to meet high safety requirements. Travis et al. (2010) compiled a large scale database comprised of 301 actual failure cases. The authors report calculated factors of safety of the 301 failure cases based on the original publications in which these case histories were presented. The major drawback of the reported predicted factors of safety is the lack of consistency in the methods of prediction between the different cases. For example, some were based on methods assuming circular failure surfaces, but some were not. Some were based on total stress analyses while others were based on effective stress analyses. These inconsistencies in the reported factors of safety do not allow for a systematic and uniform analysis of these published failure case histories of slopes. A similar effort at compiling a database of slope failures was undertaken by Wu (2009)

where eight failure cases were analyzed using various limit equilibrium methods and finite element methods. Jha and Ching (2013) collected information about 34 idealized real engineered slope failures (cut and fill slopes). They predicted the factor of safety of these slopes using finite element method and only total stress analysis was adopted. Finally, Bahsan et al. (2014) collected 43 case histories, 34 of them were the same as those collected by Jha and Ching (2013). Bahsan et al. (2014) recalculated the factor of safety by adopting Limit equilibrium methods (Simplified Bishop's method and the Spencer's method) using a MATLAB code for the LEM calculations.

3.2. Database collection

In this study, 52 case histories are collected from documented failure cases of undrained slopes and embankments from the year 1956 to 2002 (Table 3.1). These cases are divided into 43 embankments/fill slopes, 8 cut slopes, and 1 natural slope. Site locations were spread from Europe, US, South America, Arabian Gulf to Asia. Most of the cut slopes and fill slopes are parts of road facilities, especially road embankments located in relatively remote areas such that the failures didn't have critical consequences on the surroundings, while others are test embankments that were built to fail. Slope heights range from 2 to 22 m, and slope angles range from 9 to 69 degrees. The subsoil natural materials are mostly clays and silty clays with unit weights ranging from 1.1 to 2 t/m³. The embankment fills are typically sandy or silty. The most common tests used to obtain undrained shear strengths are Unconfined Compression tests (UC) and Field Vane Tests (FVT). The observed failure surfaces tended to be circular except for two cases.

Table 3. 1. Database of Undrained Slope Failure Cases

No.	Site/Country	Reference	Slope Type	Slope Angle	Slope Height
1	Nesset/Norway	Flaate and Preber(1974)	Fill	27°	3m
2	Presterødbakken/ Norway	Flaate and Preber(1974)	Fill	34°	3m
3	Âs/Norway	Flaate and Preber(1974)	Fill	27°	7m
4	Skjeggerod/Norway	Flaate and Preber(1974)	Fill	27°	7m
5	Tjernsmyr/Norway	Flaate and Preber(1974)	Fill	27°	1.5m
6	Aulielva/Norway	Flaate and Preber(1974)	Fill	24°	2m
7	Falkenstein/Norway	Flaate and Preber(1974)	Fill	27°	4m
8	Jalsberg/Norway	Flaate and Preber(1974)	Fill	27°	2.5m
9	Saint Alban/ Canada	Pilot et al.(1982) La Rochelle et al. (1974) Talesnick and Baker (1984)	Test Fill	34°	4m
10	Narbonne/France	Pilot (1972) Pilot et al (1982) Talesnick and Baker (1984)	Test Fill	37°	9.6m
11	Lanester/France	Pilot (1972) Pilot et al (1982) Talesnick and Baker (1984)	Test Fill	32°	4m
12	Cubzac-les Ponts/France	Pilot et al (1982) Talesnick and Baker (1984)	Test Fill	38°	4.5m
13	Lodalen1/Norway	Sevalson(1956)	Cut	27°	15.9m
14	Lodalen2/Norway	Sevalson(1956)	Cut	28°	18.8m
15	Lodalen3/Norway	Sevalson(1956)	Cut	27°	16.3m
16	Rio de janeiro/Brazil	Ramalho-Ortigao et al (1983) Ferkh and Fell (1994)	Test Fill	27°	2.8m
17	New Liskeard/Canada	Lacasse et al(1977)	Test Fill	26°	6m
18	Bangkok A/Thailand	Eide and Holmberg (1972)	Test Fill	27°	2m
19	DrammenV/Norway	Kjærnsli and Simons (1962) Bjerrum and Kjærnsli (1957)	Natural	27°	17.7m
20	DrammenVI/Norway	Kjærnsli and Simons (1962) Bjerrum and Kjærnsli (1957)	Natural	26°	15.8m
21	DrammenVII/Norway	Kjærnsli and Simons (1962) Bjerrum and Kjærnsli (1957)	Natural	28°	13.2M
22	Pornic/France	Pilot(1972)	Fill	47°	3.25m
23	Saint-Andre/France	Pilot(1972)	Fill	22°	3m
24	South of France/France	Pilot(1972)	Fill	9°	6m

No.	Site/Country	Reference	Slope Type	Slope Angle	Slope Height
25	NBR Development /Canada	Dascal et al. (1972)	Test Fill	18°	4m
26	Portsmouth/USA	Ladd(1972)	Test Fill	18°	6.5m
27	Kameda/Japan	Hanzawa et al.(1994)	fill	32°	6.3m
28	KhorAl - Zubair no.4/Iraq	Hanzawa (1983) Hanzawa et al. (1980)	Fill	32°	11.5m
29	Lian-Yun- Gang/China	Chai et al.(2002)	Fill	30°	4m
30	Congress Street/USA	Ireland(1954)	Cut	42°	14.3m
31	Daikoku-Cho Dike/Japan	Kishida et al.(1983) Hanzawa (1983)	fill	28°	14.7m
32	Cuyahoga AA/USA	Wu et al.(1975)	fill	27°	18.7m
33	King's Lynn(England)	Wilkes(1972)	fill	35°	10.5m
34	Muar/Malaysia	Indraratna et al.(1992)	Test fill	54°	5.5m
35	North Ridge Dam/Canada	Rivard et al.(1978)	Fill	13°	18.3m
36	Seven Sisters Dike/Canada	Rivard et al. (1978) Peterson et al. (1957)	Fill	12°	4.3m
37	Shellmouth Dam/Canada	Rivard et al.(1978)	Fill	27°	16.5m
38	Juban I/USA	Zhang et al.(2005)	Fill	17°	6m
39	Bradwell/England	Skempton and LaRochelle (1965) Duncan and Wright (2005)	Cut	45°	4.60m
40	Genesee/ Canada	Been et al.(1986)	Fill	16°	7m
41	Precambrian/Canada	Dascal et al. (1975)	Fill	23°	7.6m
42	Scrapsgate/England	Golder et al.(1954)	Fill	27°	6m
43	Scottsdale/Australia	Parry(1968)	Fill	17°	6m
44	Iwai/Japan	Shogaki et al.(2008)	Fill	34°	4.5
45	Fair Haven/USA	Haupt and Olson(1972)	Fill	20°	13.8m
46	Boston Marine Excavation/USA	McGinn et al. (1993)	Cut	90°	14m
47	Desert View Drive/USA	Day(1996)	Cut	33°	21.7m
48	Siburua October 5	Wolfskill et al. (1967)	Natural	22°	7m
49	Tianshenqiao/China	Chen et al. (1988)	Natural	34°	14.5m
50	San Francisco Bay/USA	Duncan and Buchignani (1973)	Cut	41°	18m
51	Carsington/England	Skempton and Coats (1985)	Fill	18°	12.2m
52	Atchafalaya/USA	Kaufman et al. (1967)	Natural	14°	10.5m

This chapter includes brief descriptions for all the failure cases found in the literature. The geometries right before failures were considered to estimate the near failure condition in the LEM due to the fact that all these cases are failure cases. The 52 cases studied are re-analyzed and the factors of safety are evaluated using four different limit equilibrium methods (Simplified Bishop method, Ordinary method of slices, Janbu, and Spencer's method). Table 3.2 illustrates all the soil properties adopted for the slope stability analysis of the 52 case histories.

3.2.1. Slide at Nasset

In October 1957 a 50m slide occurred at Nasset in Norway during the construction of the embankment. The embankment is 3m high and is mostly comprised of granular soil (sand and gravel) with a probable angle of internal friction of 35° and a unit weight of 1.9 t/m^3 . This embankment was built with 2 (horizontal):1 (vertical) side slopes. The foundation soil at the site consisted of a 2-8m thick deposit of soft clay soil over a 1m thick layer of silty sand that is placed at 10m below the ground level over bedrock. The site showed no evidence of the presence of a dry crust; however, quick clays of the type involved in this slide are noted for their great sensitivity and extremely brittle failure. This layer of quick clays is present at 8m below the ground surface close to the permeable sand layer. Soil properties including unit weight, index parameters, undrained shear strength and sensitivity for the site soils are summarized in the borehole profile in Fig.3.1. The clay has undrained shear strength of $0.8\text{-}2 \text{ t/m}^2$ that is measured by unconfined compression tests, fall-cone tests and vane shear tests and a unit weight

between 1.50 and 1.80 t/m³. Due to the small movements and disturbances that occurred after failure, the slip failure was close to cylindrical.

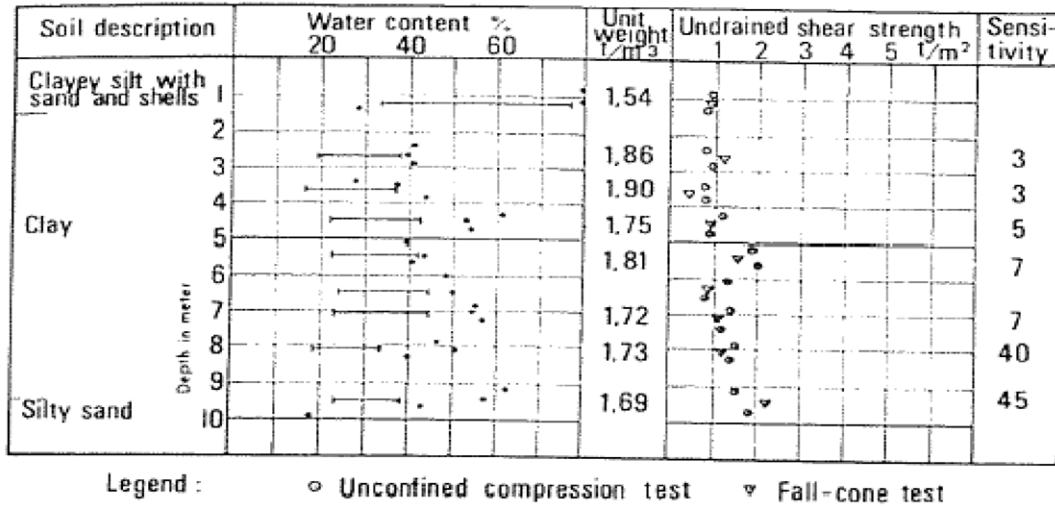


Figure 3.1 Borehole Profile at Nasset (Flaate and Preber 1974)

Flaate and Preber (1974) computed the minimum factor of safety for the profile shown in Fig.3.2 by adopting a short term stability analysis using the Swedish slip circle method and obtained a factor of safety of 0.88. Re-calculation of the factor of safety for the profile shown in Fig.3.3 was accomplished using the SLIDE software that can evaluate the factor of safety using different methods (Bishop, Ordinary Method of Slices, Janbu, and Spencer). The analysis is carried out by adopting the field vane measurements for assigning the undrained shear strength values for the layers.

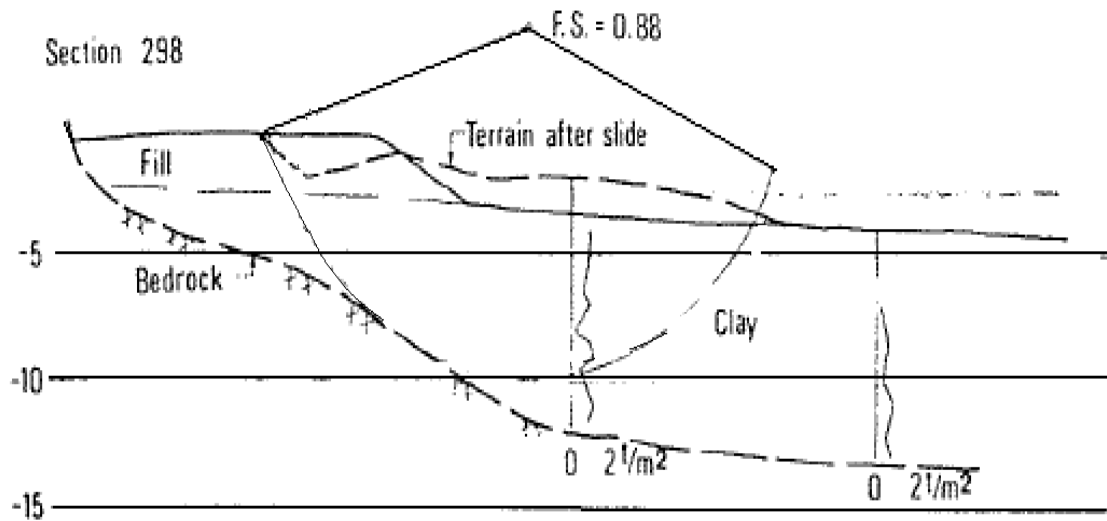


Figure 3. 2 Critical Slip Surface (Flaate and Preber 1974)

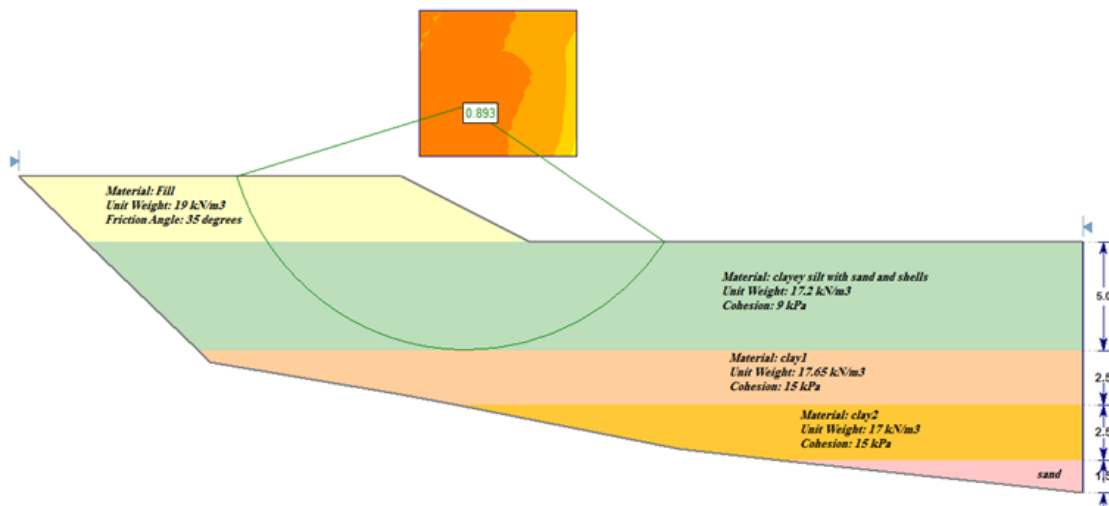


Figure 3. 3 Critical Slip Surface using SLIDE software

3.2.2 Slide at Presterødbakken

The Presterødbakken slide occurred in May 1962 during the construction of a 3m high embankment. The failure was due to workmanship mistake, when workers noticed that slight depression occurred in the surface of the embankment they hurried up to solve the problem by filling the depression with an additional material without seeking an engineer. That resulted in a slide that began at the centerline of the road with an area of 50x25m. The embankment was constructed of granular fill with an assumed angle of internal friction of 30° and unit weight of 1.9t/m^3 and it was laid at a slope of 1:1.5. The foundation soil is composed of 1-2m dry crust underlain with 8-10m of clayey silt. Soil properties are shown in Fig.3.4. The undrained shear strength values are measured using Unconfined Compression test, field vane test, and Fall-cone tests.

The slide failure was assumed as mere rotational about an axis resulting in a circular slip surface due to the presence of the same vane shear strength values inside and outside the sliding zone. Flaate and Preber (1974) analyzed the profile in Fig.3.5 by using the Swedish slip circular method where $FS=0.83$ was obtained. The slope is reanalyzed using SLIDE software to evaluate the minimum factor of safety for the sliding body and the results are shown in Fig.3.6.

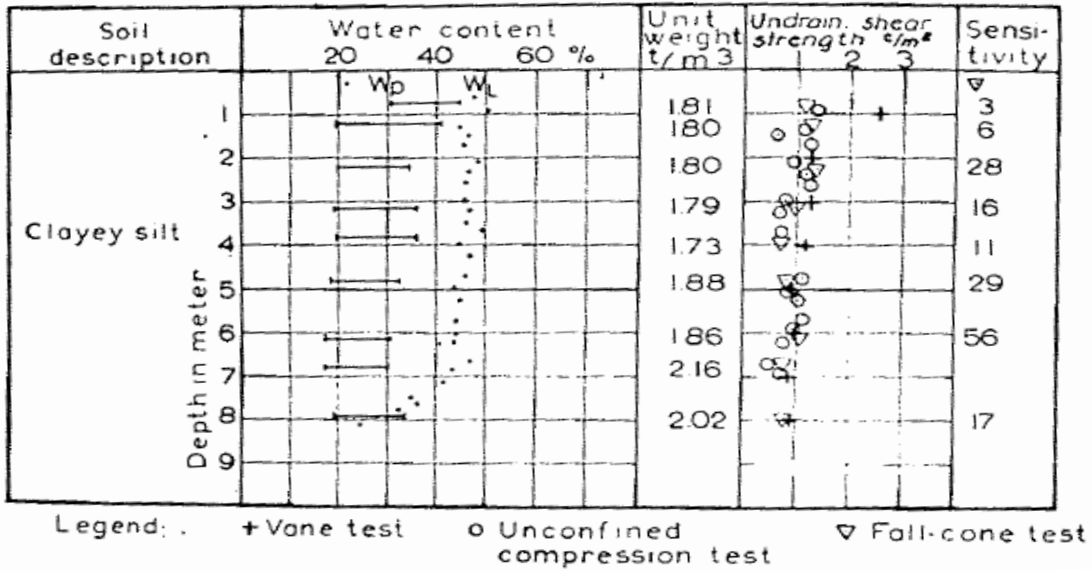


Figure 3. 4 Borehole Profile at PresterØdbakken (Flaate and Preber 1974)

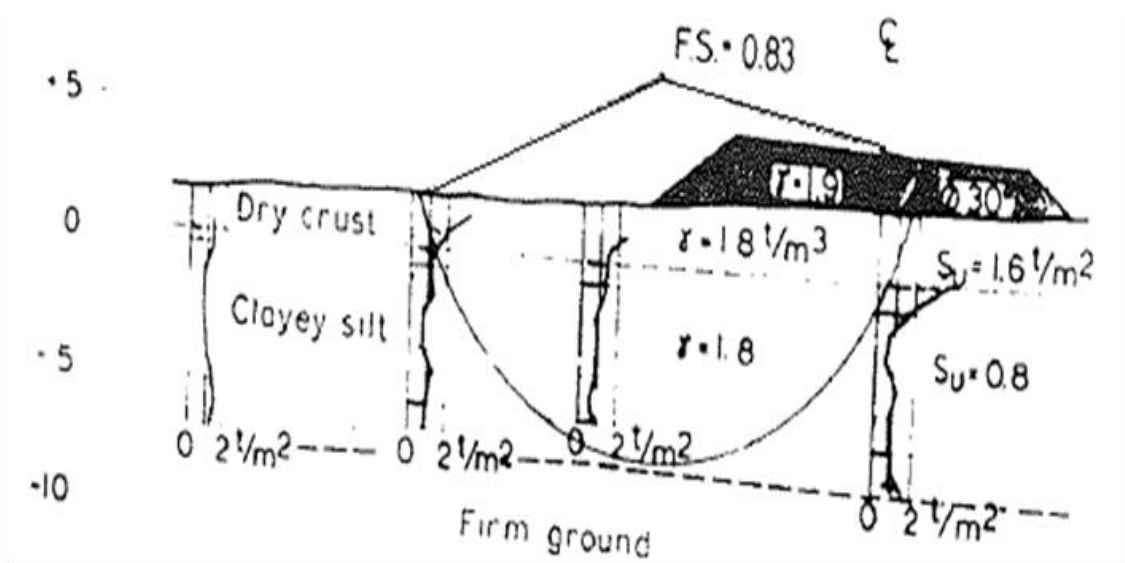


Figure 3. 5 Critical Slip Surface at PresterØdbakken (Flaate and Preber 1974)

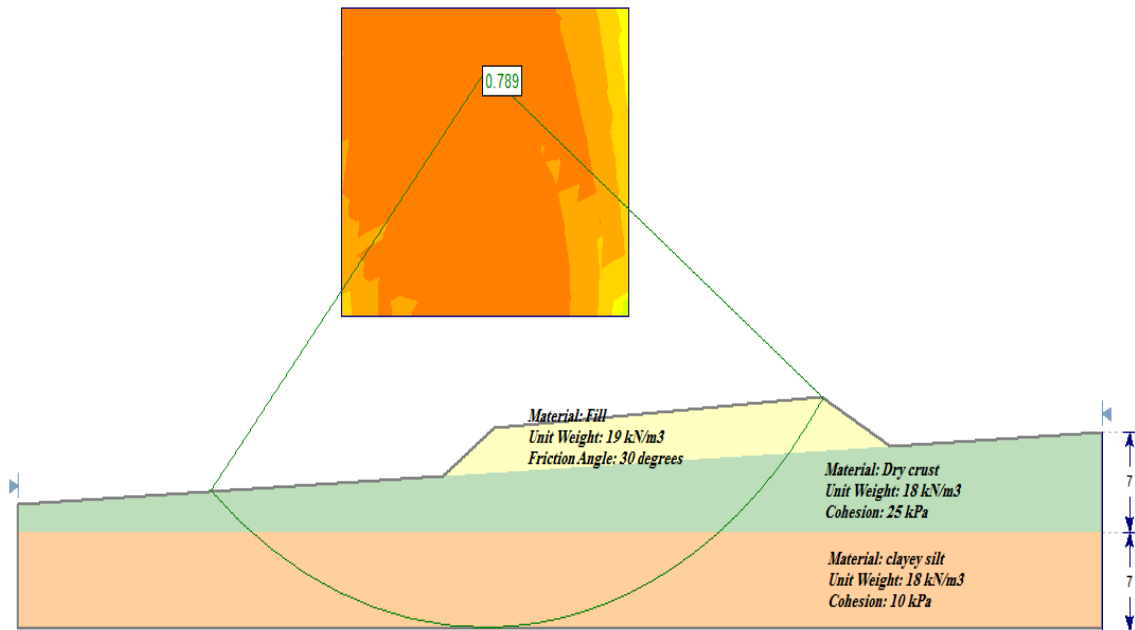


Figure 3. 6 Critical Slip Surface using SLIDE

3.2.3 Slide at Ås

The 25x35m area slide took place during the night at the end of September 1962 at Ås in Norway. A depression of about 1-1.5m occurred at the end of construction of the road embankment when the workers started with the bituminous surfacing. The embankment height is close to 7m and the slope is inclined at about 27°. The embankment fill is formed from compacted silt or clay with little amount of crushed stone. Soil investigation showed that the foundation soil consisted of a 2-3m thick dry crust underlain by 7m of silty clay. The soil properties of the foundation soil are shown in Fig.3.7.

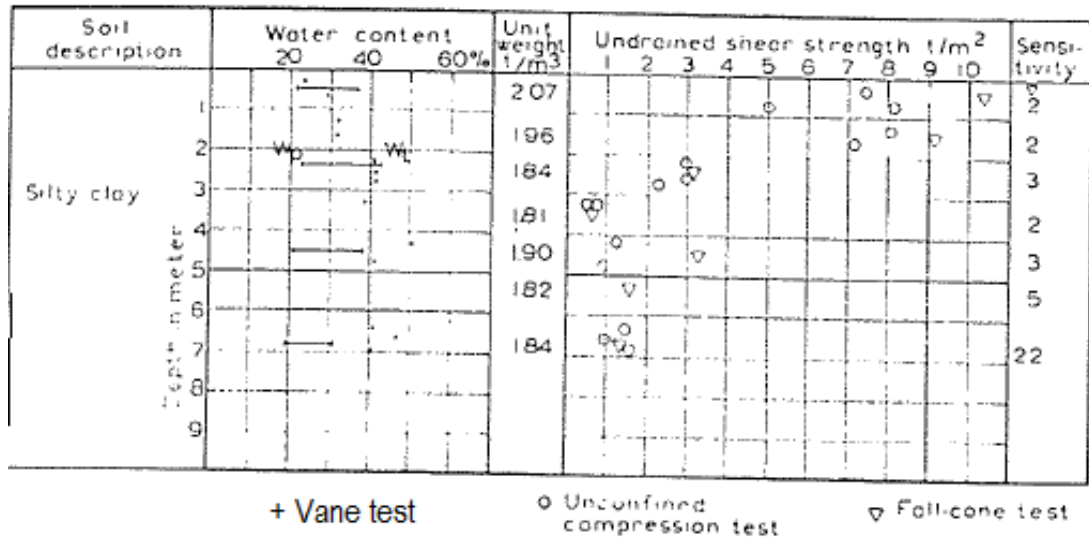


Figure 3.7 Borehole Profile at Ås in Norway (Flaate and Preber 1974)

When the depression occurred, no cracks were formed and the vane tests showed no disturbance. Hence, a circular failure surface was assumed and the factor of safety for the profile shown in Fig.3.8. was calculated using Swedish slip circle method and $FS=0.80$ was obtained. The minimum factor of safety is recalculated using SLIDE software and the results are shown in Fig.3.9.

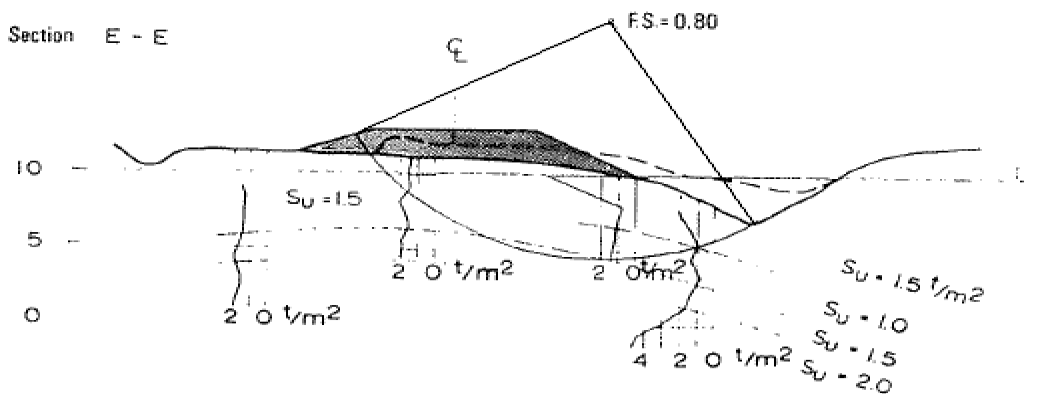


Figure 3.8 Critical Slip Surface at Ås in Norway (Flaate and Preber 1974)

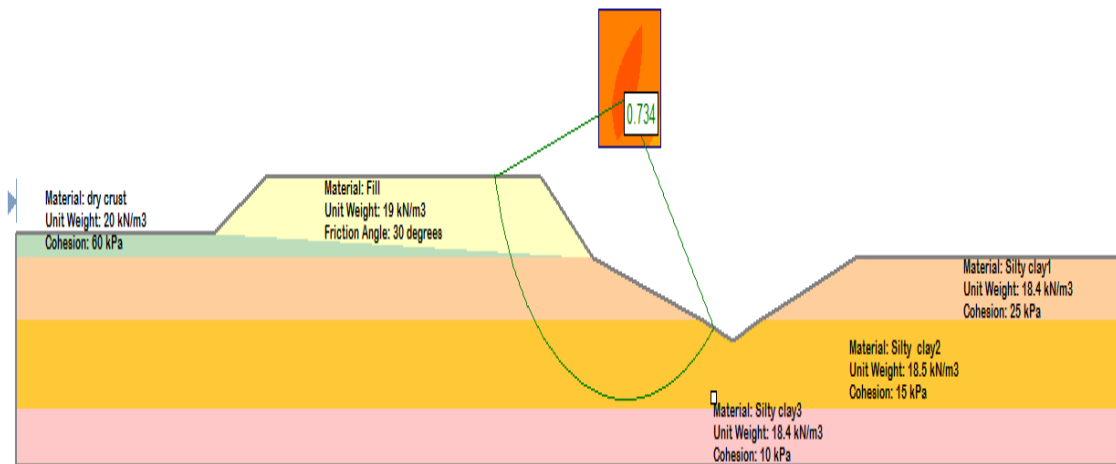


Figure 3. 9 Critical Slip Surface using SLIDE

3.2.4 Slide at Skjeggerod

Fig.3.10 shows a slope failure that occurred during the night in the beginning of September 1963 at Skjeggerod in Norway. The soil mass slid over a distance of 45m perpendicular to the road forming a slope that is 5-6m high at an inclination of 27°.

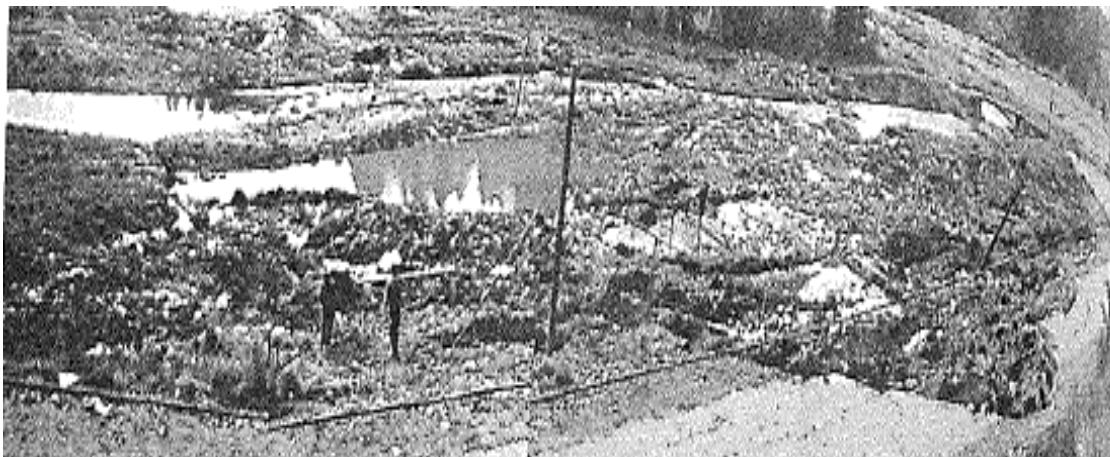


Figure 3. 10 View of the Slide Occurred at Skjeggerod in Norway (Flaate and Preber 1974)

Soil investigation after the slide resulted in the soil properties shown in Fig.3.11.

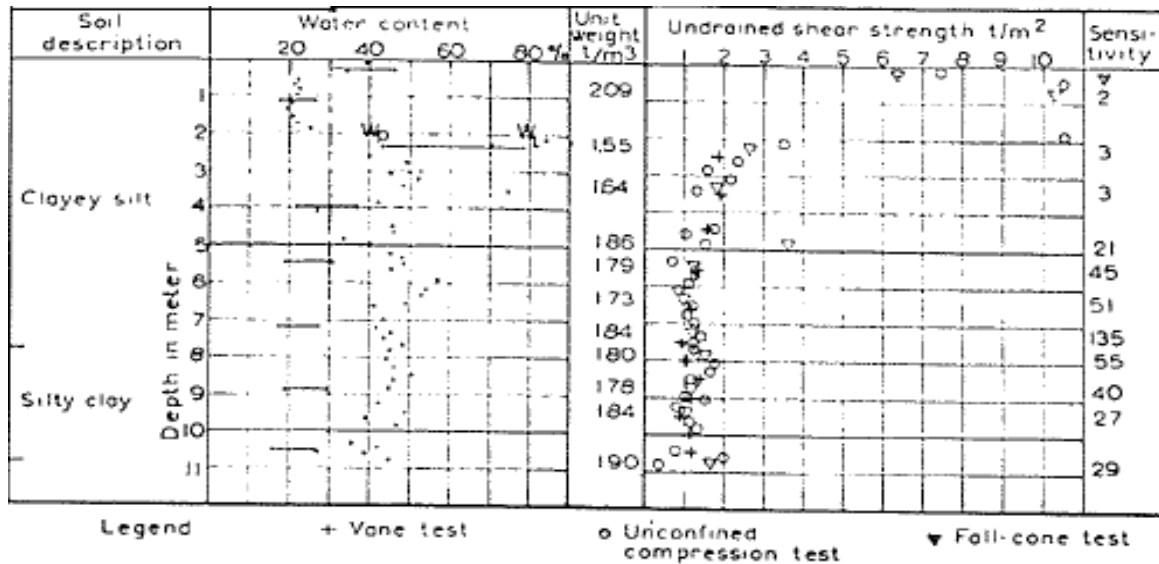


Figure 3. 11 Borehole Profile at Skjeggerod in Norway (Flaate and Preber 1974)

The road embankment is mostly of granular material with an angle of internal friction of 30° and unit weight of 2t/m³. According to Flaate and Preber (1974), the slip surface is assumed to be composite due to the strong disturbance of the soil masses. The authors computed the factor of safety for the profile shown in Fig.3.12 using the Swedish slip circle method and a value of 0.73 was obtained. However, in this study the surface is assumed circular and the factor of safety value is presented in Fig.3.13.

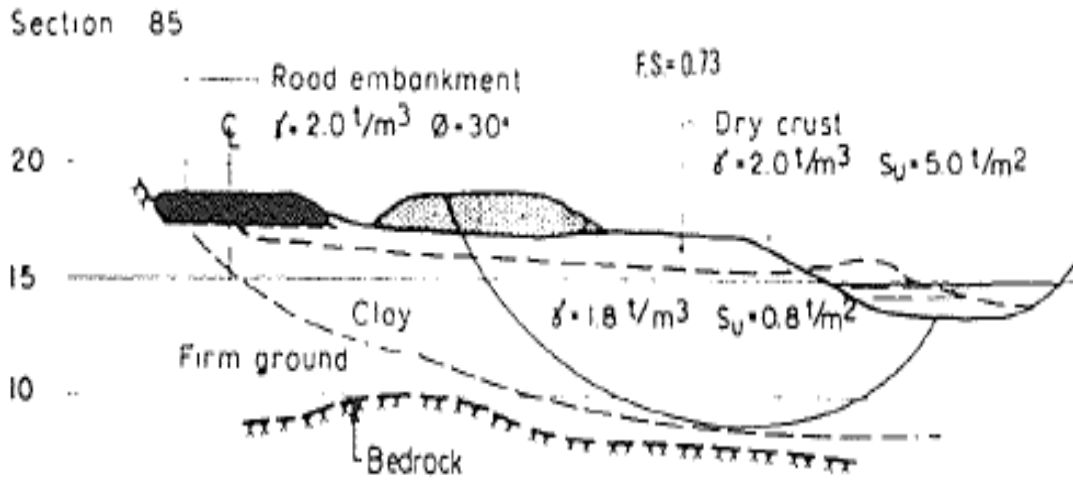


Figure 3. 12 Critical Slip Surface at Skjeggerod (Flaate and Preber 1974)

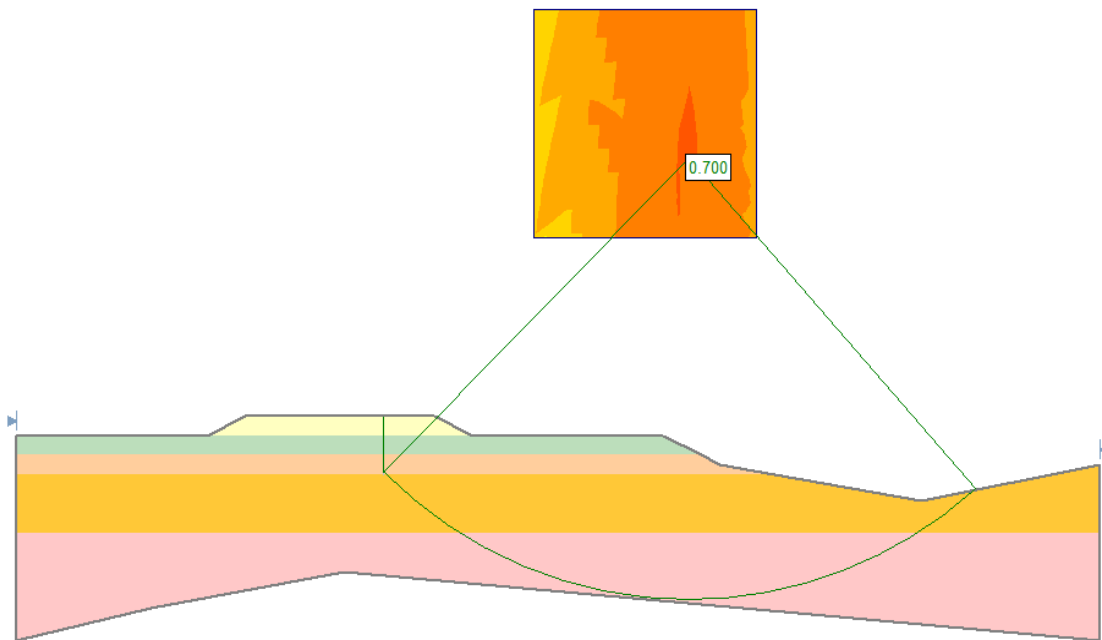
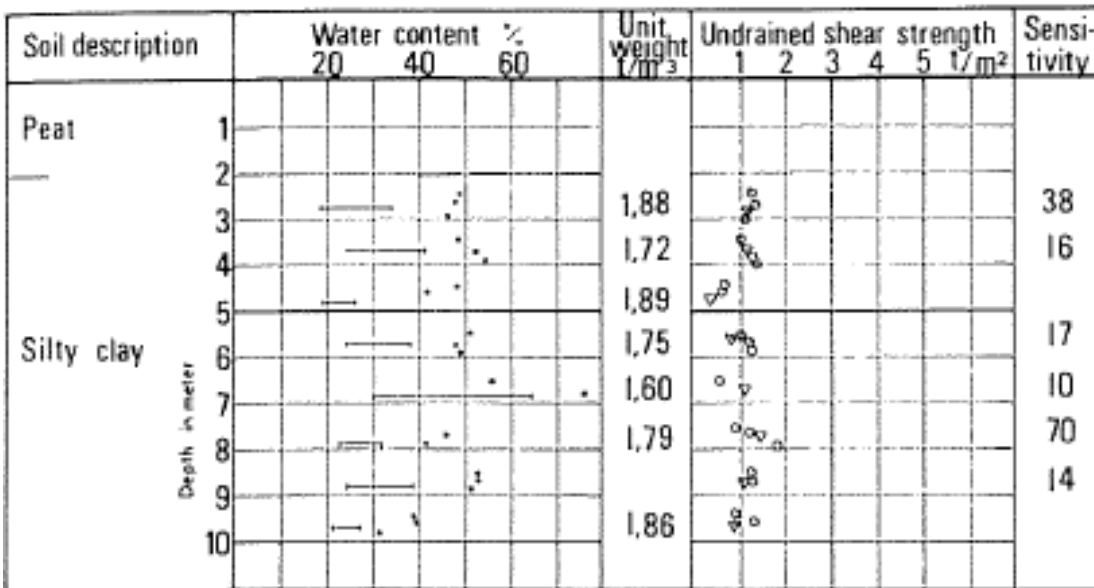


Figure 3. 13 Critical Slip Surface using SLIDE

3.2.5 Slide at Tjernsmyr

On November 29, 1957, a slide took place at Tjernsmyr in Norway. At the end of the road construction, 80m of the embankment slid out. The embankment was between 1-2m high and was built with 2 (horizontal) : 1 (vertical) side slopes. The fill consisted of granular material with an angle of internal friction of about 40° and a unit weight of 1.9 t/m³. The foundation soil consisted of 1-2m layer of peat over a 10-20m layer of soft silty clay with high sensitivity. Soil properties are shown in Fig.3.14.



Legend: ○ Unconfined compression test ▽ Fall-cone test

Figure 3. 14 Borehole Profile at Tjernsmyr (Flaate and Preber 1974)

The movements were small and very few cracks on the surface of the sliding body were seen so very little disturbance of the soil occurred. Due to the presence of only small movements, the slip surface was assumed circular and the factor of safety was calculated

by Flaate and Preber (1974) using the profile shown in Fig.3.15. and by adopting the Swedish slip circle method. A factor of safety of 0.87 was obtained by the authors. The slide at Tjernsmyr is analyzed using SLIDE software and a minimum FS= 0.834 is obtained as shown in Fig.3.16.

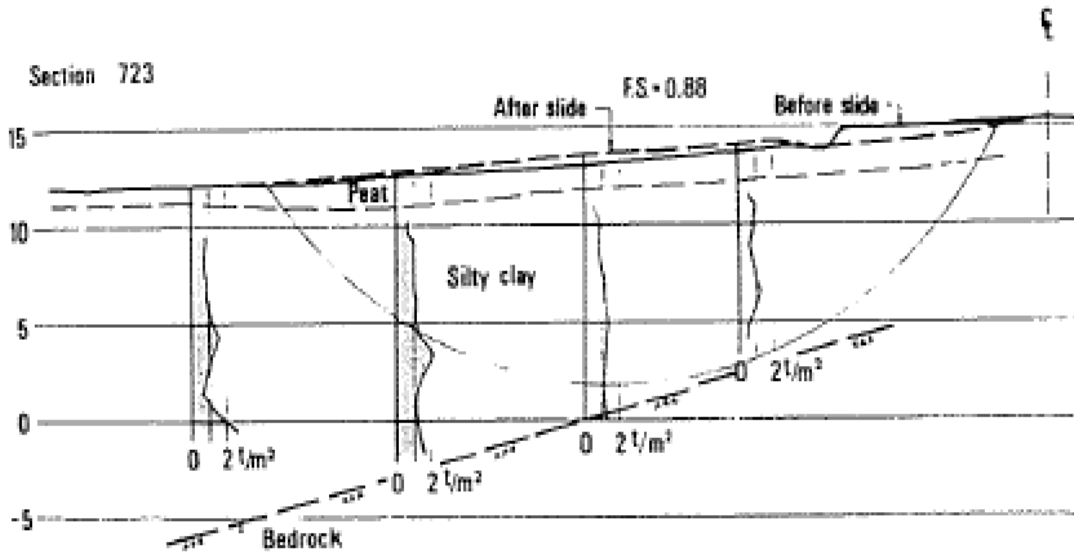


Figure 3. 15 Critical Slip Surface at Tjernsmyr (Flaate and Preber 1974)

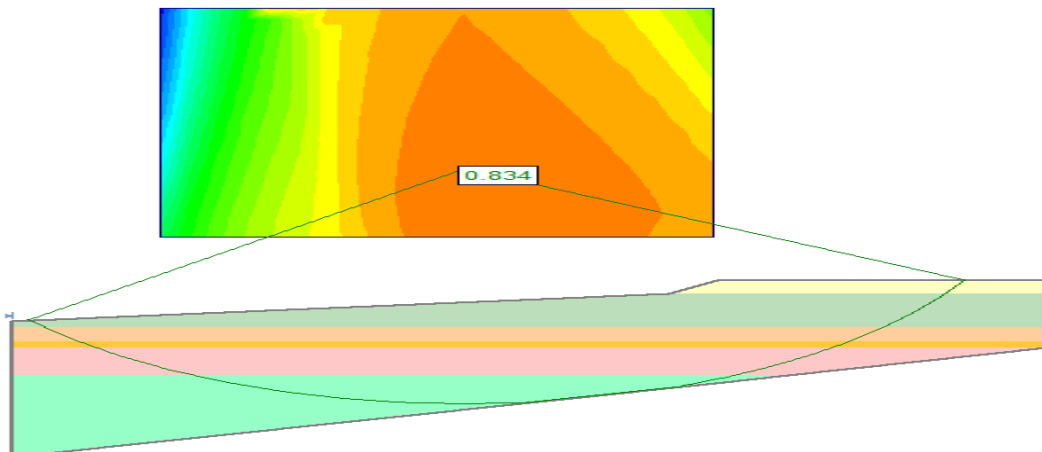


Figure 3. 16 Critical Slip Surface using SLIDE

3.2.6 Slide at Aulielva

In March 1963 and after the completion of the road construction at Aulielva in Norway by six months, a slide occurred and the materials slid out perpendicular to the road towards the Auli river. A photograph of the slide is shown in Fig.3.17.



Figure 3. 17 Slide at Aulielva (Flaate and Preber 1974)

The embankment was 2m high and was laid at an angle of 24° with an angle of internal friction of 30° and unit weight of 1.9t/m^3 . The soil investigation indicated the presence of a 2-4m thick dry crust underlain by a silty clay layer. Fig.3.18. shows the soil properties of the foundation soil. High disturbance and remolding that occurred within the sliding body indicated that the slip surface is composite.

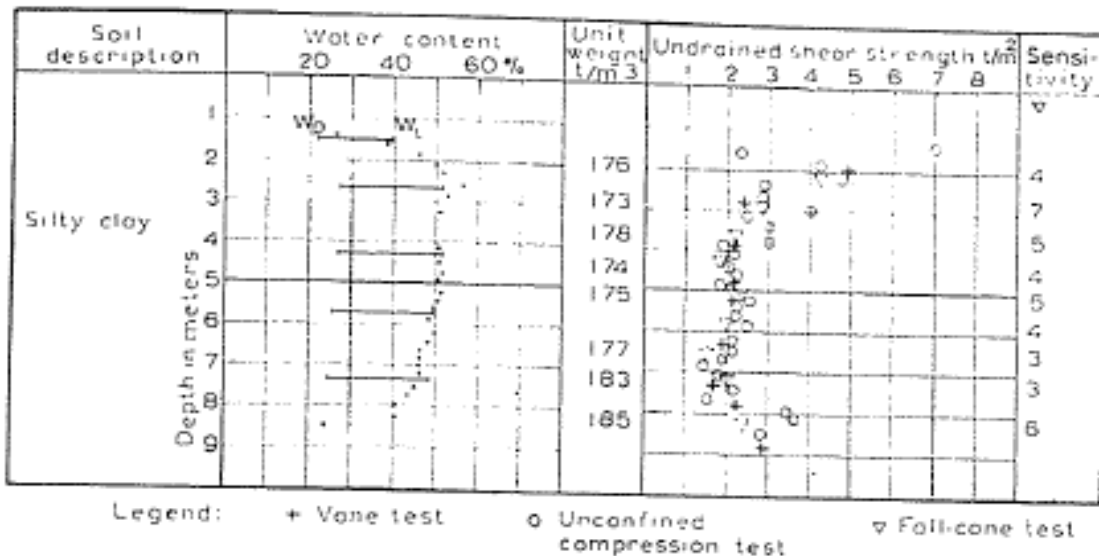


Figure 3. 18 Borehole Profile at Aulielva (Flaate and Preber 1974)

Flaate and Preber (1974) analyzed the slope profile shown in Fig.3.19. and obtained a factor of safety of 0.92 using the Swedish slip circle method by assuming both composite and circular slip surface. In this study the factor of safety is evaluated using SLIDE software and the results are shown in Fig.3.20.

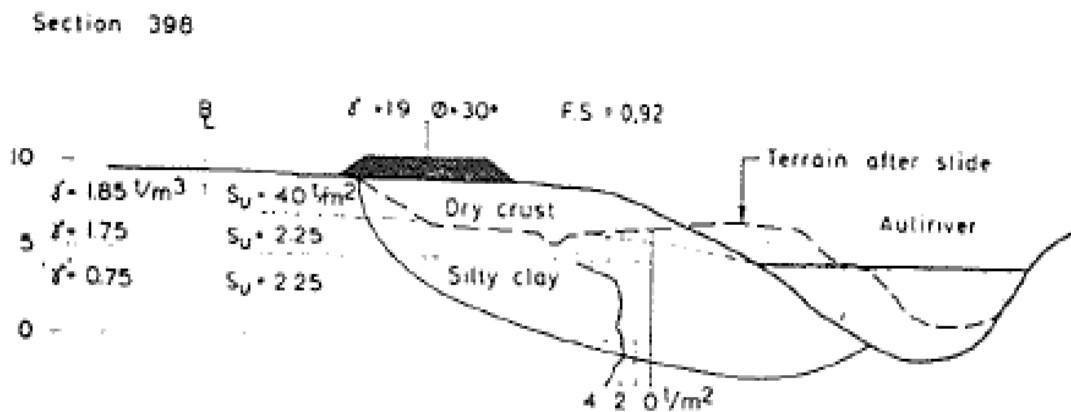


Figure 3. 19 Critical Slip Surface at Aulielva (Flaate and Preber 1974)

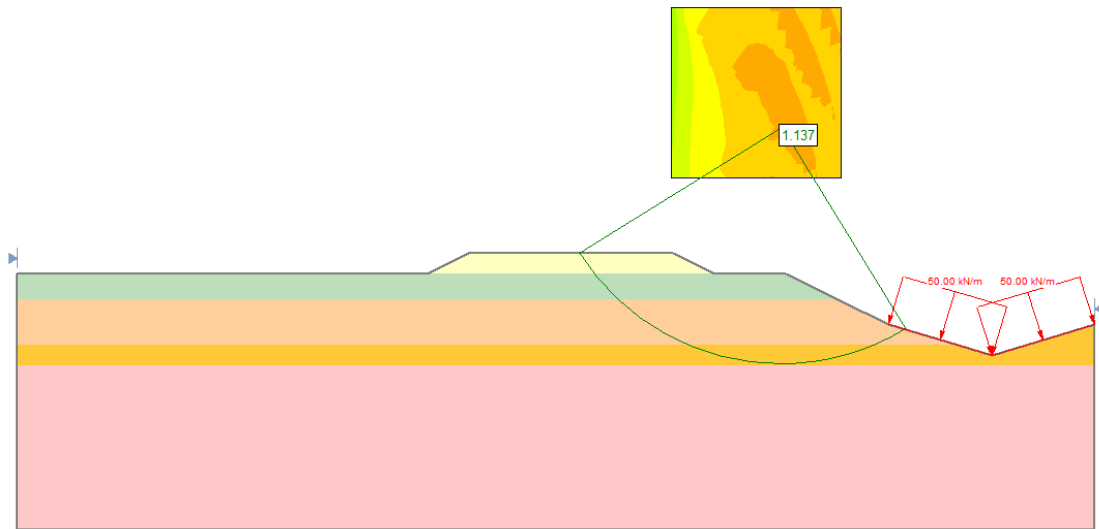


Figure 3. 20 Critical Slip Surface using SLIDE

3.2.7 Slide at Falkenstein

The slide at Falkenstein in Norway took place in April 1964. The slide occurred over a 40m width of a recently placed embankment. The fill consisted of granular material with an assumed angle of internal friction of 35° and unit weight of 1.9t/m^3 . Moreover, the embankment was 4m high inclined at 27° .

According to the soil investigation done in the site, no evidence of a dry crust was found at the site. The soil profile consisted of a 15m soft silty quick clay layer. The soil properties of the foundation soil material are shown in Fig.3.21.

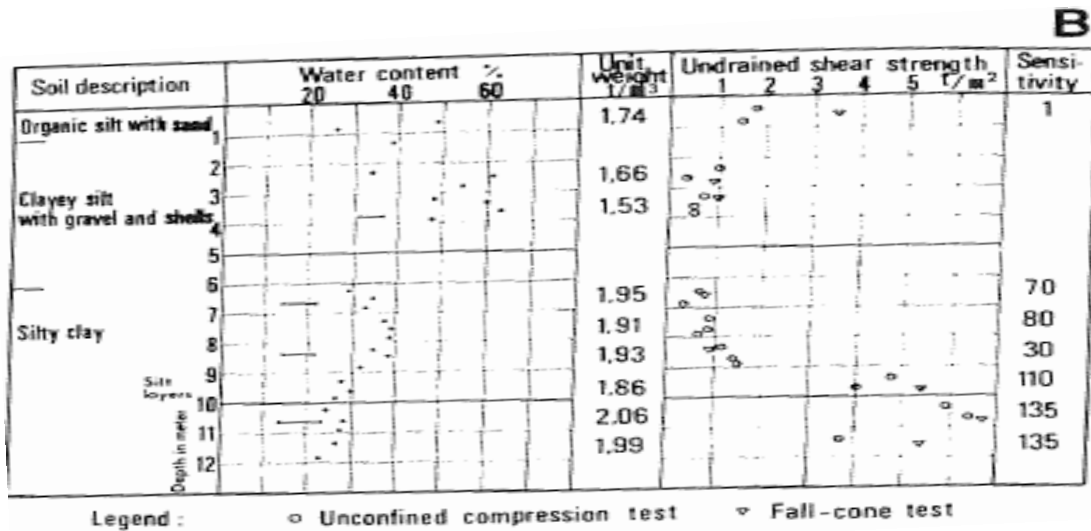


Figure 3. 21 Borehole Profile at Falkenstein (Flaate and Preber 1974)

Flaate and Preber (1974) evaluated the factor of safety of the slope using the Swedish Slip Circle method and by assuming a circular slip surface as shown in Fig.3.22. In this study the factor of safety is evaluated using the profile shown in Fig.3.23.

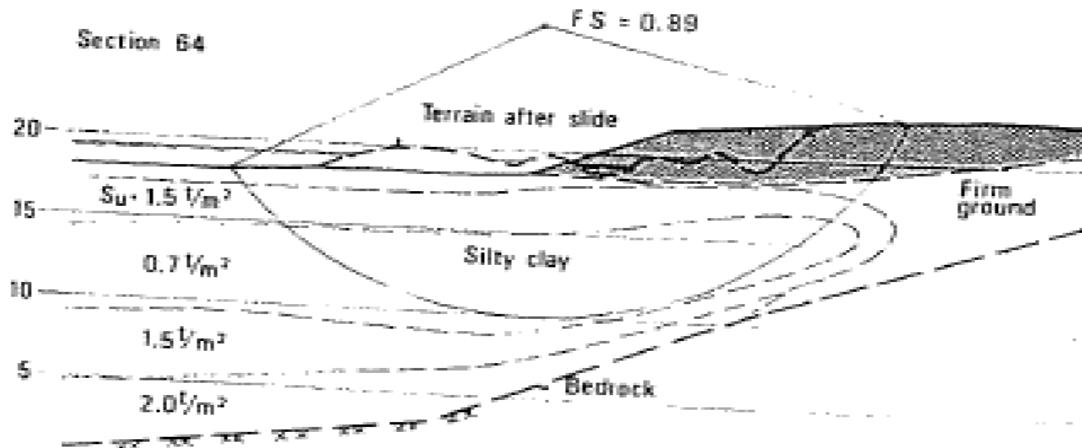


Figure 3. 22 Critical Slip Surface at Falkenstein (Flaate and Preber 1974)

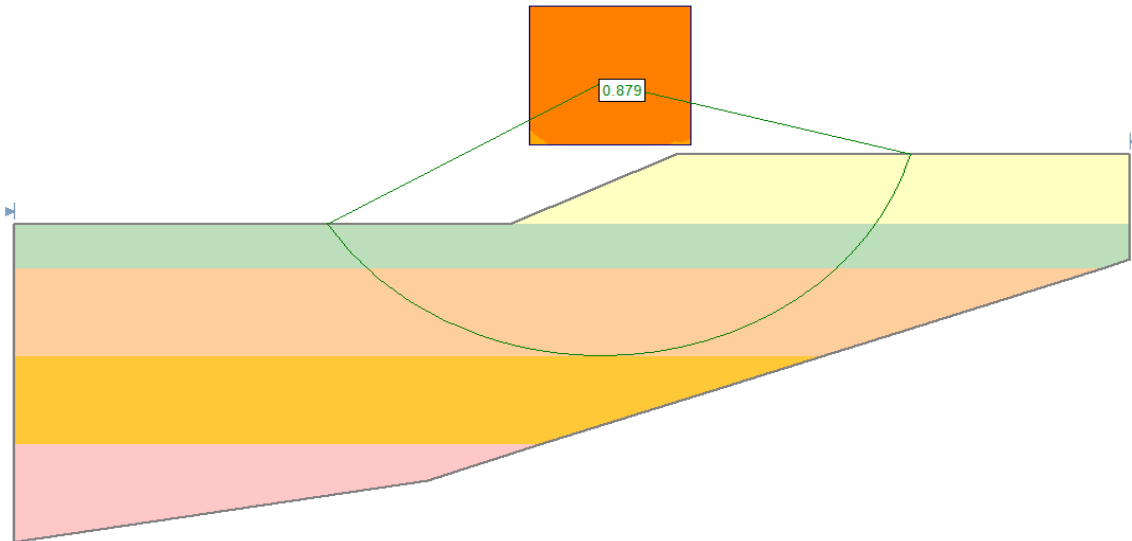


Figure 3. 23 Critical Slip Surface Using SLIDE

3.2.8 Slide at Jalsberg

In October 1964, a slide took place at Jalsberg in Norway during the construction of road embankment. The embankment was about 2.5m high and was built at 27° inclination. The fill consisted of granular soil with an internal friction angle of 35° and a unit weight of 1.9 t/m³. Soil investigation was carried out and showed the presence of 1-2m dry crust over a thick deposit of medium to low sensitivity silty clay.

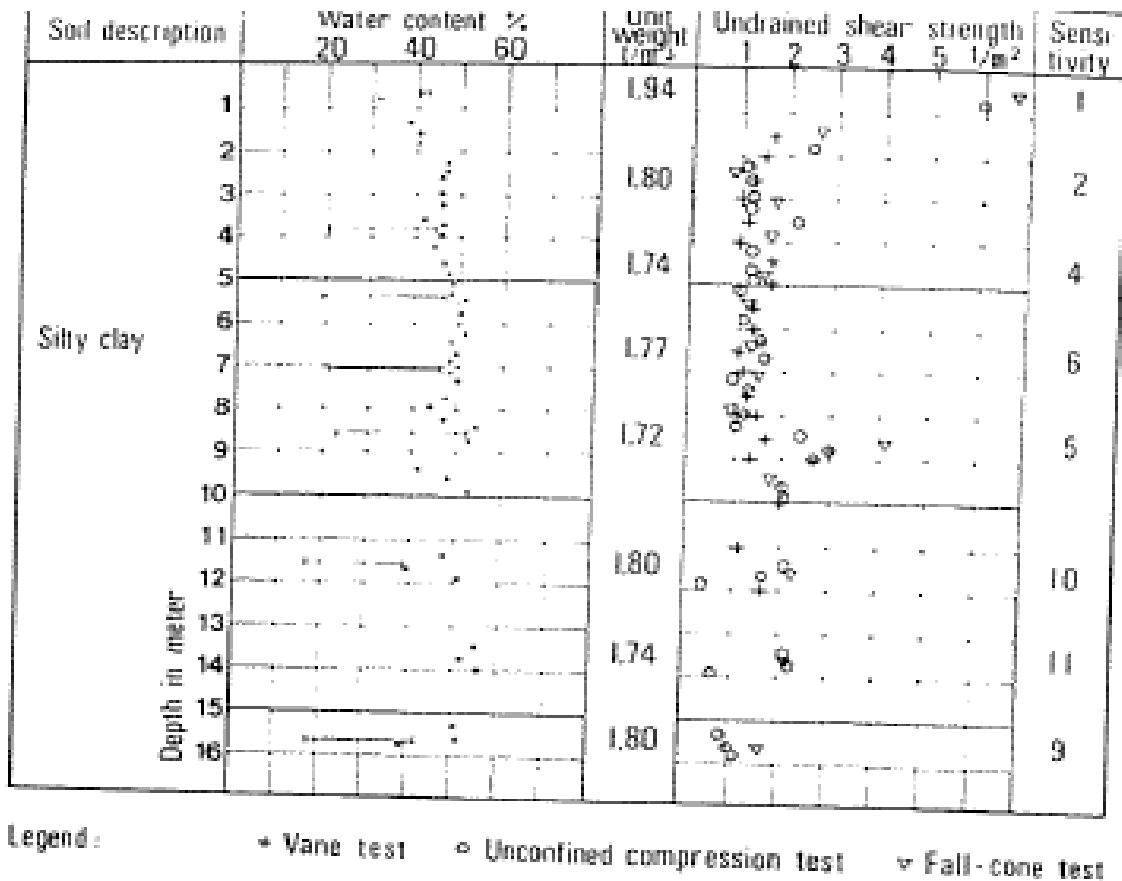


Figure 3. 24 Borehole Profile at Jalsberg (Flaate and Preber 1974)

The soil borehole profile is shown in Fig.3.24. No strong soil deformation occurred due to the slide and no soil disturbance was detected within the sliding body. Hence, a circular slip surface was assumed by Flaate and Preber (1974) and the minimum factor of safety was found to be 1.10 for the profile shown in Fig.3.25. The factor of safety is recalculated by using SLIDE software and the results are shown in Fig.3.26.

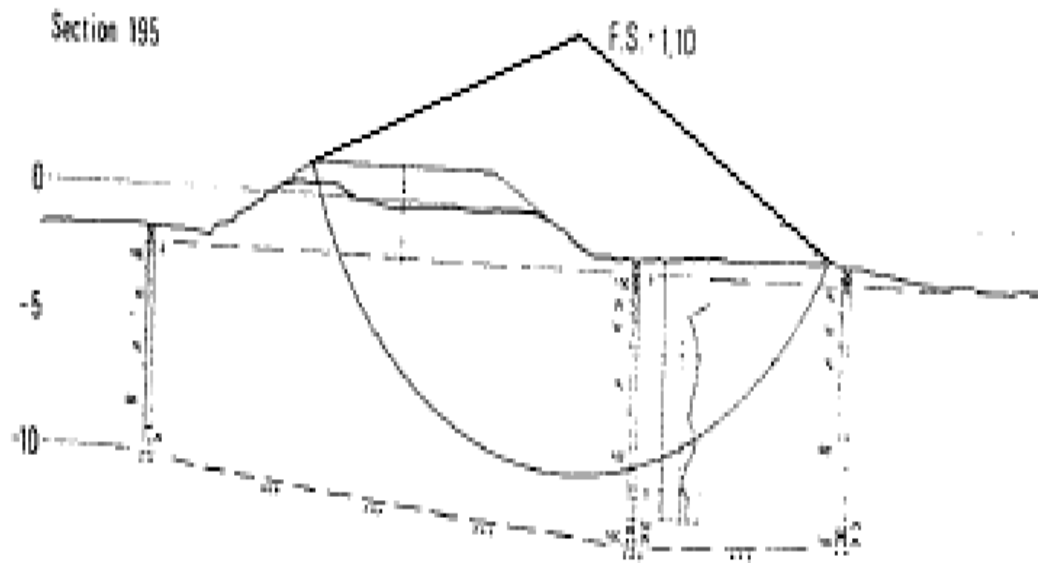


Figure 3. 25 Critical Slip Surface at Jalsberg (Flaate and Preber 1974)

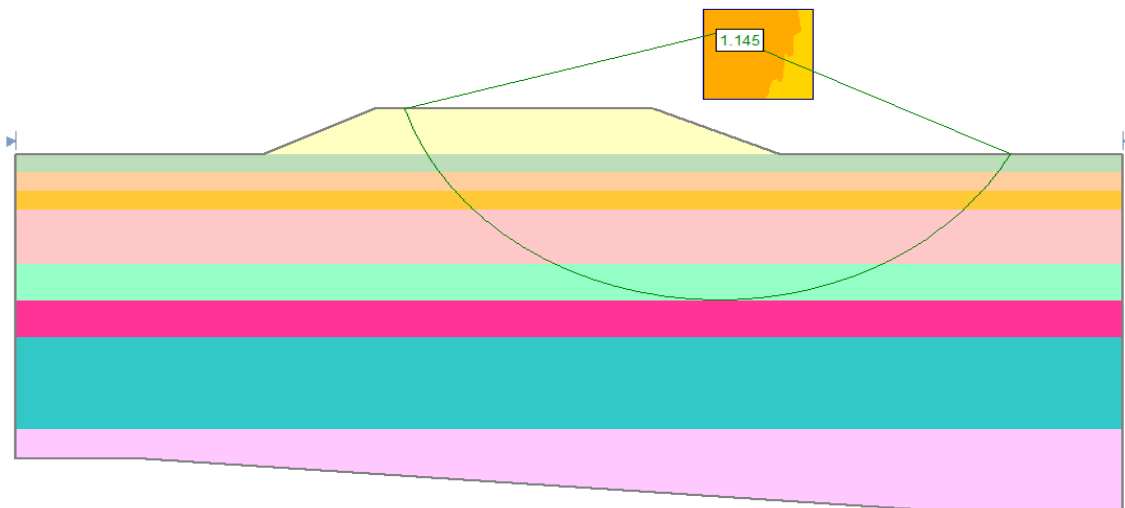


Figure 3. 26 Critical Slip Surface using SLIDE

3.2.9 Slide at Saint- Alban

In October 13, 1973 a failure of a test embankment occurred in Saint-Alban, Quebec in Canada. Numerous fissures opened on the top surface of the fill and massive failure occurred. The purpose of the project was to investigate the failure conditions of fills built on foundations of soft sensitive clays. The fill was built up until failure occurred with a height of 4.6m and with a front slope of 1.5 horizontal to 1 vertical. Moreover, the fill consisted mostly of uniform medium to coarse sand containing about 10% fine sand and 10% gravel. This fill has an internal friction angle of 44° due to the presence of very pronounced angular-shaped grains. A detailed soil investigation was conducted in the site indicating the presence of a weathered clay crust extending down to a depth of 1.8m. This layer is overlain by 0.3m top soil and underlain by a gray to blue soft silty marine clay with a more silty layer at 5.2m. Below this silty clay layer, a layer of soft and sensitive clayey silt with sand is found. Finally, a dense fine to medium sand constitutes the lower part of the deposits from 13.7 to 24.4 m depth. Soil properties including index parameters, unit weight, and undrained shear strength are shown in Fig.3.27.

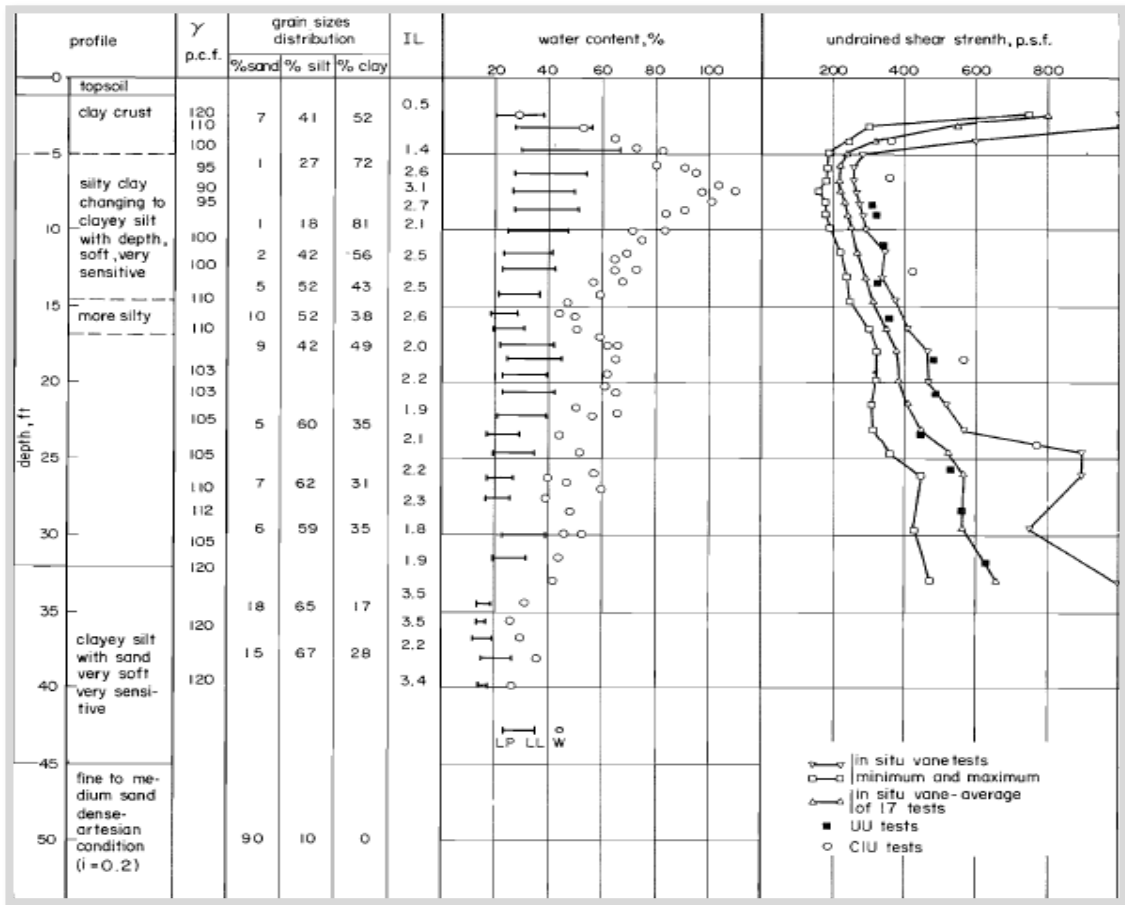


Figure 3.27 Soil Profile at Saint-Alban (L_A Rochelle et al. 1982)

An instrumentation program was conducted and from the observations of the displacements of the reference points at the toe and of the surface of the fill after failure, it is evident that the failure surface developed along a circular arc. L_A Rochelle et al. (1974) performed a slope stability analysis using a computer program made by Lefebvre (1968) that adopt both the simplified Bishop and the $\phi = 0$ methods. Using the profile shown in Fig. 3.28., the authors ended up with a factor of safety of 1.2. The slope is

reanalyzed with SLIDE software and a FS of 1.27 is obtained. The results are shown in Fig.3.29

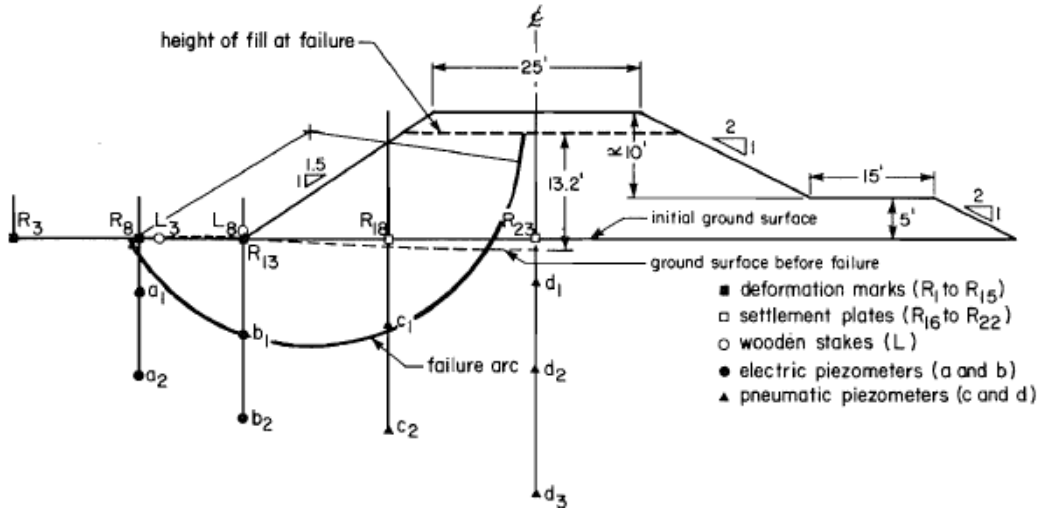


Figure 3. 28 Cross- section of the Saint-Alban embankment (L_A Rochelle et al. 1982)

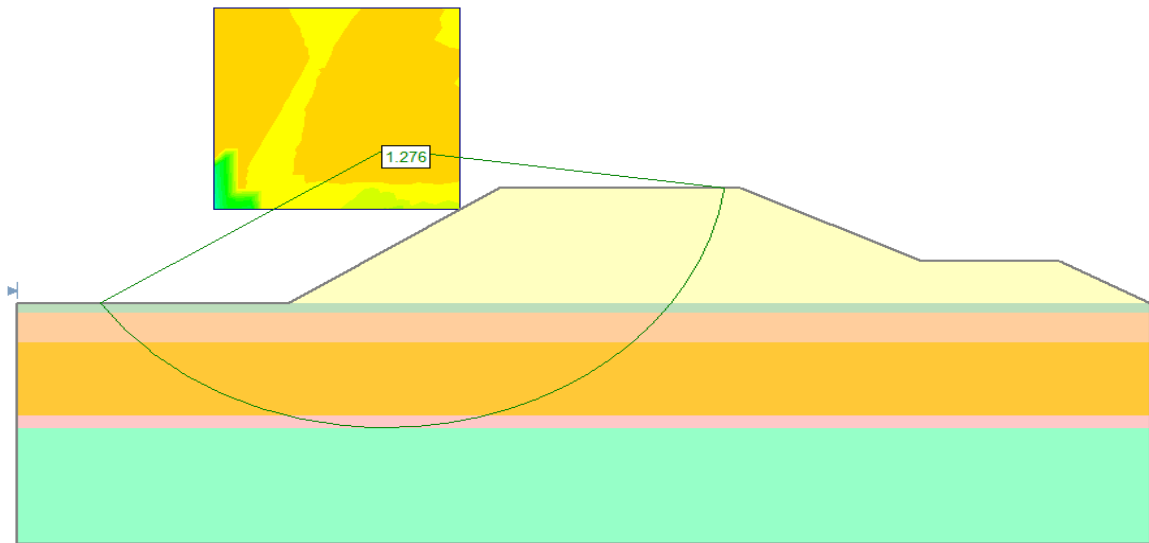


Figure 3. 29 Critical Slip Surface using SLIDE

3.2.10 Slide at Narbonne

The embankment failure took place in 1972 in France. The embankment was built to failure in order to verify the validity of the methods of analysis used in the design of Narbonne motorway. The foundation soil is relatively heterogeneous and is mainly made up of a soft low plasticity clay deposit with 12-14m thickness that rests on a layer of gravel that overlies very sound marls. Fig.3.30. shows the different soil properties of the foundation material.

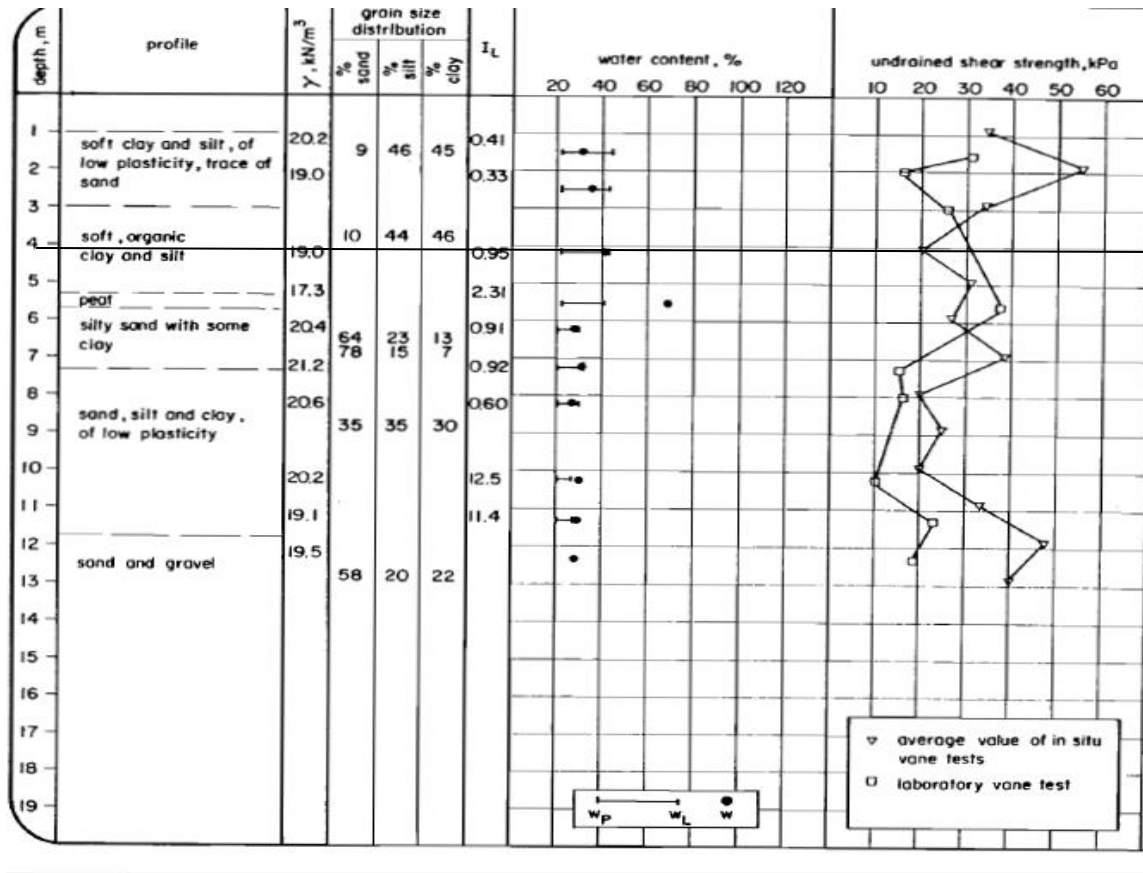


Figure 3. 30 Soil Profile at Narbonne (L_ARochelle et al. 1982)

The embankment was constructed in five days and failure occurred at a height of 9.60m with 37° slope angle. The embankment material is a gravelly and clayey compacted sand with unit weight = 2.07t/m³ and with the strength parameters $c = 53\text{KPa}$ & $\phi = 26^\circ$. When the large movements took place at failure, the embankment practically moved by rotation and a circular shape of the failure was formed. Pilot (1972) conducted a total stress analysis and a factor of safety = 0.83 was obtained using the profile shown in Fig.3.31. and using the computer program developed by the Geotechnical Group of Université Laval, Québec that adopts the simplified Bishop (1955) method for slope stability analysis. The slope is re-analyzed by using SLIDE software for the evaluation of the factor of safety. Fig.3.32. shows the results of the analysis.

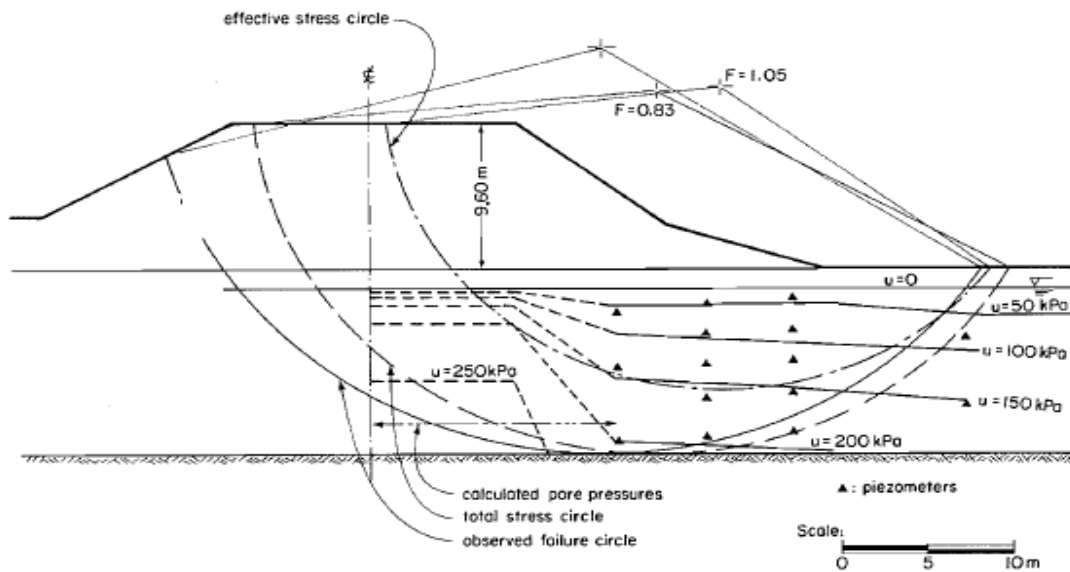


Figure 3. 31 Cross-section of the Narbonne embankment (L_A Rochelle et al. 1982)

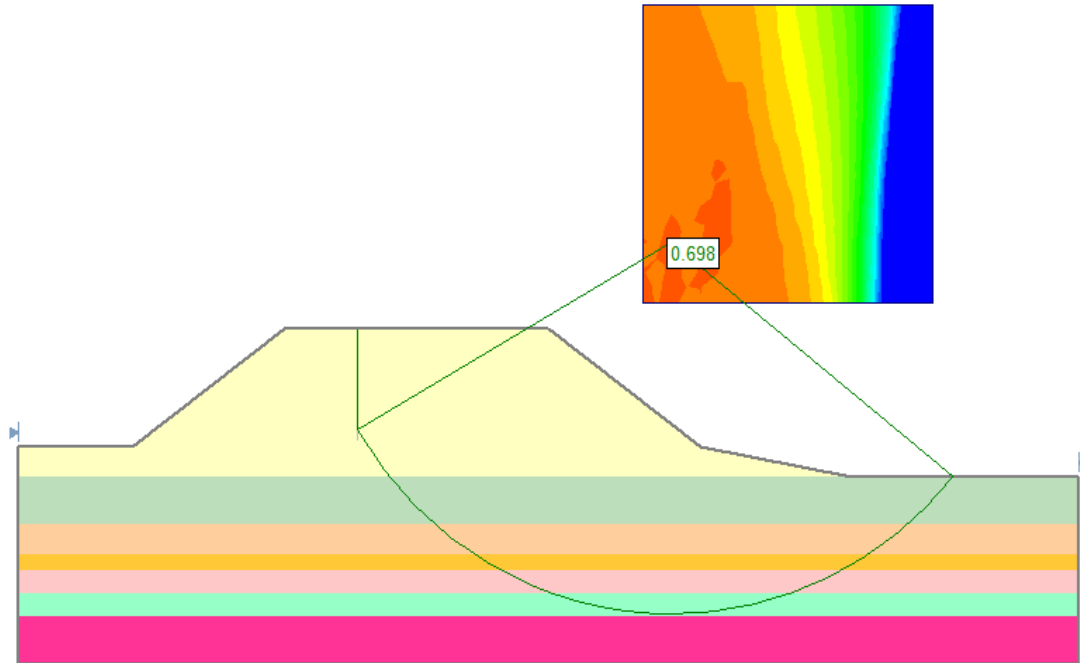


Figure 3. 32 Critical Slip Surface using SLIDE

3.2.11 Slide at Lanester

In 1969 in France, engineers constructed the Lanester embankment to provide them with all the necessary data about the pore pressures generated in the foundations. A compacted sandy clayey gravel embankment with a density of 1.82 t/m^3 and strength parameters ($c = 30 \text{ KPa}$ & $\phi = 31^\circ$) was constructed on foundation soil consisting of a layer of soft, organic sandy clay and silt layer with 8-10m thickness, overlying a layer of gravel over bedrock. Fig.3.33 shows the different soil parameters of the foundation material.

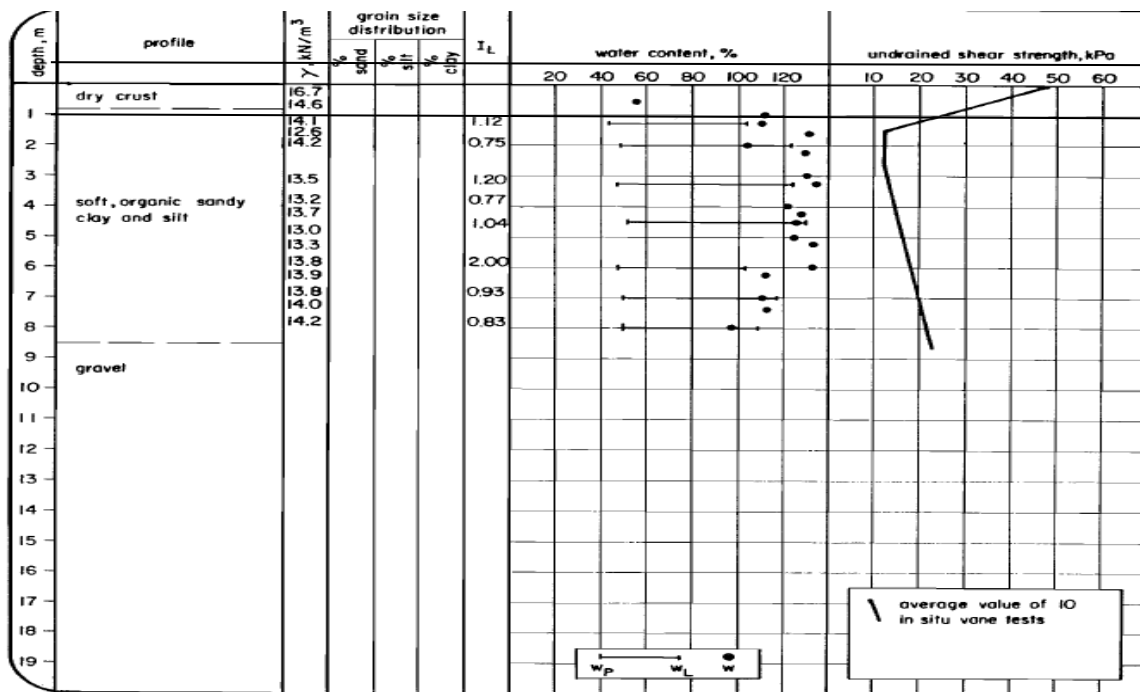


Figure 3. 33. Soil Profile at Lanester (L_A Rochelle et al. 1982)

Before the occurrence of the slide, lateral displacements formed causing the formation of vertical cracks in the embankment. Failure occurred when the embankment reached a 4m height. Fig.3.34 shows a photograph for the embankment failure.



Figure 3. 34 View of the Lanester embankment after Failure(L_A Rochelle et al. 1982)

Pilot (1972) conducted a total stress analysis for the profile shown in Fig.3.35. and a factor of safety of 1.27 was obtained. The factor of safety is reevaluated using SLIDE software and the factor of safety shown in Fig.3.36. was obtained.

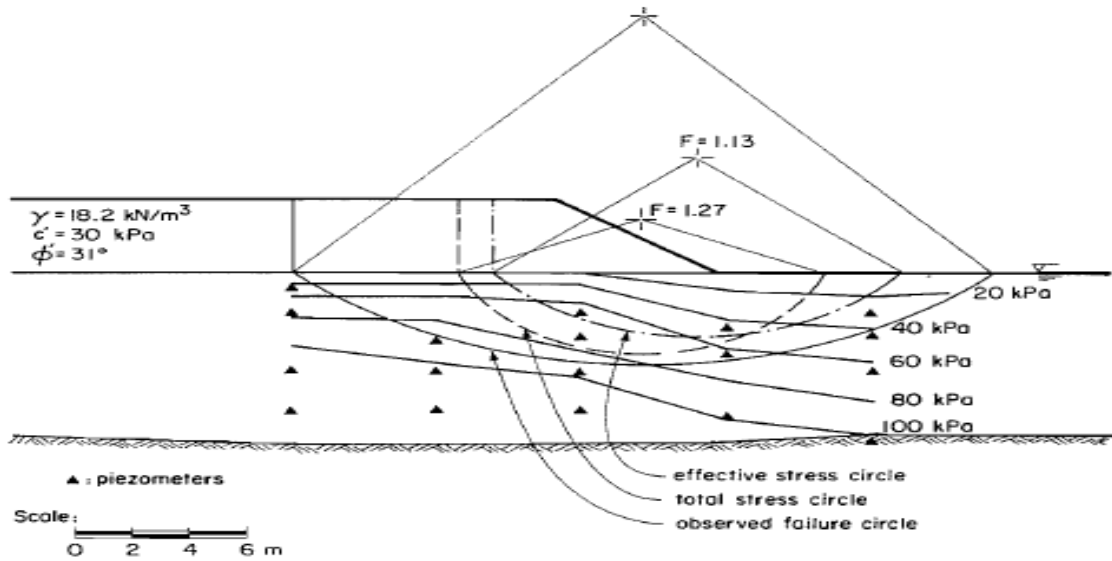


Figure 3. 35 Cross-section of the Lanester embankment ((L_A Rochelle et al. 1982)

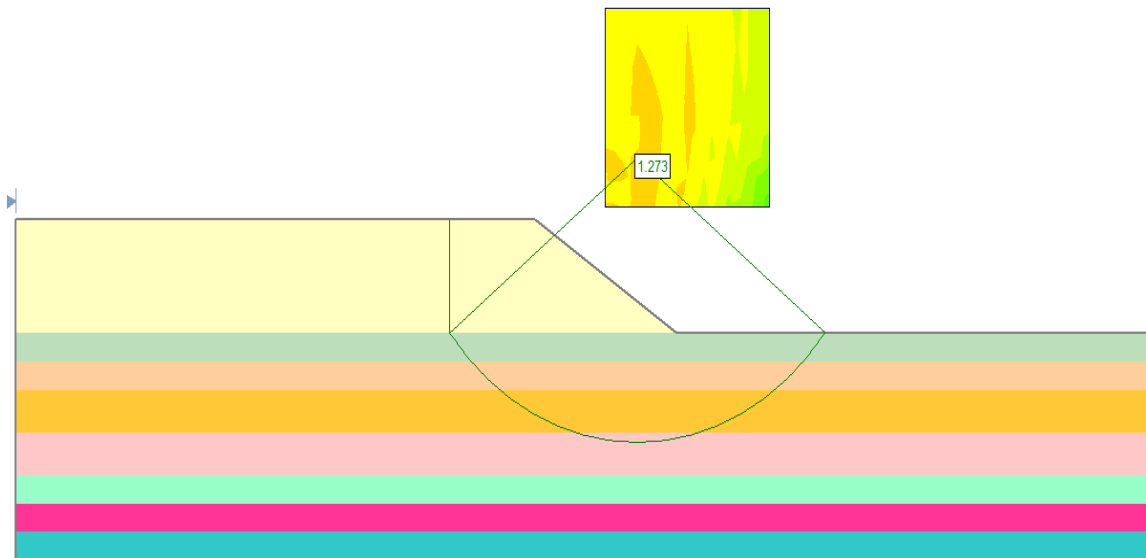


Figure 3. 36 Critical Slip Surface using SLIDE

3.2.12 Slide at Cubzac les-ponts

In 1971 a test embankment failure took place at Cubzac-les-Ponts near Bordeaux in France (Fig.3.37.). The construction of the embankment was part of a research program aimed at settlement evaluation. The embankment was constructed on soft alluvial deposits of 9m thickness. An overconsolidated clayey and silty crust (1m in thickness) overlies a thin layer of strongly organic silty clay of 1m thickness which in turn overlies slightly organic, soft silty clay 6m in thickness (Fig.3.38.). Failure occurred when the embankment reached a height of 4.5m. The embankment fill consisted of clean gravel with unit weight of 2.1t/m^3 and an internal friction angle of 35° . The shape of the slip surface appeared to be circular. Stability analysis was carried out by total stress analysis method using the computer program developed by the Geotechnical Group of Université Laval, Québec that adopts the simplified Bishop (1955) method for slope stability analysis and a factor of safety of $F = 1.44$ was obtained (Fig.3.39). The factor of safety is reevaluated by using SLIDE software as indicated in Fig.3.40.



Figure 3. 37 View of the Cubzac embankment after failure (L_A Rochelle et al. 1982)

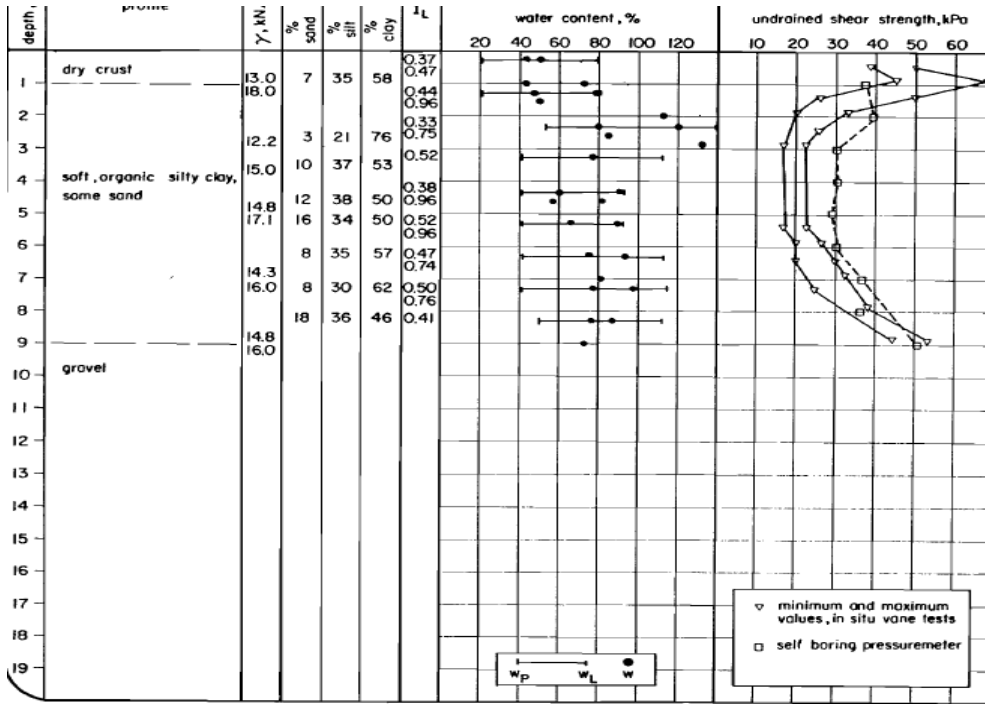


Figure 3.38 Soil Profile at Cubzac-les-Ponts (L_A Rochelle et al. 1982)

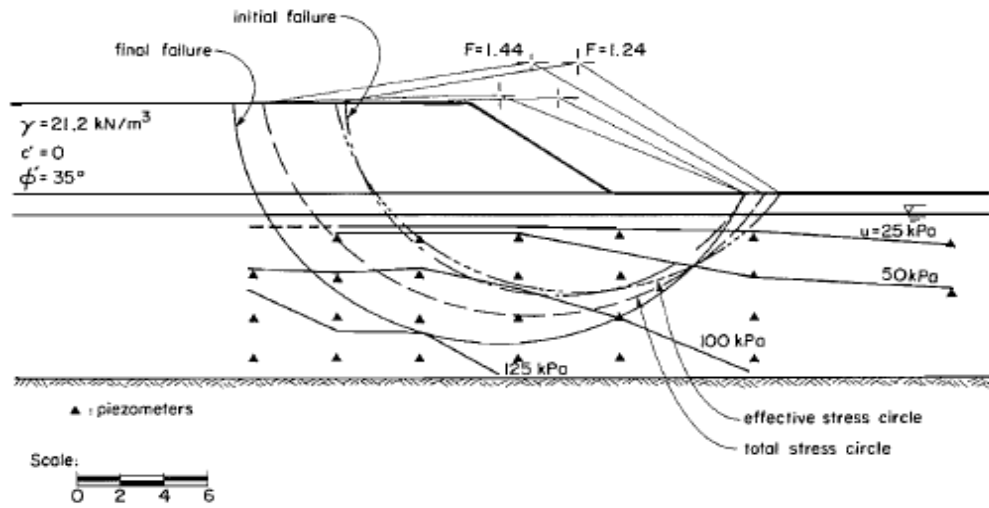


Figure 3.39 Cross-Section of the Cubzac embankment (L_A Rochelle et al. 1982)

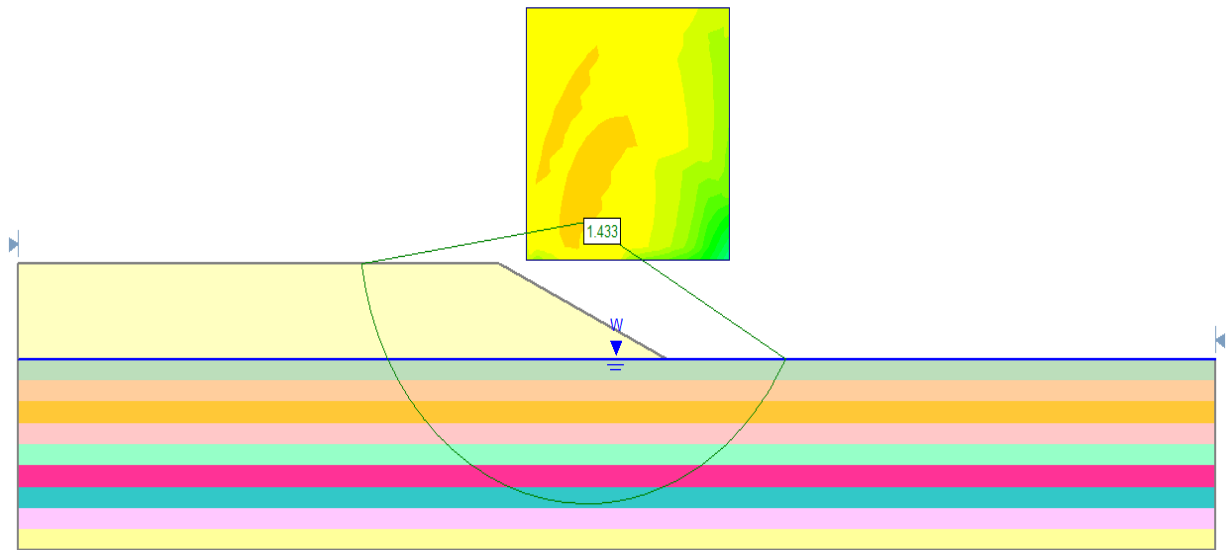


Figure 3. 40 Critical Slip Surface using SLIDE

3.2.13 Slide at Lodalen 1

The slide occurred in Oslo in 1954. The slope was produced by an excavation of a natural slope. The slope originally had an inclination of approximately 1:2.5 and was excavated 5-6m and steepened to an inclination of 1:2. The result of a typical boring in the slide area is shown in Fig.3.41. Underneath the upper layers, the drying crust is found to be a firm comparatively homogenous marine clay with some thin silt layers. The study done by Sevaldson (1956) adopted the so-called $\phi=0$ analysis for the evaluation of the factor of safety. The authors ended up with $F = 0.93$ (Fig.3.42.). Using SLIDE software, the factor of safety obtained = 1.012 (Fig.3.43).

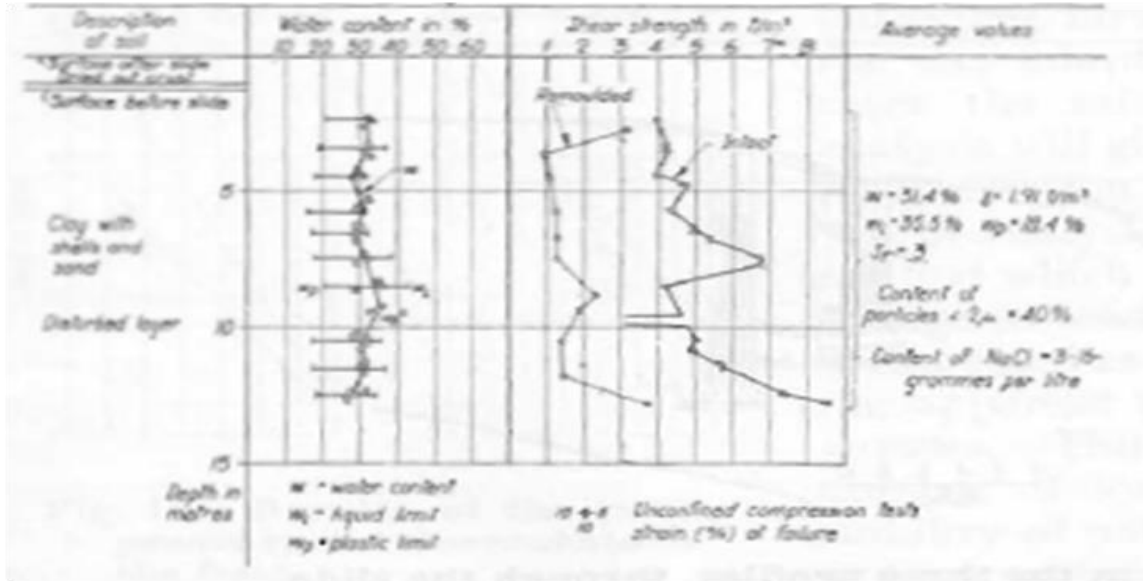


Figure 3. 41 Boring Profile at Lodalen (Sevaldson 1956)

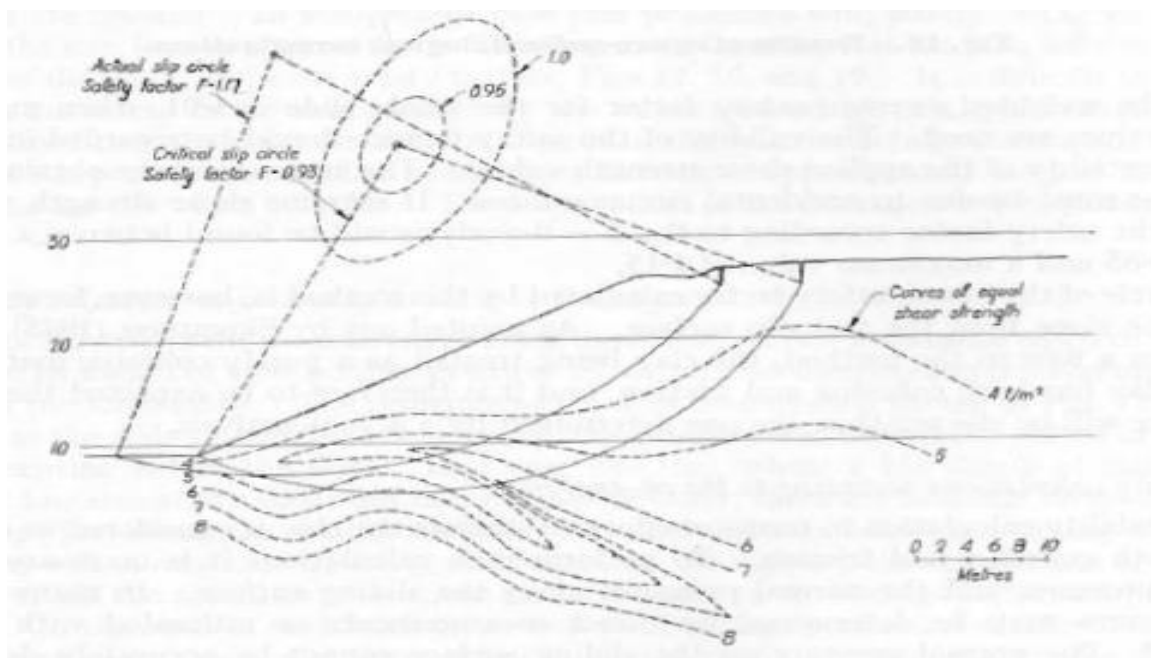


Figure 3. 42 Actual and Critical Slip Surfaces at Lodalen (Sevaldson 1956)

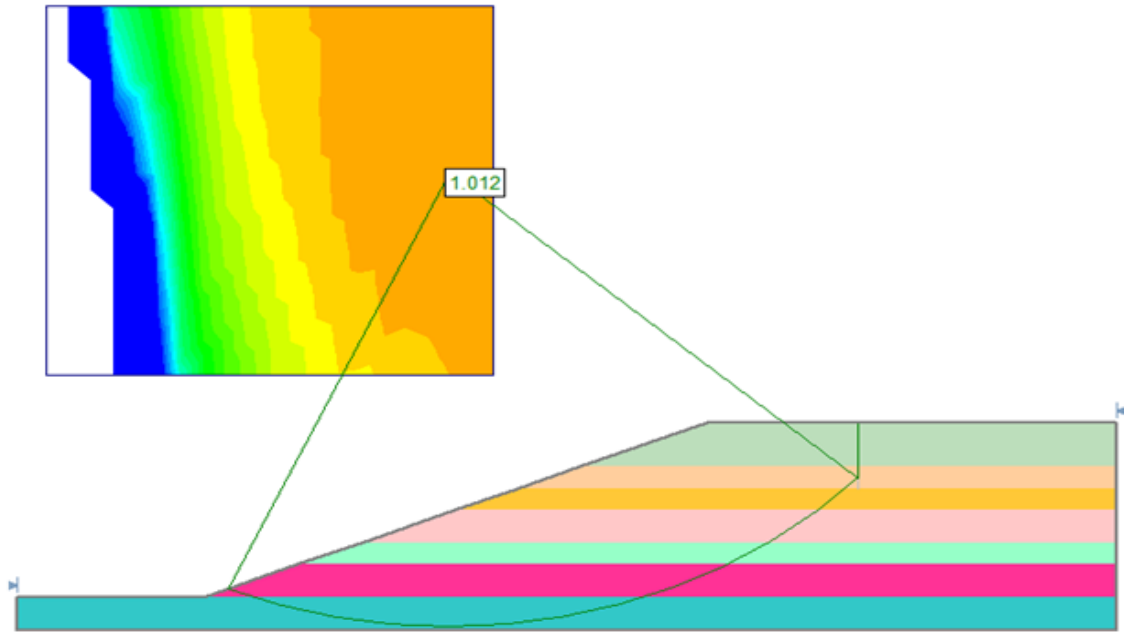


Figure 3. 43 Critical Slip Surface using SLIDE

3.2.14 Slide at Lodalen 2

This slide occurred in another section through the Lodalen site. At this profile, the slide took place when the cutting reached 18.8m. Slope stability analysis was carried out by Sevaldson (1956) using the same soil properties for Lodalen 1. A factor of safety of 0.93 was obtained. The results of the analysis conducted using SLIDE are shown in Fig.3.44.

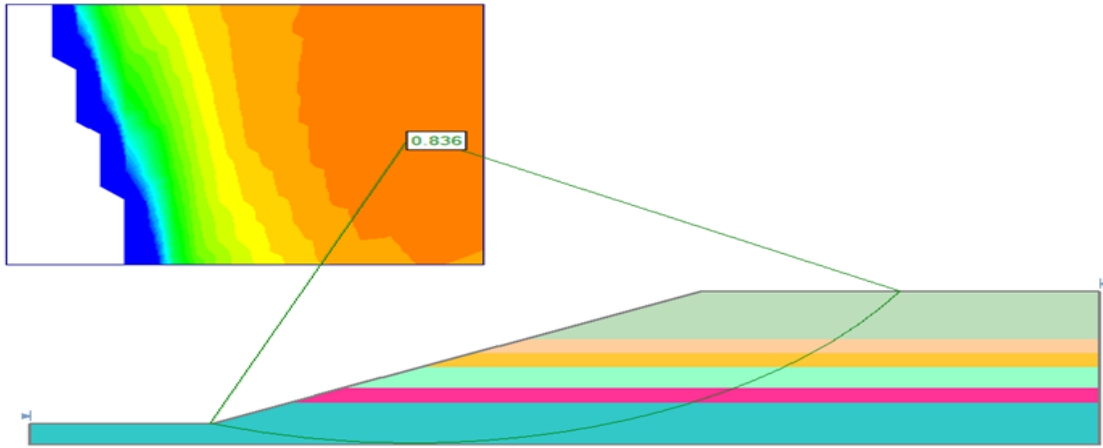


Figure 3. 44 Results of Total Stress Analysis using Slide Software at Lodalen 2

3.2.15 Slide at Lodalen 3

Another section was analyzed through the Lodalen slide. The slide occurred when the cutting reached a 16.3m height. Sevaldson (1956) conducted an analysis for the slide using the $\phi=0$ analysis method and a factor of safety of 1.35 was obtained. In this study, the slide is reanalyzed using SLIDE. The results are shown in Fig.3.45.

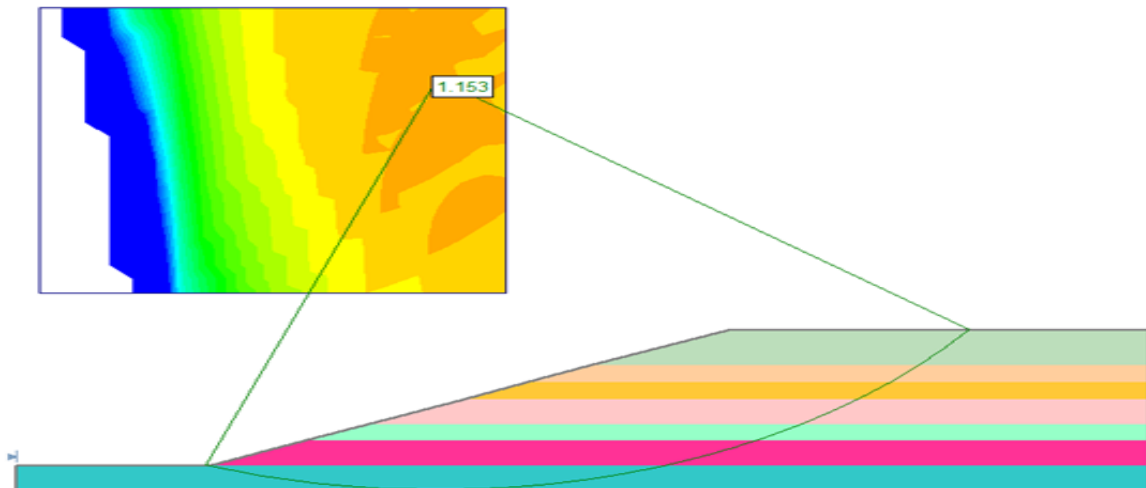


Figure 3. 45 Results of Total Stress Analysis using Slide Software at Lodalen 3

To investigate the behavior of embankments founded on soft soils, the Brazilian Highway Research Institute conducted an extensive research program on an instrumented trial embankment. The testing site consisted of a clay deposit that is 11m thick and that overlies sand and gravel layers. Fig. 3.46. illustrates a summary of the geotechnical properties of the site.

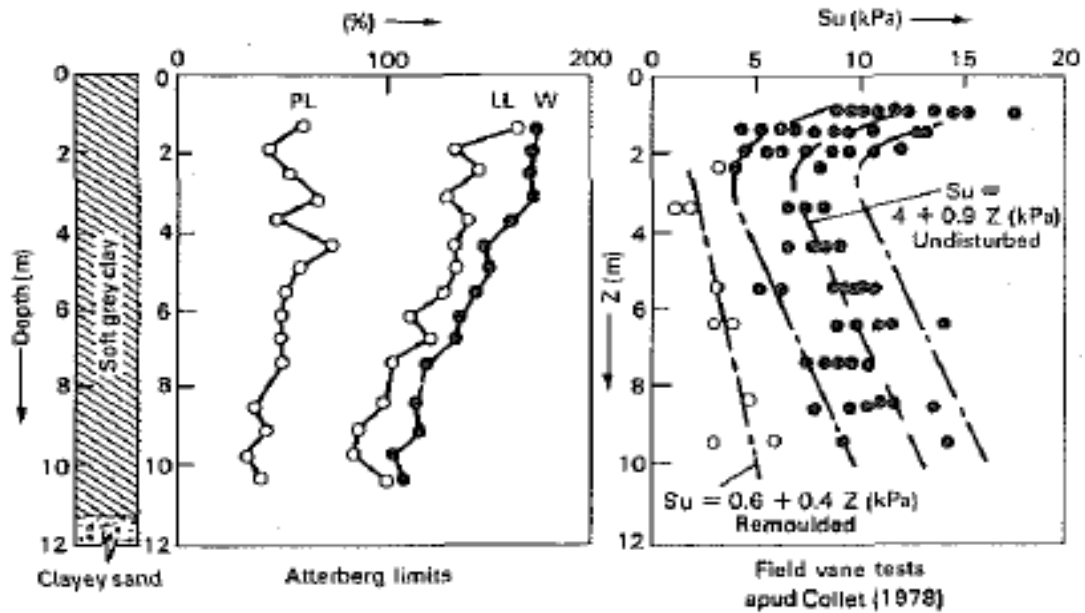


Figure 3. 46 Summary of Geotechnical Properties, Rio de Janeiro Soft Gray Clay (Ramalho-Ortigão et al. 1983)

The trial embankment was constructed with a steeper slope (1v:2h), a stable slope (1v:6h), a base length of 80m, and a base width of 40m. Moreover, two triangular berms were constructed to avoid the possibility of failure occurring outside the instrumented zone. The embankment fill material was a silty-sand residual soil with unit weight of $1.8t/m^3$ and strength parameters ($c = 10-20$ KPa & $\phi = 35^\circ$). The slide occurred when the

embankment height was raised to 2.80 m. Ramalho- Ortigao et al. (1983) conducted a total stress stability analysis employing Bishop's modified circular arc analysis. The analysis was made through a program named BISPO and a factor of safety of 1.11 was obtained (Fig. 3.47.). The slope stability analysis is repeated by using SLIDE and the results are shown in Fig.3.48.

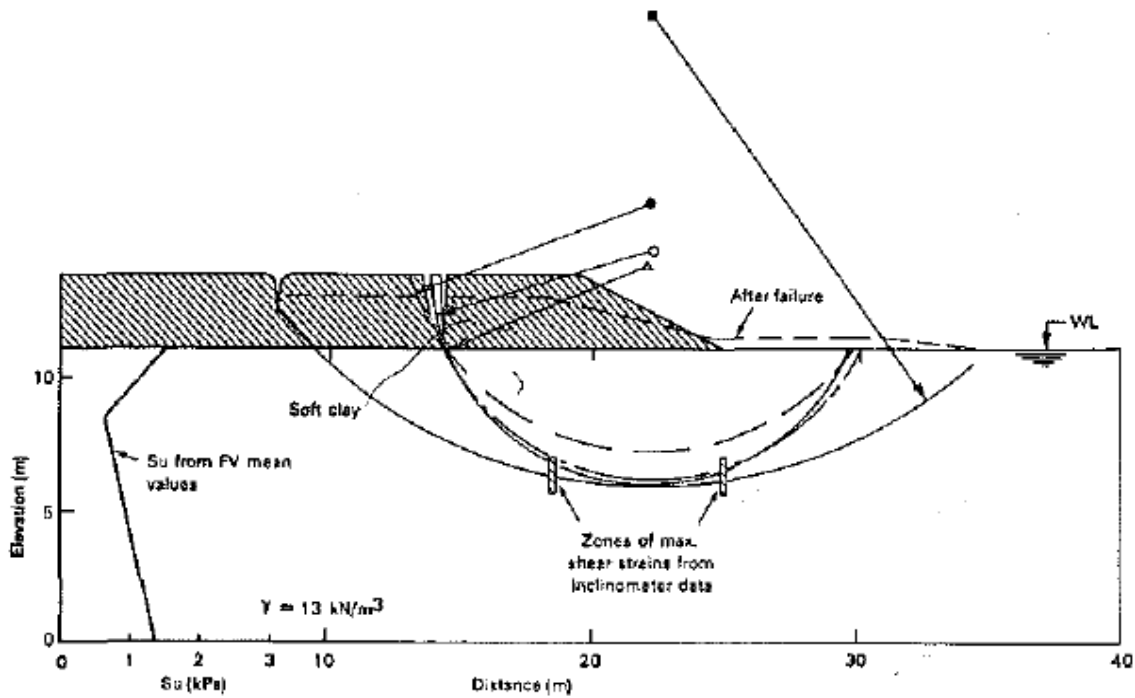


Figure 3. 47 Results of Total Stress Stability Analysis (Ramalho-Ortigão et al. 1983)

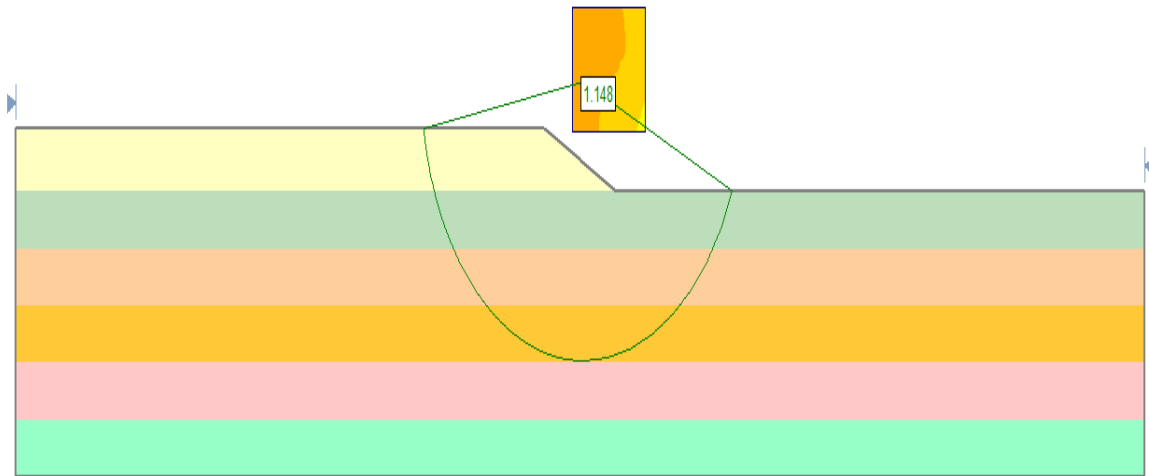


Figure 3. 48 Results of Total Stress Stability Analysis using SLIDE software

3.2.17 Slide at New Liskeard

On June 27, 1963, an embankment failed at New Liskeard in Canada. The embankment rests on 43m of soft to medium varved clay with a 2.7m thick silty clay crust. Fig.3.49. shows the undrained shear strength used in the total stress analyses. The fill material was a gravelly sand with cobbles, boulders and traces of silt and clay with unit weight of 2.04t/m^3 and angle of internal friction of 40° . Failure occurred when the embankment reached 6m. Lacasse et al. (1977) analyzed the stability of New Liskeard embankment using the ICES-LEASE-I computer program (Bailey and Christian 1969) with circular arc failure Fig. 3.50. The analysis resulted in a factor of safety of 1.10. However, using SLIDE software a larger factor of safety is obtained as shown in Fig.3.51.

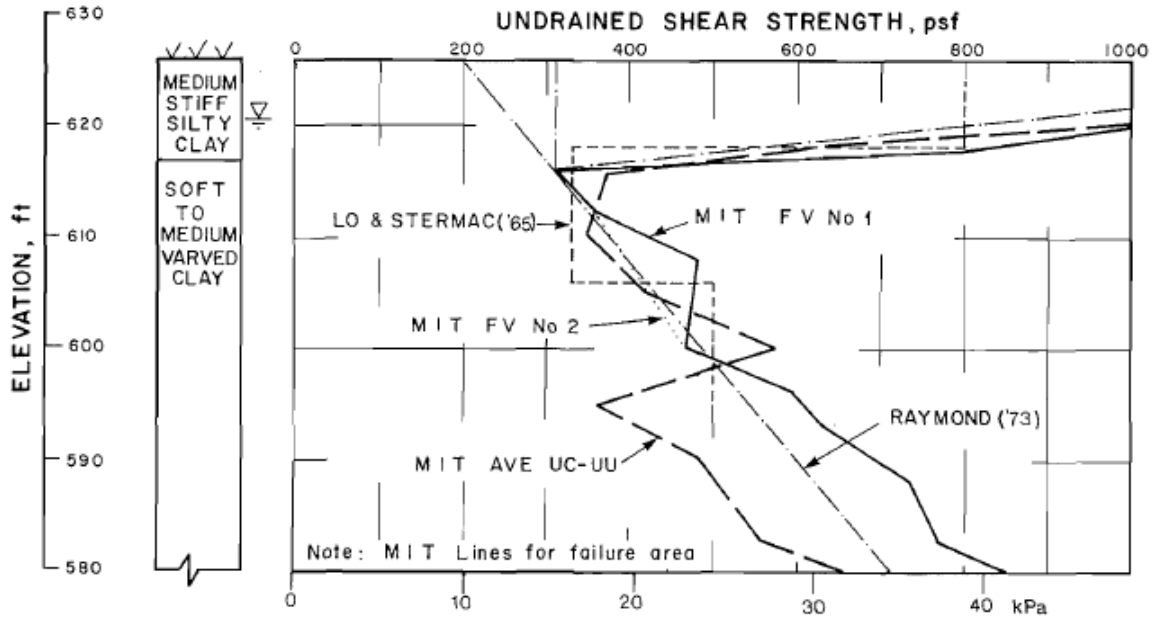


Figure 3.49 Undrained shear strengths used in total stress stability analyses (Lacasse et al. 1977)

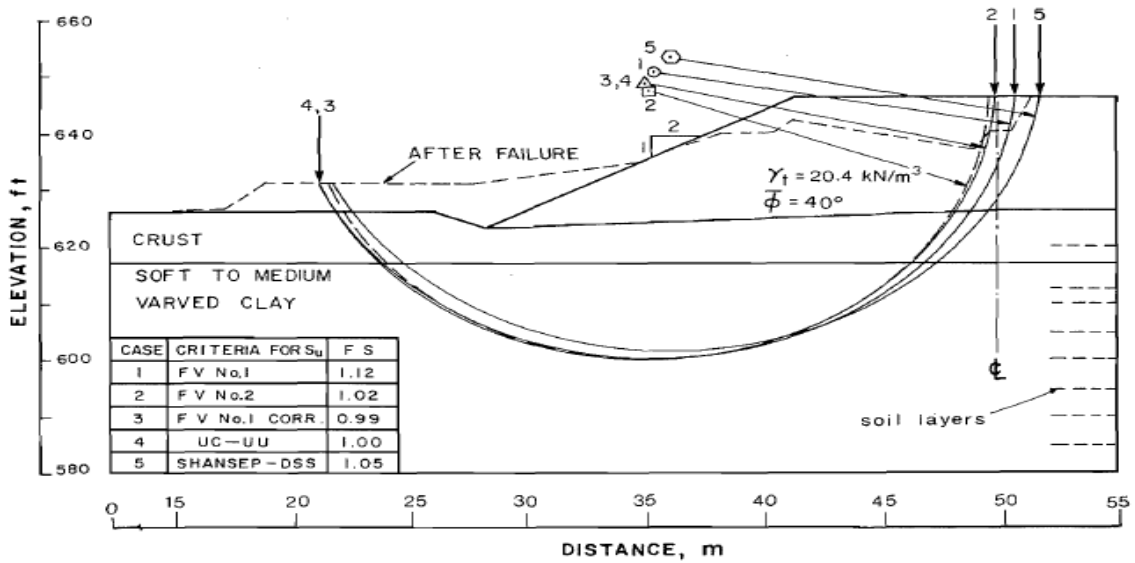


Figure 3.50 LEASE-I critical failure arcs at New Liskeard (Lacasse et al. 1977)

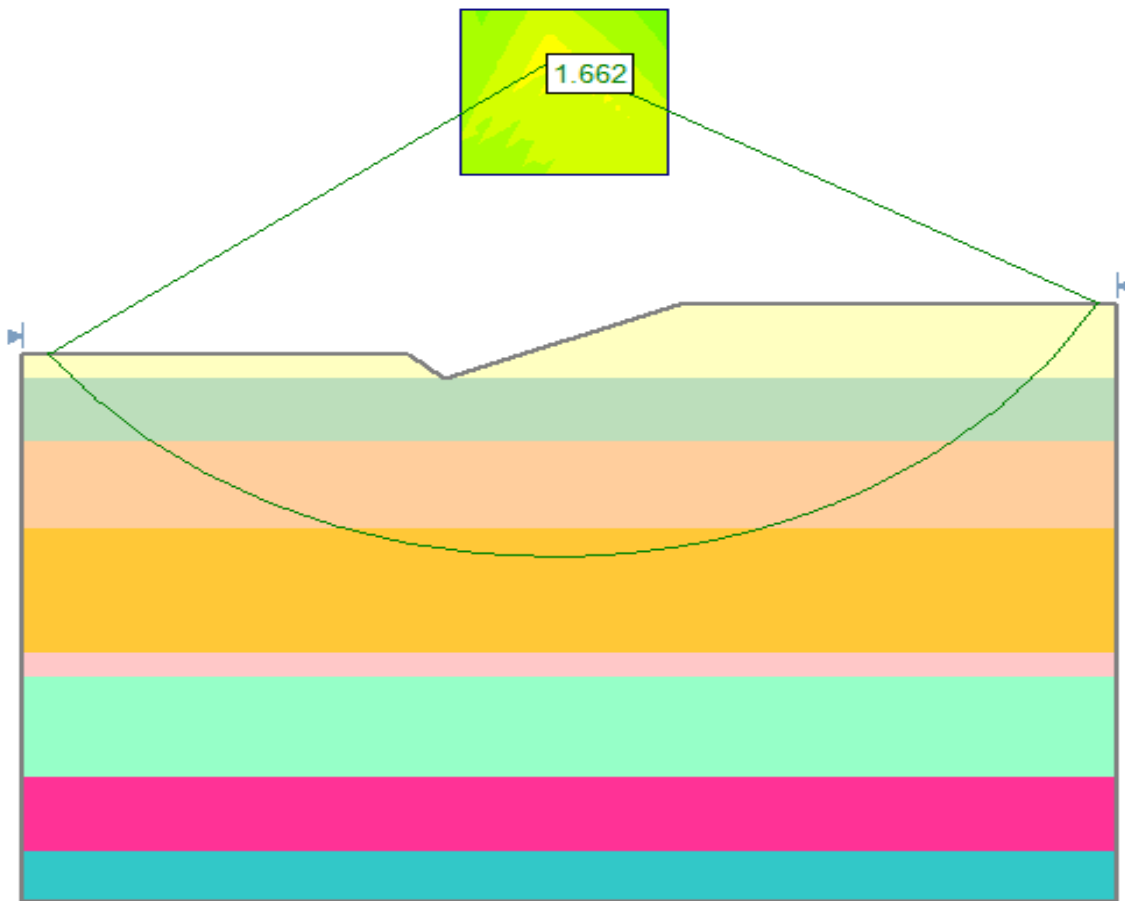


Figure 3. 51 SLIDE critical failure arc at New Liskeard

3.2.18 Slide at Bangkok A

At noon on the 12th of April in 1972, a slide occurred in Bangkok in Thailand. The failure took place several days after the critical fill height of an embankment had been reached. The fill was a test fill constructed to study the bearing capacity of the soft Bangkok clay and to study the efficiency of sand drains. The embankment height at failure was 2m with a 2:1 slope and consisted of uniform sand material except for a 20cm

layer of gravel material placed at a fill height of 1.6m. The fill material was of unit weight of $2t/m^3$ and of internal friction angle of 35° . The fill is placed on foundation soil composed of 1m dry crust. Beneath it, the soft clay extends to a depth of 23m and is underlain by stiff clay. Fig.3.52. shows the geotechnical profile of the site.

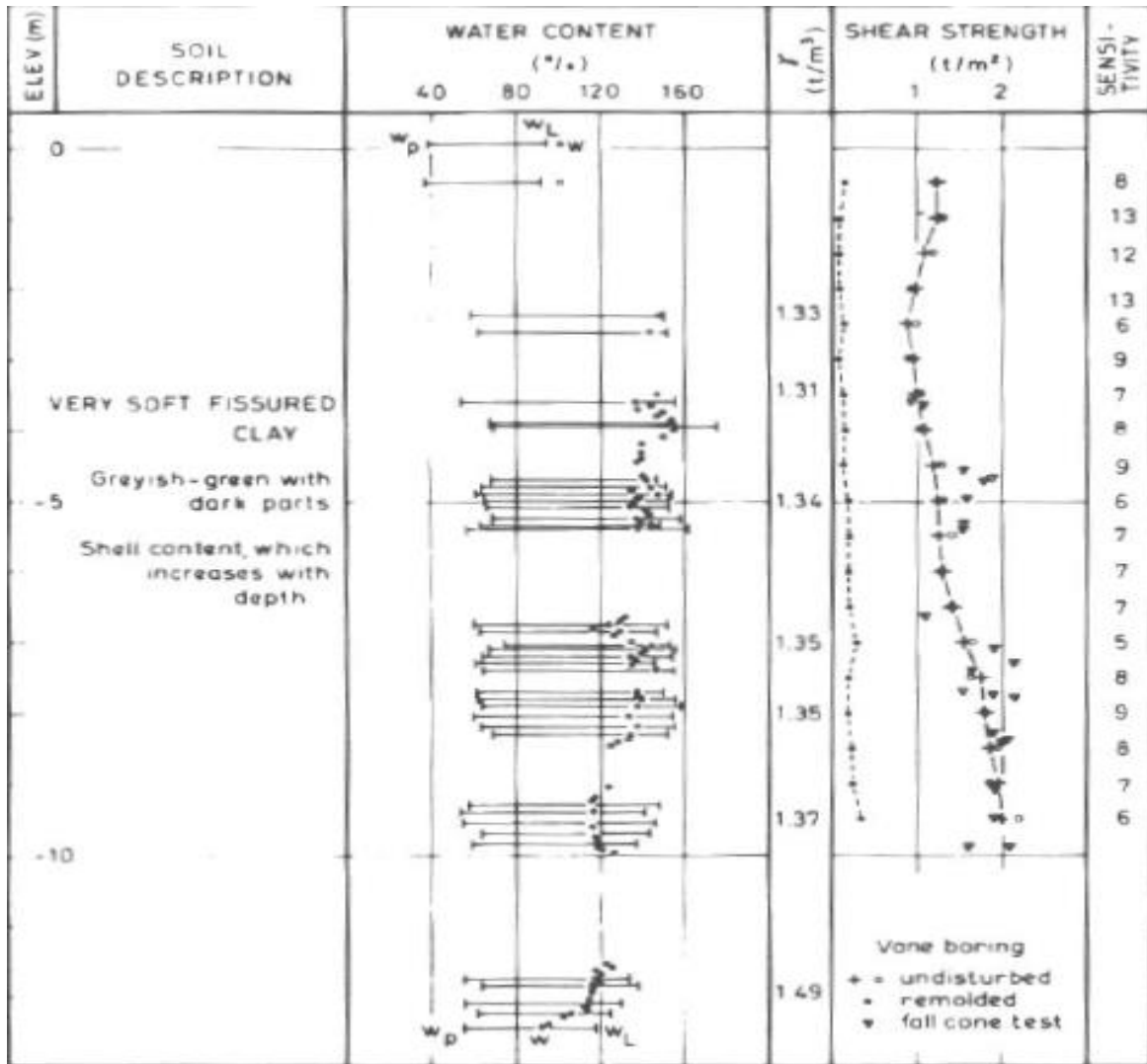


Figure 3.52 Geotechnical Profile at Bangkok Site (Eide and Holmberg 1972)

A stability analysis was conducted by Eide and Holmberg (1972) by adopting undrained total stress analysis. The calculated factor of safety at failure was 1.46 (Fig.3.53). The slope is reanalyzed using SLIDE software and the results are shown in Fig.3.54.

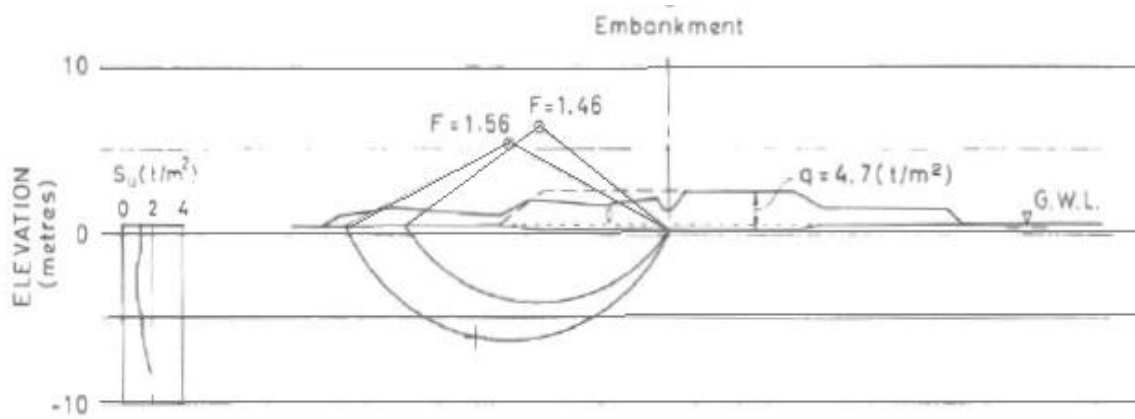


Figure 3. 53. Critical Slip Surface (Eide and Holmberg 1972)

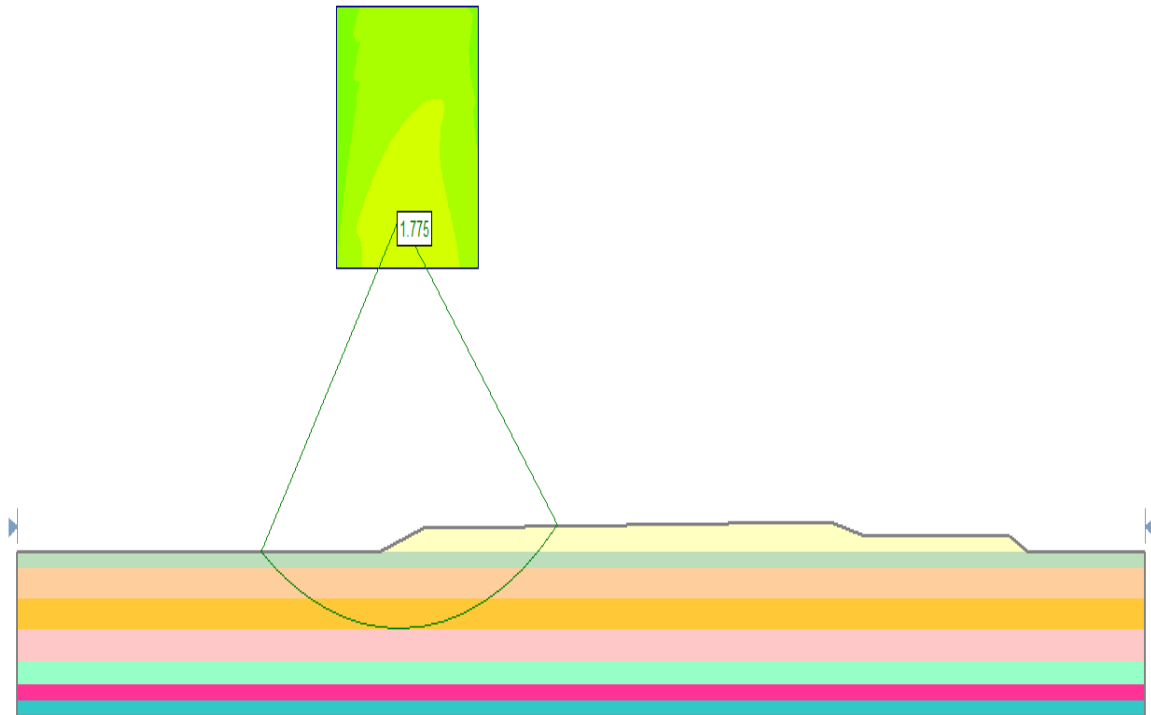


Figure 3. 54 Critical Slip Surface using SLIDE software

3.2.19 Slide at Drammen V

On January 6, 1955, a slide occurred along the river in Drammen, a town 40 km west of Oslo in Norway. The slide took place in a natural slope made up of normally consolidated clay to a great depth. The Norwegian Geotechnical Institute investigated the slide by adopting $\phi = 0$ analysis for the evaluation of the factor of safety. The stability analysis was made in the ordinary way, assuming circular sliding surface and using the soil properties shown in Fig.3.55. Kjærnsli and Simons (1962) reported the analysis and a factor of safety of 0.74 was obtained (Fig.3.56). The same analysis is carried out by using SLIDE software and the results are shown in Fig.3.57.

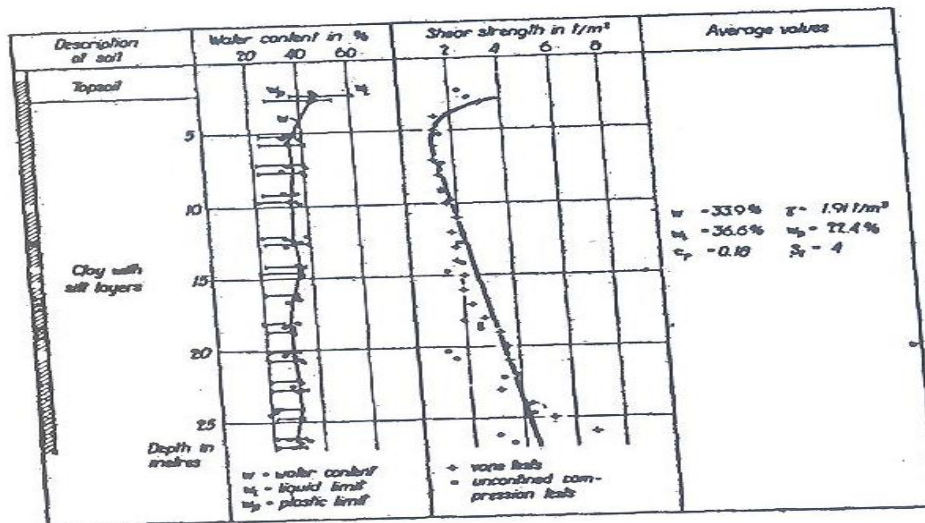


Figure 3. 55. Soil Properties at Drammen (Kjærnsli and Simons (1962))

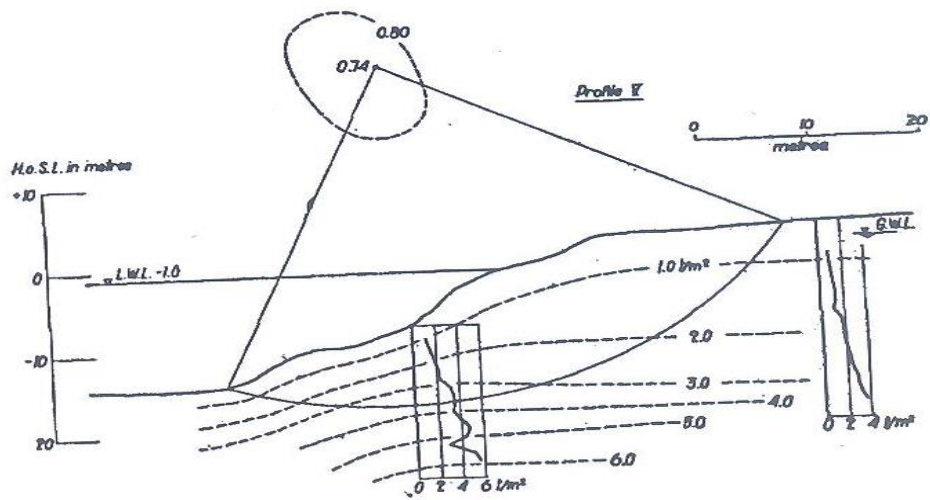


Figure 3. 56 Critical Slip Surface (Kjærnsli and Simons 1962)

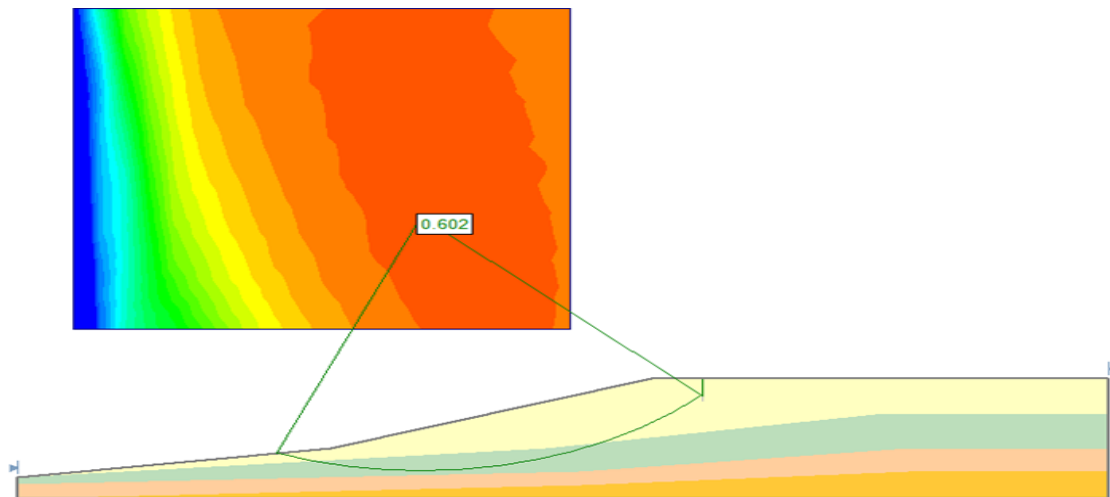


Figure 3. 57 Critical Slip Surface using SLIDE

(Kjærnsli and Simons 1962) conducted a total stress analysis for the center profile of the slide described above for Drammen V. Using the soil properties shown above in Fig.3.55. the authors ended up with a factor of safety of 0.59. Total stress analysis is carried out using SLIDE. The results are shown in Fig.3.58.

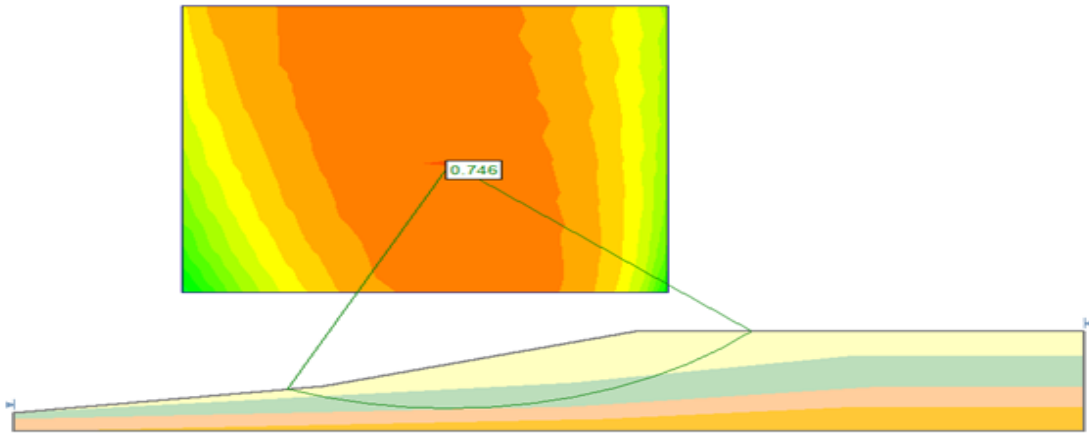


Figure 3. 58 Critical Slip Surface using SLIDE software at Drammen VI

3.2.21 Slide at Drammen VII

In addition to the analysis carried out for the downstream and the center of the slide profiles, Kjærnsli and Simons (1962) carried out a total stress analysis for the upstream profile from the slide. A factor of safety of 0.70 was obtained. However, the analysis using SLIDE ended up with a factor of safety of 0.87 as shown in Fig.3.59.

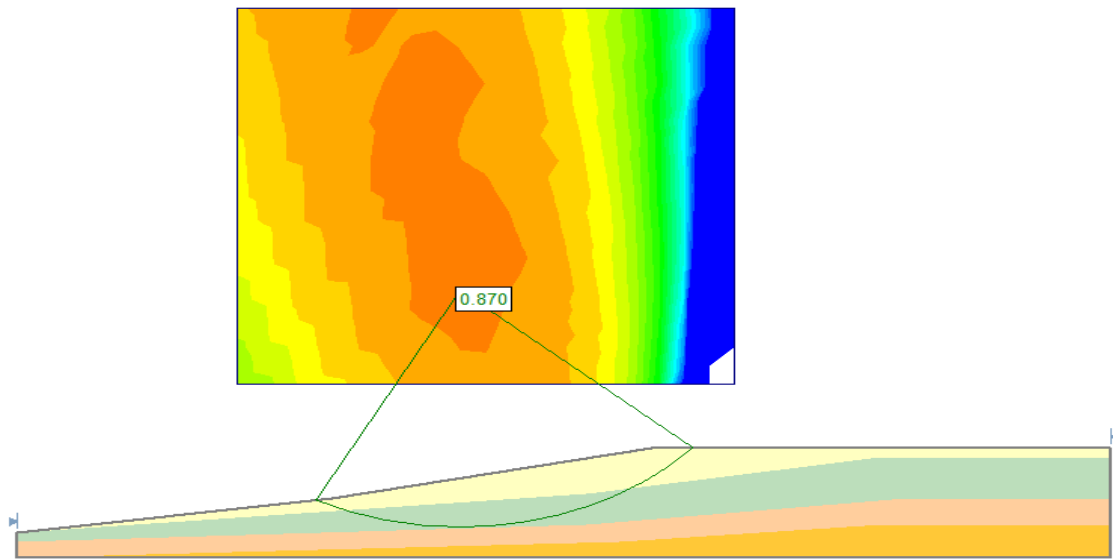


Figure 3. 59 Critical Slip Surface using SLIDE software at Drammen VII

3.2.22 Slide at Pornic

In 1963, an embankment failure took place at Pornic in France. The embankment was built by the highway and motorway construction in France. The embankment height required was about 8 meters needed to construct a highway by-pass to cross a valley over about 250m; however, failure occurred when the critical height of the embankment was 4m. This happened four months after the beginning of its construction. Stability analysis was adopted with the embankment characteristics: unit weight of 2 t/m^3 , $c = 1 \text{ t/m}^2$, $\phi = 40^\circ$. The embankment placed on a deposit of normally consolidated clay, except for a dessicated crust of 2m overconsolidated clay. Pilot (1972) conducted stability analyses under total stress analysis by the Bishop calculation method (circular failure) and a factor

of safety of 1.17 was obtained using the profile and soil properties shown in Fig.3.60.

Analysis using SLIDE software is presented in Fig.3.61.

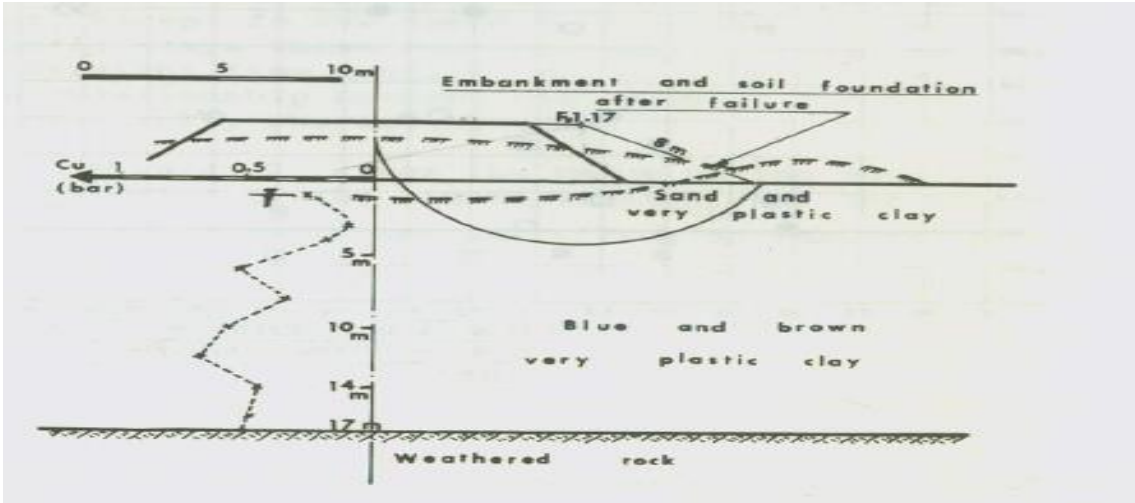


Figure 3. 60 Embankment Failure at Pornic (Pilot 1972)

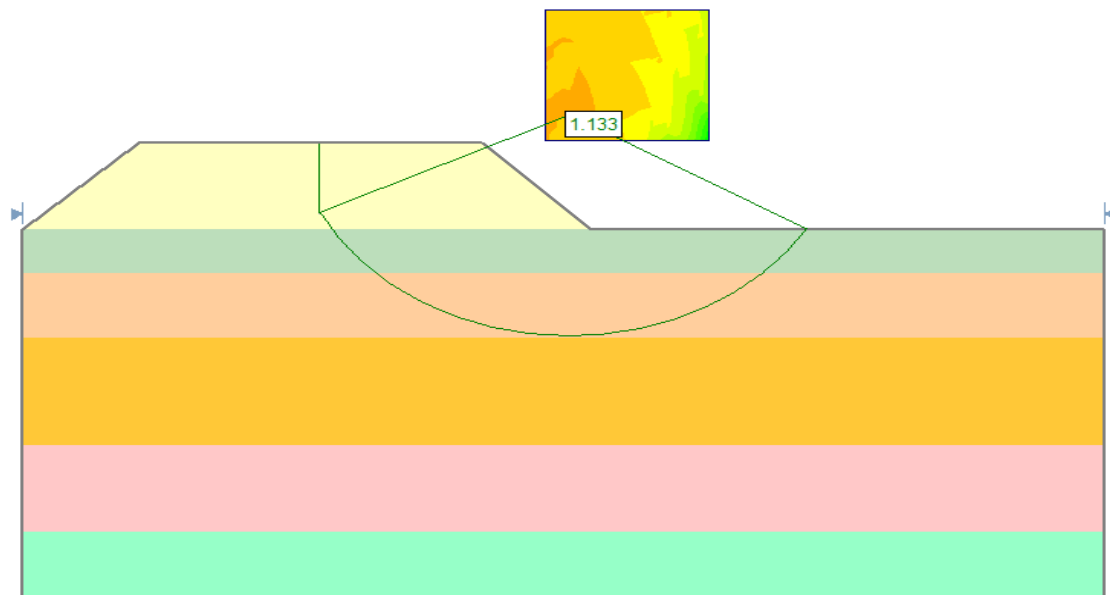


Figure 3. 61 Embankment Failure at Pornic using SLIDE

3.2.23 Slide at Saint-Andre

The slide occurred in 1969 at Saint-Andre (Gironde) in France. Failure happened at the last stage construction of the embankment. The failure started with a sinking of about 40cm, then a rotational movement appeared resulting in another sinking of the platform. Failure occurred when the embankment reached 3m height. Stability analysis was performed after failure, taking into account the exact geometry of the embankment at the instant of sliding as shown in Fig.3.62. and using the geotechnical soil properties shown in Table 3.3. A factor of safety of $F=1.38$ was obtained (Pilot 1972). Using SLIDE, the slope is reanalyzed and the results obtained are shown in Fig.3.63.

Table 3.3 Main soil characteristics of soils at Saint-Andre in France (Pilot 1972)

Depth	γ_d t/m ³	W %	W _L	IP	Type of soil
0 to 1 m	1.15	49	83	37	Organic clay
1 to 3 m	0.27	300	-	-	Very peaty clay
3 to 3.50 m	0.15	600	-	-	Peat
3.50 to 8.50 m	0.70	110	102	47	Organic mud
Below 8.50 m	-	-	-	-	Sand and gravel

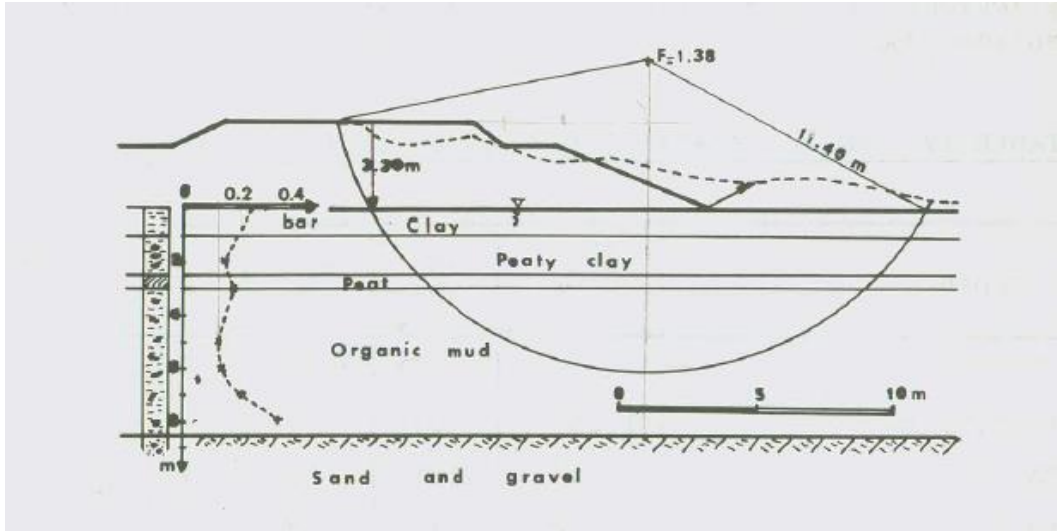


Figure 3. 61 Embankment Failure at Saint-Andre (Pilot 1972)

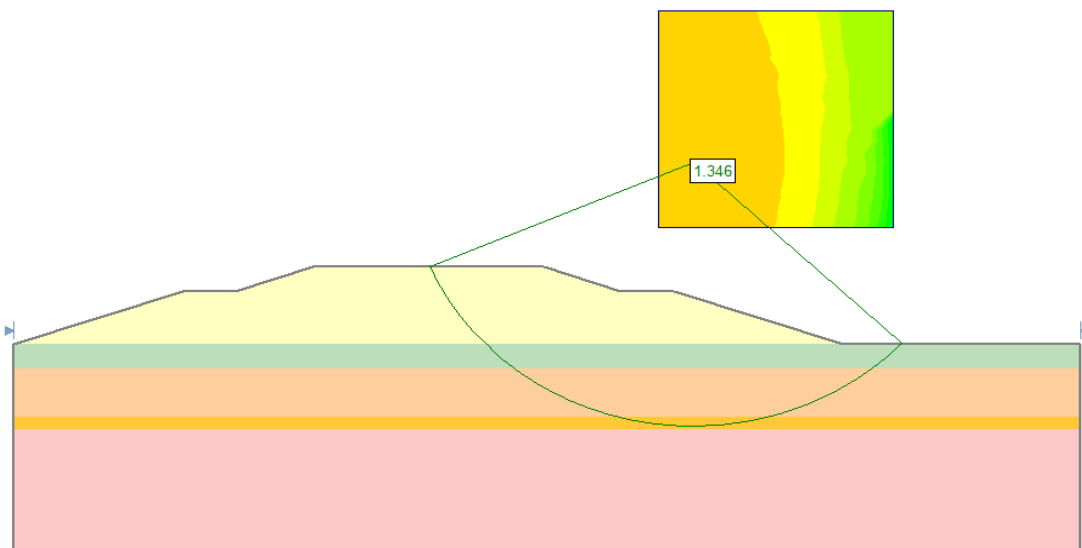


Figure 3. 62 Embankment Failure at Saint-Andre using SLIDE

3.2.24 Slide at South of France

In 1971 during the construction of an embankment on an approach to a bridge in South of France, a rapid failure occurred in this embankment. The embankment consisted of slightly muddy loose sand with unit weight of 1.7t/m^3 and angle of friction of 35° that is laid on a 2m-thick river deposit of more or less muddy sands, overlying a 25m thick layer of lagoonal marine deposits consisting of slightly underconsolidated muddy shelly clay. Stability analysis was carried out under total stress analysis by the Bishop calculation method (circular failure) and a factor of safety of 1.30 was obtained using the profile and soil properties shown in Fig.3.64. The embankment was re-analyzed using the SLIDE software and the results are shown in Fig.65.

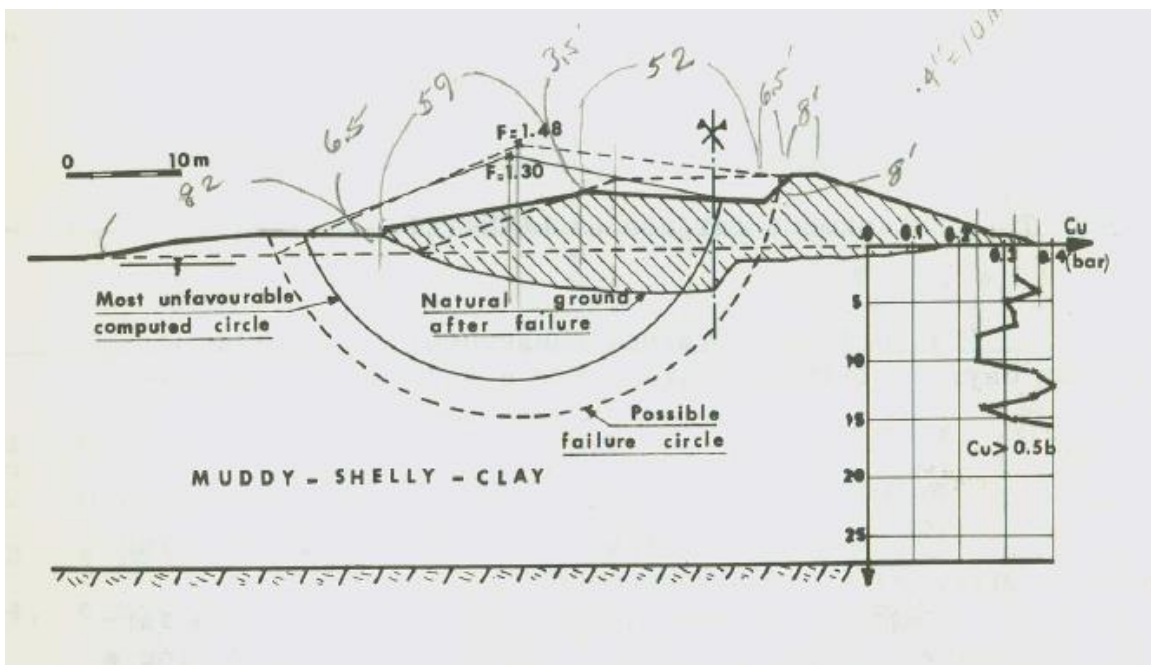


Figure 3. 63 Embankment Failure at South of France (Pilot 1972)

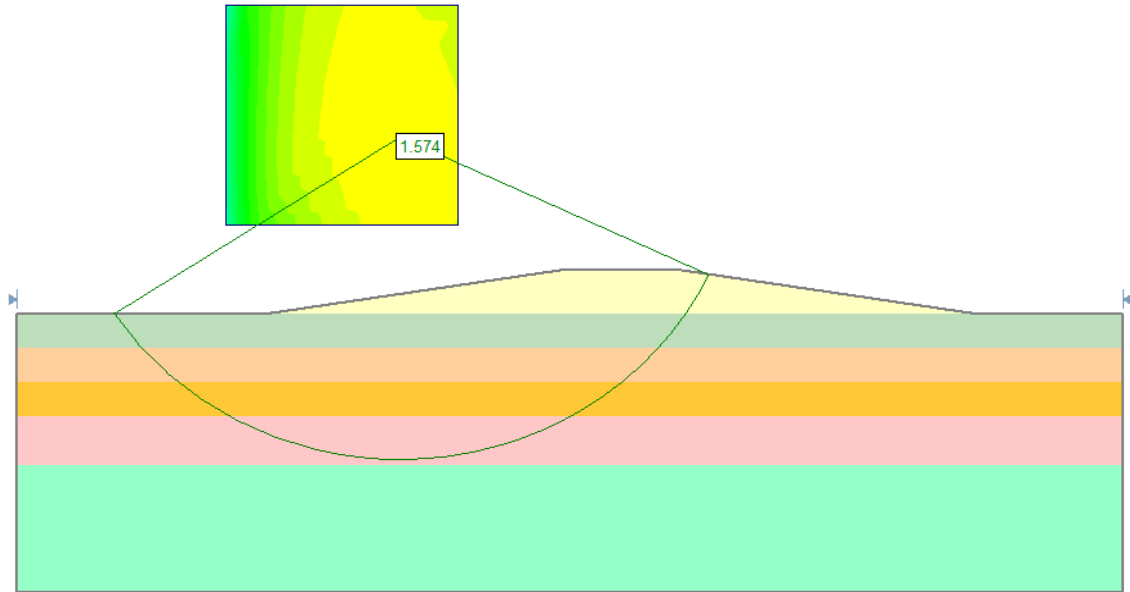


Figure 3. 64 Critical Slip Surface at South of France using SLIDE

3.2.25 Slide at NBR Development

On Friday morning, September 17th, 1971, a failure occurred on a dyke in Canada. The dyke was erected as a part of the James Bay water resources exploitation project. The dyke's dimensions were selected in order to induce failure in a selected direction and at the same time to involve a large enough soil mass so that the failure could be considered representative.

Transverse cross section:

- West slope: 1:5
- East slope: 1:4 for the first 15 ft height and 1:2 above 15 ft

Longitudinal cross- section: north and south slope:

- 1:8 for the first 15 ft height and 1:4 above 15 ft

The dyke which is composed of a medium compacted wet granular material with a unit weight of 130 pcf and an angle of internal friction of 35° was constructed on a 6 ft thick layer of organic material underlain by 50 ft clay deposit. The top 8 ft of the clay deposit is weathered (Fig.3.66). The stability analysis was carried out in terms of a total stress analysis using the MIT ICES-LEASE computer program (Bishop's simplified method) and using the soil properties shown above for the profile shown in Fig.3.67. Dascal et al. (1972) reported the factor of safety of 1.3.

The dyke is reanalyzed using SLIDE software and the results are shown in Fig.3.68.

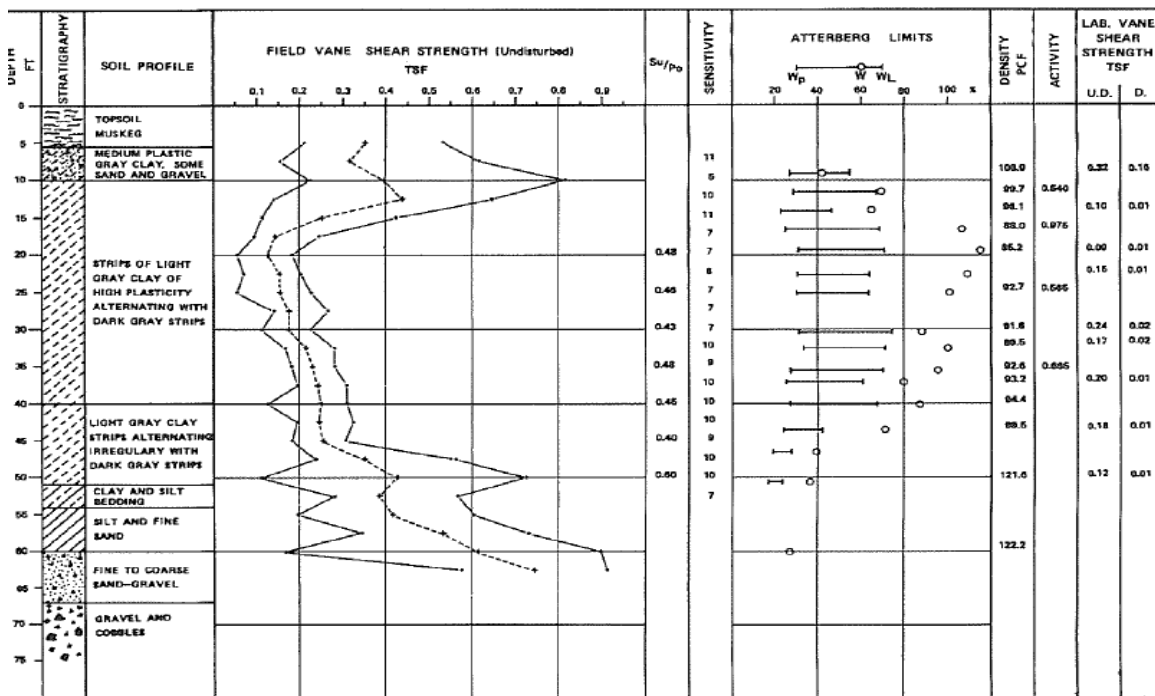


Figure 3. 65 Stratigraphy and Geotechnical Characteristics of the foundation Soil at NBR Development (Dascal et al. 1972)

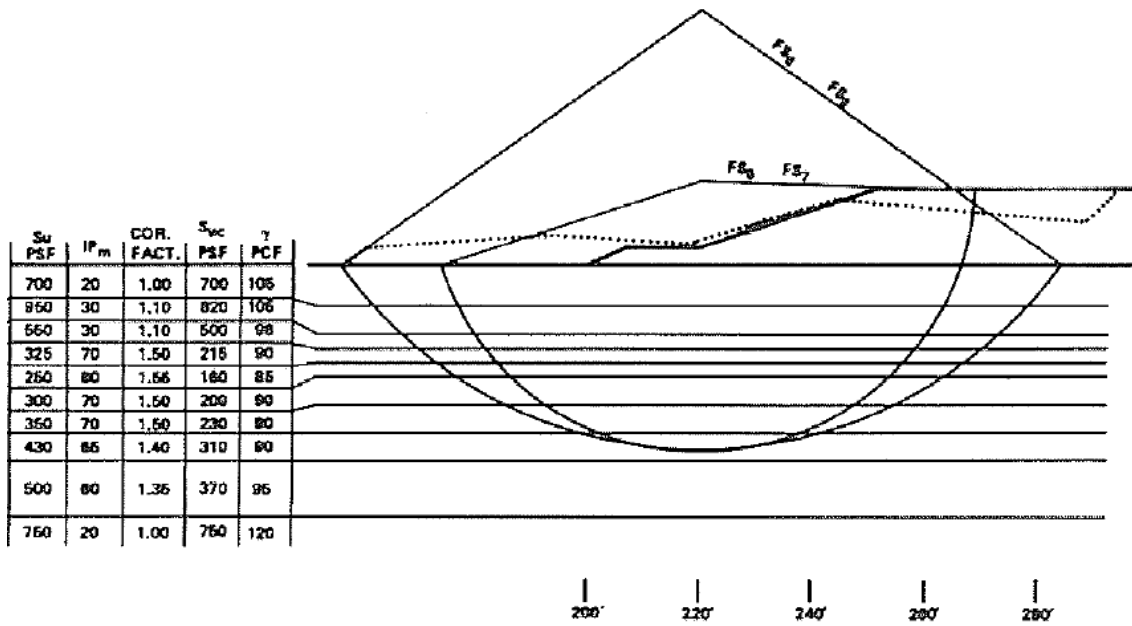


Figure 3.66 Results of the total stress stability analysis at NBR Development in France (Dascal et al. 1972)

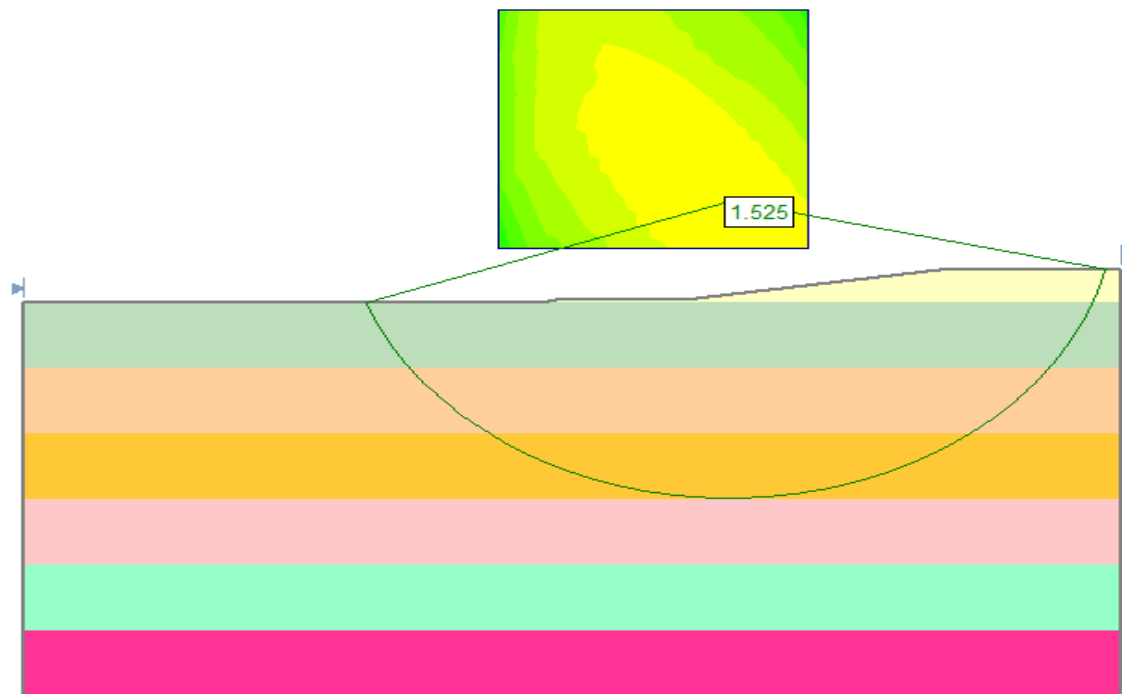


Figure 3.67 Critical Slip Surface using SLIDE

3.2.26 Slide at Portsmouth

In the spring of 1968, a test embankment was purposely constructed to failure in order to better define the in situ behavior of the foundation clay. The experimental test embankment was constructed on a weathered drying crust of several feet underlain by grey silty clay. Beneath this layer, a non-plastic sand silt layer that overlain a soft clay soil layer. Soil properties are shown in Fig.3.69. The fill used to construct the test embankment consisted of fairly clean and well graded sand with an average unit weight of 115.5 pcf and with an angle of internal friction of 41° . Failure occurred when the embankment reached a height of 21.50 ft. Total stress stability analysis of the failure was performed by Ladd (1972) using ICES LEASE1 program using the simplified Bishop and the normal Fellenius method of slices. The factor of safety from this analysis is 0.84 (Fig.3.70). The factor of safety is recalculated using SLIDE and a value of 0.843 is obtained as shown in Fig.3.71.

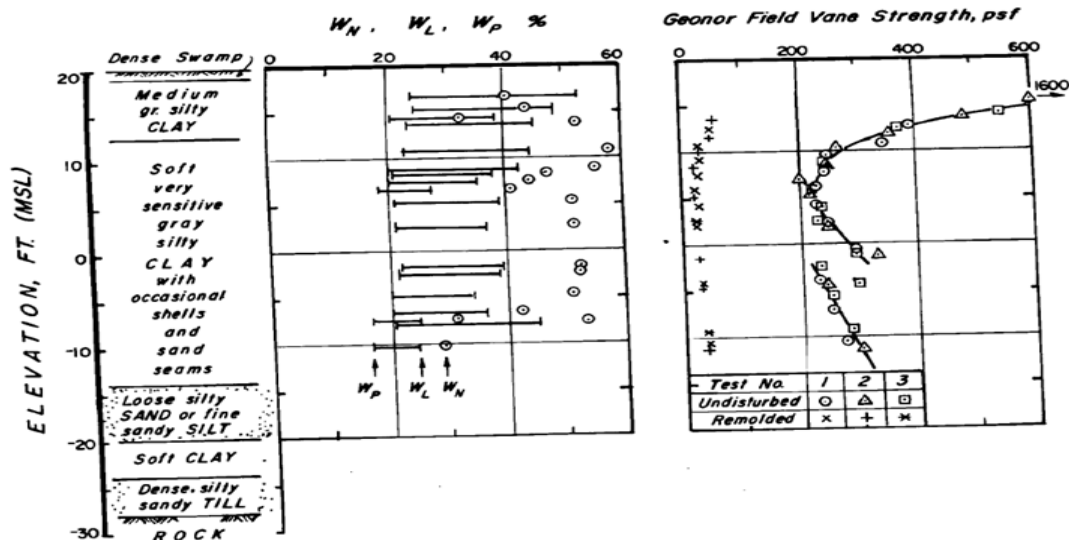


Figure 3. 68 Soil Profile, Index Properties and Field Vane Strengths at Portsmouth in USA (Ladd 1972)

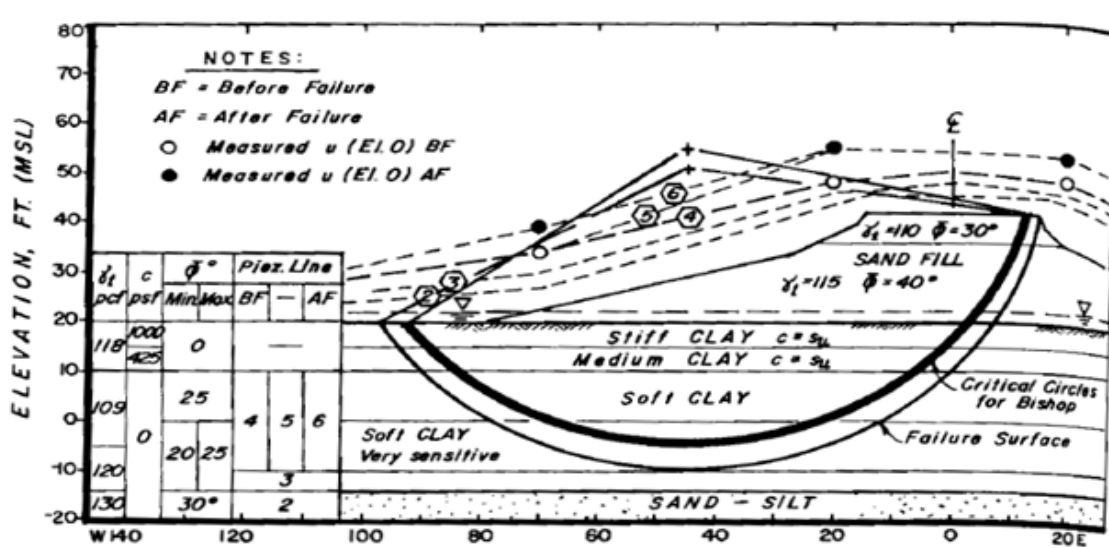


Figure 3. 69 Results of Total Stress Analysis (Ladd 1972)

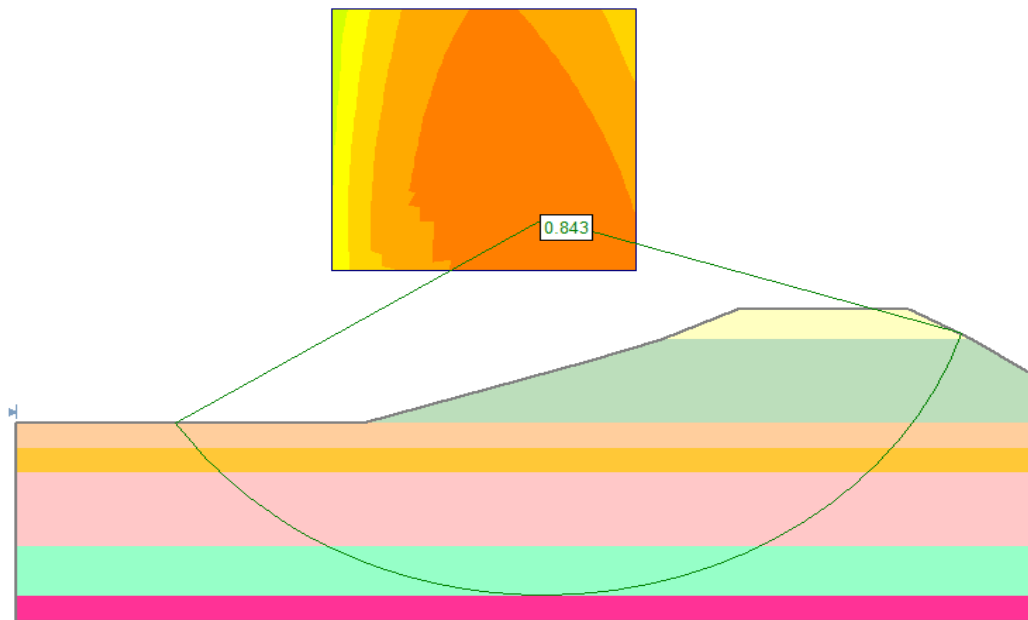


Figure 3. 70 Critical Slip Surface using SLIDE

3.2.27 Slide at Kameda

An expressway embankment was constructed on peaty subsoil to investigate the application of direct shear and cone penetration tests to soil investigation. The construction site was the Kameda Interchange for the Hokuriku Expressway in Niigata Prefecture. A detailed stability analysis was made on the embankment that is placed on peaty soils that vary in thickness from 2m to 6m, and can be classified into two layers; peat with water content from 100% to 400% and another layer of sandy clay with peaty material with water content from 45% to 75%. Fig.3.72. shows the soil conditions at the proposed site and the physical properties of the peaty soils. Fig.3.73. shows the undrained shear strength of the soil. The fill material used for the embankment consists of upland sand containing about 10% of fine particles smaller than 0.074mm and Tertiary mudstone with more fine particles up to 20% maximum. The unit weight of the sand was 1.9 t/m³ and the angle of internal friction was 35°.

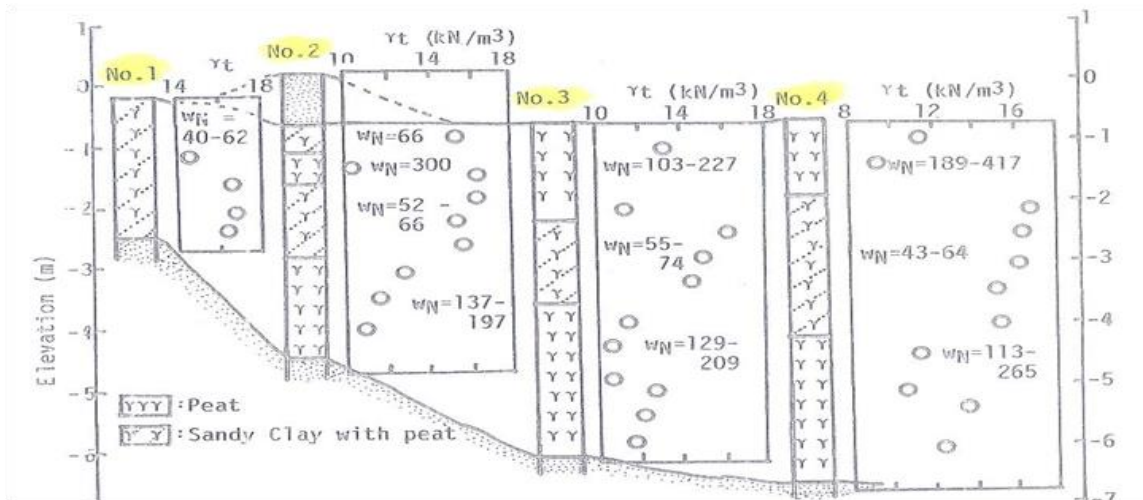


Figure 3. 71 Soil conditions at Kameda site (Hanzawa et al. 1994)

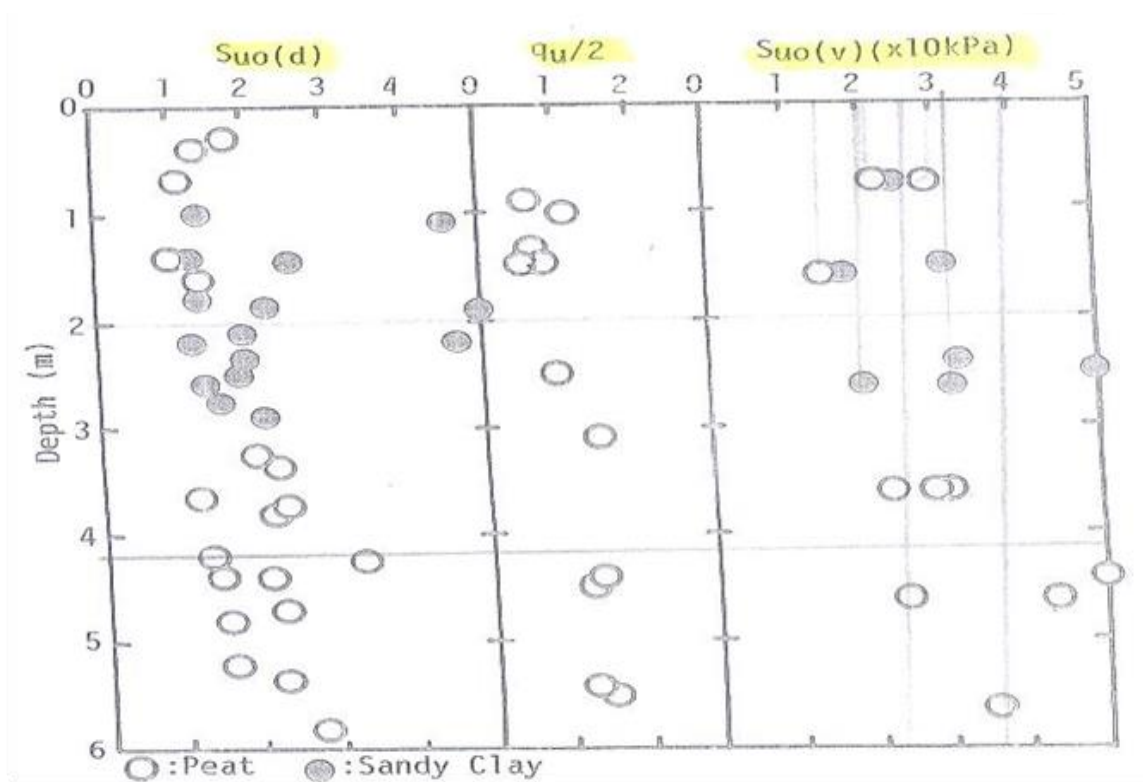


Figure 3.72 Undrained Shear Strength at Kameda Site (Hanzawa et al. 1994)

Failure occurred when the embankment height reached 6.3m where large deformations took place together with settlement causing tension cracks and heave. The failure occurred during the stage where an excavation for an irrigation canal was under construction. Stability analysis was carried out and a factor of safety of 0.98 was obtained (Fig.3.74).The factor of safety is re-evaluated again using SLIDE software and the results are shown in Fig.3.75.

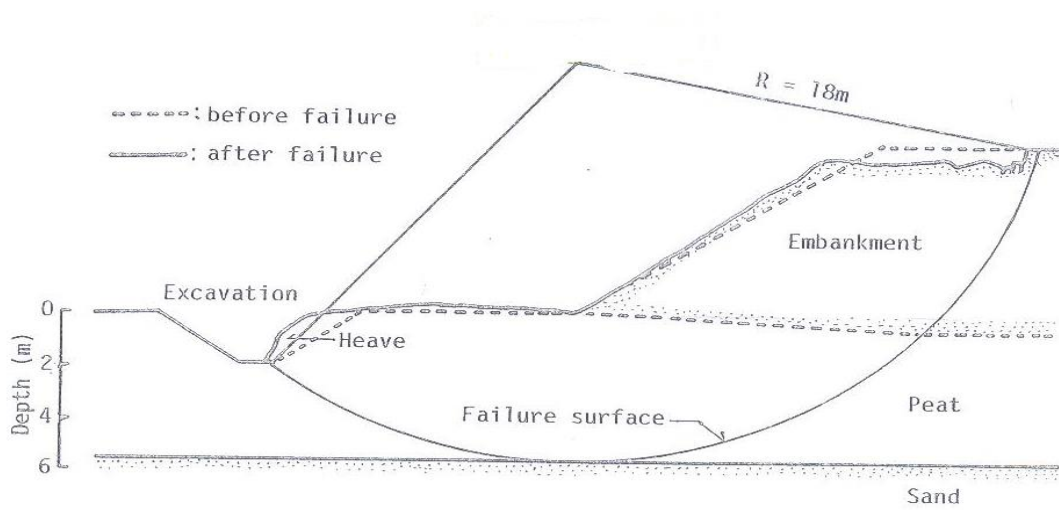


Figure 3.73 Circular Slip Surface (Hanzawa et al. 1994)

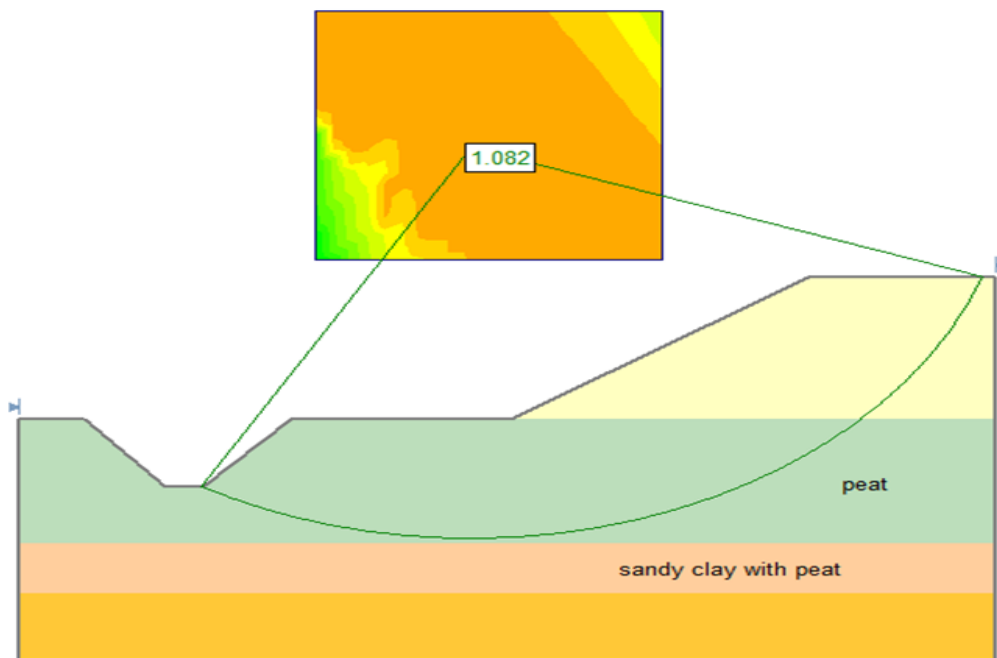


Figure 3.74 Circular Slip Surface using SLIDE

3.2.28 Slide at Khor Al - Zubair no.4

Five earth fills were constructed for the aim of preloading of an alluvial marine clay with an area of 500mx500m. The unit weight of the fill was suggested to be 2 t/m^3 with an angle of internal friction of 35° . The fill was placed on a 17m layer of Alluvial marine clay underlain by 2m silt and fine sand and finally with 1m dilluvial hard clay.

Fig.3.76. shows the soil properties of the site.

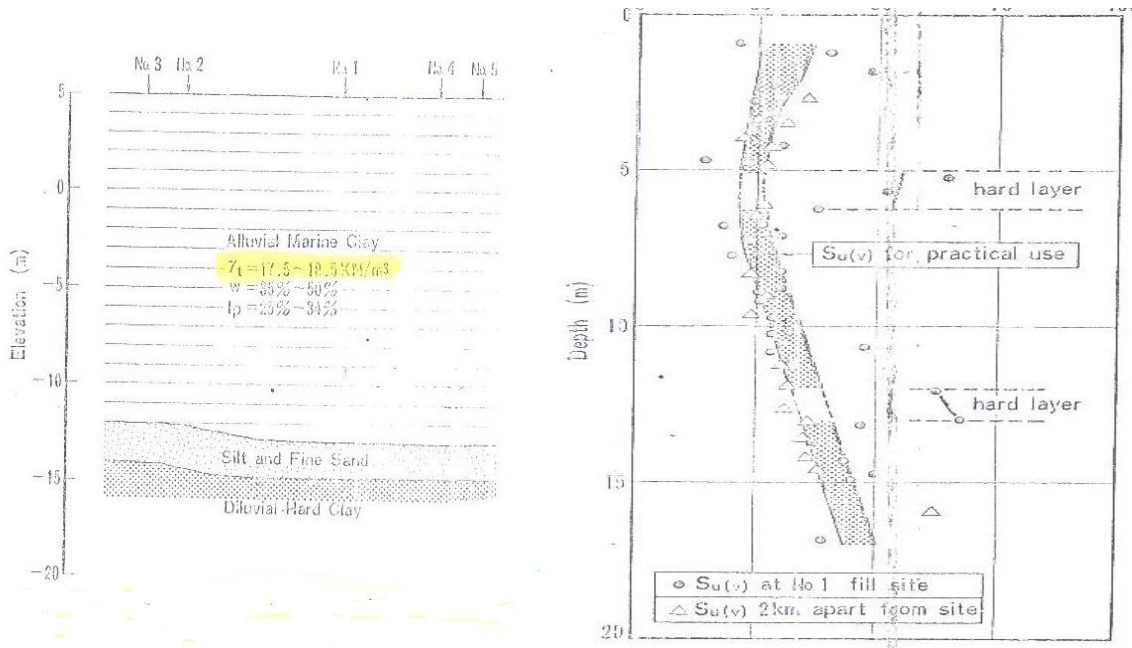


Figure 3. 75 Soil Properties at Khor Al-Zubair Site (Hanzawa 1983)

Failure occurred when the fill reached 11.5m height. Stability analysis was accomplished using circular arc method as shown in Fig.3.77 and the factor of safety obtained was 1.03. Moreover, the slope is analyzed by using SLIDE and a factor of safety of 1.387 is obtained Fig.3.78.

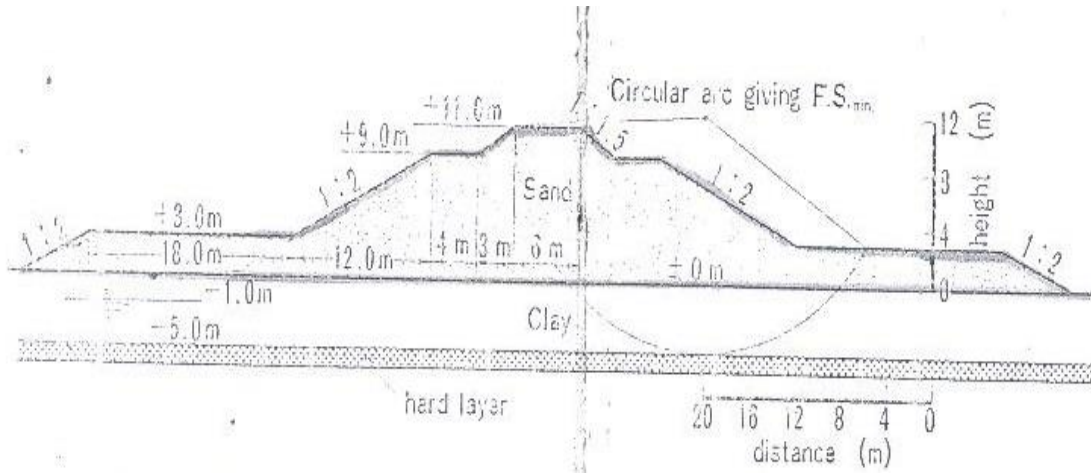


Figure 3. 76 Circular Slip Surface at Khor Al-Zubair Site (Hanzawa 1983)

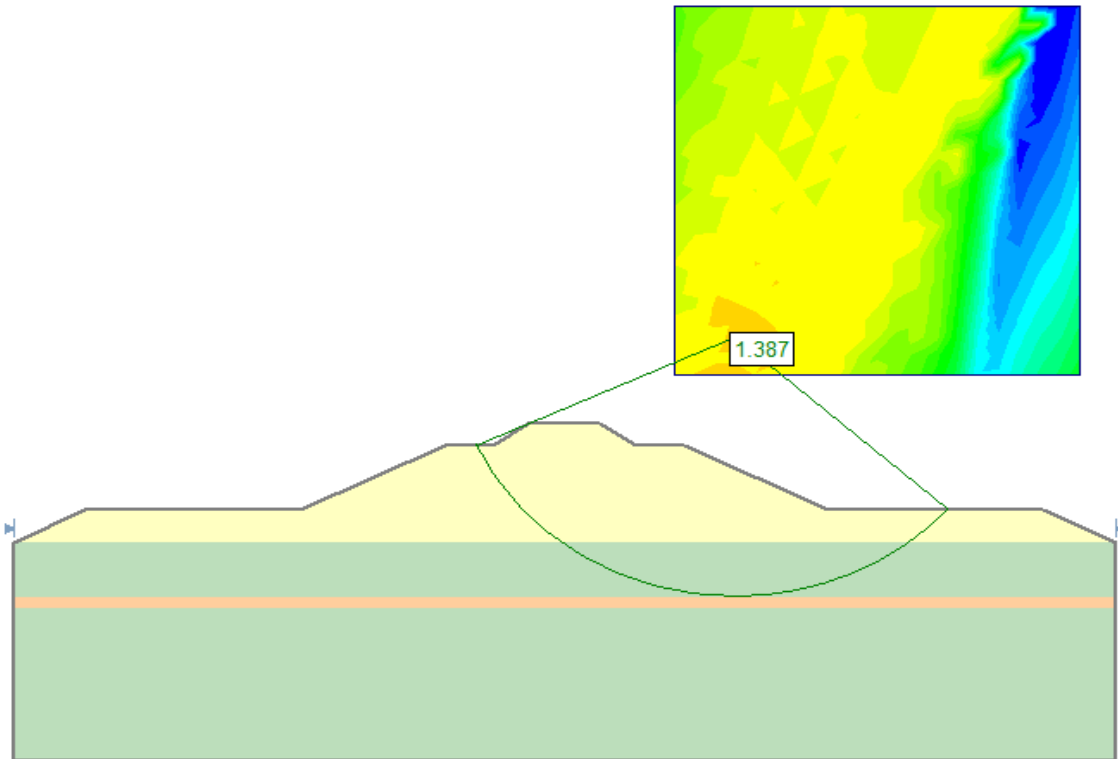


Figure 3. 77 Embankment Failure at Khor-Al-Zubair using SLIDE

3.2.29 Slide at Lian-Yun-Gang

The test site is located in an alluvial plain in the Lian-Yun-Gang area, Jiangsu province, China (Chai et al. 2002). The built-to-failure embankment had a length of 45m with a base width of 42m. The embankment has a 1V:1.75H slope and comprised of compacted sandy clay with unit weight of 1.9 t/m³ and an angle of internal friction of 35°. The soil profile where the embankment was placed consisted of a 2m thick clay crust underlain by an 8.5m thick soft clay layer. Below the soft layer there were medium-to-stiff sandy clay and silt sand layers. The soil properties of the soft deposit are summarized in Fig.3.79. Slope stability analysis was carried out using the finite element method and the subsoil and embankment fill material were represented by 8-node quadrilateral and 6-node triangular elements. Failure occurred when the embankment height reached a height of 4.04m. The factor of safety obtained from Chai et al.(2002) analysis equals to 1.01 with a circular slip surface as shown in Fig.3.80. The slope is re-analyzed by adopting Limit equilibrium method not the finite element method using SLIDE software and the results are shown in Fig.3.81.

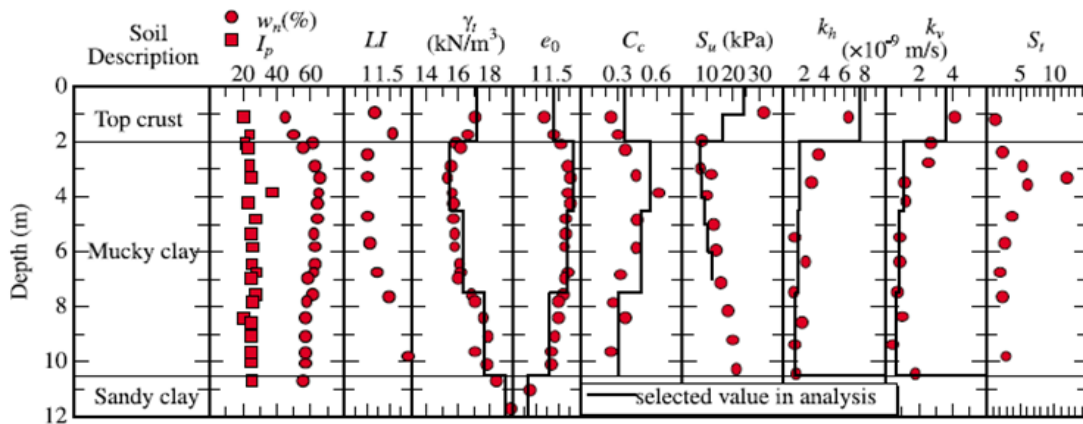


Figure 3.78 The Index and the Mechanical Properties of the Subsoil (Chai et al. 2002)

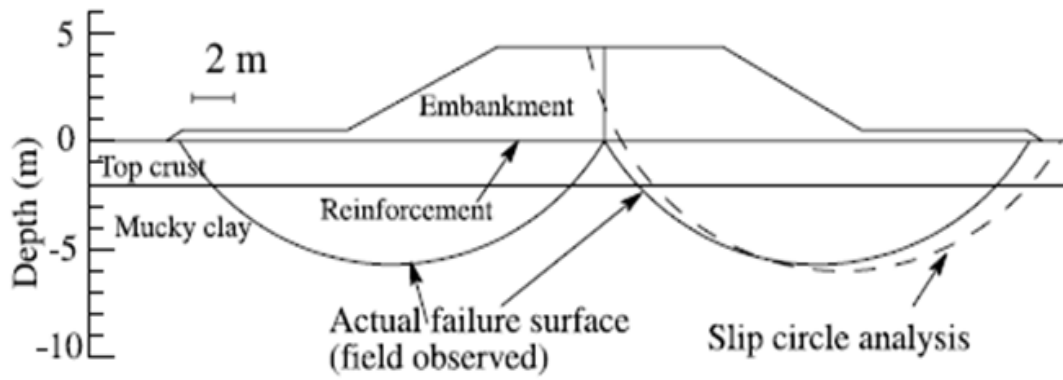


Figure 3.79 Failure Surfaces from Field Observations and in Slip Circle Analysis (Chai et al. 2002)

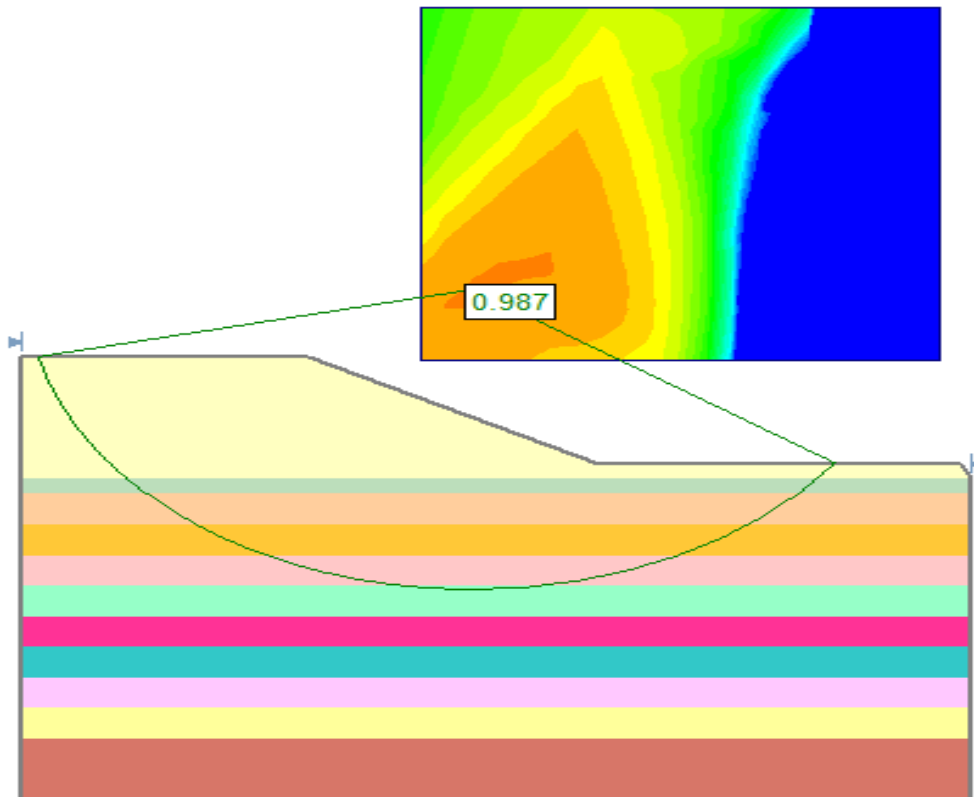


Figure 3.80 Failure Surface using SLIDE

3.2.30 Slide at Congress Street

During the spring and summer of 1952, a portion of the Congress Street “superhighway”, just east of Halsted Street, in Chicago, was built in an open cut. The cut was for the most part in glacial clay and failed when the excavation reached a depth of 47 feet. The soil profile consisted of a deposit of sand and miscellaneous fill underlain by a gritty blue clay as shown in Fig.3.82.

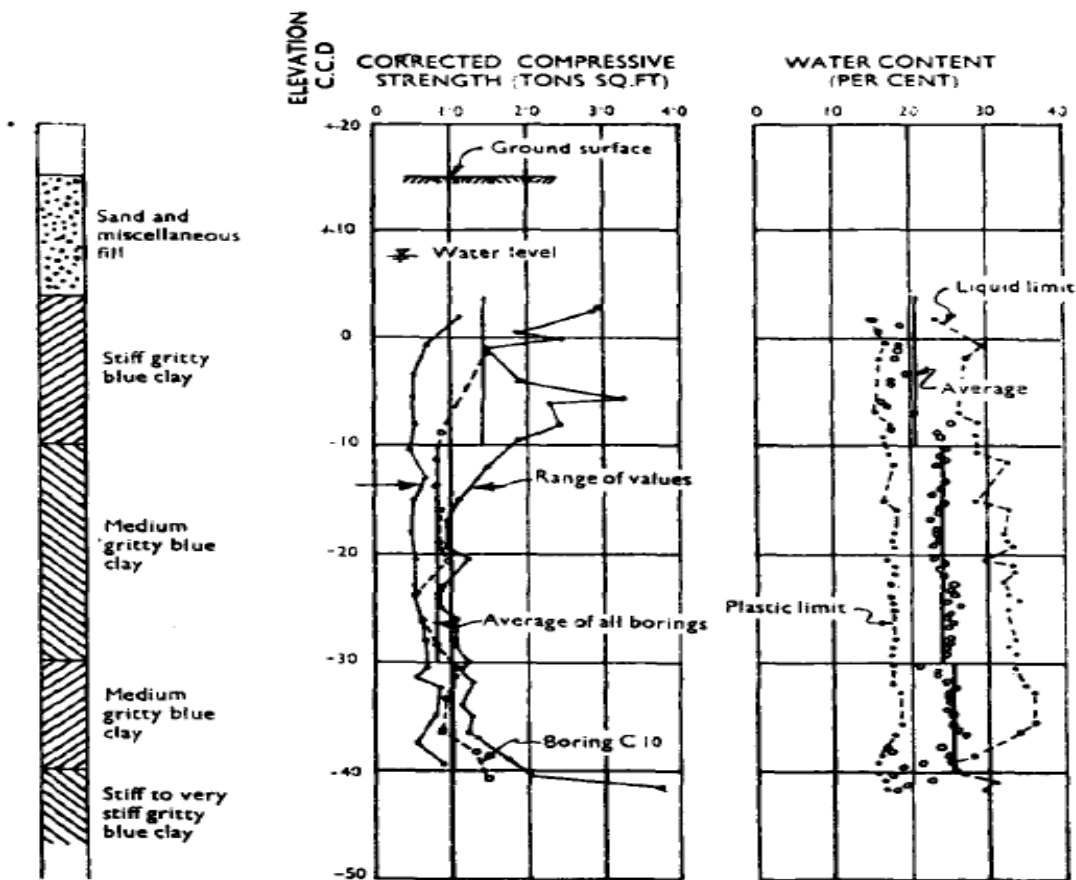


Figure 3. 81 Compressive Strength and Water- Content at Congress Street (Ireland 1954)

The approximate location of the slip surface is known from field evidence. A nearly vertical escarpment formed at the top of the slope and a crack formed in the bottom of the cut near the center line. It was assumed that the slip surface must be tangential to the stiff layer. Slope stability analysis was conducted using the $\phi=0$ analysis and a factor of safety of 1.11 was obtained (Ireland 1954) as shown in Fig. 3.83. The slope failure is analyzed using SLIDE and a factor of safety of 1.486 is obtained Fig.3.84.

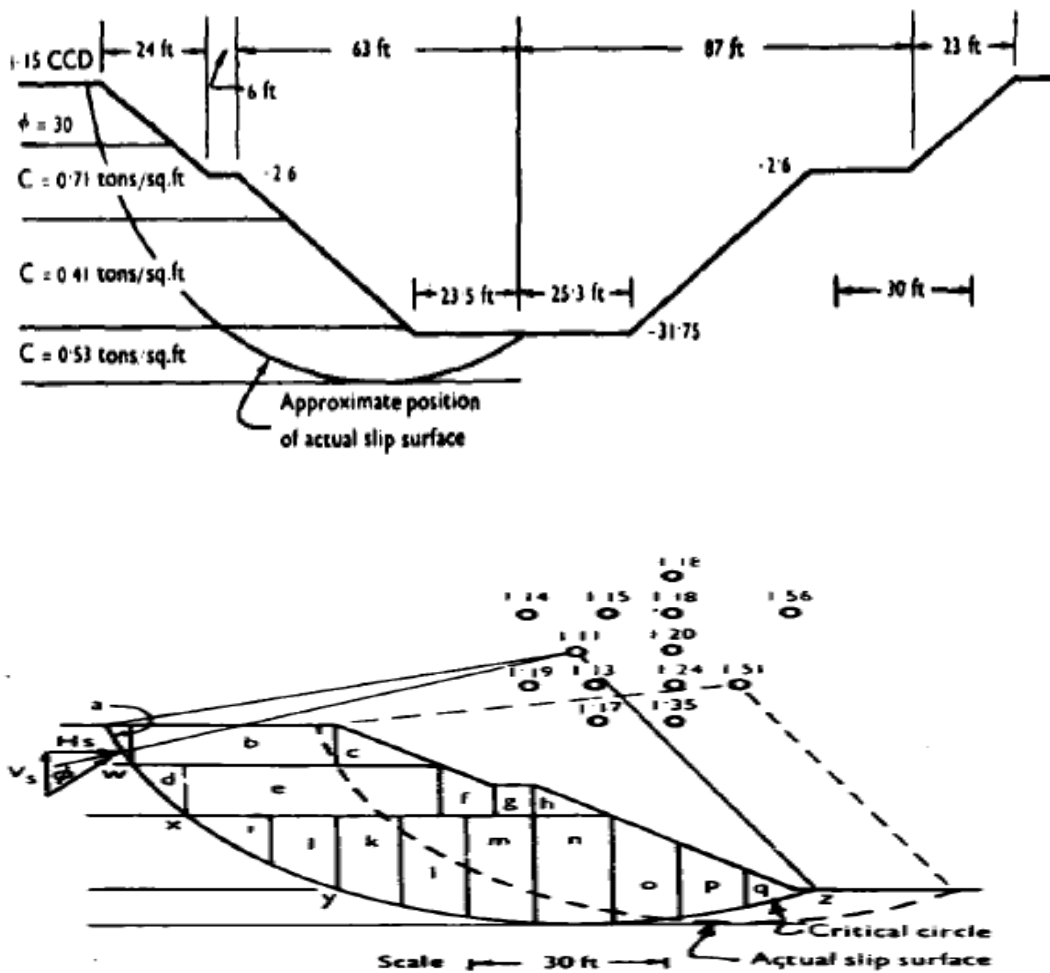


Figure 3. 82 Total Stress Stability Calculations (Ireland 1954)

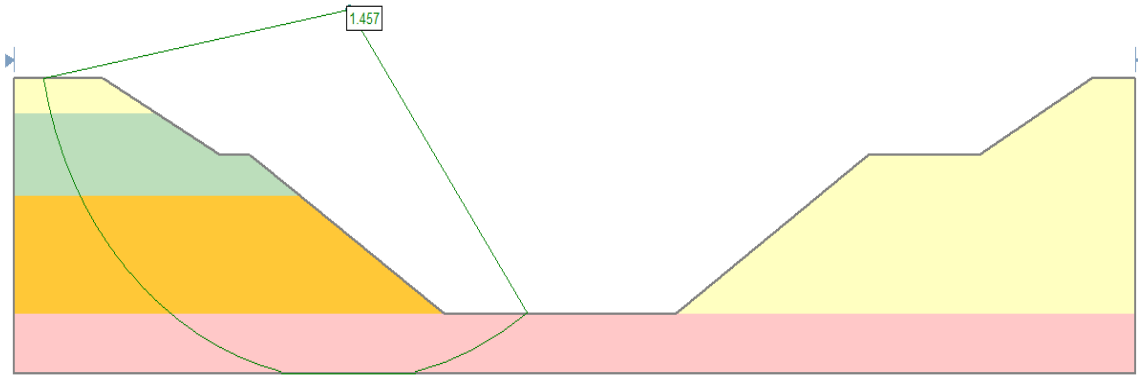


Figure 3.83 Critical Slip Surface using SLIDE

3.2.31 Slide at Daikoku-Cho Dike

On March 19, 1981, a dike failed in Japan. The dike was constructed for a reclaimed land for the urban waste material on a highly plastic marine clay which is considered a normally consolidated clay. The soil profile consisted of a highly plastic marine clay 10m to 15m thick underlain by a sandy gravel with N values more than 50. Below the sandy gravel, a stiff clay and a fine sand with some gravels were found. The undrained shear strength profile used for analysis is shown in Fig.3.85. The embankment consisted of mudstone with unit weight of 1.5t/m^3 and with an angle of friction of 35° . Kishida et al. (1983) and Hanzawa (1983) carried out slope stability analysis by adopting both the simplified and the advanced $\phi=0$ method. The difference between the simplified and advanced methods is the undrained shear strength values either from unconfined compression test or SHANSEP. The authors ended up with a factor of safety of 0.91 Fig.3.86. Slope stability analysis is carried out using SLIDE and a factor of safety of 1.042 is obtained Fig.3.87.

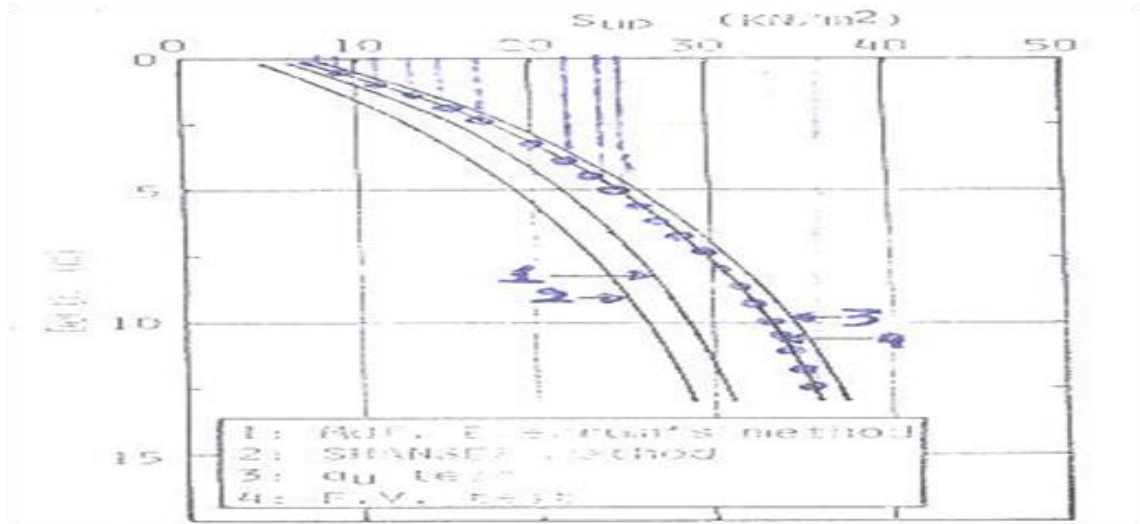


Figure 3.84 Undrained Shear Strength at Daikoku (Kishida et al. 1983)

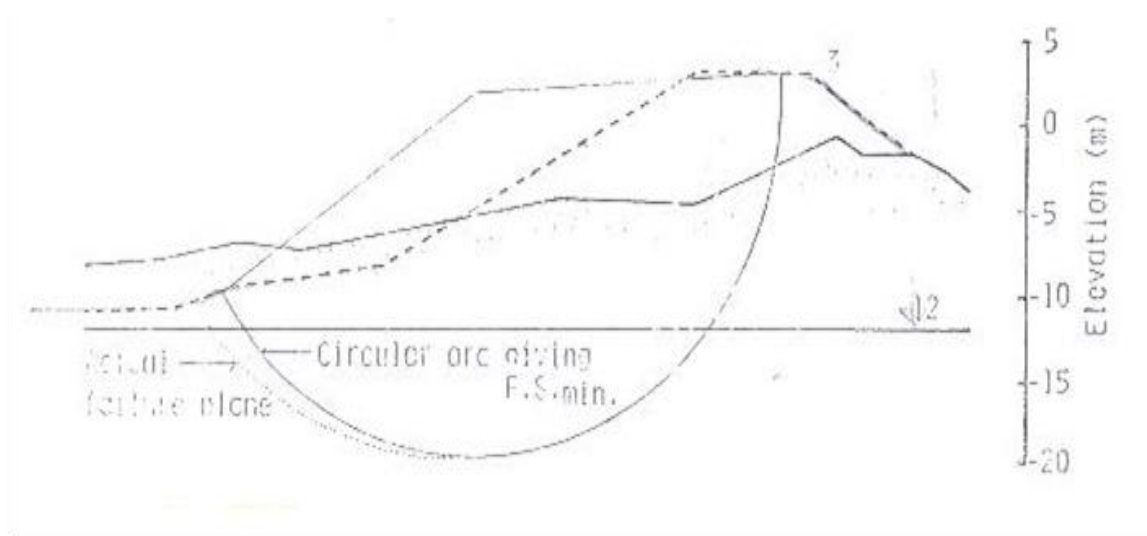


Figure 3.85 Circular Slip Surface at Daikoku Site (Kishida et al. 1983)

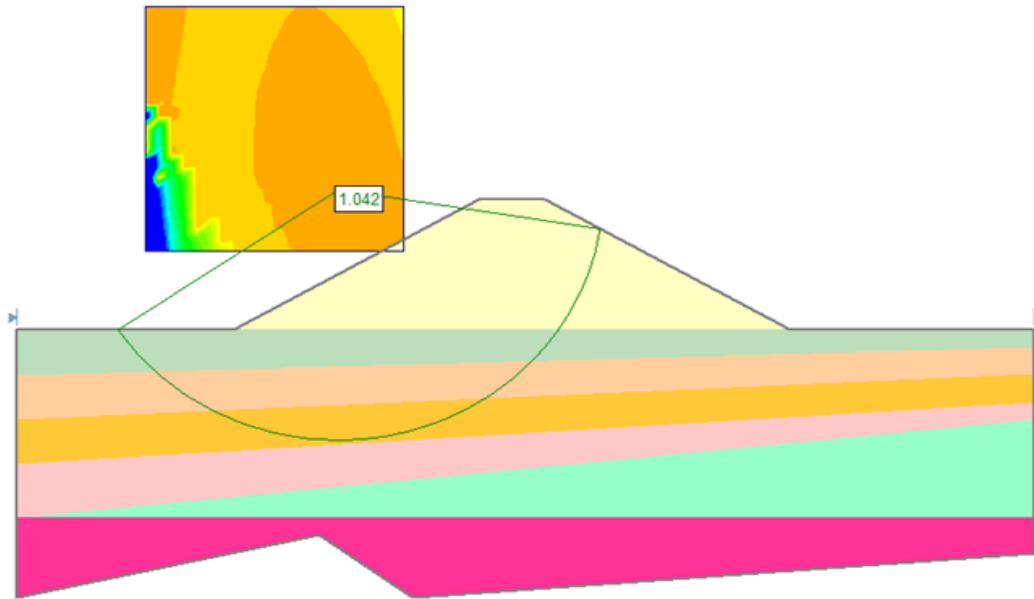


Figure 3. 86 Total Stress Stability Analysis using SLIDE

3.2.32 Slide at Cuyahoga AA

In March 1971, an embankment failure occurred in the Cuyahoga River valley about 5 miles south of Cleveland in Ohio in USA. The embankment fill consisted of clayey silt with an undrained shear strength of 4.3t/m^2 . The subsoil conditions at the site consisted of thick layer of lacustrine clay made up mainly of varved clay which is a silty clay with silt and fine sand laminations. This layer overlies a layer of glacial till. An organic silty sand layer is found below the glacial till (Fig.3.88).

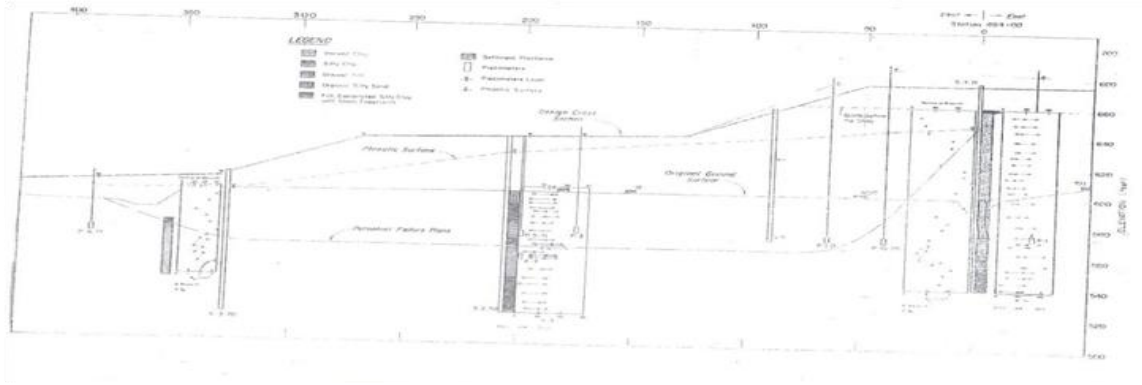


Figure 3. 87 Soil Properties and Critical Slip Surface at Cuyahoga AA site (Wu et al. 1975)

Wu et al. (1975) analyzed the stability of the embankment by the Morgenstern and Price method using the circular arc method. The authors assumed a total stress analysis assuming that the loading takes place in the undrained condition. A factor of safety of 1.25 was obtained. A slope stability analysis is conducted using SLIDE and a factor of safety of 0.815 is obtained as shown in Fig.3.89.

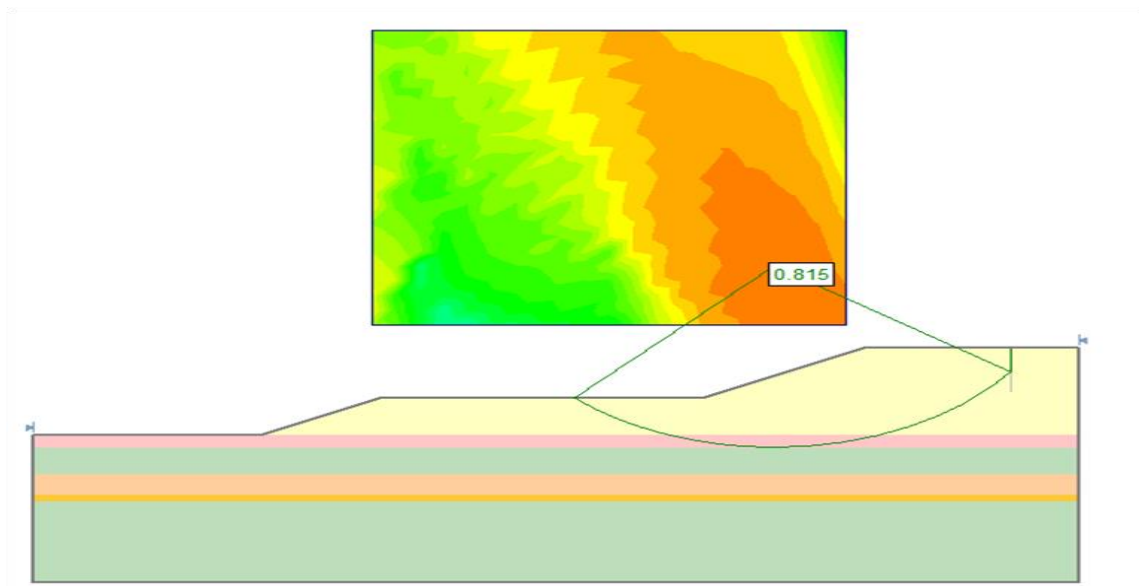


Figure 3. 88 Critical Slip Surface using SLIDE

3.2.33 Slide at King's Lynn

In 1972, an induced failure occurred in a trial embankment at King's Lynn in England. The trial aimed at getting data regarding the installation of the sand drains (type, spacing, diameter) and investigating the types of instruments needed for monitoring the final work. The fill consisted of a light weight material called Carstone. The embankment was laid on an upper alluvial layer composed of firm blue silty clay, soft brown clay and soft blue peaty clay. The upper alluvial layer is underlain by a layer of peat of 2m thick. Below the peat layer, a soft blue clay with traces of peat was found. Finally, a blue brown clayey sand was present that overlies a weathered Kimmeridge layer (Fig.3.90.). Wilkes et al. (1972) conducted a total stress stability analysis based on a circular slip surface and a factor of safety of 1 was resulted as shown in Fig.3.91.

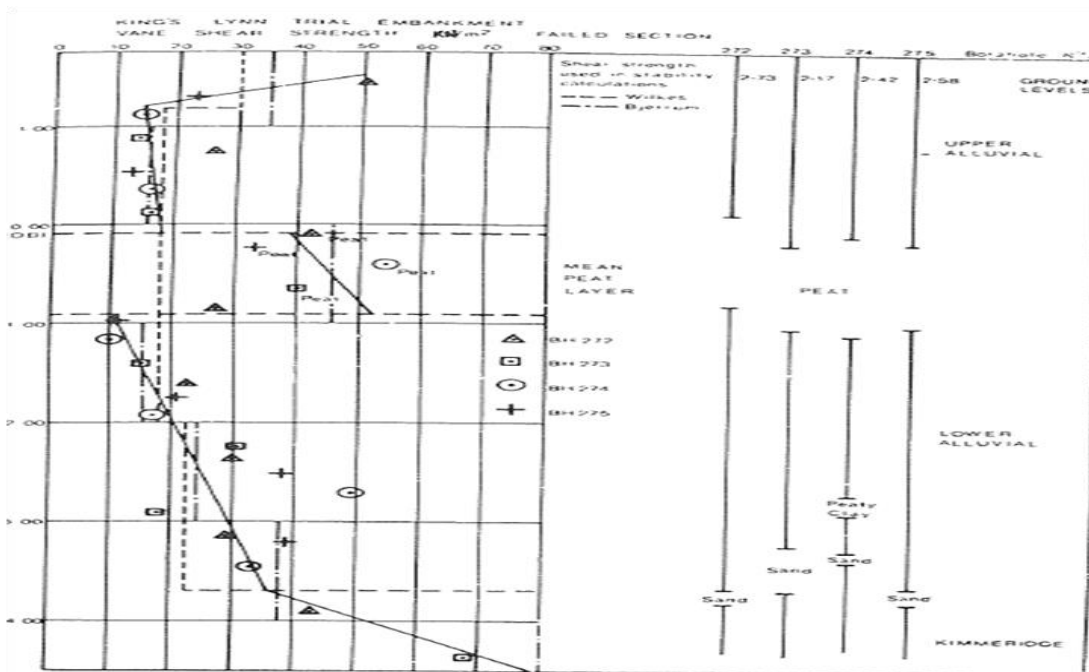


Figure 3. 89 Soil Properties at King's Lynn (Wilkes et al. 1972)

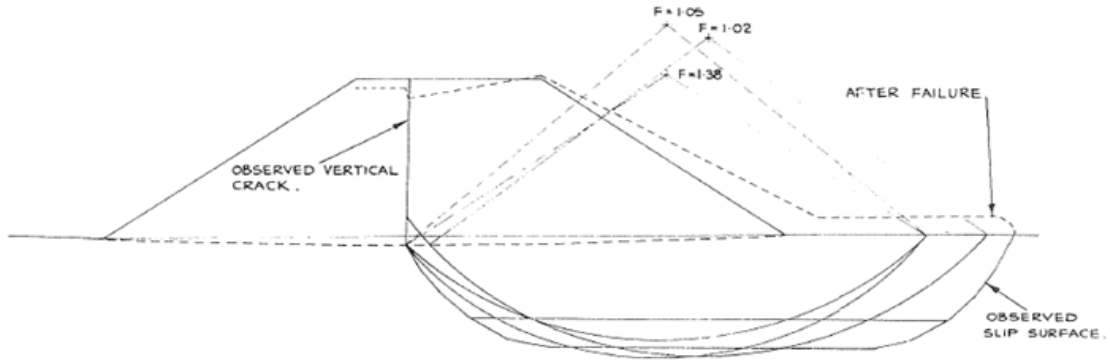


Figure 3. 90 Observed and calculated Slip Surface (Wilkes et al. 1972)

When failure occurred, the final slip zone was non-circular and was deeper than anticipated. Thus, total stress analysis was adopted for analyzing the slope using SLIDE software by assuming an irregular slip surface and the results are shown in Fig.3.92.

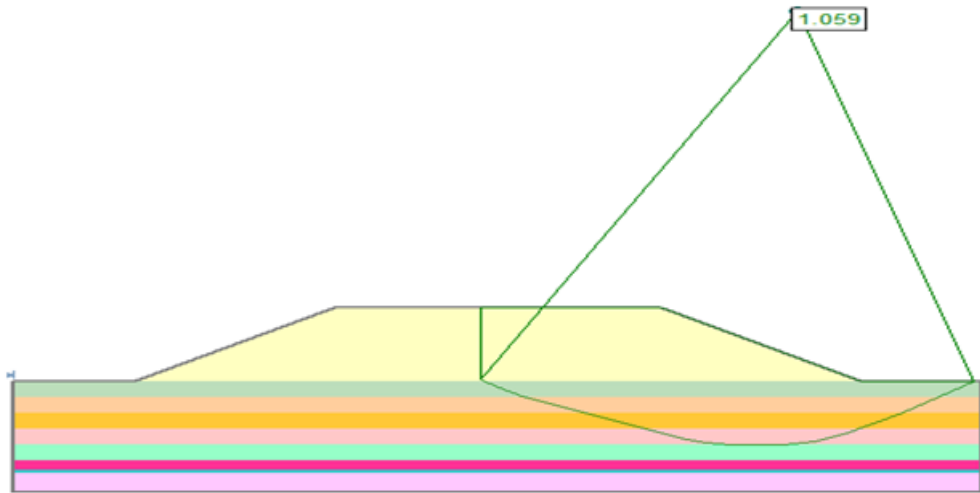


Figure 3. 91 Critical Slip Surface using SLIDE

3.2.34 Slide at Muar

The Malaysian Highway Authority selected an appropriate site on the Muar plain to construct full-scale test embankment built to failure to investigate in detail the behavior of Muar clay deposits. The subsurface geology at the site revealed the existence of a 2m thick weathered crust overlying a 16.50 thick layer of soft silty clay. This soft silty clay is composed of an upper very soft and a lower soft silty clay. Below this lower clay layer a thick peaty soil layer was found followed by a stiff sandy clay layer (Fig.3.93).

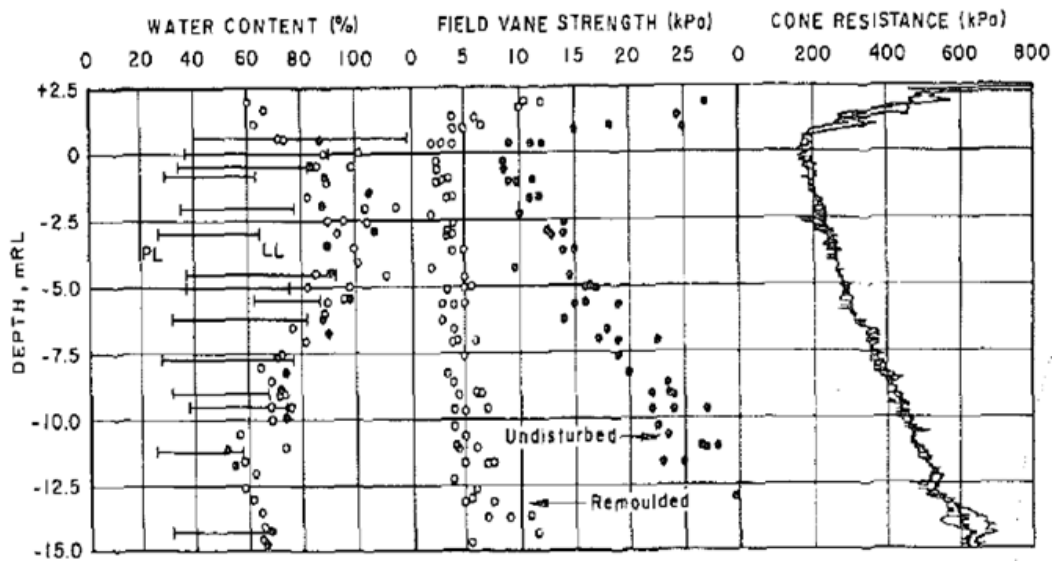


Figure 3. 92 Variation of Soil Properties with Depth (Indraratna et al. 1992)

The embankment fill consisted of soil material with unit weight of 2.05t/m^3 and strength parameters of $c=1.9\text{t/m}^2$ and an angle of internal friction of 26° . The embankment failed by the development of a quasi-slip circle type of rotational failure at a critical height of

5.5m with a tension crack propagating vertically through the crust and the fill. Indraratna et al. (1992) conducted both finite element analysis and limit equilibrium method to evaluate the stability of the slope. The slope is reanalyzed using SLIDE software and the factor of safety is evaluated. The result is shown in Fig.3.94.

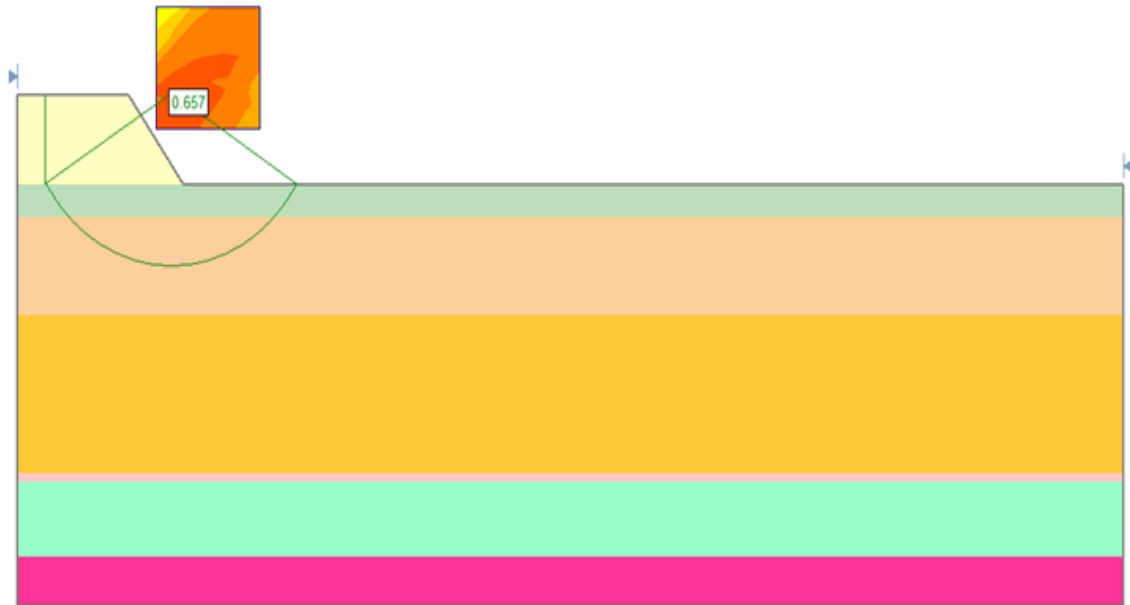


Figure 3. 93 Critical Slip Surface at Muar using SLIDE

3.2.35 Slide at North Ridge Dam

The North Ridge Dam is a 21.30 m high homogenous earth dam located southeast of Raymond, Alberta. The fill material consisted of lean to medium plastic clay of glacial origin with an average liquid limit of 31%, and an average plastic limit of 15%. The fill was compacted to an average dry density of 17.9 t/m^3 at an average water content of 14.6%. The fill had a $c= 41.4 \text{ KPa}$ and $\phi= 27^\circ$ and was placed on a foundation soil

consisting of 3-5.8m of sand overlying 11-15m of soft highly plastic clay. A lower sand layer underlies the clay to an unknown depth. The sand has an angle of internal friction of 29°. The highly plastic clay has the properties shown in Table 3.4.

Table 3.4. Soil Properties of Highly Plastic Clay, North Ridge Dam (Rivard et al. 1978)

Soil property	Average	Range
Wet density (kN/m ³)	18.1	16.6–19.2
Water content (%)	37	22–50
Liquid limit (%)	72	47–91
Plastic limit (%)	21	15–29
Unconfined compressive strength (kPa)	96.5	62.1–144.8
Water content from unconfined compression tests (%)	37	33–42

Construction of the earth dam started in June 1953 and failure occurred at a fill height of 18.30m in mid-September. Failure of the embankment was indicated by cracks and slope bulging. Rivard et al. (1978) carried out an effective stress analysis. However, Peterson et al. (1957) conducted a total stress analysis as shown in Fig.3.95. and a factor of safety of 1.23 was obtained. Using SLIDE software, a total stress analysis is conducted using the soil properties illustrated above by assuming a circular slip surface. The results are shown in Fig.3.96.

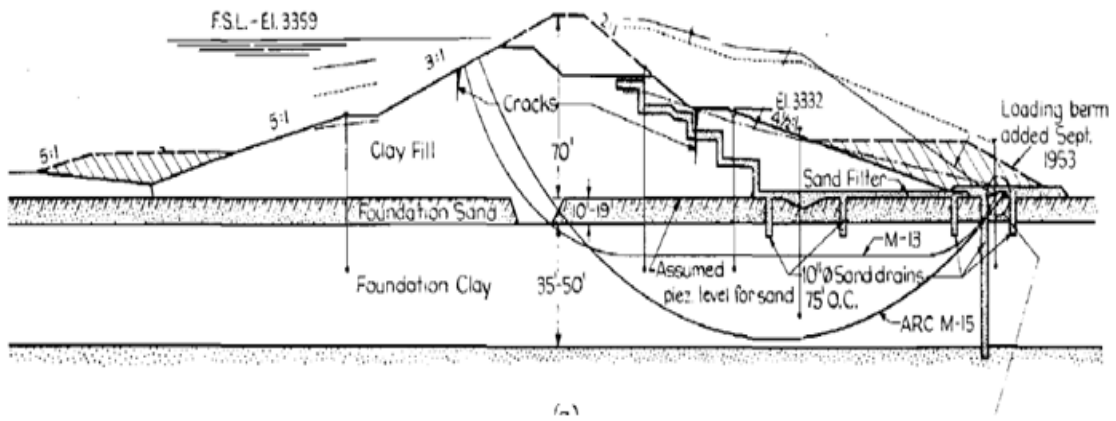


Figure 3. 94 Stability Analyses, North Ridge Dam(Rivard et al. 1978)

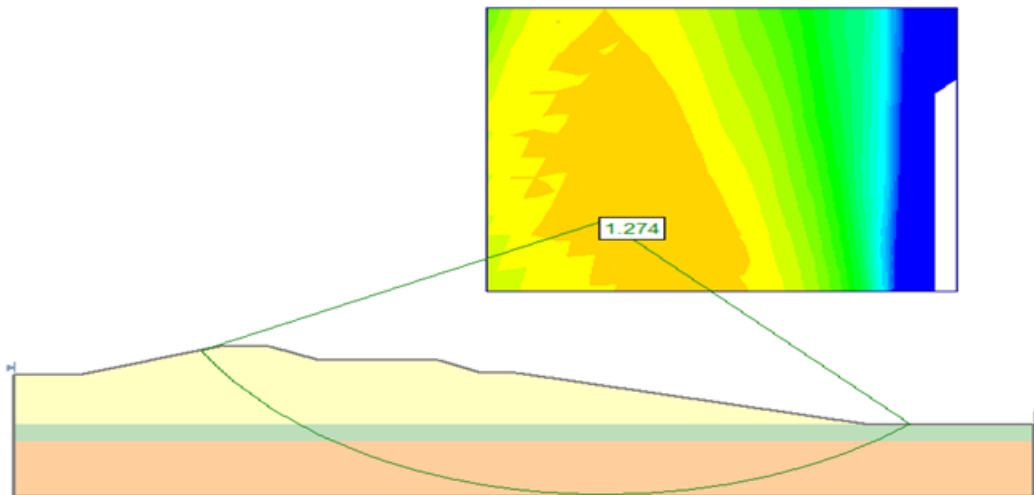


Figure 3. 95 Stability Analyses, SLIDE software

3.2.36 Slide at Seven Sisters Dike

In 1953, a slide took place at Seven Sisters on the Winnipeg River, Manitoba. The dike failed when the embankment reached a critical height of 4.3m. The dike was constructed of medium to highly plastic clay compacted to greater than 90% standard proctor density at a water content of 5-10% above the Standard Proctor optimum water content. The foundation conditions of the site consisted of 4.6m of highly plastic clay underlain by a low to medium plastic glacial clay. Table 3.5 summarizes the physical characteristics of the highly plastic clay.

Table 3.5 Soil Properties of the Highly Plastic Clay, Seven Sisters Dike (Peterson et al. 1957)

Soil property	Average	Range
Wet density (kN/m³)	17.4	15.2–18.5
Water content (%)	39	19–67
Liquid limit (%)	58	27–84
Plastic limit (%)	21	13–29
Unconfined compressive strength (kPa)	68.9	13.8–248.2
Water content from unconfined compression tests (%)	40	15–66

A total stress analysis was conducted by Peterson et al. (1957) using the profile shown in Fig.3.97. and a factor of safety of 1.4 was obtained. Another total stress analysis was conducted using SLIDE software and the results are shown in Fig.3.98.

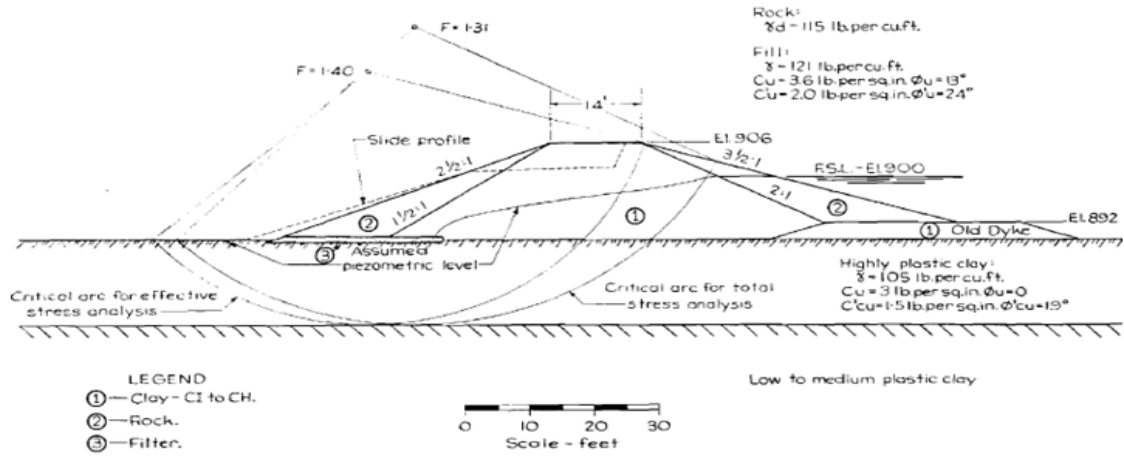


Figure 3. 96 Stability Analyses, Seven Sisters Dike (Rivard et al. 1978)

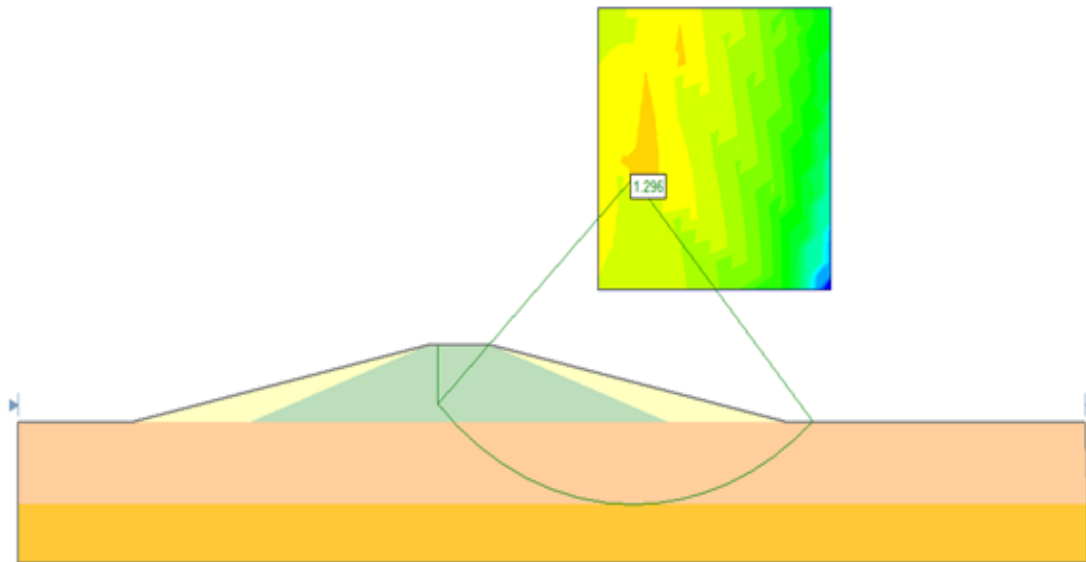


Figure 3. 97 Stability Analyses using SLIDE

3.2.37 Slide at Shellmouth Dam Test Fill

To evaluate the shear strength and the development of pore pressures for the design of Shellmouth Dam, the Prairie Farm Rehabilitation Administration (PFRA)

constructed the Shellmouth Dam Test Fill. The fill was constructed of a well-graded mixture of sand and gravel to a height of 16.8m with slopes of 1.75:1, 2:1, and 5:1. The foundation of the test fill consisted of two clay layers, each about 6-7.6m thick, separated by a 3m continuous sand layer. The two clay layers possessed similar soil properties as shown in Table 3.6.

Table 3.6. Stability Analyses, Shellmouth Dam Test Fill (Rivard et al. 1978)

Soil property	Average	Range
Wet density (kN/m ³)	17.4	15.2–18.5
Water content (%)	39	19–67
Liquid limit (%)	58	27–84
Plastic limit (%)	21	13–29
Unconfined compressive strength (kPa)	68.9	13.8–248.2
Water content from unconfined compression tests (%)	40	15–66

The sand layer between the clay layers was a mixture of poorly-graded and silty sands with an angle of internal friction of 38°. At a fill height of 16.80m, failure occurred and construction stopped. An effective stress analysis was carried out by Rivard et al. (1978) by assuming a circular arc surface. A total stress analysis was conducted using SLIDE software and a factor of safety of 0.94 was obtained as shown in Fig.3.99.

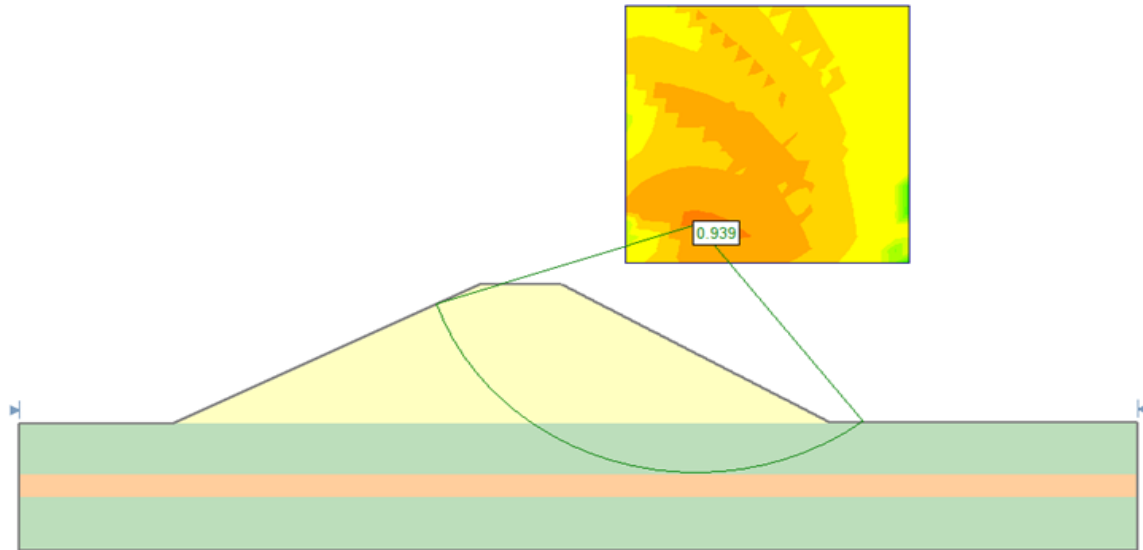


Figure 3. 98 Stability Analyses using SLIDE

3.2.38 Slide at Juban

In late 2002, the south approach embankment of the overpass of the Juban Road experienced slope surface failures. The Juban Road is classified as a local collector that crosses Interstate Highway 12 in Livingston Parish, Louisiana (Zhang et al. 2005). Based on the field observations and laboratory results, the failure occurred due to the shrinkage cracks that formed during the dry season. During the wet season, the water infiltrates into the soil mass through the shrinkage cracks causing swelling that lead to the decrease in the shear strength of the soil. The slope consisted of cohesive soil with a specific gravity of 2.72 and contained 30.6% silt, 41.5% sand, and 27.9% clay. Its index parameters are as follows (PL=15, LL= 37, PI=22). The soil has a maximum unit weight of 1.868t/m^3 and an unconfined compressive strength of 10.6 KPa. Both the embankment soil and the foundation soil have the same soil properties. Zhang et al. (2005) conducted a total stress

analysis of the slope profile shown in Fig.3.100. The authors reported a factor of safety of 0.991 for an assumed circular slip surface.

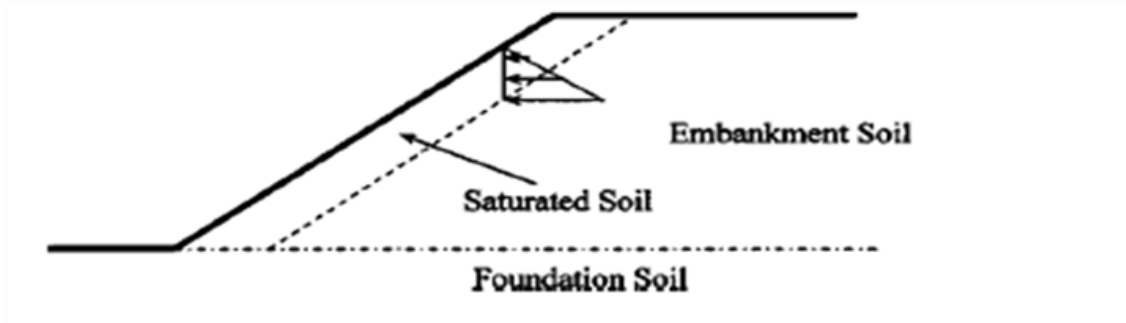


Figure 3. 99 Schematic Model used in the analysis (Zhang et al. 2005)

Another total stress analysis is conducted by using SLIDE software and the factor of safety is calculated by adopting different methods (Bishop, Ordinary method of slices, Janbu, and Spencer). The results are shown in Fig.3.101.

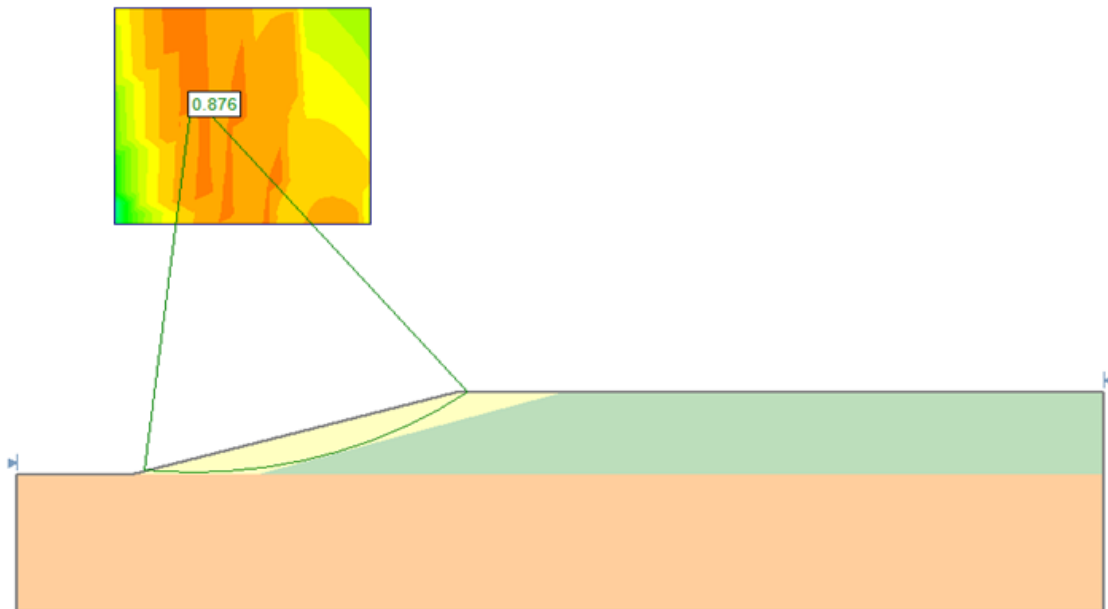


Figure 3. 100 Critical Slip Surface using SLIDE

3.2.39 Slide at Bradwell

Five days after the excavation was completed in the London clay at Bradwell, the slope failed. The excavation is 48.5 ft deep. The lower 28 ft of the excavation is in London Clay and is inclined at 0.5(Horizontal) : 1(vertical). The London Clay is overlain by 9ft of Marsh clay where the excavation slope was inclined at 1:1 (45°). About 11.5 ft of clay from the excavation was placed at the top of the excavation, over the marsh clay. The clay fill was also inclined at 1:1. Fig.3.102. shows the soil properties of the site. A representative unit weight for the London clay at the site was 120 pcf. The clay fill was assumed to crack to the full depth of the fill and thus its strength was ignored. The marsh clay was reported to have a total unit weight of 105 pcf. The analysis and the cross-section adopted by Skempton and La Rochelle (1965) in the analysis of the slope is shown in Fig.3.103. The SLIDE analysis (Fig.3.104) resulted in a factor of safety of 1.76.

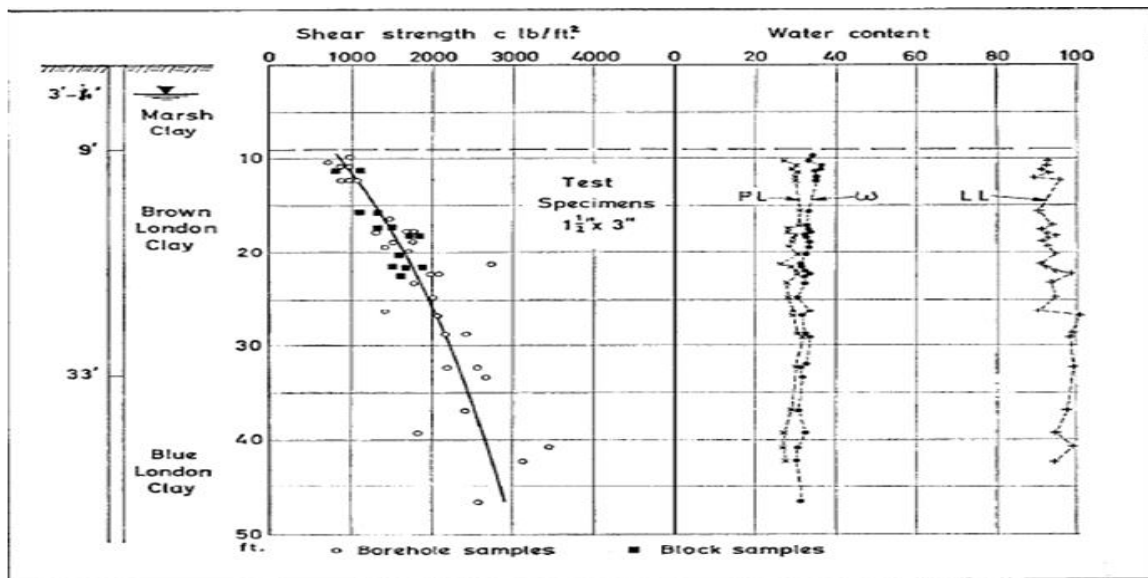


Figure 3. 101 Properties of London Clay at Bradwell (Skempton and LaRochelle 1965)

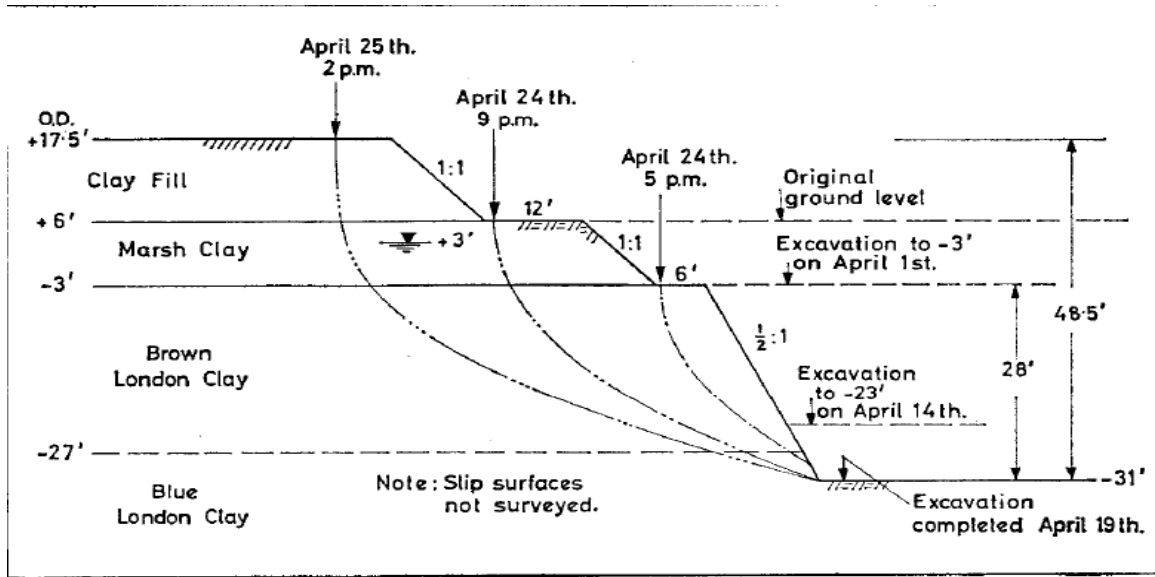


Figure 3.102 Cross Section of Excavated Slope at Bradwell (Skempton and LaRochelle 1965)

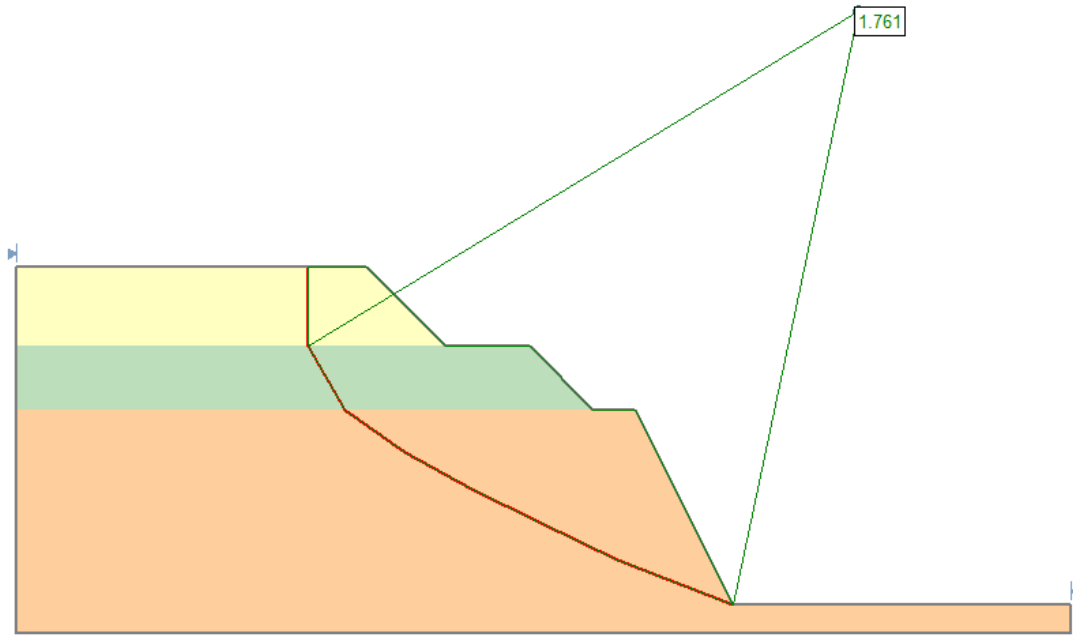


Figure 3.103 Critical Slip Surface at Bradwell using SLIDE

3.2.40 Slide at Genesee

On July 28, 1982, longitudinal cracking was observed along the top of an embankment located in Genesee, 60 km southwest of Edmonton. The fill was constructed using a weathered clay shale compacted to 95% of standard Proctor maximum dry density. The Genesee site is underlain by bedrock of the Late Cretaceous Paskapoo Formation consisting of a sequence of shale, siltstone, sandstone, and coal deposits. Moreover, the site is located on the side of a pre glacial valley in the bedrock surface and was covered by a till deposit during glaciations. Fig.3.105. shows the stratigraphy of the soil deposit. The failure occurred on a clay foundation with a thick crust, so the failure surface is more likely to be circular. The failure took place when the embankment reached a critical height of 12m. The slope was analyzed by Been et al. (1986) (Fig.3.106) by adopting a total stress analysis and a factor of safety of 1 was obtained. Another total stress analysis of the slope is conducted using SLIDE and the same factor of safety is obtained as indicated in Fig.3.107.

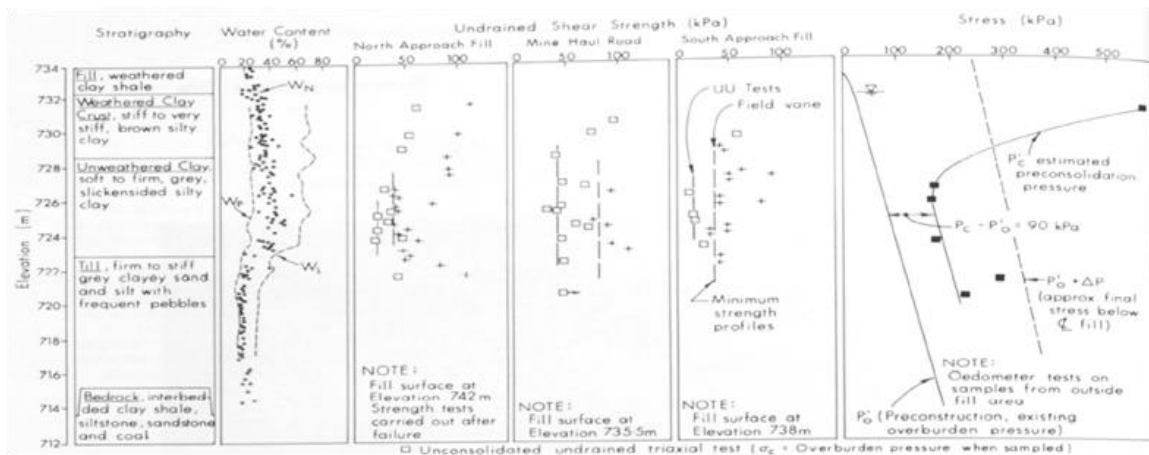


Figure 3. 104 Stratigraphy and Engineering Properties of the soil at Genesee (Been et al. 1986)

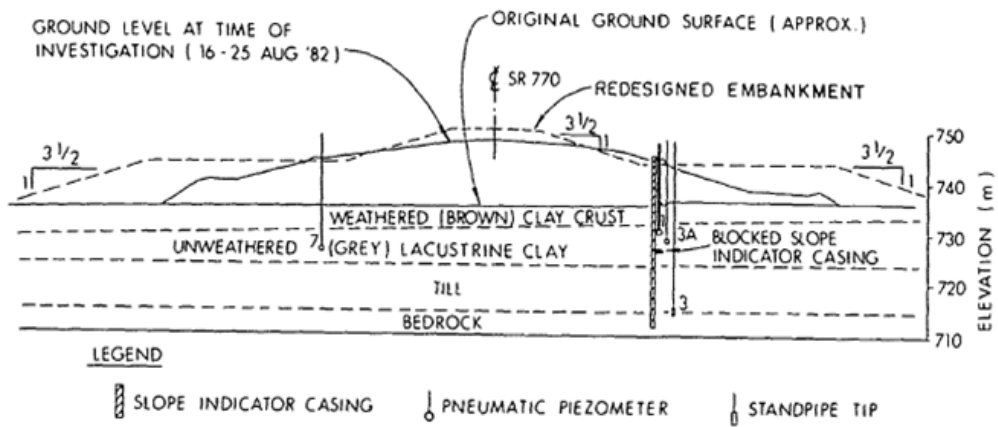


Figure 3. 105 Slope Geometry at Genesee (Been et al. 1986)

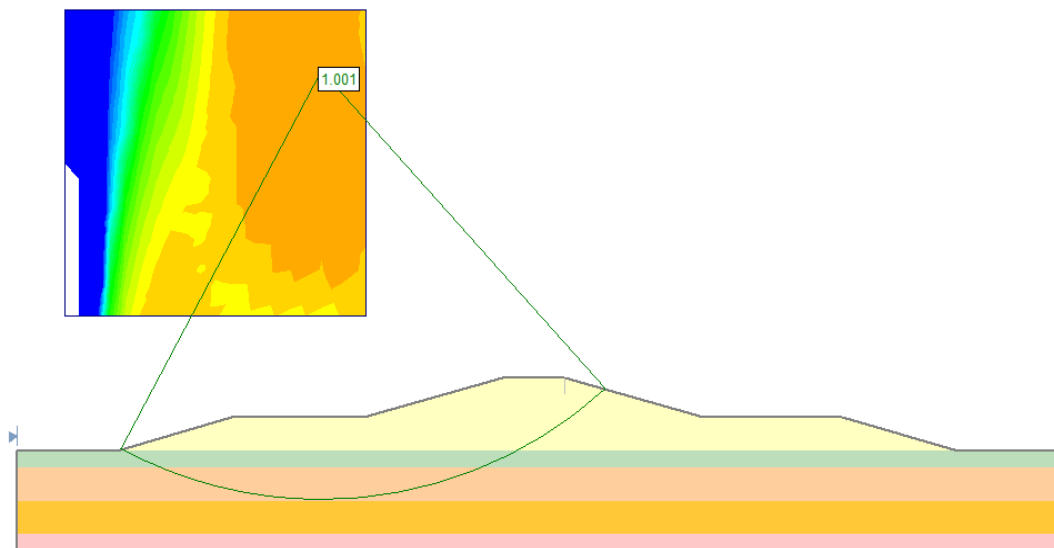


Figure 3. 106 Critical Slip Surface at Genesee using SLIDE

3.2.41 Slide at Precambrian

On the morning of August 22, 1973, an embankment failure occurred at Precambrian in Canada. The failure happened when the height of the embankment reached 30 ft (7.6m). The fill material was a well-graded granular material, with particles ranging from fine sand to cobbles. The density of the embankment material was considered to be 130 pcf and the angle of internal friction was 35°. The soil profile of the foundation soil consisted of a 3-ft thick organic soil (muskeg) overlying a marine clay formation with a 45 ft thickness. The marine formation consisted of an irregular sequence of silty clay layers and thin seams of silt or fine sand. Below the marine formation, a layer of fine to medium sand containing some gravel, cobbles and rocks having a thickness of about 50 ft underlies the clay formation and rests directly on the bedrock (Fig.3.108). Dascal et al. (1975) carried out the stability analysis by adopting a total stress analysis and a circular slip surface was assumed (Fig.3.109) resulting in a factor of safety of 1.1. The factor of safety is re-evaluated using SLIDE and the results are shown in Fig.3.110.

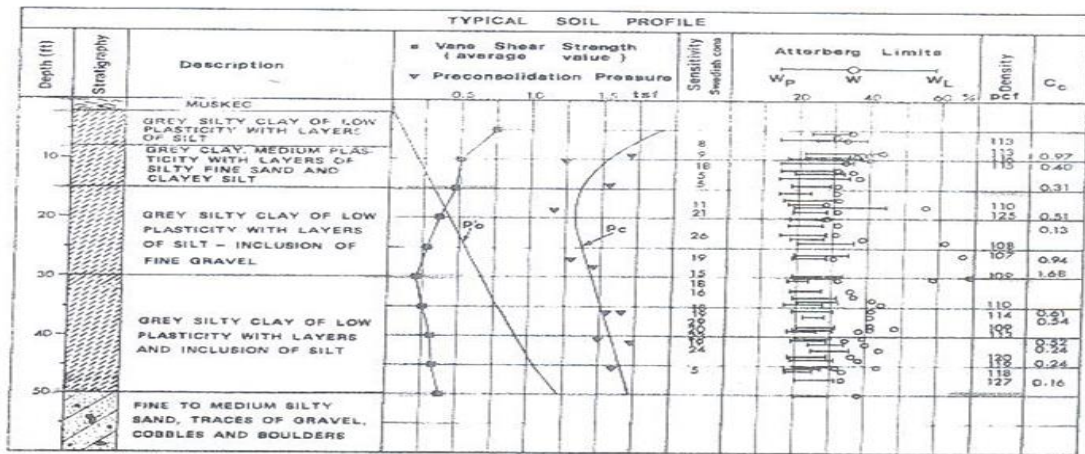


Figure 3.107 Soil Profile at Precambrian (Dascal et al. 1975)

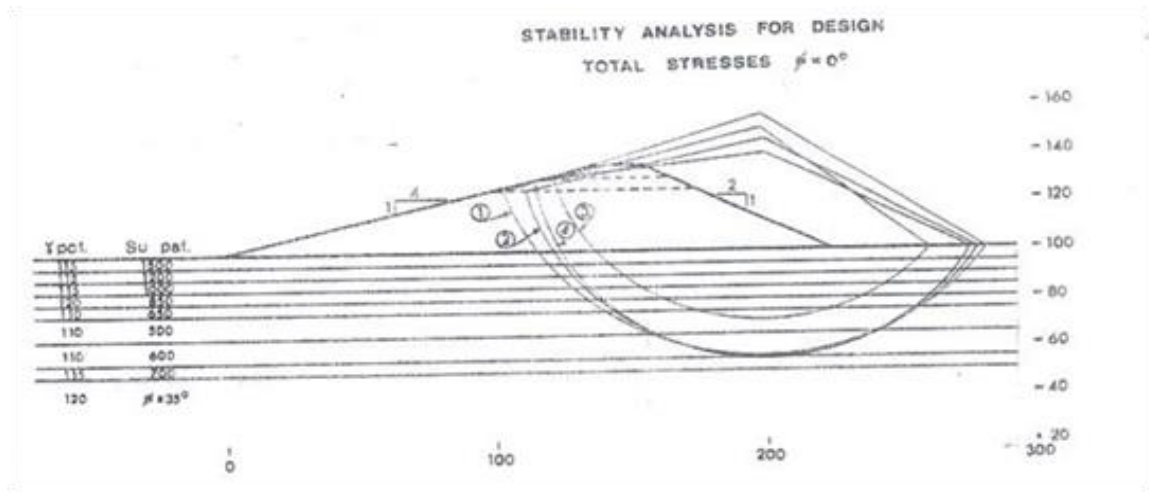


Figure 3. 108 Total Stress Analysis (Dascal et al. 1975)

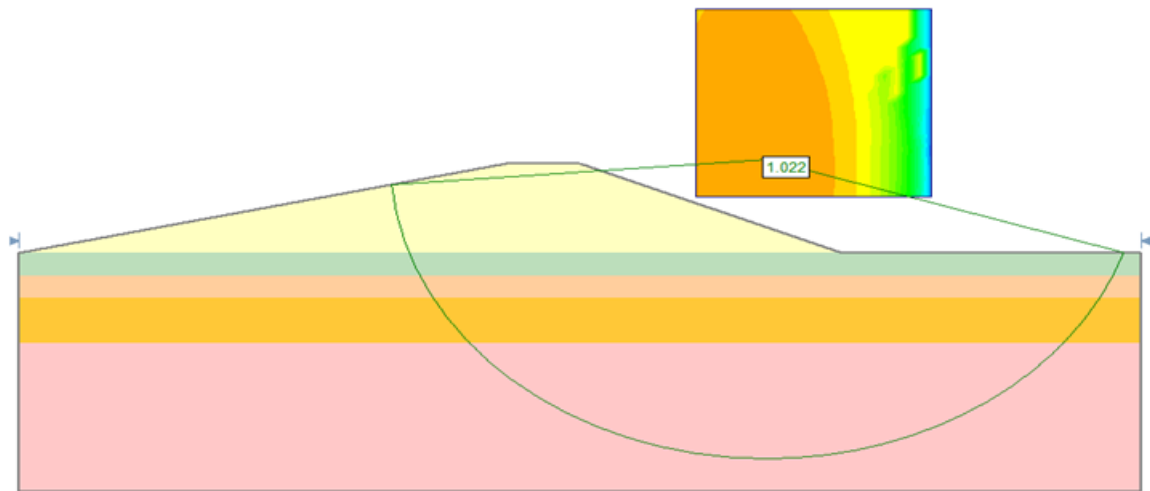


Figure 3. 109 Stability Analysis at Precambrian using SLIDE

3.2.42 Slide at Scrapsgate

At the end of January 1953, disastrous floods occurred on the east coast of England. These floods led to the failure of many banks of earth constructed on saltings. The slide at Scrapsgate is one of these banks failures. The failure occurred towards the landward side and extended from a vertical tension crack near the top of the seaward slope to the toe of the slip. The bank fill consisted of brown London Clay. The fill was placed on a foundation site consisting of a 22-ft deep layer of soft grey organic peaty silty clay. A layer of firm to stiff grey-brown London Clay underlies the soft clay (Fig.3.111). Golder et al. (1954) conducted a short term analysis for the bank fill using the profile shown in Fig.3.112. and a factor of safety of 1.3 was obtained. Fig.3.113. shows the results of analyzing the slope using SLIDE.

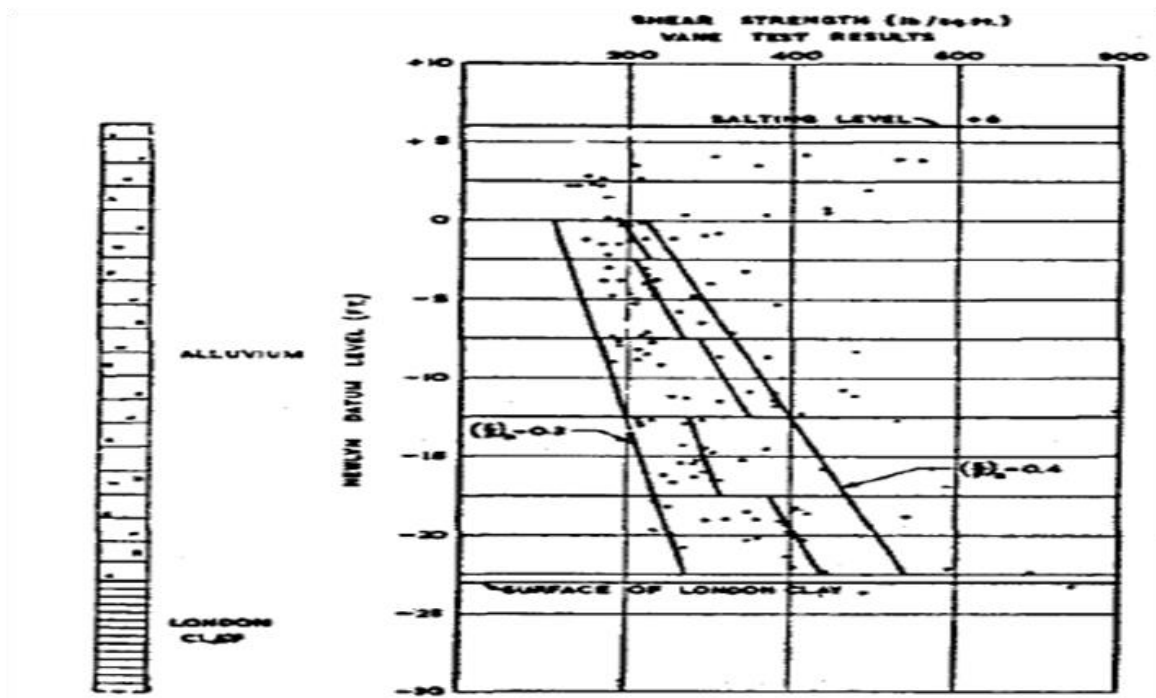


Figure 3. 110 Shear Strength Values at Scrapsgate (Golder et al. 1954)

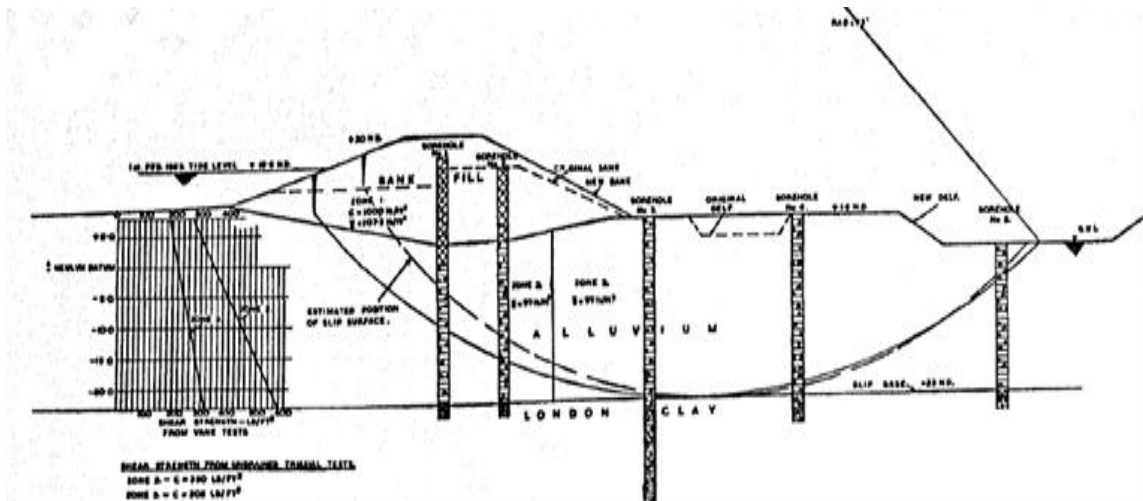


Figure 3. 111 Stability Analysis at Scrapsgate (Golder et al. 1954)

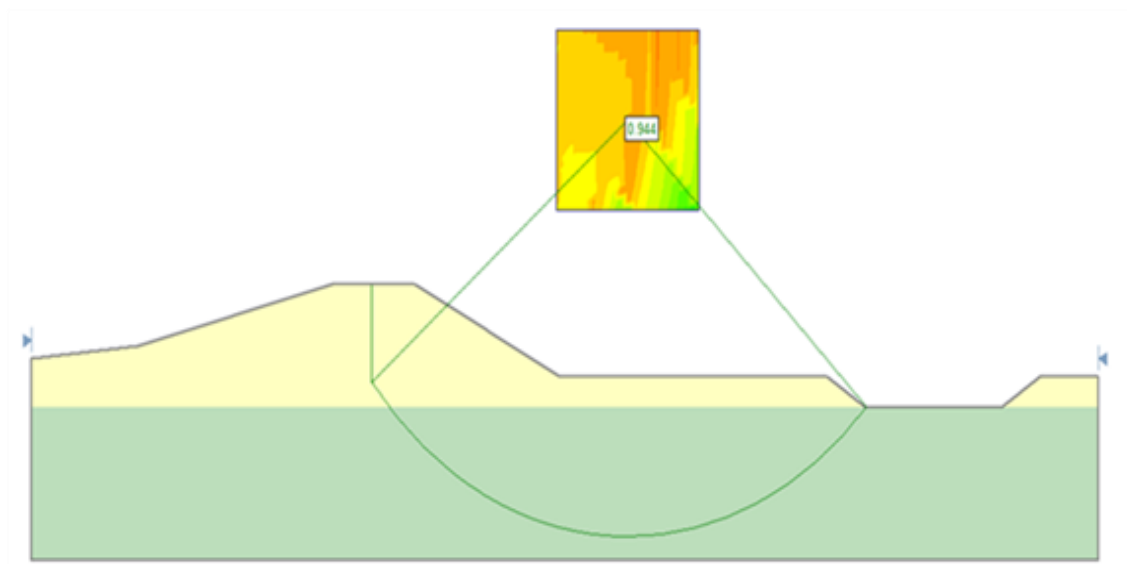


Figure 3. 112 Stability Analysis using SLIDE

3.2.43 Slide at Scottsdale

In February 1965, a major slip failure occurred along the Scottsdale Railway Levée in Launceston, Australia. The Scottsdale Railway portion of the levee was designed to be built in three stages. The first stage was constructed as an extension to the existing railway embankment and was completed in July 1962. The second stage began in January 1965 and was completed on 5th February, 1965. One day after the construction of the second stage, the slip occurred. The levees consisted of an imported sandy clay. It was constructed with a total length of 150 ft and net height of 7 ft above ground level. The foundation soil consisted of a soft black clay layer extending to a depth of 50 ft. A sand layer underlies the clay. Fig.3.114. shows the soil properties of the site.

Parry (1968) conducted a total stress analysis for the Scottsdale levee and a minimum factor of safety of 1.6 was obtained. The factor of safety is recalculated by adopting the total stress analysis and using SLIDE software (Fig.3.115).

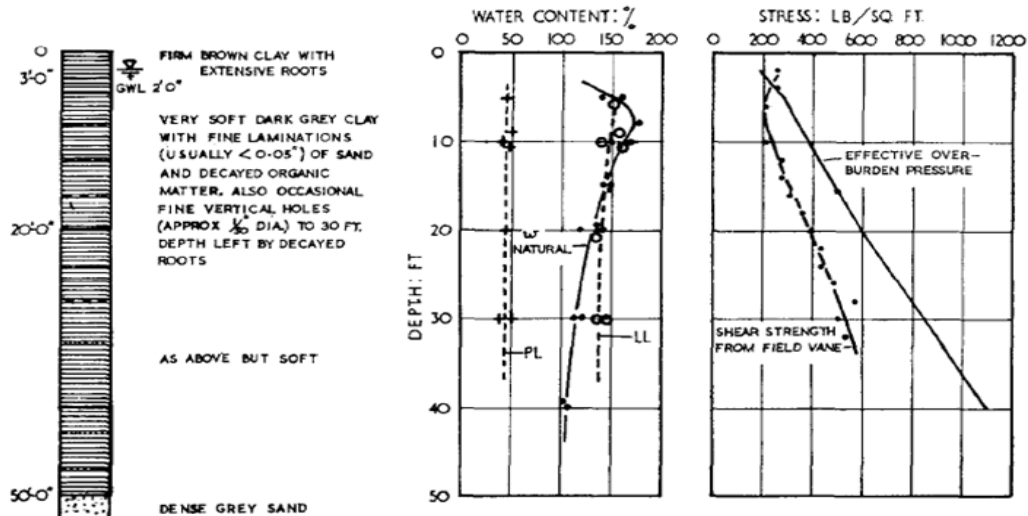


Figure 3. 113 Soil Properties at Scottsdale (Parry 1968)

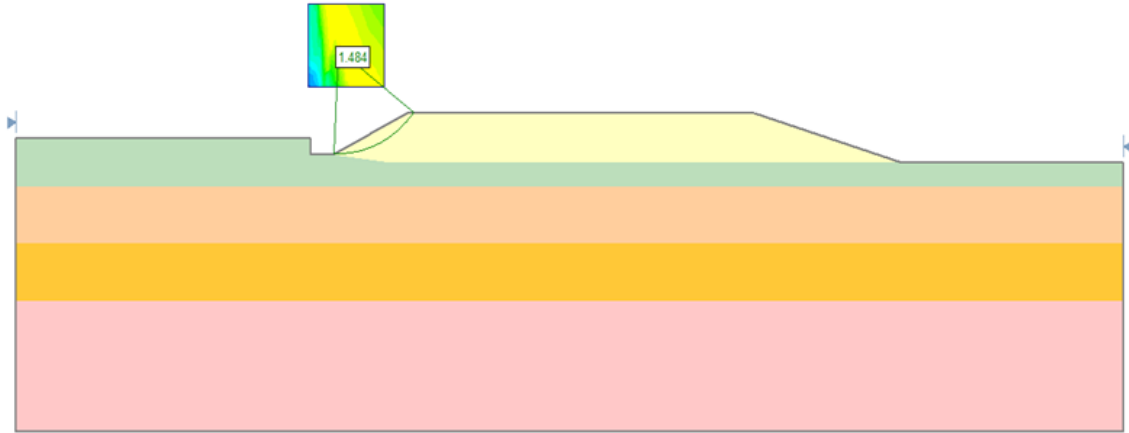


Figure 3.114 Critical Slip Surface using SLIDE

3.2.44 Slide at Iwai

The site is located on the Holocene lowland in Ibaraki Prefecture in Japan. The foundation soil consisted of an organic clay layer bounded between two clay layers (C1 & C2). The soil properties of the layers are shown in Fig.3.116. and Fig.3.117.

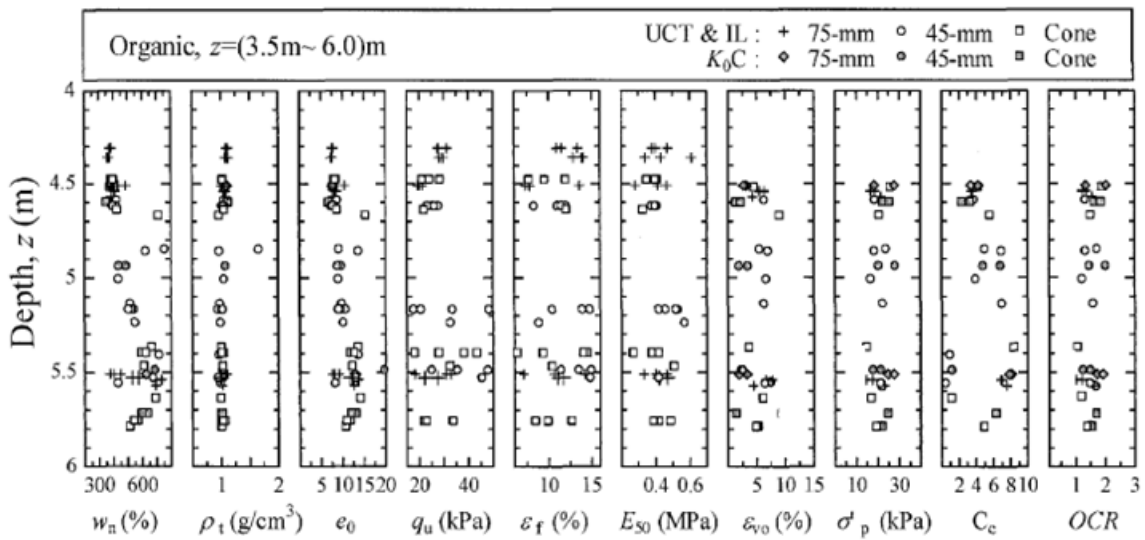


Figure 3.115 Soil Properties of Organic Clay (Shogaki et al. 2008)

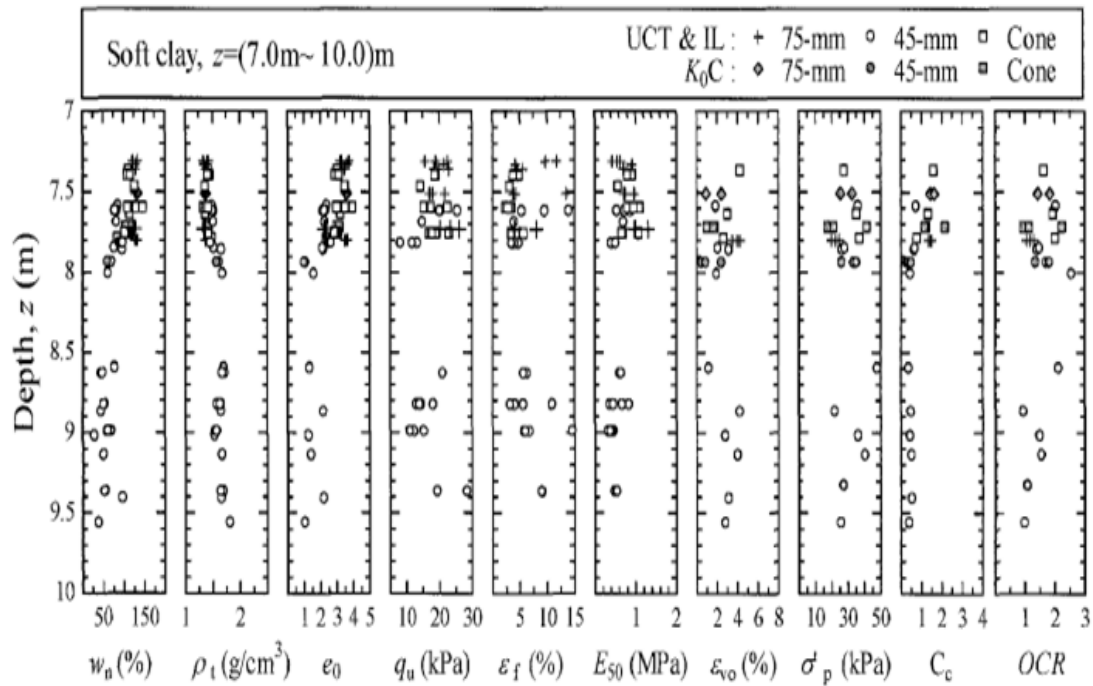


Figure 3.116 Soil Properties of Clay1 & Clay2 (Shogaki et al. 2008)

The failure embankment was studied by Shogaki et al. (2008) to examine the effect of soil variability and plasticity index on the inherent strength anisotropy of the soft clay layers. Shogaki et al. (2008) conducted a total stress analysis by using the strength measured by Unconfined Compression tests for the slope geometry shown in Fig.3.118. The failure surface was assumed circular with a tension crack appearing in the embankment height. The factor of safety is recalculated using SLIDE software and the results are shown in Fig.3.119.

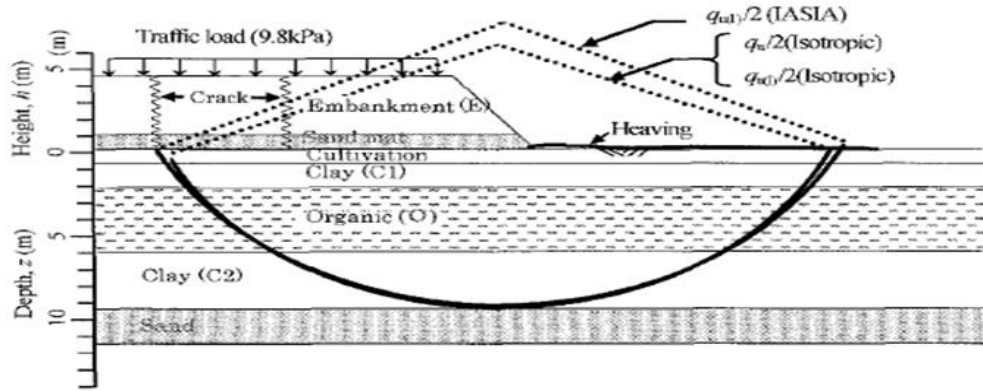


Figure 3. 117 Total Stress Stability Analyses (Shogaki et al. 2008)

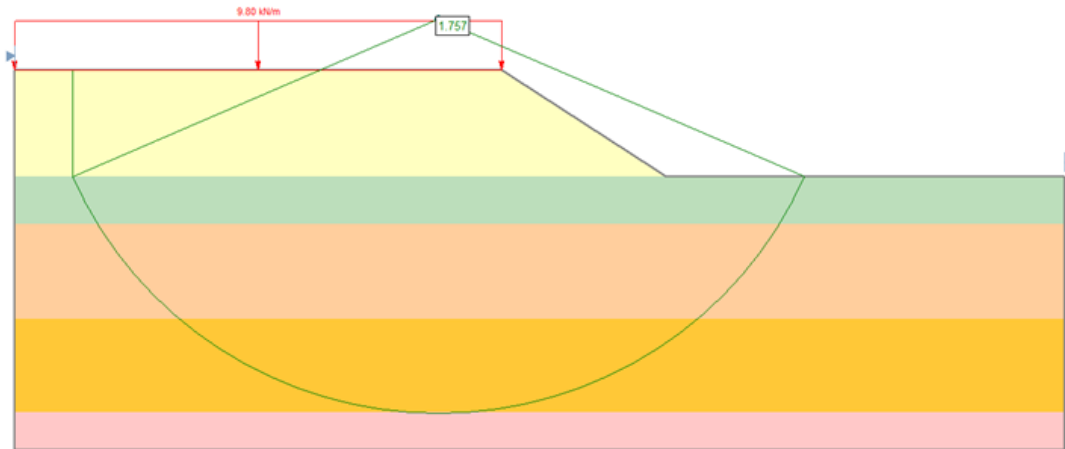


Figure 3. 118 Critical Slip Surface using SLIDE

3.2.45 Slide at Fair Haven

During the construction of a highway beginning at the New York State Border in Fair Haven, Vermont and ending at a section open to traffic in Castleton, Vermont, an embankment failure occurred in November 1971. The subsurface conditions consisted of a layer of brown and grey varved silt extending from the surface to a depth of 15 to 20 ft

(layer A). A layer of grey and blue varved silt (layer B) 10 to 15 ft in thickness was placed beneath layer A. Underlying layer B, a stratum of grey varved silty clay 10 ft in thickness (layer C) existed. Below the varved clay a 5 to 10 ft thick layer of grey silty sand resting on a shale bedrock was found. Atterberg Limits tests indicate that the clay had a LL = 37, PL = 21, and PI = 16 while the silt has a LL = 30 and is non-plastic. The fill has a unit weight of 130 pcf and an angle of internal friction of 35°. The properties of the different layers in the soil profile are:

- First layer: $\lambda = 119$ pcf, $c = 0$, $\phi = 30^\circ$
- Second layer: $\lambda = 57$ pcf, $c = 0$, $\phi = 30^\circ$
- Third layer: $\lambda = 57$ pcf, $c = 700$, $\phi = 0$
- Fourth layer: $\lambda = 165$ pcf, $c = 20000$, $\phi = 45^\circ$

Haupt and Olson (1972) performed a total stress analysis by assuming a circular failure surface (Fig.3.120.) a factor of safety of 1.66 was obtained. The factor of safety is re-evaluated by using SLIDE and a factor of safety of 1.88 resulted as shown in Fig.3.121.

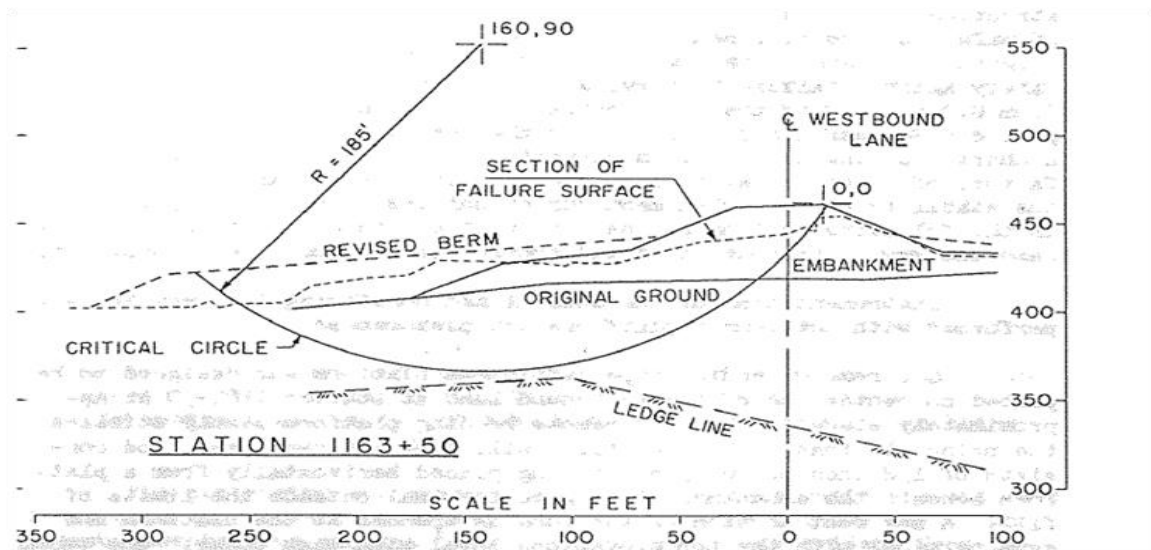


Figure 3. 119 Stability Analyses (Haupt and Olson 1972)

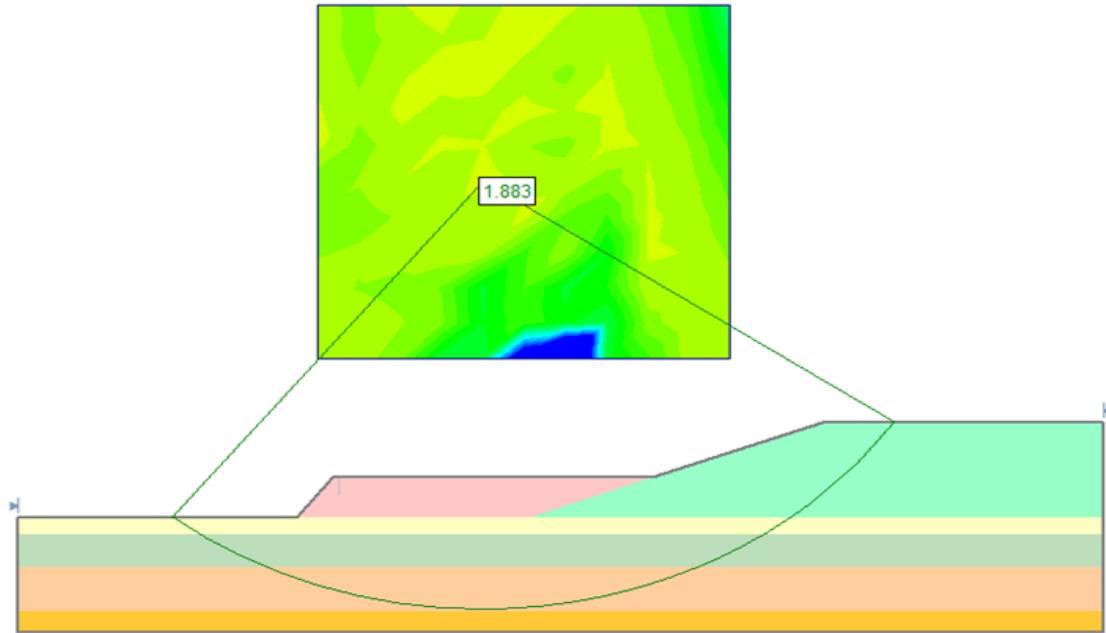


Figure 3.120 Critical Slip Surface using SLIDE

3.2.46 Slide at Boston Marine Excavation

In September 1993, an excavation failure occurred in Boston Marine Clay. The excavation is for the construction of 915m of I-90 adjacent to Logan Airport, Boston, Massachusetts. The failure took place when the excavation reached a depth of 13.4m. The stratigraphy from the ground surface downwards consisted of granular and cohesive fill, organic silt, and a thick layer of marine clay formed from a grey clay with inter layered silt seams of fine sands. The marine clay overlying glacial deposits (Fig.3.122) shows the undrained shear strength used for the analysis.

Limit equilibrium analyses were performed by McGinn et al. (1993) and a factor of safety of 0.97 was obtained as shown in Fig.3.123. Analysis using SLIDE is conducted and the results are shown in Fig.3.124.

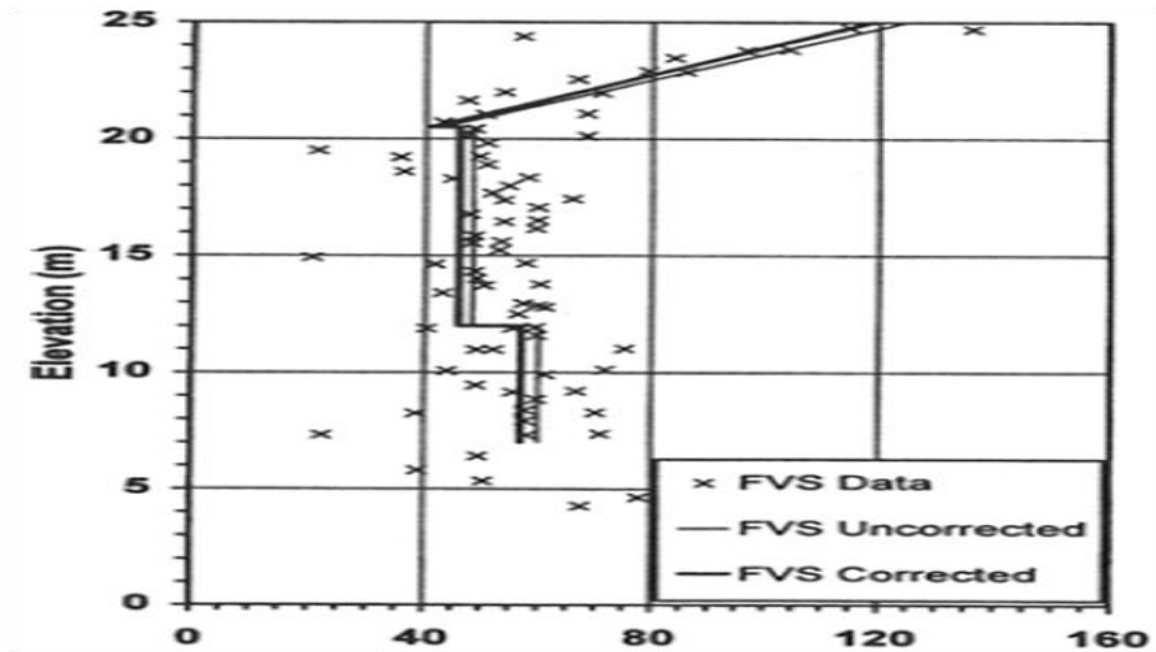


Figure 3. 121 Undrained Shear Strength using Field Vane (McGinn et al. 1993)

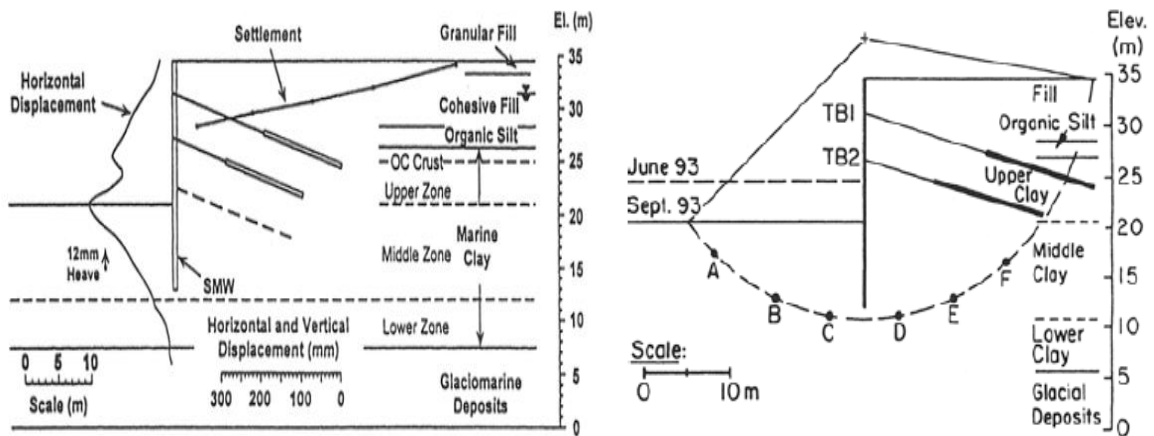


Figure 3. 122 Stability Analyses (McGinn et al. 1993)

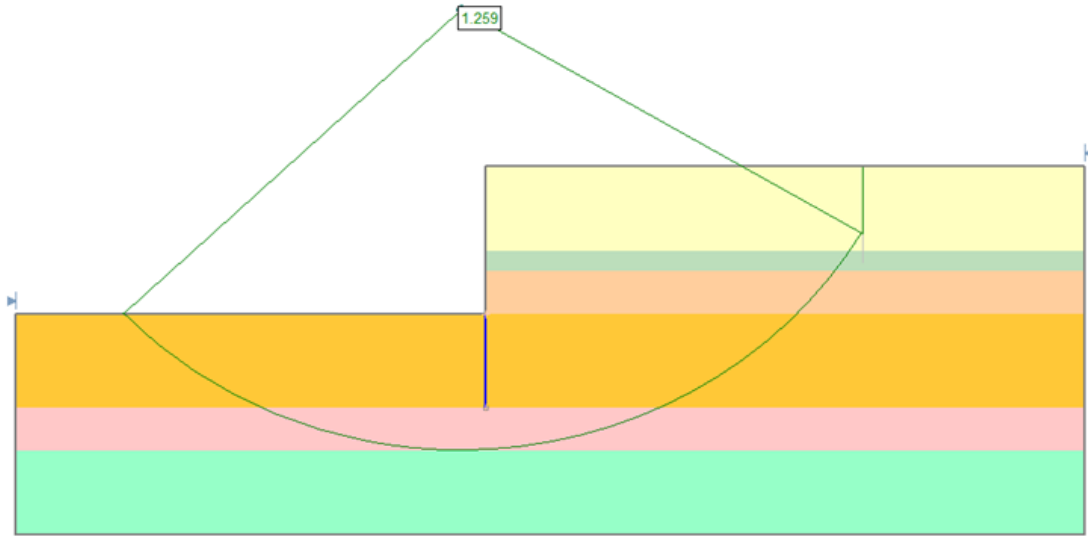


Figure 3. 123 Stability Analyses using SLIDE

3.2.47 Slide at Desert View Drive

In 1990, the failure of the Desert View Drive fill embankment occurred in La Jolla. The failure took place when an excavation group cut into the embankment to construct a building pad and house. The failure started as a circular mode and eventually increasing to a wedge type movement of the entire fill embankment. Total stress analysis was conducted by Day (1996) using the section shown in Fig.3.125. and the shear strength parameters $\phi = 18^\circ$ and $c = 24$ KPa. The analysis was carried out using the STABL computer program. The computer program, using the modified Janbu method of slices, calculated a minimum factor of safety of 1.15 for the fill embankment. The location of the critical failure surface is shown in Fig.3.125. Another analysis is conducted using SLIDE software. The results are shown in Fig.3.126.

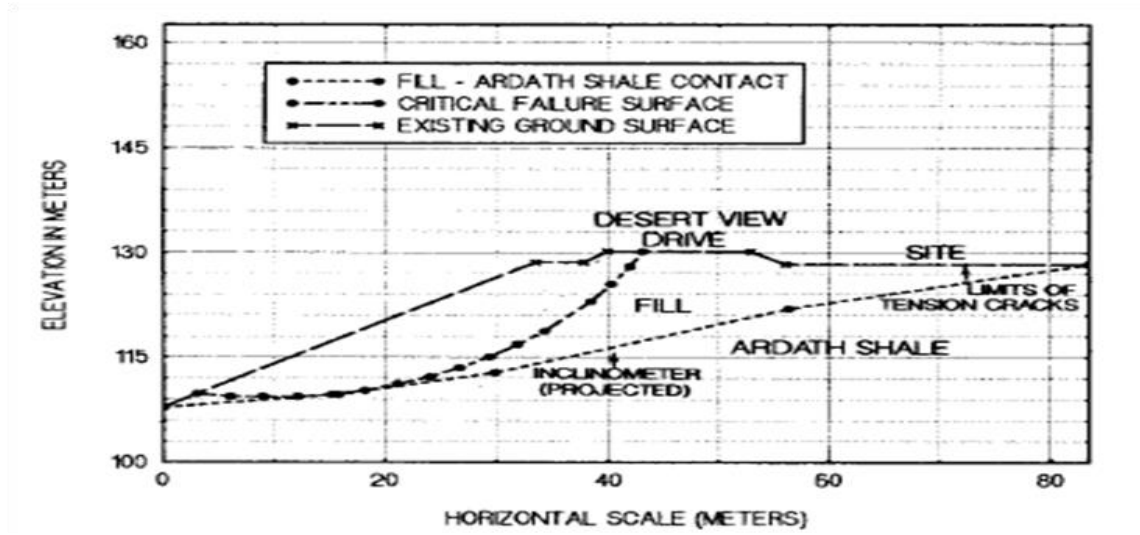


Figure 3. 124 Critical Slip Surface at Desert View Drive (Day 1996)

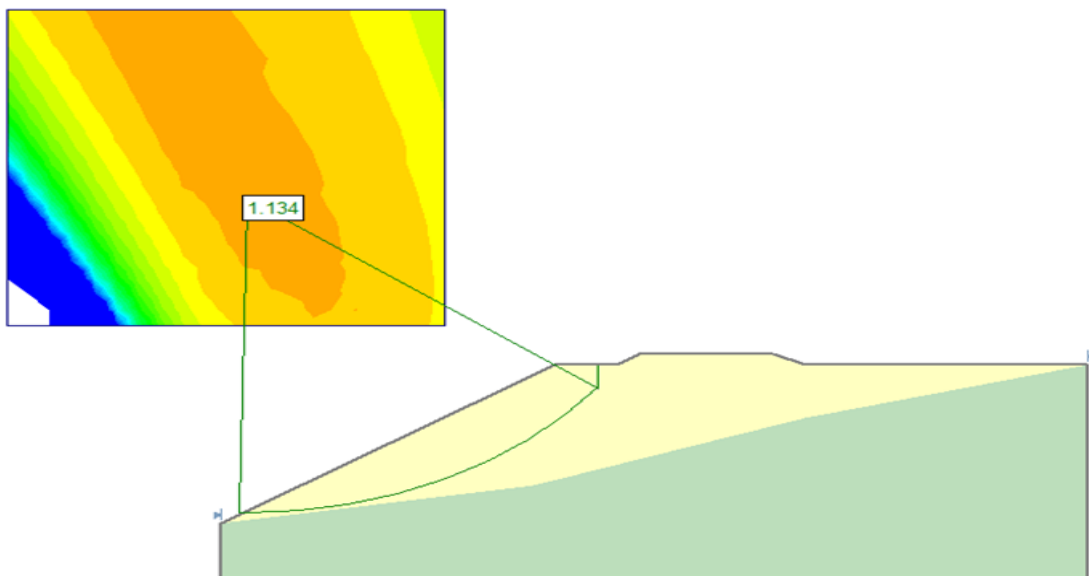


Figure 3. 125 Critical Slip Surface using SLIDE

3.2.48 Slide at Siburua

In the late evening of August 12, 1964, a slide took place in the downstream slope of a dam composed of shaley clay. The foundation soil consisted of a thin layer of sand and gravel underlain by a stratum of compacted clay core. Below the clay core, a layer of cored sandstone overlies a stiff shaley fat clay with brown and red weathering planes. Finally, an extremely hard red clay is found at the bottom. Wolfskill et al. (1967) conducted total stress analysis using different methods. The first method requires the equilibrium of a rigid free body of circular failure surface. The second method was the ordinary method of slices. Moreover, the authors used Bishop method for comparing the results of the factor of safety and finally they used the Morgenstern –Price general method of slices.

The authors conducted the analysis for the slides that occurred during different periods. They did the analysis for the slides that occurred on July 15, August 12, and October 5. The following table illustrates the results they obtained using different slope stability analyses methods. Fig.3.127. shows the geometry of the slope and the slip surface that was obtained.

Total stress analysis is conducted for the slide that occurred on October 5 which is considered the major slide in the dam. The analysis conducted using SLIDE software and the results are shown in Fig.3.128.

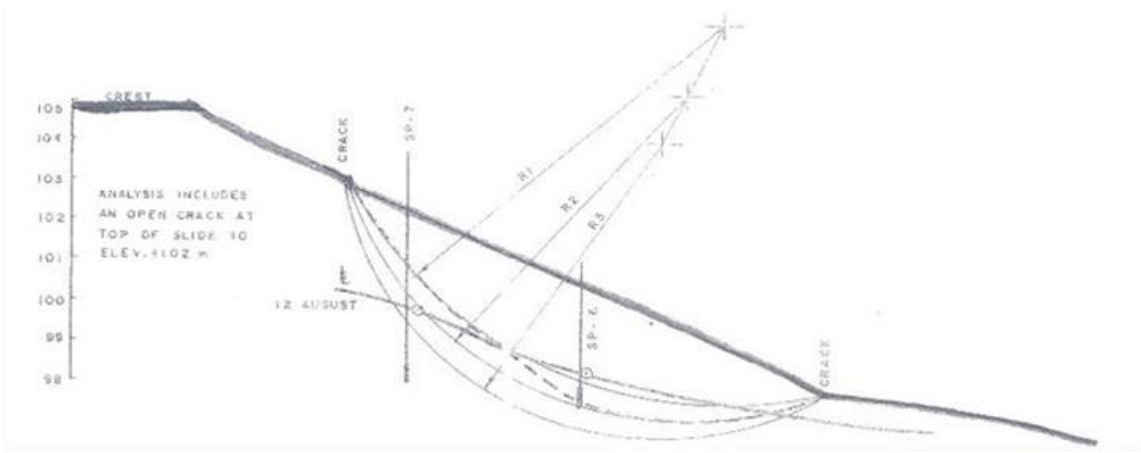


Figure 3.126 Total Stress Analysis at Siburua (Wolfskill et al. 1967)

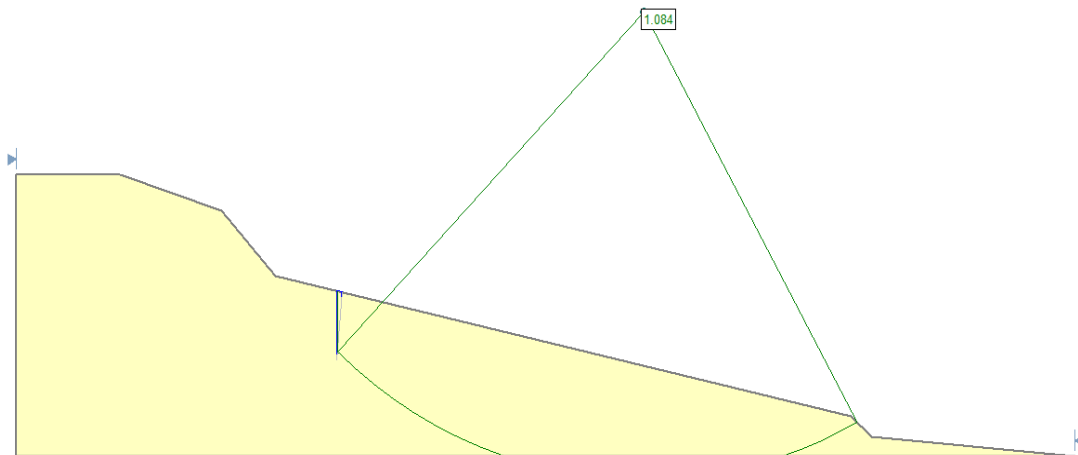


Figure 3.127 Stability Analyses using SLIDE

3.2.49 Slide at Tianshenqiao

On December 24, 1985, a landslide occurred at the Tianshenqiao Hydroelectric Power Project in Guangxi Province, China. The landslide killed 48 people. The slide area is on the right bank of the Nanpanjiang River. The slope consisted mainly of Quaternary alluvium and talus covered by road fill and underlain by middle Tertiary bedrock, composed of shales and sandstones. Table 3.7. shows the soil properties of the slope soil materials.

Table 3. 7 Geotechnical Soil Parameters used in the Stability Analysis for Tianshenqiao (Chen and Shoe 1988)

Soil layer	Description	Density ρ (g/cm ³)	Shear strength parameters	
			ϕ (deg)	C (kPa)
1	New fill, clay and debris mixture	1.85	21.8	19.6
2	Old fill, sand, clay, and debris mixture	1.85	21.8	19.6
3	Quaternary talus, clay with rock fragments	1.85	21.8	0.0
4	Quaternary alluvium, fine sand and medium sand	1.85	20.8	29.4
5	Quaternary alluvium, grey and dark silty clay	1.81	10.2	34.3
6	Quaternary alluvium, gravels and sands	1.90	24.2	0.0
7	Tertiary bedrock, shales, sandstones with limestone intercalations	2.40	45.0	39.2

Chen and Shoe (1988) conducted a total stress analysis for the profile shown in Fig.3.129. and using the soil properties shown in Table.3.6. A factor of safety of 1.03 was obtained. The factor of safety is re-calculated using SLIDE (Fig.3.130).

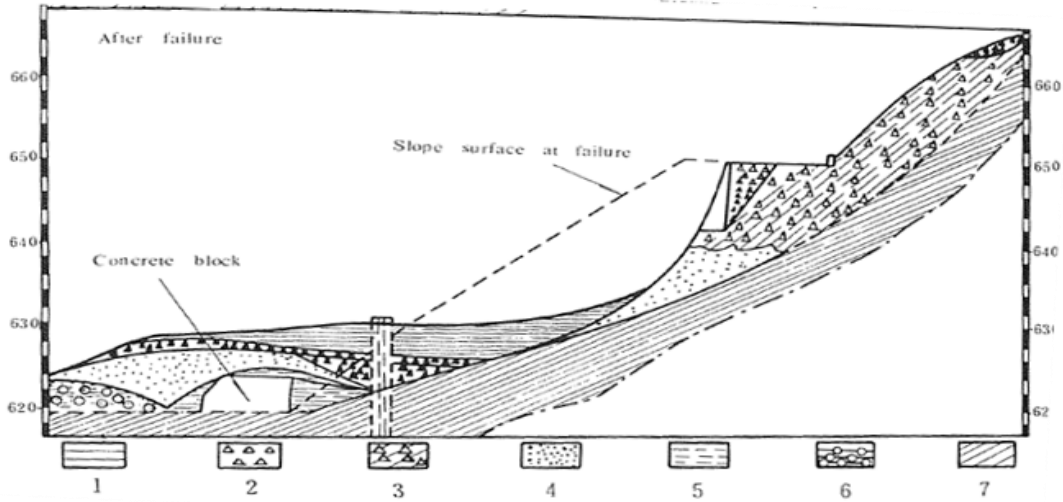


Figure 3. 128 Geological Profile at Tianshenqiao (Chen and Shoe 1988)

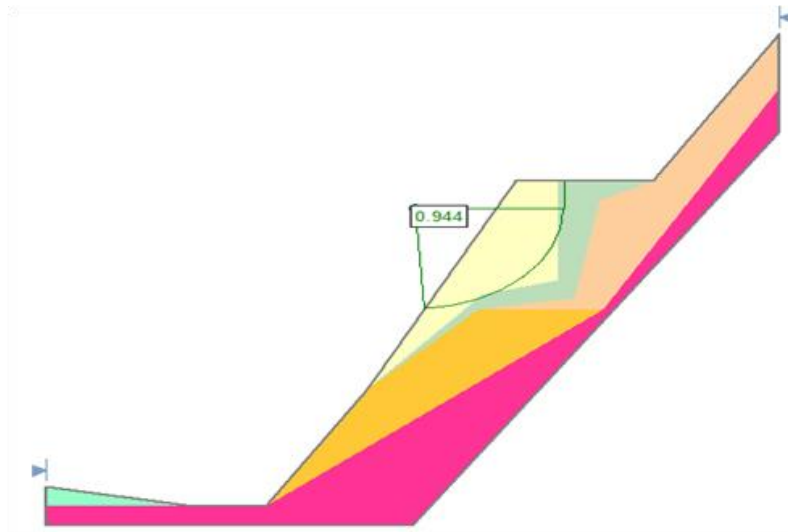


Figure 3. 129 Critical Slip Surface using SLIDE

3.2.50 Slide at San Francisco Bay

On August 20, 1970, a failure of a slope excavated underwater took place during construction of a new shipping terminal at the port of San Francisco. The soil conditions at the site were found to be quite uniform over the entire area. The profile consisted of about 80 ft to 100 ft of San Francisco bay mud underlain by firmer clays and sands. The San Francisco bay mud is a normally consolidated, slightly organic clayey silt or silty clay of marine origin. The clay has moderate plasticity, with a liquid limit of about 50% and a plastic limit of about 30%. Fig.3.131. shows the undrained shear strength profile determined by the Field Vane shear tests. Duncan and Buchignani (1973) conducted a total stress analysis of the site based on the undrained shear strengths and using the slope geometry shown in Fig.3.132. The authors obtained a factor of safety of 1.17. Moreover, the authors showed that the effect of sustained loading (creep) under undrained conditions was probably the reason to reduce the shear strength and cause the failure.

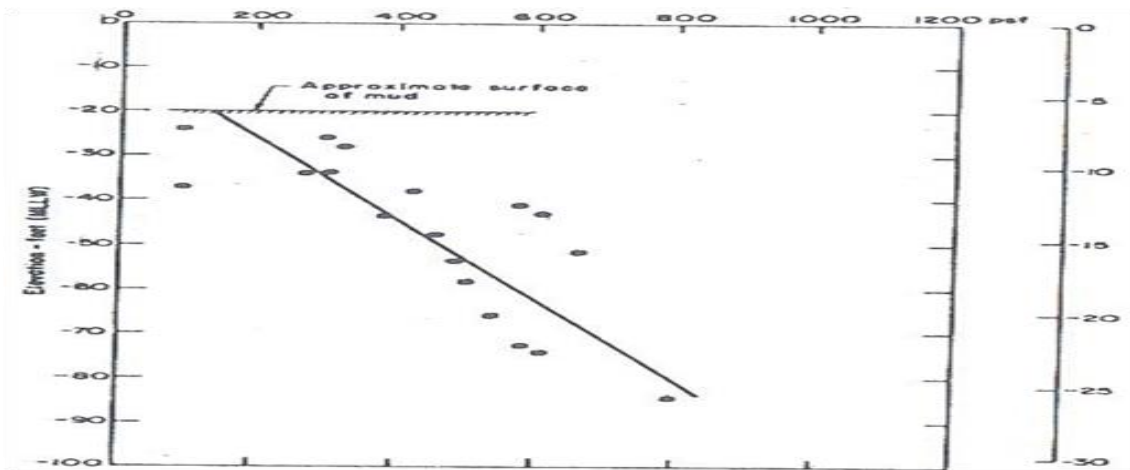


Figure 3. 130 Undrained Shear Strength using Field Vane Tests (Duncan and Buchignani 1973)

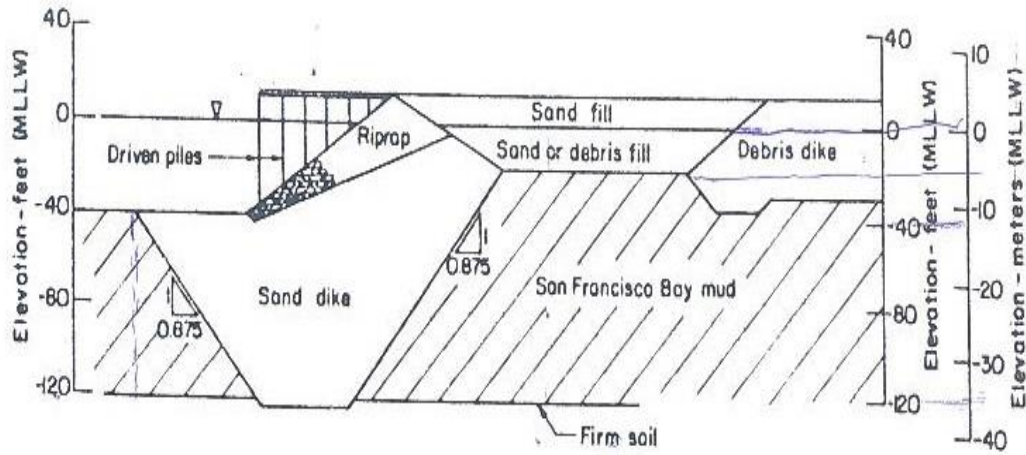


Figure 3.131 Slope Geometry at San Francisco (Duncan and Buchignani 1973)

Duncan and Wright (2003) performed new slope stability calculations using a program with Spencer's procedure of slices. The minimum factor of safety calculated was 1.17.

The factor of safety is re-calculated by using SLIDE software and a factor of safety of 1.2 is obtained as shown in Fig.3.133.

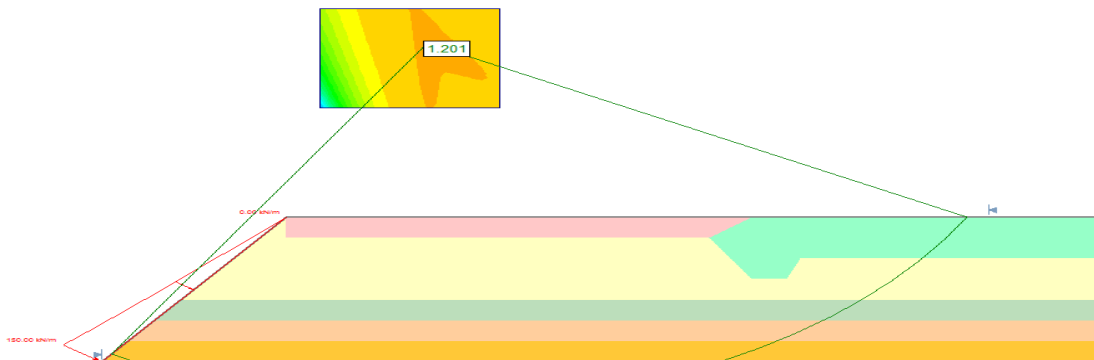


Figure 3.132 Critical Slip Surface using SLIDE

3.2.51 Slide at Carsington

In June 1984, a failure occurred in Carsington Dam. The dam is located near the village of Hognaston in Derbyshire. The failure occurred due to the heavy rainfall that caused cracks in the dam followed by total failure. The foundation strata consisted of the materials shown in Table 3.8.

Table 3.8 Soil Stratification at Carsington Dam (Skempton and Coats 1985)

SITE IDENTIFICATION		SYMBOL IN TRIAL PIT LOGS	CLASSIFICATION AND DESCRIPTION
Topsoil		TS	Topsoil
Subsoil		a ₁	<u>Head deposits</u> Stiff brown and grey friable clay
Yellow Clay	Yellow Clay (a)	a ₂	Firm and stiff light grey and yellow/orange mottled clay. Both a ₁ and a ₂ contain some angular/subangular sandstone and limestone fragments, and rare rounded quartz pebbles
	Yellow Clay (b)	b ₁ & b ₂	<u>Weathered Bedrock</u> Soft to stiff grey, brown & yellow mottled clay with rare sandstone and coal fragments [Residual Soil]
Dark Clay		b ₃	Soft dark grey and black clay with some very weak mudstone peds. [Highly brecciated and completely weathered mudstone]
Brecciated Mudstone		b ₄	Dark grey laminated, highly weathered mudstone; very weak
Blocky Mudstone		b ₅	Dark grey laminated, moderately weathered mudstone

A stability analysis was carried out by Skempton and Coats (1985) by dividing the sliding mass above the slip surface into a number of vertical slices and by assuming that the forces between the slices are inclined at an angle of 10° to the horizontal. The authors used the profile shown in Fig.3.134. to evaluate the factor of safety. A factor of safety of

1.1 was obtained. Another total stress analyses is carried out in this study by taking the same profile and soil properties. The results are shown in Fig.3.135.

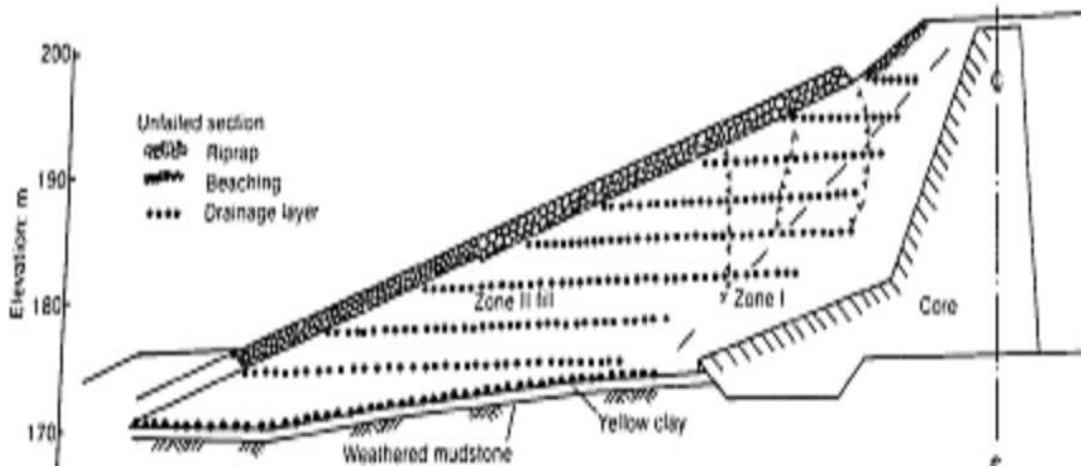


Figure 3. 133 Profile at Carsington Dam (Skempton and Coats 1985)

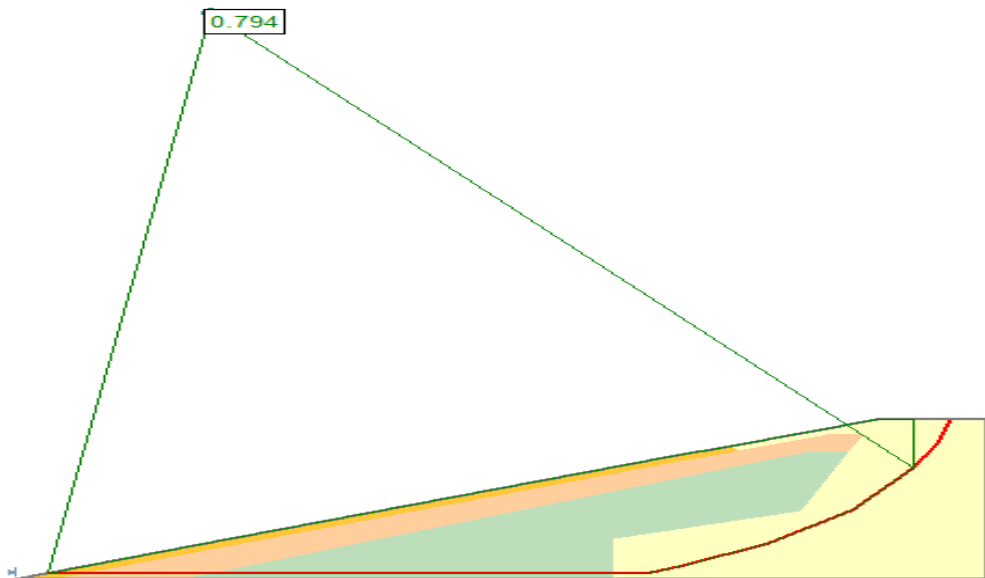


Figure 3. 134 Critical Slip Surface using SLIDE

3.2.52 Slide at Atchafalaya

In December 1964, the construction of the Atchafalaya test sections was commenced. Six months after construction of the test sections, two test sections had moved laterally to the extent that cracks developed in the surface of the fills. In this study the test section that exhibited more cracks was considered for analysis. The fill consisted of fat clay and the soil properties of the site including the index parameters, undrained shear strength, unit weight and the preconsolidation pressures are shown in Fig.3.136.

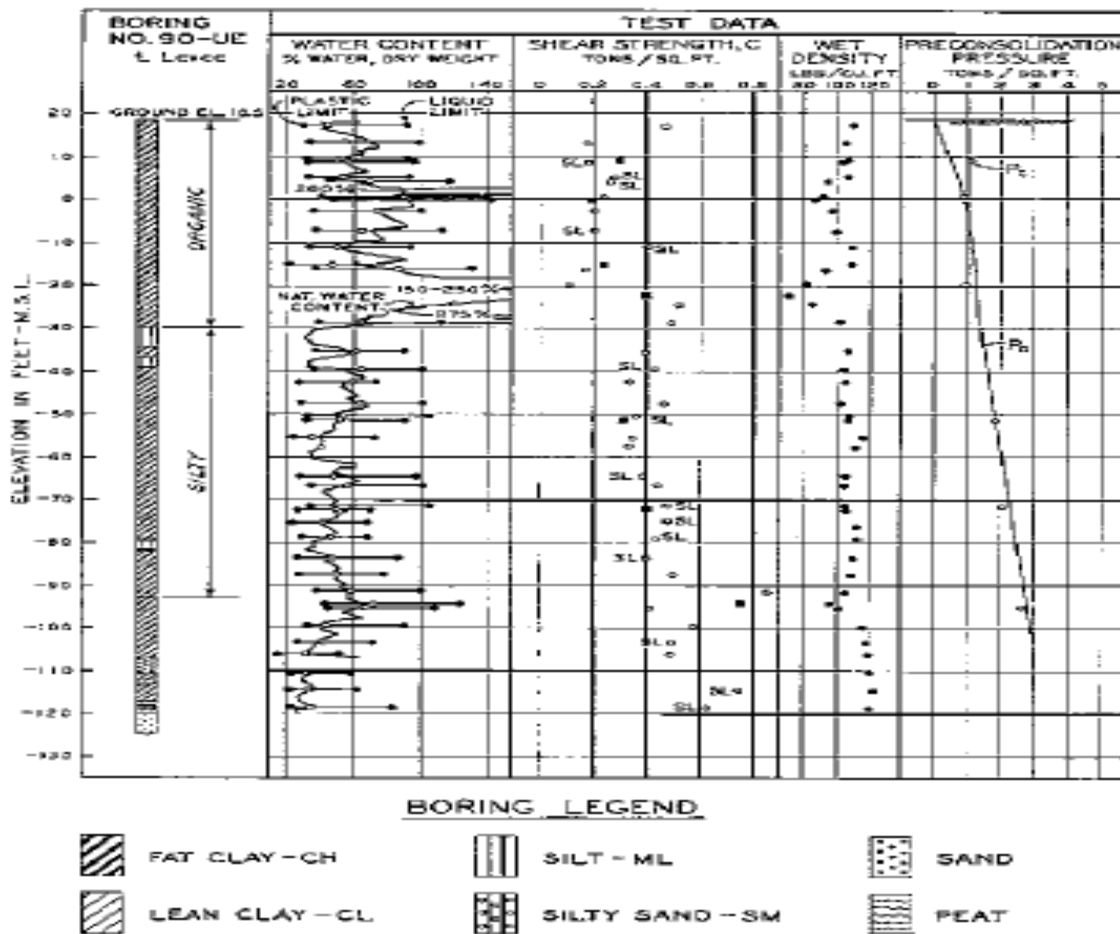


Figure 3. 135 Soil Properties at Atchafalaya Levees (Kaufman et al.1967)

Kaufman et al. (1967) conducted a total stress analysis for the test section using the soil properties shown in Fig.3.136 and using the geometry shown in Fig.3.137. The factor of safety was evaluated and a value of 1.10 was obtained. The factor of safety is recalculated using the SLIDE software as shown in Fig.3.138.

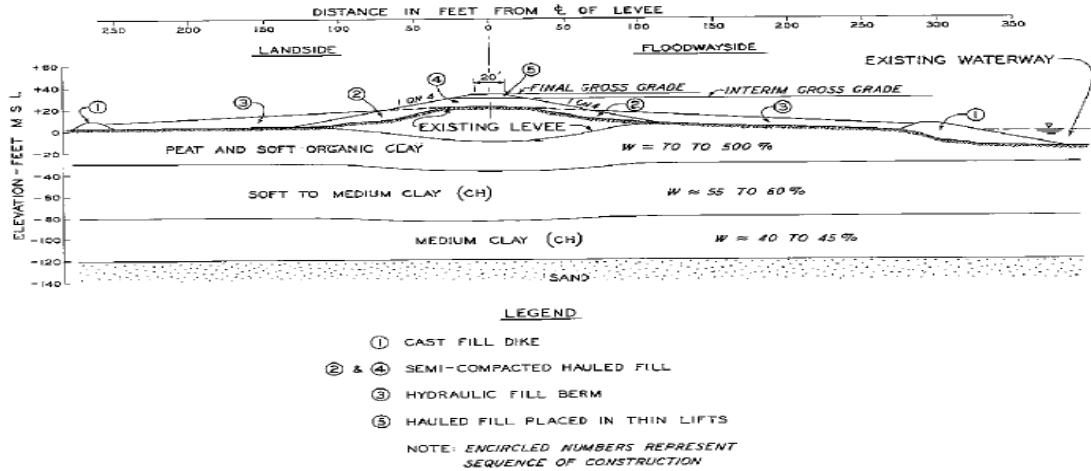


Figure 3. 136 Geometry and Soil conditions at Atchafalaya Site (Kaufman et al. 1967)

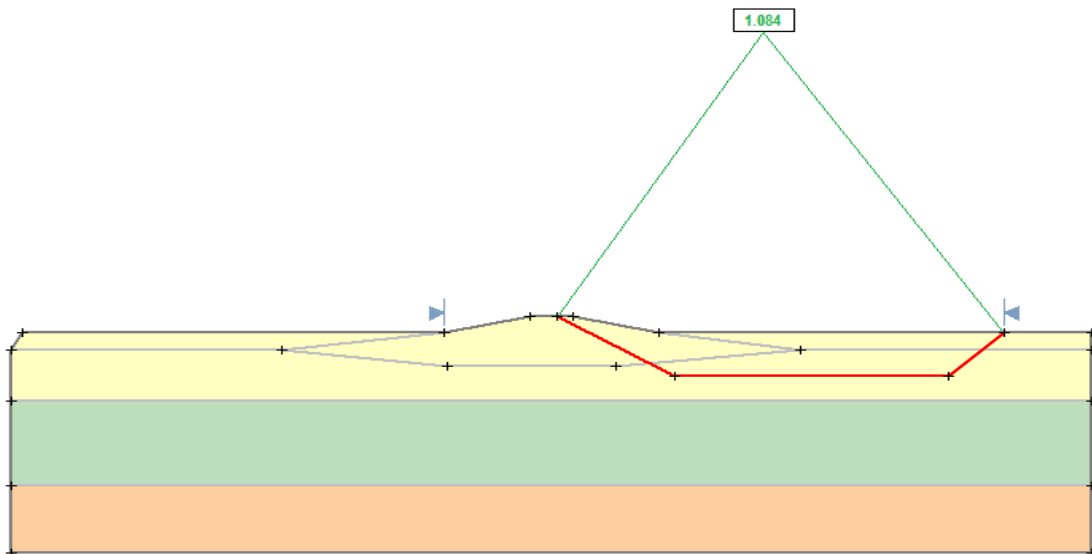


Figure 3. 137 Critical Slip Surface using SLIDE

Table 3. 2. Soil Properties Adopted for the Analyses of the 52 Cases

Case Number/ Slope Name	Slope Type/ Fill Type	Ø° Fill	Layer Name	H (m)	γ (t/m ³)	Su_U (t/m ²)	Su_R (t/m ²)	Su test type	LL (%)	PI	LI	S	Notes	
(1) Nesset	Fill/ granular	35	Fill	3	1.9	-	-	-	-	-	-	-		
			Clayey silt	5	1.72	0.9	2.71			40	40	1	3.5	
			Clay I	2.5	1.77	1.5	2.2	FC,UC	44	50	1.27	7	a,c,m	
			Clay II	2.5	1.7	1.5	0.36			39	50	1.69	42	
			Sand (Ø = 30°)	7	2	-	-			-	-	-	-	
(2) Presterødbakken	Fill/ granular	30	Fill	3	1.9	-	-	-	-	-	-	-		
			Dry Crust	7	1.8	2.2	0.48	FC,UC,VT	43	45	1.111	4.5	a,c,m	
			Clayey Silt	13	1.8	1	0.333			35	45	1.667	30	
(3) As	Fill/ clayey	-	Fill	2	1.9	2	2			-	-	-	-	
			Dry Crust	2	2	4.5	2.25			38	30	0.53	2	
			Silty Clay 1	1	1.84	2.5	0.833	FC,UC,VT	42	21	0.14	3	a,c,m	
			Silty Clay 2	3	1.85	1.5	0.5			38	18	0.38	3	
			Silty Clay 3	14	1.84	1	0.045			38	18	1.6	22	
(4) Skjeggerød	Fill/ granular	30	Fill	2	2	-	-	-	-	-	-	-		
			Dry Crust 1	2	2.1	8	4			45	15	0.167	2	
			Dry Crust 2	2	1.6	2	0.667	FC,UC,VT	78	36	0.916	3	a,b	
			Clayey silt	6	2.1	1	0.016			30	10	1.5	62	
			Silty Clay	10	1.9	1	0.034			28	10	1.22	29	
(5) Tjernsmyr	Fill granular	40	Fill	1.5	1.9	-	-	-	-	-	-	-		
			Peat	2	1.4	0.6	-			-	-	-	-	
			Silty Clay 1	1	1.88	1.2	0.0315	FC,UC	35	16	2	38	a,c,n,m	
			Silty Clay 2	4	1.74	1.1	0.073			40	15	1.2	15	
			Silty Clay 3	1	1.79	1.5	0.021			32	10	2.5	70	
			Silty Clay 4	12	1.86	1.1	0.078			38	13	1.5	14	
(6) Aulielva	Fill/ granular	30	Fill	2	1.9	-	-	-	-	-	-	-		
			Dry Crust	2.5	1.76	4	1			40	18	0.8	4	
			Silty Clay 1	4.5	1.75	2	0.4	FC,UC,VT	52	24	0.85	5	a,b	
			Silty Clay 2	2	1.8	1.85	0.617			58	33	0.5	3	
			Silty Clay 3	11	1.85	3	1			58	33	0.5	3	
(7) Falkenstein	Fill/ granular	35	Fill	4	1.9	-	-	-	-	-	-	-		
			Organic Silt with Sand	2	1.74	3.2	3.2			-	-	-	-	
			Clayey silt with gravel and shells	5	1.64	0.8	0.011	FC,UC	25	5	3	70	a,b	
			Silty Clay 1	2	1.92	1.2	0.022			21	9	2.2	50	
			Silty Clay 2	11	2	5.25	0.04			22	10	2.9	127	
(8) Jalsberg	Fill/ granular	35	Fill	2.5	1.9	-	-	-	-	-	-	-		
			Dry Cryst 1	1	1.94	1.5	2			-	-	-	1	
			Dry crust 2	1	1.8	1.5	0.75			-	-	-	2	
			Silty Clay 1	1	1.8	0.9	0.456			-	-	-	2	
			Silty Clay 2	3	1.78	0.9	0.225	FC,UC,VT	-	-	-	-	4	a,b
			Silty Clay 3	2	1.77	1	0.167			-	-	-	6	
			Silty Clay 4	2	1.72	2.5	0.5			-	-	-	5	
			Silty Clay 5	5	1.76	1.25	0.125			-	-	-	10	
Silty Clay 6	5	1.8	1	0.111			-	-	-	9				

Table 3.2.(Continued.)

(Case Number) Slope Name	Slope Type/ Fill Type	∅° Fill	Layer Name	H (m)	γ (t/m ³)	Su _U (t/m ²)	Su _R (t/m ²)	Su test type	LL (%)	PI	LI	S	Notes	
(9) Saint Alban	Fill/ granular	35	Fill	4	1.88	-	-		-	-	-	-		
			Top Soil	0.4	1.92	4	1.333		-	-	-	-		
			Clay Crust 1	1.2	1.68	3	0.2	CIU,UU,VT		55	25	1.4	15	a,b,d
			Clay Crust 2	3	1.68	3	0.2			60	100	1.4	15	
			More Silty 1	0.5	1.76	1.6	0.025			42	22	2.5	64	
			More silty 2	4.7	1.73	3	0.077			40	20	2	39	
(10) Narbonne	Fill/ granular	26	Fill	9.6	2.07	-	-		-	-	-	-		
			Soft Clay and Silt	2	1.96	2.8	1.12		42	21	0.4	2.5		
			Soft, organic clay and silt	2	1.9	3	0.375		42	21	0.95	8		
			Peat	1	1.73	2.9	0.045		40	19	2.31	64		
			Silty Sand with some clay	1.5	2.08	2.5	0.312	LVS,VS		30	10	0.91	8	a,b,d
			Sand, silt and clay of low plasticity 1	1.5	2.06	1.9	0.585			30	10	0.6	3.25	
			Sand, silt and clay of low plasticity 2	3	1.98	2	0.002			30	10	12	1000	
(11) Lanester	Fill/ granular	30	Fill	4	1.82	-	-		-	-	-	-		
			Dry Crust 1	1	1.6	3.6	3.6		-	-	-	1		
			Dry Crust 2	1	1.4	1.4	0.175		100	58	1.12	8		
			Dry crust 3	1.5	1.35	1.3	0.108		120	70	1.2	12		
			Soft, organic sandy clay and silt 1	1.5	1.33	1.533	0.191		120	70	1.12	8		
			Soft, organic sandy clay and silt 2	1	1.36	1.8	0.075	VS		100	50	2	24	a,b,d
			Soft, organic sandy clay and silt 3	1	1.39	1.95	0.244			120	70	1.12	8	
(12) Cubzac-les ports	Fill/ granular	35	Soft, organic sandy clay and silt 4	1	1.41	2.05	0.293		100	50	0.83	7		
			Fill	4.5	2.21	-	-		-	-	-	-		
			Dry Crust 1	1	1.3	4.5	1.56		80	60	0.42	2.88		
			Dry Crust 2	1	1.8	3	0.43		80	60	0.9	7		
			Dry Crust 3	1	1.22	2.2	0.667		140	90	0.52	3.3		
			Dry Crust 4	1	1.5	2.2	0.667		110	70	0.52	3.3		
			Soft, organic silty clay 1	1	1.48	2.2	0.55		90	50	0.75	4		
			Soft, organic silty clay 2	1	1.71	2.2	0.275	VS		90	50	0.7	8	a,b,d
			Soft, organic silty clay 3	1	1.43	2.2	0.55			110	70	0.75	4	
			Soft, organic silty clay 4	1	1.6	5	0.125			114	75	0.75	4	
Soft, organic silty clay 5	1	1.48	5	0.172		110	65		0.41	2.9				

Table 3.2. (Continued.)

Case Number) Slope Name	Slope Type/ Fill Type	∅° Fill	Layer Name	H (m)	γ (t/m ³)	Su _U (t/m ²)	Su _R (t/m ²)	Su test type	LL (%)	PI	LI	S	Notes
(13) Lodalen 1 (14) Lodalen 2 (15) Lodalen 3	Cut/ -	-	Clay with shells and sand 1	4	2	4	2	UC	38	18	0.3	2	c,e
			Clay with shells and sand 2	2	1.9	4	1		30	10	0.9	4	
			Clay with shells and sand 3	2	2	4	1.2		30	15	0.7	3.33	
			Clay with shells and sand 4	3	2	4	1.7		40	20	0.1	2.35	
			Clay with shells and sand 5	2	2	4	2		35	15	0.2	2	
			Clay with shells and sand 6	3	2	4	1.5		35	15	0.4	2.67	
			Clay with shells and sand 7	3	2	5	2.5		35	15	0.2	2	
(16) Rio de Janeiro	Fill/ granular	35	Fill	2.8	1.8	-	-	VS, UU	-	-	-	-	b,e
			Crust	2.5	1.5	1.5	1.5		160	100		1	
			Soft Grey Clay 1	2.5	1.3	0.75	0.21		130	80	0.8	3.6	
			Soft Grey Clay 2	2.5	1.3	0.96	0.31		120	80	0.75	3.1	
			Soft Grey Clay 3	2.5	1.3	1.2	0.41		100	65	0.65	2.9	
			Soft Grey Clay 4	2.5	1.3	1.4	0.51		100	65	0.4	2.74	
(17) New Liskeard	Fill/ granular	40	Fill	6	2.04	-	-	UC,UU,VS,SHANSEP	-	-	-	-	a,b
			Crust	5	2	4.8	0.1		70	10	2.5	48	
			Soft clay 1	7	1.3	2	0.067		30	10	4	200	
			Soft clay 2	10	1.3	1.2	0.06		30	10	4	200	
			Soft clay 3	2	1.3	2	0.06		30	10	4	200	
			Soft clay 4	8	1.3	3.2	0.16		30	10	4	200	
(18) Bangkok A	Fill/ granular	20	Fill	2	2	-	-	VS	-	-	-	-	a,b
			Crust	1	1.5	2.9	-		90	50	1.2	13	
			Clay 1	2	1.33	0.991	0.123		150	90	1	8	
			Clay 2	2	1.32	0.838	0.105		150	90	1	8	
			Clay 3	2	1.34	1.117	0.14		150	90	1	8	
			Clay 4	1.5	1.35	1.33	0.166		150	90	1	8	
			Clay 5	1	1.35	1.62	0.2		150	90	1	8	
Clay 6	1	1.37	1.755	0.22	150	90	1	8					
(19) DrammenV (20) DrammenVI (21) Drammen VII	Cut/ -	-	Very soft to soft grey silty clay 1	5	1.85	1	0.12	CIU,CID, UC, VS	38	18	1	8	b,e
Very soft to soft grey silty clay 2			5	0.85	1	0.123	35		15	1	8		
Very soft to soft grey silty clay 3			3	0.9	2	0.215	32		12	1.08	9		
Very soft to soft grey silty clay 4			4	0.95	2.5	0.4	32		12	0.83	6		

Table 3.2. (Continued.)

(Case Number) Slope Name	Slope Type/ Fill Type	∅° Fill	Layer Name	H (m)	γ (t/m ³)	Su _U (t/m ²)	Su _R (t/m ²)	Su test type	LL (%)	PI	LI	S	Notes
(22) Pornic	Fill/ clayey	40	Fill	4	2	1	1		-	-	-	-	
			Crust	2	2	2.5	2.5		-	-	-	1	
			Blue and brown very plastic Clay 1	3	1.5	1.4	0.14		80	45	1.22	10	
			Blue and brown very plastic Clay 2	5	1.5	4.2	0.42	VS	80	45	1.22	10	a,b
			Blue and brown very plastic Clay 3	4	1.5	5	0.5		80	45	1.22	10	
			Blue and brown very plastic Clay 4	3	1.5	4.5	0.45		80	45	1.22	10	
(23) Saint -Andre	Fill/ granular	35	Fill	3	2	-	-		-	-	-	-	
			Organic Clay	1	1.15	1.5	0.6		83	37	0.08	2.5	
			Very Peaty Clay	2	0.27	1.2	0.004	VS	-	-	-	300	a,b
			Peat	0.5	0.15	1.3	0.0048		-	-	-	300	
			Organic Mud	5	0.7	1.6	0.16		102	47	1.17	10	
(24) South of France	Fill/ granular	35	Fill	6.5	1.7	-	-		-	-	-	-	
			Soil 1	5	1	2.8	0.7		64	32	1	4	
			Soil 2	5	1	2.2	0.55	VS	64	32	1	4	a,b
			Soil 3	5	1.7	3	0.75		64	32	1	4	
			Soil 4	5	1.7	3	0.75		64	32	1	4	
(25) NBR Development	Fill/ granular	35	Fill	1.5	2.08	-	-		-	-	-	-	
			Medium plastic grey clay	3	1.75	3.8	0.475		58	33	1.2	8	
			Grey Clay of high plasticity 1	3	1.4	3	0.333		70	40	1.21	9	
			Grey Clay of high plasticity 2	3	1.48	2	0.286	VS	62	32	1.1	7	a,b
			Grey Clay of high plasticity 3	3	1.48	2.4	0.267		75	40	1.21	9	
			Light Grey Clay	3	1.7	3.2	0.32		42	12	1.22	10	
			Silt and Fine Sand	3	1.96	5	0.72		42	12	0.8	7	
(26) Portsmouth	Fill/ granular	30	Fill	-	17.28	-	-		-	-	-	-	
			Medium Clay	1.5	18.54	48	3.83		45	20	1.2	12.5	
			Soft Clay 1	1.5	18.54	14.4	3.83	VS	35	15	0.5	3.75	b,e
			Soft Clay 2	4.6	17.12	14.4	3.83		35	15	0.5	3.75	
			Soft Clay 3	3	18.85	14.4	3.83		35	15	0.5	3.75	
			Sand Silt (∅ =30°)	1.5	20.4	-	3.83		35	15	0.5	3.75	
(27) Kameda	Fill/ granular	35	Fill	6.3	1.9	-	-		-	-	-	-	
			Peat	5.5	1.15	2.4	0.8		-	-	-	3	
			Sandy Clay with Peat	2.2	1.6	3.35	1.116	UC,VS,qc	-	-	-	3	a,b,l
			Peat 2	3	1.212	4.025	1.35		-	-	-	3	
(28) KhorAl - Zubair no.4	Fill/ granular	35	Fill	11	1.85	-	-		-	-	-	-	
			Clay	5	1.8	2.5	0.156	VS	55	27	1.48	16	b,f,g
			Hard Failure	1	1.8	5000	1428		45	20	0.55	3.5	
			Clay	14	1.75	2.5	0.714		55	30	0.567	3.5	

Table 3.2. (Continued.)

Case Number)	Slope Type/ Slope Name	Fill Type	∅° Fill	Layer Name	H (m)	γ (t/m ³)	Su _U (t/m ²)	Su _R (t/m ²)	Su test type	LL (%)	PI	LI	S	Notes	
(29) Lian-Yun-Gang	Fill/ clayey	25		Fill	2	1.9	0.5	-			20	1.25	4		
				Top Crust 1	0.5	1.7	2.4	1.6			20	1	1.5		
				Top Crust 2	1	1.7	1.6	1.067			21	1	1.5		
				Clay 1	1	1.5	0.76	0.304			25	1.2	2.5		
				Clay 2	1	1.5	0.8	0.08			22	1	10		
				Clay 3	1	1.6	0.92	0.23	VS		30	1.25	4	a, b, h	
				Clay 4	1	1.6	1.06	0.424			30	1.5	2.5		
				Clay 5	1	1.6	1.2	0.6			30	1.75	2		
				Clay 6	1	1.7	1.7	0.68			30	2	2.5		
				Clay 7	1	1.7	1.8	0.72			30	2	2.5		
				Clay 8	4	1.7	1.9	0.76			30	2	2.5		
(30) Congress Street	Cut/ -	-		sand and miscellaneous fill (∅ = 30°)	1.8	17.3	-	-			28	13	0.385	3.25	
				Medium gritty blue clay 1	4.3	20.74	74.8	23	UC, VS	31	13	0.538	3.63	a, b	
				Medium gritty blue clay 2	6.1	20.11	43.18	11.87		32	14	0.538	3.63		
				Stiff to very stiff gritty blue clay	2.7	20.11	43.18	11.87		31	14	0.643	4		
(31) Daikoku-Cho Dike	Fill/ granular	30		Fill	15	1.5	-	-							
				Marine Clay 1	2.5	1.9	3	0.43		100	60	0.833	7		
				Marine Clay 2	2.5	1.9	4	1.334		110	55	0.64	3		
				Marine Clay 3	2.5	1.9	4	1.6	VS	120	61	0.426	2.5	a, b	
				Sand 1(∅ = 40°)	2.5	2	3.5	-		-	-	-	-		
				Sand 2(∅ = 30°)	-	2	-	-		-	-	-	-		
				Sand 3(∅ = 40°)	-	2	-	-		-	-	-	-		
(32) Cuyahoga AA	Fill/ granular	35		Fill	20	22	-	-							
				Glacial Till	3	18.9	191.5	83.3		30	20	1	2.3		
				Varved Clay	6	19.6	96	41.6	UC	30	20	1	2.3	a, c	
				Silty Clay	4.5	19.6	43	18.7		30	20	1	2.3		
				Organic Silty Clay	1.5	19.6	33.5	14.55		30	20	1	2.3		
				Varved Clay	18	19.6	96	41.6		30	20	1	2.3		
(33) King's Lynn	Fill/ granular	35		Fill	4.5	2.02	-	-							
				Upper Alluvial	1	1.7	3	1.2		62	22	0.091	2.5		
				Peat	1	1.2	1.8	0.1125		45	25	1.6	16		
				Lower Alluvial	1	1.7	2.2	0.0346		62	41	2.2	52		
				Lower Alluvial 2	1	1.7	3	0.0236	VS	60	32	2.72	93	a, b	
				Lower Alluvial 3	1	1.7	3	0.107		20	10	1.8	28		
				Sand(∅ = 30°)	0.6	2	-	-		-	-	-	-		
				Weathered Kimmeridge	1.2	1.7	4.2	1.3		60	42	0.476	3.25		
(34) Muar	Fill/ clayey	26		Fill	5.5	2.05	1.9	-							
				Crust	2	1.65	2.5	0.5		70	40	1.25	5		
				Very Soft Clay	6.1	1.55	1.1	0.3		80	45	0.888	3.67		
				Soft Clay	9.7	1.55	2	0.5	VS	70	40	1.125	4	b, e	
				Peat	0.5	1.5	1.1	0.5		75	45	0.67	2.2		
				Sandy Clay	4.6	1.6	3.5	0.75		68	43	1.2	4.67		
				Sand(∅ = 30°)	3	1.6	3.5	-		-	-	-	-		

Table 3.2. (Continued.)

(Case Number) Slope Name	Slope Type/ Fill Type	∅° Fill	Layer Name	H (m)	γ (t/m ³)	Su _U (t/m ²)	Su _R (t/m ²)	Su test type	LL (%)	PI	LI	S	Notes
(35) North Ridge Dam	Fill/ clayey	27	Fill	19	2.01	4.14	-		-	-	-	-	
			Sand(∅ = 29°)	4	1.81	-	-	UC	-	-	-	-	a,c
			Highly Plastic Clay	13	1.81	4.825	1.93		72	51	0.313	2.5	
(36) Seven Sisters Dike	Fill/Clay Fill Fill/Rock	13 35 -	Fill	4.2	1.94	2.54	-		-	-	-	-	
			Highly Plastic Clay	4.6	1.686	1.5	0.6	UC	-	-	-	-	
			Highly Plastic Clay	17	1.98	-	-		-	-	-	-	
(37) Shellmouth Dam Test Fill	Fill/ granular	43.5	Highly Plastic Clay (upper clay)	6.1	1.74	3.445	0.984		58	37	0.486	3.5	
			Sand(∅ = 38°)	2.8	1.96	-	-	UC	-	-	-	-	a,c
			Highly Plastic Clay (Lower clay)	6.4	1.74	3.445	0.984		58	37	0.486	3.5	
(38) Juban I	Fill/ Clayey	-	Fill 1	6	1.55	0.53	0.212		-	-	-	2.5	
			Fill 2	10	1.6	1.89	0.756	UC	-	-	-	2.5	c,i
			Foundation Soil	10	1.65	2.9	1.16		-	-	-	2.5	
(39) Bradwell	Cut/ -	-	Clay Fill	3.5	17.3	0.1	0.1		-	-	-	-	
			Marsh Clay	2.8	16.5	14.4	14.4	VS	-	-	-	-	a,b
			London Clay	9.8	18.9	86.2	43.1		92	67	0.104	2	
(40) Genesee	Fill/ clayey	-	Fill, weathered clay shale	22	1.8	7	7		-	-	-	-	
			Clay Crust	5	1.8	7	2.3		60	40	0.25	3	
			Un-weathered Clay	10	1.8	2.3	2.3	VS, UU	60	30	0	1	a,b,g
			Firm to stiff grey clay	10	1.8	5	2.3		25	7	0.2	2	
			Bedrock	5	2	500	500		-	-	-	-	
(41) Precambrian	Fill/ granular	35	Fill	9	20.5	-	-		-	-	-	-	
			Clay with low plasticity	2.3	17.75	72	8.95		40	25	-	8	
			Clay with medium plasticity	2.3	18.06	47.9	5.3	VS	30	15	-	9	a,b
			Low plastic clay with silt	4.6	17.3	38.3	2.54		30	2	-	15	
			Clay	15	18.9	24	1.484		30	2	-	16	
(42) scrapsgate	Fill/ clayey	-	Bank Fill	6.1	16.88	47.87	16.75		-	-	-	-	
			Sogt Organic silty clay with peat	7.6	15.71	16.75	3.35	UU,VS	67	47	-	3	a,b
(43) scottsdale	Fill/ granular	25	Fill	1.8	17.3	-	-		-	-	-	-	
			Brown Clay	0.9	17.3	10.53	4.25		145	100	0.4	2.5	
			Dark Grey Clay 1	2.1	17.3	10.05	4.02	VS	-	-	-	2.5	a,b
			Dark Grey Clay 2	2.1	17.3	14.36	5.75		-	-	-	2.5	
			Soft Clay	4.9	17.3	24	9.6		-	-	-	2.5	

Table 3.2. (Continued)

(Case Number) Slope Name	Slope Type/ Fill Type	ϕ° Fill	Layer Name	H (m)	γ (t/m ³)	Su_U (t/m ²)	Su_R (t/m ²)	Su test type	LL (%)	PI	LI	S	Notes
(44) Iwai	Fill/ granular	25	Fill	4.5	1.5	-	-		-	-	-	-	
			Clay 1	2	1.36	1.21	0.4033		67	34	0.5	3	
			Organic	4	1.01	1.55	0.484	UC	655	370	0.6	3.2	a,c
			Clay 2	4	1.36	1.23	0.41		67	34	0.5	3	
			Sand($\phi=30^\circ$)	1.5	1.6	-	-		-	-	-	-	
(45) Fair Haven	Fill/ granular	35	Fill	14	20.5	-	-		-	-	-	-	
			Berm($\phi=30^\circ$)	5.8	22	-	-		-	-	-	-	
			Brown and grey varved silt($\phi=30^\circ$)	2.6	18.7	-	-		-	-	-	-	
			Grey and blue varves silt($\phi=30^\circ$)	4.7	9	-	-	LVS	-	-	-	-	a
			Grey varved silty clay	6.4	9	33.5	2.6		37	16	1.31	13	
			Grey Silty($\phi=45^\circ$)	3	26	960	960		-	-	-	-	
(46) Boston Marine Excavation	Cut/ -	-	Cohesive Fill	8.1	1.8	6	6		-	-	-	-	
			Organic Silt	1.9	1.75	6.5	1.86		35	5	0.6	3.5	
			Upper Marine Clay	4	1.6	8	0.62		30	12	1.42	13	
			Middle Marine Clay	9	1.6	5	0.385	VS	30	12	1.42	13	a,b
			Lower Marine Clay	4	1.6	6	0.462		30	12	1.42	13	
			Glaciomarine Deposits	8	1.78	7	0.54		26	7	1.29	11	
(47) Desert View Drive	Fill/ clayey	18	Fill	V	2	2.4	0.96		-	-	-	2.5	
			Bedrock	V	2	500	-		-	-	-	-	a,b,j
(48) Siburua October 5		-	Compacted Clay Core	9	2.04	0.8	0.8	UU	45	21		1	a,k
(49) Tianshenqiao	Fill/ clayey	21.8	New Fill	V	1.85	1.96	0.784		-	-	-	-	
			Old Fill	V	1.85	1.96	0.784		-	-	-	-	
			clay with rock ($\phi=21.8^\circ$)	V	1.85	0	0		-	-	-	-	
			fine sand and medium sand ($\phi=20.8^\circ$)	V	1.85	2.94	1.176		-	-	-	-	
			grey and dark silty clay($\phi=10.2^\circ$)	V	1.81	3.43	1.372		-	-	-	-	
			gravels and sands ($\phi=24.2^\circ$)	V	1.9	0	0		-	-	-	-	
			Tertiary Bedrock ($\phi=45^\circ$)	V	2.4	3.92	1.568		-	-	-	-	
(50) San Francisco Bay	Cut/ -	-	Debris	V	0.39	4	-		-	-	-	-	
			Sand($\phi=30^\circ$)	V	2	-	-		-	-	-	-	
			Mud	10	0.6	1.6	0.04		50	20	2	40	
			Clay 1	5	0.6	2	0.05	UU	50	20	2	40	a,b
			Clay 2	5	0.6	3	0.075		50	20	2	40	
			Clay 3	5	0.6	4.2	0.105		50	20	2	40	

(Case Number)	Slope Type/ Fill Type	Ø° Fill	Layer Name	H (m)	γ (t/m ³)	Su _U (t/m ²)	Su _R (t/m ²)	Su test type	LL (%)	PI	LI	S	Notes
(51) Carsington	Fill/ clayey	-	Core	V	1.85	6.5	4.333		74	42	0.048	1.5	a
			Zone I	V	2.05	6.5	2.167	-	79	45	0.2	3	
			Zone II	V	2.1	6.5	6.5	-	-	-	-	1	
			Protection	V	1.85	6.5	6.5	-	-	-	-	-	
(52) Atchafalaya	Fill/ Clayey	-	Peat and soft organic Clay	12	15.71	31.6	1.975		100	70	1.5	16	a,c
			Soft to Medium Clay	15	17.28	42	14	UC,UU	90	65	0.492	3	
			Medium Clay	12	18.06	52.66	21		80	50	0.2	2.5	

Abbreviations

H: Layer Thickness

γ : Unit Weight

Su_U: Undisturbed Undrained Shear Strength

Su_R: Remolded Shear Strength

S: Sensitivity

FC: Fall Cone

UC: Unconfined Compression

VT: Vane Test

UU: Unconsolidated Undrained

CIU: Consolidated Isotropic, Undrained

LVS: Laboratory Vane Test

SHANSEP: Stress History and Normalized soils Engineering Parameters

CID: Consolidated Isotropic, Drained

q_c: Point Resistance measured in CPT

V : Variable

Notes

a : Remolded shear strength is calculated from sensitivity

b : Analysis based on Uncorrected Field Vane test

c : Analysis based on Unconfined compression test

d : Liquidity index is given

e : Remolded shear strength is given

f : Assume Atterberg limits

g : Assume high shear strength (500 t/m²) to indicate the presence of a hard layer

h : PI is estimated from figure

i : Correlation between dry unit weight and water content to get Unconfined compression strength

LVS : laboratory field vane

j : Sensitivity is assumed

k : Analysis based on Unconsolidated Undrained Testing

l: sensitivity is assumed

m: Field vane shear strength values are not clear in the paper

n: Peat properties are assumed

o: Fill properties are assumed

p: Lodalen (1), (2), and (3) have same properties but differ in the slope angle and the slope height

q:Drammen V, Drammen VI, and Drammen VII have same soil properties but different slope angle and height

CHAPTER 4

Quantification of Model Uncertainty and Investigation of the lower-bound factor of safety for slopes

4.1 Introduction

In slope stability analysis and design, one frequently uses models to evaluate the stability of slopes. These models represent the physical phenomenon of slope stability by mathematical or numerical solutions for the factor of safety of slopes. For instance, the Limit Equilibrium Methods of Bishop, Ordinary Method of slices, Janbu, and Spencer are popular methods among engineers for studying the stability of slopes. The effectiveness of these models has never been thoroughly tested due to the lack of databases of historical published records of slope failures. Databases are needed for evaluating biases and uncertainties in these models for predicting the factor of safety of slopes. In this chapter, the database discussed in chapter 3 and summarized in Table 3.1. is used to accomplish the following objectives: (1) quantify the model uncertainty of these slope stability models by evaluating the statistics {mean and coefficient of variation (COV)} and the probability distribution of the ratio of measured to predicted factor of safety for each method, and (2) investigate the presence of a lower-bound factor of safety that can be calculated using information on the slope geometry and site-specific soil properties.

4.2 Quantification of model uncertainty

4.2.1 The Importance of Quantification of Model Uncertainty

Model uncertainty is the uncertainty associated with the geotechnical model due to the inability of the model to fully represent the true physical behavior of a geotechnical system. Model uncertainty arises from unavoidable idealizations in analytical or numerical models for predicting engineering behavior. Mathematical modeling of any physical process generally requires approximations to create a usable model. Unavoidably, the resulting models are simplifications of complex real world phenomenon. Consequently there is uncertainty in the model prediction even if the model inputs are known with certainty.

The magnitude of model uncertainty is important for geotechnical decision making. If model uncertainty is not considered, the geotechnical predictions and hence the decisions based on the geotechnical predictions might be biased. Tang and Gilbert (1993) and Lacasse and Nadim (1994) noted that the calculated probability of failure without considering model uncertainty was not the actual failure probability of geotechnical systems.

4.2.2 Mean, COV, and Distribution Type of Model Uncertainty

The model uncertainty in a slope stability calculation method could be quantified from a database of slope failure case histories in terms of a mean (bias), a standard deviation (and/or Coefficient of variation) and a probabilistic density distribution of the

ratio of the measured to predicted factor of safety of the failed slopes. In this study, a framework for characterizing model uncertainty using observation data is proposed. The proposed framework is illustrated by characterizing the model uncertainty of four limit equilibrium methods for slope stability analysis (Bishop, Ordinary method of slices, Janbu, and Spencer).

4.2.2.1 Evaluation of the Statistical Parameters of the Model Uncertainty

In an initial analysis, predicted factors of safety for the 52 case histories presented in Table 3.1. are calculated using the SLIDE software for the four Limit Equilibrium Methods. In this analysis, values of undrained shear strength as reported in the original references (see Table 3.2) are used as input to the model. An investigation of the original references for the different case studies indicates that different types of tests were conducted for each case history to evaluate the undrained shear strength. In this initial analysis, only the results of field vane tests are adopted. For cases that do not include field vane records, the unconfined compression test results are adopted instead.

The 52 case histories include cohesive soils in the upper portion of the slope. Slope stability calculations usually show tension at the interfaces between slices as well as on the bottom of the slices. When tension develops, numerical problems in the slope stability calculations could occur (Duncan and Wright 2005). To overcome these problems the tension forces should be eliminated. Introducing tension cracks to the analysis can eliminate these tensile stresses. In the analysis conducted in this research study, an automatic tension crack search procedure using SLIDE software is applied.

To quantify the model uncertainty, the ratio of the measured factor of safety to that of the predicted factor of safety (λ) is calculated using SLIDE for the four Limit Equilibrium Methods for all the cases in the database. The predicted factors of safety from the different methods are presented in Table 4.1 for the 52 cases. Since the cases are actual historical failed slopes, the measured factor of safety could be realistically assumed to be approximately equal to 1. Based on this assumption, the ratio of measured to predicted factors of safety λ was calculated for all the cases in the database and for the different slope stability methods considered.

The calculated values of λ for the four models are presented in Fig.4.1 for the 52 cases analyzed in this study. Results on Fig. 4.1 indicate that the ratio of the measured to predicted factor of safety varies significantly between the different cases with minimum and maximum values of about 0.5 and 1.8, respectively. The mean value of the ratio of measured to predicted factor of safety λ is found to vary from 0.964 (for the Spenser method) to 1.036 (for the Janbu method). The mean of λ is a direct measure of the “bias” in the prediction model. Based on the statistics of λ as reflected in Table 4.2, it could be concluded that the 4 limit equilibrium methods could be considered to be relatively unbiased with mean values of λ that are very close to 1.0. The coefficient of variation (COV) of λ is an indication of model uncertainty. Results on Fig. 4.1 and Table 4.2 indicate that the predictions of the different models show considerable scatter with COVs ranging from 0.256 (for the ordinary method of slices) to 0.285 (for the method of Janbu). These COV values could be considered to be significant and in line with model uncertainties that are generally encountered in other areas of geotechnical engineering.

Table 4. 1 Predicted and Lower-Bound Factors of Safety for the Slopes in Database

NO	Slope Name	FS Bishop	FS OMS	FS Janbu	FS Spencer	LB Bishop	LB OMS	LB Janbu	LB Spencer
1	Neset	1.205	1.1	1.080	1.198	0.271	0.274	0.266	0.267
2	Presterødbakke	0.987	0.9	0.940	0.986	0.089	0.089	0.087	0.089
3	As	0.810	0.8	0.674	0.808	0.525	0.504	0.489	0.519
4	Skieggerod	0.700	0.7	0.642	0.702	0.01	0.011	0.01	0.012
5	Tiernsmvr	0.834	0.8	0.740	0.832	0.078	0.078	0.071	0.073
6	Aulielva	1.137	1.1	1.078	1.134	0.228	0.228	0.214	0.228
7	Falkenstein	1.071	1.0	1.067	1.067	0.318	0.322	0.616	0.546
8	Jalsberg	1.145	1.1	1.094	1.141	0.384	0.381	0.603	0.602
9	Saint Alban	1.276	1.1	1.197	1.272	0.047	0.047	0.048	0.05
10	Narbonne	0.698	0.7	0.657	0.697	0.18	0.18	0.142	0.148
11	Lanester	1.273	1.2	1.136	1.267	0.529	0.636	0.614	0.624
12	Cubzac-les	1.438	1.3	1.333	1.433	0.388	0.383	0.388	0.386
13	Lodalen1	1.012	1.0	0.926	1.010	0.399	0.399	0.371	0.398
14	Lodalen2	0.879	0.8	0.836	0.881	0.409	0.409	0.38	0.407
15	Lodalen3	1.153	1.1	1.115	1.156	0.496	0.496	0.463	0.493
16	Rio de ianeiro	1.148	1.1	1.139	1.150	0.586	0.591	0.635	0.626
17	New Liskeard	1.662	1.2	1.668	1.670	0.005	0.01	0.005	0.007
18	Bangkok A	1.803	1.7	1.727	1.800	0.057	0.057	0.058	0.057
19	DrammenV	0.602	0.6	0.547	0.600	0.052	0.052	0.047	0.053
20	Drammen VI	0.746	0.7	0.694	0.750	0.1	0.1	0.085	0.094
21	DrammenVII	0.870	0.8	0.819	0.873	0.109	0.109	0.103	0.111
22	Pornic	1.133	1.1	1.040	1.128	0.43	0.465	0.486	0.447
23	Saint -Andre	1.346	1.2	1.207	1.330	0.145	0.154	0.146	0.148
24	South of France	1.574	1.5	1.394	1.569	0.412	0.407	0.373	0.412
25	NBR	1.525	1.4	1.487	1.560	0.195	0.194	0.191	0.196
26	Portsmouth	0.843	0.8	0.805	0.839	0.2	0.198	0.177	0.198
27	Kameda	1.082	0.9	0.941	1.058	0.41	0.393	0.35	0.413
28	KhorAl - Zubair	1.387	1.1	1.319	1.396	0.421	0.417	0.409	0.448
29	Lian-Yun- Gang	0.987	0.8	0.958	0.987	0.608	0.459	0.613	0.605
30	Congress Street	1.457	1.4	1.349	1.456	0.624	0.622	0.621	0.624
31	Daikoku-Cho	1.042	0.9	0.890	1.029	0.365	0.358	0.3	0.361
32	Cuvahoga AA	0.900	0.9	0.803	0.901	0.391	0.391	0.353	0.392
33	King's Lvn	1.059	1.0	1.013	1.140	0.105	0.01	0.114	0.197
34	Muar	0.660	0.6	0.583	0.652	0.161	0.162	0.137	0.157
35	North Ridge	1.515	1.4	1.409	1.508	0.868	0.794	0.834	0.872
36	Seven Sisters	1.646	1.6	1.490	1.642	0.723	0.729	0.664	0.72
37	Shellmouth	1.125	1.0	1.051	1.113	0.323	0.442	0.272	0.302
38	Juban I	0.818	0.8	0.799	0.813	0.35	0.35	0.343	0.35
39	Bradwell	1.761	1.7	1.624	1.680	0.911	0.914	0.85	0.907
40	Genesee	1.001	1.0	0.935	1.001	0.557	0.557	0.532	0.555
41	Precambrian	1.022	0.9	1.041	1.046	0.081	0.085	0.097	0.089
42	scrapsgate	0.944	0.9	0.821	0.943	0.273	0.273	0.25	0.271
43	scottsdale	1.484	1.4	1.396	1.481	0.846	0.771	0.787	0.841
44	Iwai	1.732	1.7	1.732	1.757	0.682	0.68	0.498	0.755
45	Fair Haven	1.883	1.8	1.731	1.865	0.798	0.661	0.795	0.796
46	Boston Marine	1.259	1.2	1.147	1.254	0.251	0.251	0.251	0.251
47	Desert View	1.134	1.0	1.063	1.132	0.83	0.798	0.788	0.826
48	Siburua	1.084	1.0	0.992	1.083	0.881	0.881	0.866	0.882
49	Tianshenqiao	0.944	0.9	0.912	0.943	0.711	0.648	0.64	0.712
50	San Francisco	1.201	1.2	1.067	1.181	0.147	0.147	0.15	0.147
51	Carsington	0.830	0.7	0.751	0.822	0.466	0.484	0.443	0.477
52	Atchafalava	1.084	1.0	0.992	1.083	0.303	0.303	0.282	0.299

FS : Factor of Safety, LB: Lower-Bound

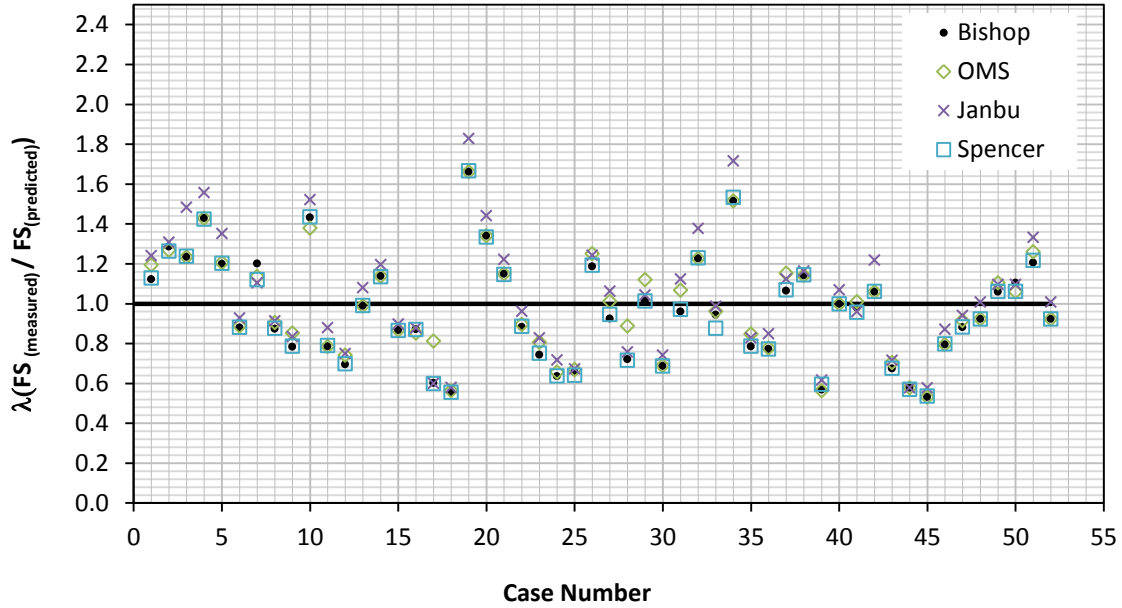


Figure 4. 1 Values of the ratio of measured to predicted factor of safety for the 52 case histories

The above results indicate that uncertainty in slope stability models for undrained slopes is considerable and needs to be incorporated in any reliability-based design analysis that aims at characterizing the risk of failure of undrained slopes. The model uncertainty as reflected by the ratio of measured to predicted factor of safety from 52 documented case histories is not sensitive to the slope stability method utilized (see Fig. 4.2). Predictions from all methods were found to be relatively unbiased but are associated with a degree of uncertainty that could be statistically reflected through a COV of about 0.27 in the ratio of measured to predicted factor of safety.

Table 4. 2 Statistical Parameters of λ for the Four LEM Slope Models

All Cases	Bishop	OMS	Janbu	Spencer
mean	0.966	0.990	1.036	0.964
Standard deviation	0.264	0.254	0.295	0.263
Coefficient of variation	0.273	0.256	0.285	0.273

To investigate the sensitivity of the model uncertainty to the choice of the test method used to measure the undrained shear strength of the soil, the undrained shear strength values that were reported in the original case histories were corrected to make them equivalent to the shear strength obtained from the Unconsolidated Undrained (UU) triaxial test, which is considered as the most representative technique for measuring the undrained strength. To this end, the undrained shear strength that was measured using field vane test procedure was considered to be equivalent to that of the UU test, while the strength that was measured using unconfined compression tests (UC) was multiplied by a factor of 1.3 to make it equivalent to a UU strength as indicated by Olson and Dennis (1982). The number of cases with UC tests are 13 out of the 52 cases (Tjernsmyr, Skejggerod, Shellmouth Dam test fill, Seven Sisters Dike, PresterØdbakken, North Ridge Dam, Nettet, Juban, Iwai, Falkenstein, Cuyahoga, Congress Street, and As).

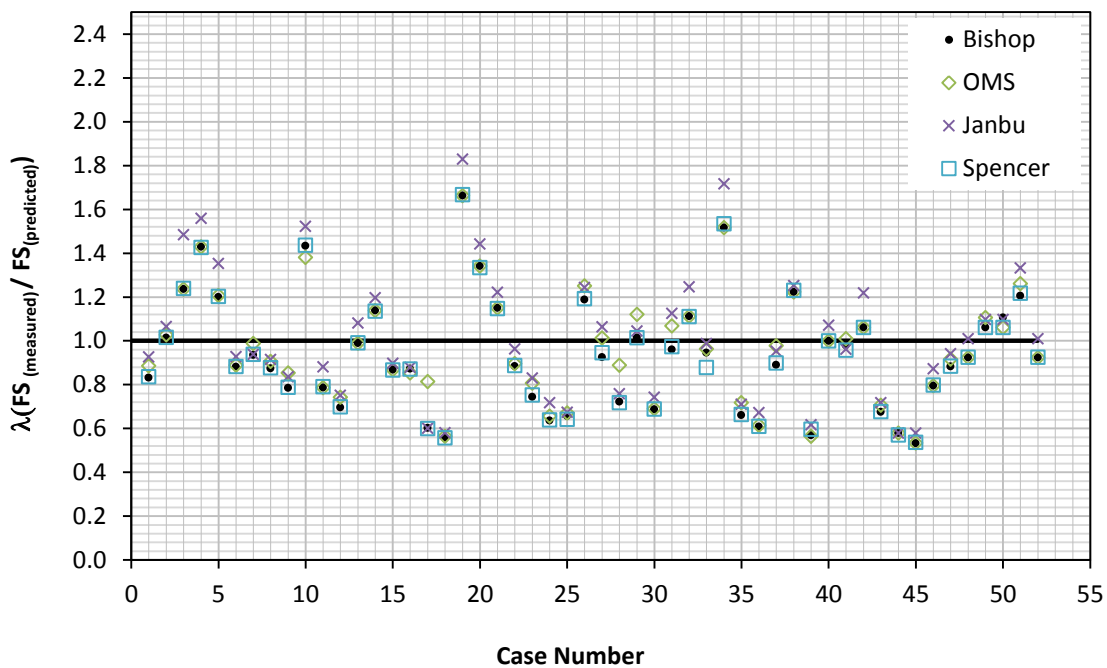


Figure 4. 2 Values of the model uncertainties for the 52 cases (Shear strength corrected to UU)

Table 4. 3. Statistical Parameters of the model uncertainty (After shear strength Correction)

All Cases	$\lambda(\text{Bishop})$	$\lambda(\text{OMS})$	$\lambda(\text{Janbu})$	$\lambda(\text{Spencer})$
mean	0.940	0.967	1.012	0.940
sd	0.262	0.252	0.295	0.262
COV	0.279	0.261	0.291	0.279

The ratio of the measured to the predicted factor of safety was reevaluated for these 13 cases with UC tests and plotted on Fig. 4.3. The updated statistics for λ are presented in Table 4.2 and indicate very small differences between the mean and COV of λ with and without the correction.

The 52 case histories that are assembled in the database are located in different countries. Some of these slopes are found on soils with high sensitivity. Sensitivity is defined as the ratio of the undrained shear strength of an undisturbed sample of soil to the undrained shear strength of a remolded sample of the same soil tested at the same water content. A more detailed analysis of the data is conducted to find if cases that have soil with high sensitivity could have a certain effect on the bias and uncertainty of the models. 9 cases out of the 52 cases have soil with high sensitivities (as high as 65). The statistical analysis that was conducted on λ was repeated without taking the cases with high sensitivities into consideration. The calculated values of the mean and the COV of λ are summarized in Table 4.3. Results in Table 4.3. indicate that removing the sensitive cases doesn't have a significant effect on the model uncertainty of the four models. There is a small decrease in the COV and the mean of λ . For instance, the COV of Bishop decreases from 0.279 to 0.273 and the mean decreases from 0.94 to 0.928. This decrease is also applicable for the other three models (OMS, Janbu, and Spencer).

Table 4. 4 Statistical parameters of model uncertainty (after removing the sensitive cases)

Non-Sensitive	$\lambda(\text{Bishop})$	$\lambda(\text{OMS})$	$\lambda(\text{Janbu})$	$\lambda(\text{Spencer})$
mean	0.928	0.957	1.003	0.930
sd	0.254	0.247	0.288	0.254
COV	0.273	0.258	0.287	0.273

In the balance of this thesis, the statistical parameters of λ as presented in Table 4.2. are adopted in any analysis related to reliability-based design of undrained slopes.

4.2.2.2 Probability Distribution of λ

Due to the limited number of research studies that target the model uncertainty for slope stability design problem, there is a lack of information on the distribution type needed to model this uncertainty for slopes. To investigate the applicability of commonly used probability distributions that could be used to model the uncertainty in λ , the cumulative distribution function (CDF) of λ was determined for the four models in Figs.4.4 (a,b,c, and d) and tested against theoretical normal and lognormal CDFs that could be used to model the data. Results in Fig.4.4 (a,b,c, and d) indicate that the lognormal distribution could provide a realistic representation of the actual data more than the normal distribution particularly at the left hand tail of the distribution. To validate the hypothesis that the lognormal distribution is considered the best fit of the data, the p-values associated with the Kolmogrov-Smirnov test for the lognormal distribution was computed using R software. The p-values for the four models were found to be greater than 0.05 indicating that there is no sufficient evidence to reject the lognormal distribution hypothesis.

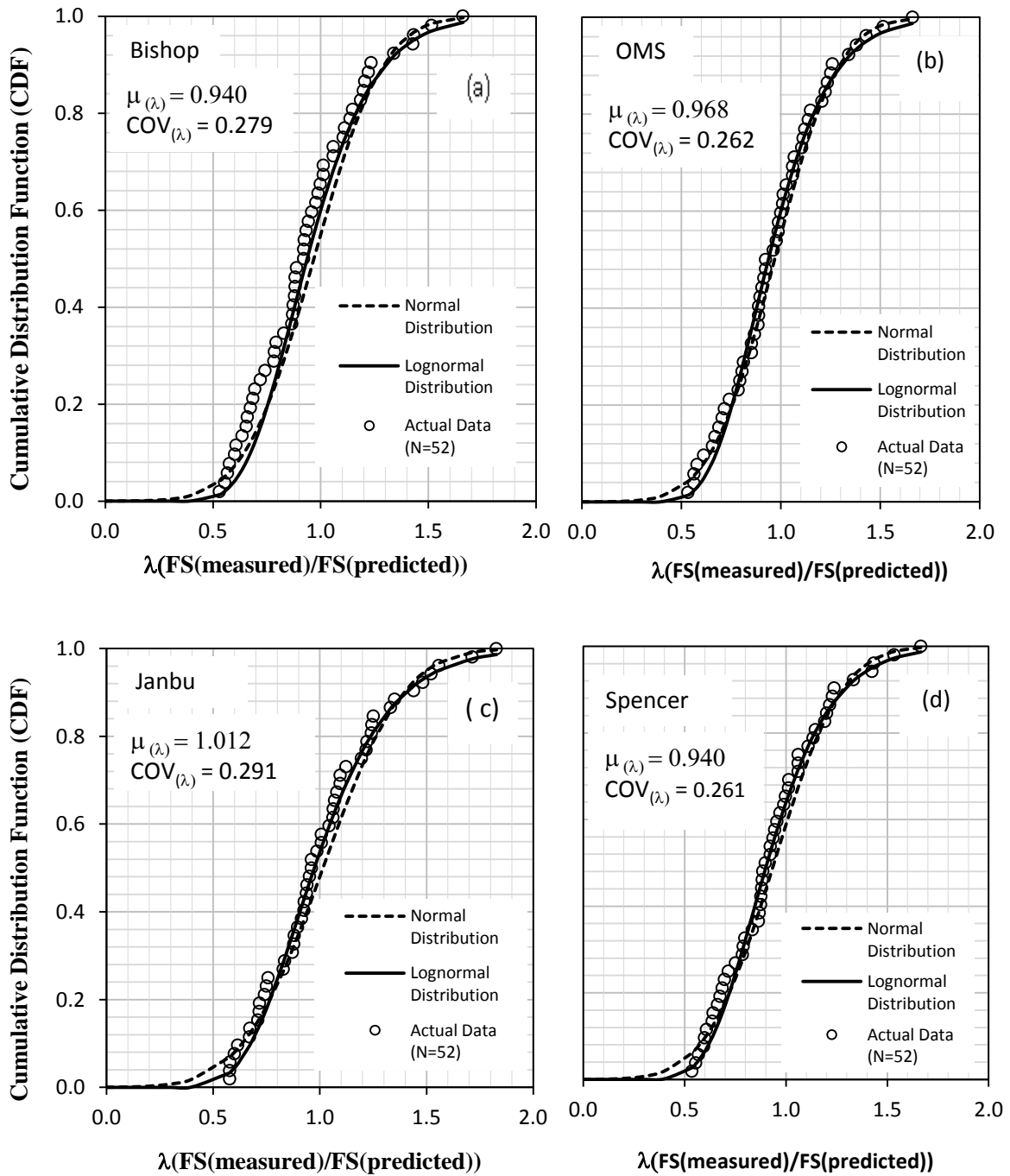


Figure 4. 3 Actual and Theoretical best-fit CDFs for the model uncertainty (λ)

4.3 Evidence of a lower-bound factor of safety of slopes

Results from 52 case histories of slope failures show significant scatter in the ratio of measured to predicted factor of safety. Part of this scatter results from the uncertainties in the values of the undrained shear strength. However, this uncertainty in the predicted factor of safety can be reduced by introducing a physical lower-bound factor of safety. The lower-bound factor of safety represents the minimum, possible factor of safety for the undrained slope and can be calculated by assuming that the shear strength of soil reduces to the fully remolded undrained shear strength. To validate the hypothesis of a lower-bound factor of safety, an analysis is presented for the slope cases available in the database. A predicted lower-bound factor of safety can be calculated using SLIDE by replacing the undisturbed undrained shear strength with the remolded shear strength. The remolded undrained shear strength represents the lowest possible strength for a clay.

Measurements of the undrained remolded shear strength are available for 6 out of 52 cases. These remolded shear strengths are typically measured using unconfined compression tests or unconsolidated-undrained Triaxial tests on soil samples that have been remolded at constant water content. For 46 out of 52 cases, information about the sensitivity of the clay was used to calculate the remolded shear strength. Sensitivity is defined as the ratio of the undisturbed strength to the remolded strength measured at the same water content. Some cases have sensitivity given in the reference that discussed the case while others have either liquidity indices as given or have index parameters that could be used to estimate the liquidity indices. The well-known correlation between liquidity index and sensitivity as presented by Bjerrum (1954) was used for this purpose. This correlation is presented in Fig. 4.5.

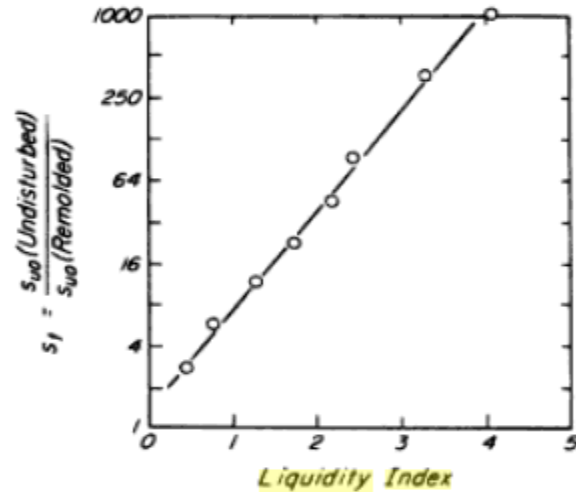


Figure 4. 4 Relation between sensitivity and liquidity index

A predicted lower-bound factor of safety was calculated using Slide for the 52 cases in the database using the 4 Limit Equilibrium methods. The lower-bound factor of safety was calculated by replacing the undisturbed undrained shear strength with the remolded undrained shear strength as mentioned above. The predicted lower-bound factor of safety are presented in Table 4.1 and plotted on Fig. 4.6. The data on Fig. 4.6 support the hypothesis of a lower-bound factor of safety because none of the data points fall above the measured factor of safety (assumed to be equal to 1.0 for a failed slope) for the four models. Each case of the database has a different calculated lower-bound factor of safety since the calculated lower-bound depends on the properties of the soil and the geometry of the slope. The predicted lower-bound factors of safety were found to range from minimum values that are almost equal to zero (for highly sensitive quick clays) to maximum values of about 0.9, with a mean value ranging from 0.37 to 0.39, depending on the method used to predict the lower-bound factor of safety. A summary of measured, predicted and lower-bound factors of safety for all cases in the database is shown in Fig. 4.7.

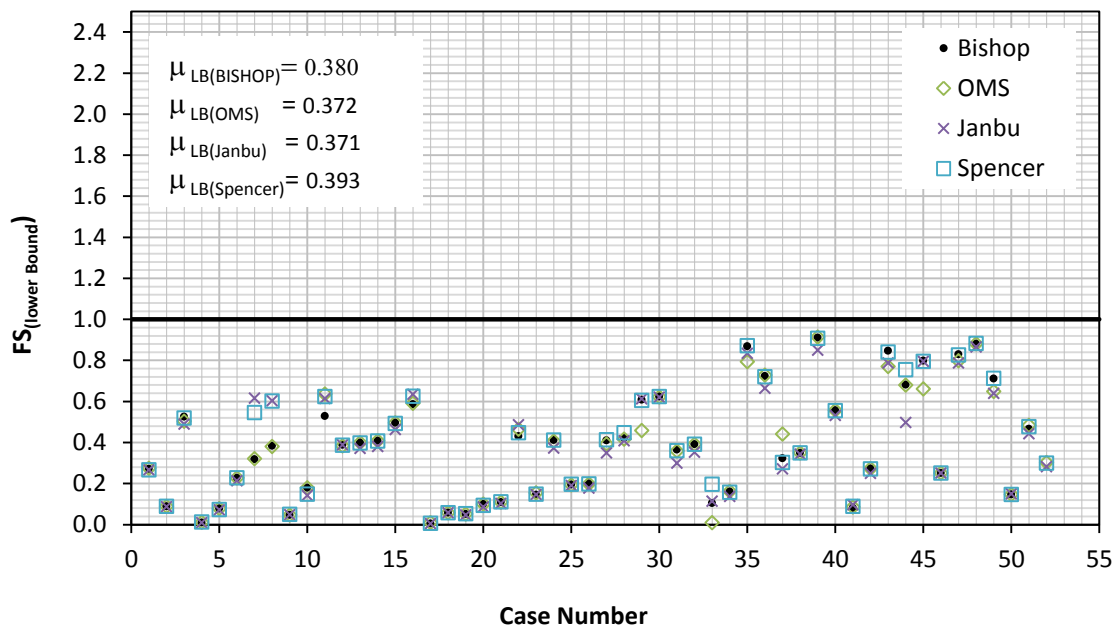


Figure 4. 5 Evidence of a lower-bound factor of safety of 52 slope failure cases

A more detailed analysis is carried out to investigate the effect of the sensitive cases on the calculated lower-bound factor of safety. The case histories that are characterized with high sensitive soils are removed from the database (Skejggerod, PresterØdbakken, Saint Alban, Narbonne, Bangkok A, NBR Development, Portsmouth, King's Lynn, New Liskeard and Precambrian). The elimination of the cases with soils with very high sensitivities resulted in a significant increase in the mean of lower-bound factor of safety for all models. The range of the mean of the lower-bound factor of safety increased from 0.37 to 0.39 to a higher range of 0.45 to 0.47 (see Fig. 4.8). This observation is important since the lower-bound factor of safety is expected to have a more considerable effect on the design of a slope as the magnitude of the lower bound increases.

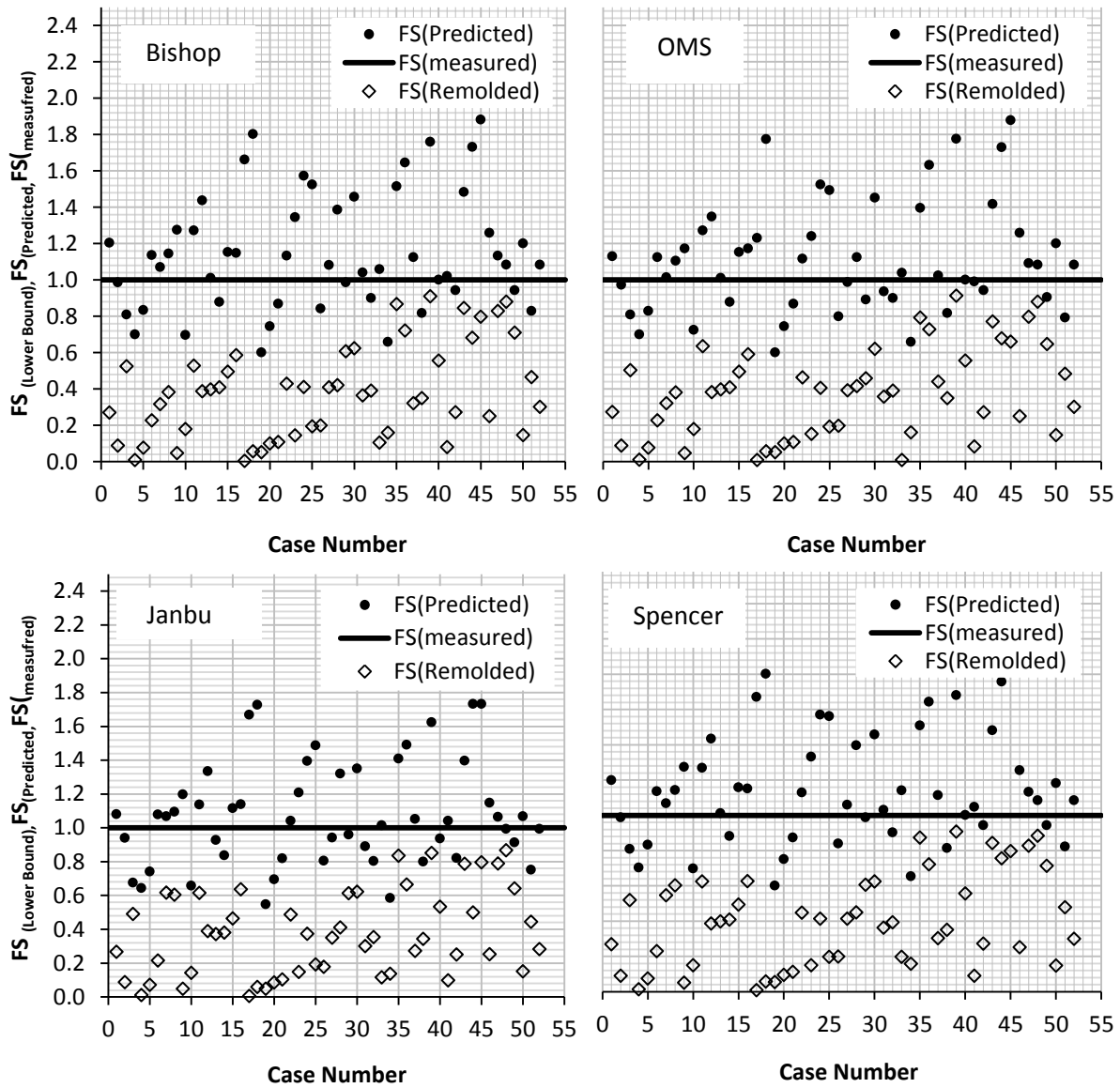


Figure 4. 6 Comparison of measured, predicted, and lower-bound factor of safety of 52 slope failures

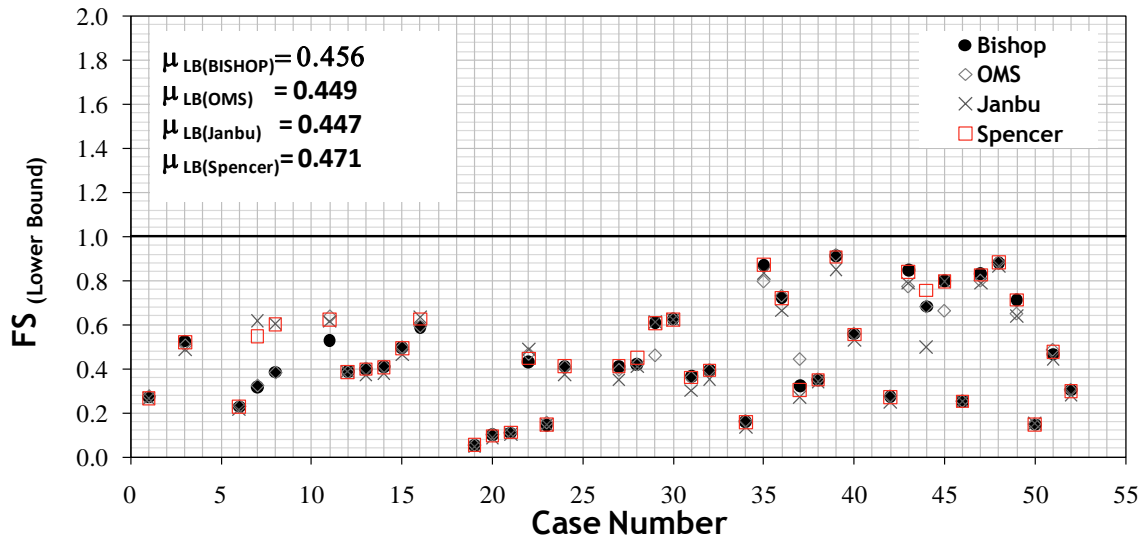


Figure 4. 7 Predicted Lower-Bound Factors of Safety Excluding Cases with Highly Sensitive Soils

4.4 Summary

Analysis of a database containing results from 52 undrained failed slopes indicates that the factor of safety of slopes can be predicted using four models (Bishop, OMS, Janbu, and Spencer) without introducing significant bias to the predicted factor of safety. The coefficient of variation in the ratio of measured to predicted factor of safety (model uncertainty λ) ranges between 0.261 to 0.291. Results from 52 slope failures provide evidence of the existence of the lower-bound factor of safety that can be calculated using the undrained remolded shear strength of the soil and information about the geometry of the slope.

CHAPTER 5

Investigation of the impact of spatial variability in the undrained shear strength on the factor of safety of undrained slopes

5.1 Introduction

Soil is a natural material. It exhibits considerable variation in space due to depositional and post depositional processes and therefore it brings unavoidable uncertainties in the estimation of input soil parameters used for defining the strength and stiffness characteristic of the in situ soil deposit. Uncertainty in the input parameters results in uncertainty in the output. In geotechnical engineering analysis and design, various sources of uncertainties are encountered and well recognized. Several features contribute to such uncertainties, like: geological details missed in the exploration program and estimation of soil properties that are difficult to quantify.

Spatial variability of soils contributes to the total uncertainty in civil engineering designs.

Reliability Based Designs provide a consistent framework to quantify the uncertainties.

One of the primary steps in the reliability analyses of geotechnical systems is to characterize the in-situ spatial variability of soil properties.

5.2 Characterization of soils

To model spatial variability of soils, generally two parameters are used as measures of variability and correlation in soils, namely, the coefficient of variation and the scale of fluctuation.

5.2.1 Coefficient of Variation (COV)

The coefficient of variation is one way of normalizing the variance and is a widely used measure of variability. Due to the fact that this parameter is simple to interpret, many soil statistical studies are based on it. The geotechnical literature has considerable information on the estimates of COV for almost all soil properties. Both Spry et al. (1988) and Phoon et al. (1999) reported typical estimates for the coefficient of variation for various geotechnical properties.

5.2.2 Scale of Fluctuation

While COV is used as a parameter to describe how variable a process is, the scale of fluctuation is used to describe the spatial correlation in a random process. Spatial variability can be effectively described by the correlation structure (Vanmarcke 1983). To describe this correlation structure, an autocorrelation distance is defined which is the distance within which soil properties show a strong correlation. A large autocorrelation distance value implies that the soil property is highly correlated over a large spatial

extent, resulting in a smooth variation within the soil profile. On the other hand, a small value indicates that the fluctuation of the soil property is large (Cho 2010).

As illustrated in Chapter 2, many studies adopted the coefficient of variation in characterizing spatial variability. The coefficient of variation (COV) does not reflect the spatial correlation of soils which is an indispensable descriptor in the geotechnical site characterization. The complexity of the problem reduces to a very simplistic level if the spatial correlation isn't taken into consideration. However, this simplicity is not realistic. In order to conduct a probabilistic geotechnical analysis in a rational framework, the method has to take the effect of soil correlation into account. According to the literature, Random Finite Element Method (RFEM) is able to combine local averaging theory, soil spatial correlation, in addition to the COV that describes how variable the soil is. Numerous reliability analyses in the literature adopted the RFEM for incorporating spatial variability in the analysis (Chapter 2).

In a recent study, Jha and Ching (2013) performed a robust and rigorous probabilistic slope stability analysis using the Random Finite Element Method to study the effect of spatial variability of soil properties on the probability of failure of undrained slopes. The following section provides a brief summary of the work done by Jha and Ching (2013) that is adopted later in the analysis.

5.3 Brief Summary of Work done by Jha and Ching (2013)

Jha and Ching (2013) performed a robust and rigorous probabilistic slope stability analysis using the Random Finite Element Method (RFEM) to study the effect of slope geometry, mean and coefficient of variation of the soil parameters, and the scale of fluctuations on the probability of failure of undrained slopes. The authors conducted the study by collecting a database for 34 real undrained engineered slope cases. The paper was aimed at quantifying the effect of spatial variability in the undrained shear strength of clays on the probability of failure of the slopes. An advanced model of spatial variability was adopted. This model took into account both vertical and horizontal spatial variability of the undrained shear strength in addition to the COV of the undrained shear strength. The vertical scale of fluctuation (δ_z) in the undrained shear strength was back-calculated for each case in the database using an approximate method proposed by Vanmarcke (1977) as follows:

$$\delta_z \approx 0.8 \bar{d} \quad (\bar{d} = (d_1 + d_2 + d_3 + d_4 + d_5)/5) \quad \text{Equation 5-1}$$

where \bar{d} is the average vertical interval of the intersection points between the S_u profile and its trend (t). Fig.5.1. shows a typical example of estimating δ_z . There are cases where the detailed S_u borehole data are not given but the trends are known. For these cases the authors assumed $\delta_z = 2.5\text{m}$.

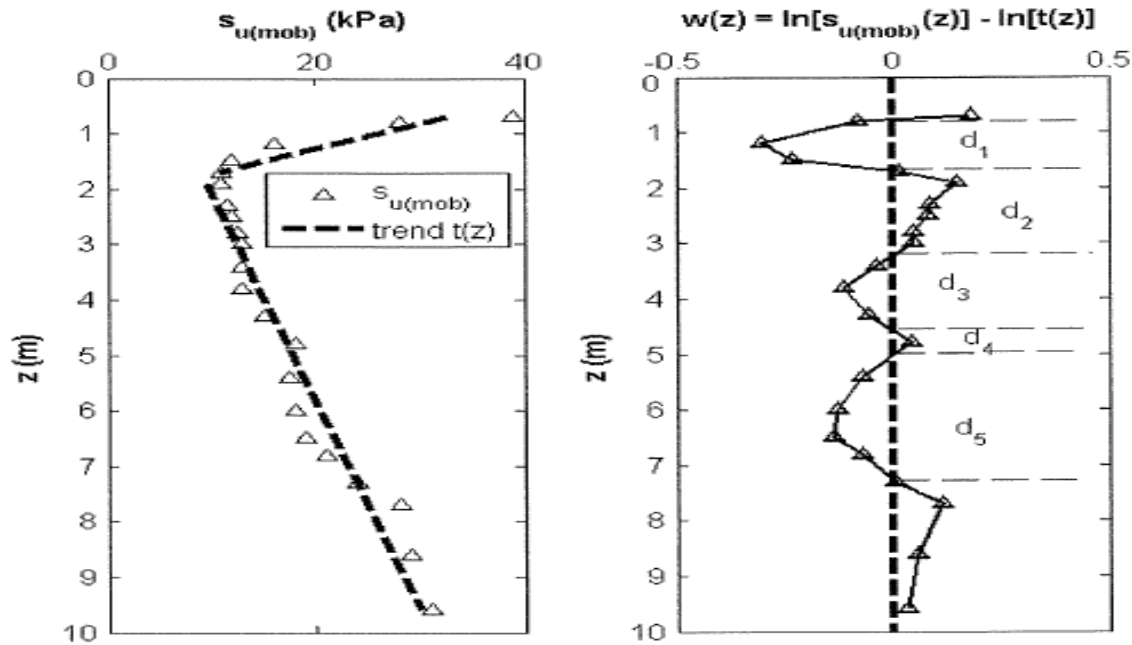
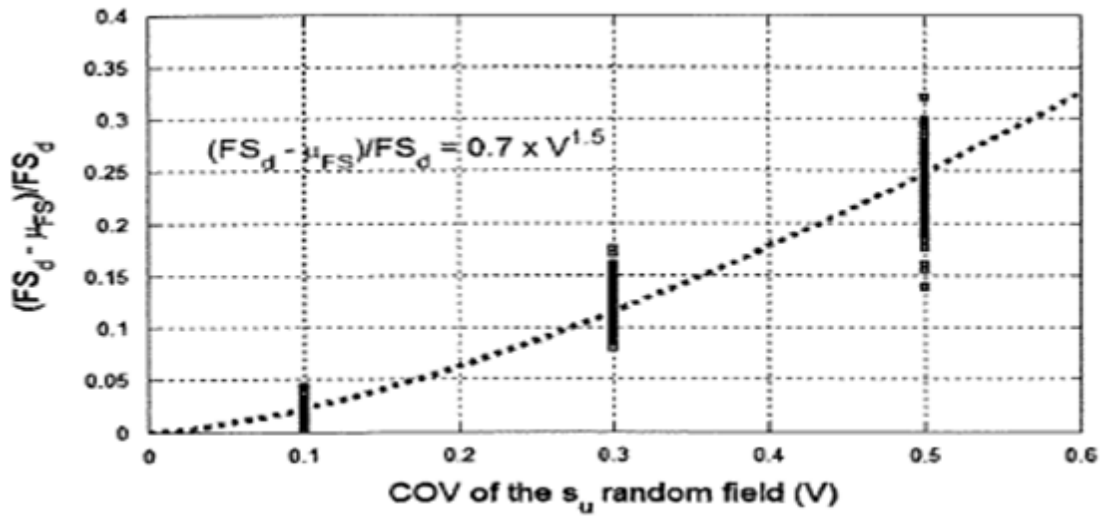


Figure 5. 1 Determination of vertical scale of fluctuation(Jha and Ching 2013)

The authors studied the effect of S_u spatial variability on the statistics of the factor of safety by quantifying the effect of the coefficient of variation (V) by varying the values of V to be 0.1, 0.3, and 0.5. Moreover, they investigated the effect of the horizontal scale of fluctuation (δ_x) by taking different values of (δ_x) to be $10\delta_z$, $20\delta_z$, and $30\delta_z$ according to Phoon and Kulhawy (1999). In addition to that, they studied the effect of both the vertical scale of fluctuation (δ_z) and the geometry of the slope by quantifying the ratio of (δ_z/L_f) where L_f is the length of the failure surface. By analyzing the 34 cases, the authors estimated the mean of the factor of safety (μ_{FS}) and the coefficient of variation of the factor of safety (V_{FS}). They concluded that μ_{FS} is always less than the deterministic factor of safety (FS_d) and V_{FS} is always less than COV of S_u . In the aim of understanding

the reasons behind this reduction, the authors studied the correlation between this reduction and V , δ_x , δ_z , and L_f . They investigated the change of the ratio $(FS_d - \mu_{FS})/FS_d$ versus the dimensionless factors (V , δ_x/δ_z , and δ_z/L_f). Their analysis showed that $(FS_d - \mu_{FS})/FS_d$ is strongly correlated to V only and this is shown in Fig.5.2.



It is shown in Fig.5.2. that there is deviation of the ratio of $(FS_d - \mu_{FS})/FS_d$ from the trend line and this variability increases as V increases. The authors took into account this variability by denoting an error term ε_1 with a standard deviation of σ_1 . Finally, they ended up with an equation for the estimation of μ_{FS} as follows:

$$\mu_{FS} = \left(1 - 0.115 \left(\frac{V}{0.3}\right)^{1.5} - \sigma_1 * Z_1\right) * FS_d \quad \text{Equation 5-2}$$

Where: V is the coefficient of variation of S_u

$$\sigma_1 = 0.06 * V^{0.85}$$

Z_1 is modeled as the standard normal random variable $N(0,1)$. As a result:

$$\mu_{FS} = (1 - 0.115 \left(\frac{V}{0.3}\right)^{1.5} - 0.06 * V^{0.85} * Z_1) * FS_d \quad \text{Equation 5-3}$$

The same analysis illustrated above was repeated by the authors to dictate the reason behind the reduction of the coefficient of variation of the factor of safety (V_{FS}). The analysis resulted in the conclusion that V_{FS} is strongly correlated with both V and δ_z/L_f and this is shown in Fig.5.3. The authors conducted a regression analysis to get an equation for the estimation of the coefficient of variation of the factor of safety (V_{FS}):

$$V_{FS} = (0.2606 * b_{\delta_z/L_f} * b_{\delta_x/\delta_z} * b_v + 0.0466 * Z_2) * V \quad \text{Equation 5-4}$$

Where

$$b_{\delta_z/L_f} = \exp[3.1226 + 1.5027 * \ln(\delta_z/L_f) + 0.1655 * \ln(\delta_z/L_f)^2]$$

$$b_{\delta_x/\delta_z} = \exp[-0.4999 + 0.1668 * \ln(\delta_x/\delta_z)]$$

$$b_v = \exp[-0.6349 - 0.731 * \ln(V) - 0.1691 * \ln(V)^2]$$

Z_2 is modelled as the standard normal variable $N(0,1)$.

The value 0.0466 that is placed in the equation is related to the standard deviation of the error between the estimated and the actual ratio (V_{FS}/V) as shown in Fig.5.4.

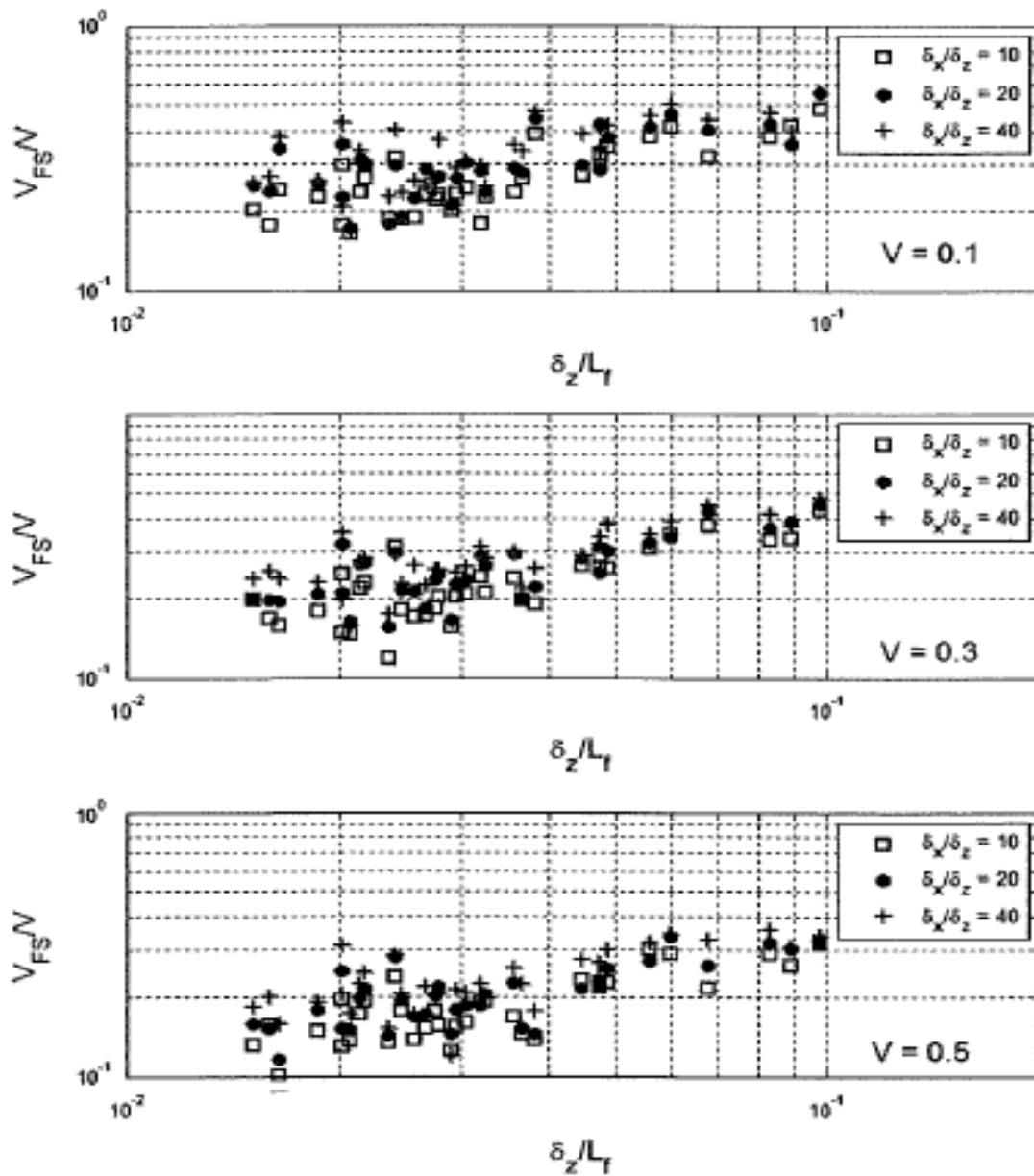


Figure 5. 3 Relationship between V_{FS}/N and $(V, \delta_z/L_f, \delta_x/\delta_z)$ (Jha and Ching 2013)

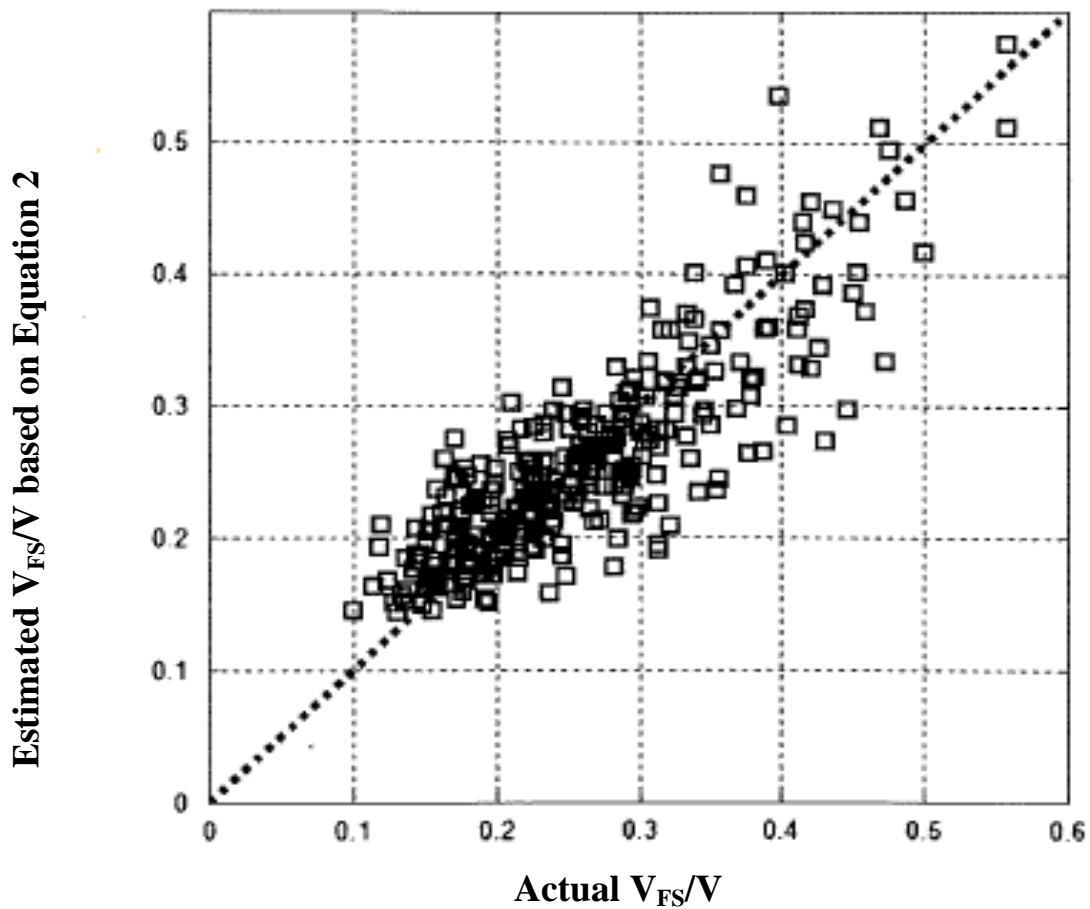


Figure 5. 4 Relationship between actual V_{FS}/V and V_{FS}/V estimated by Equation 2

5.4 Method for Combining Uncertainties

The work done by Jha and Ching (2013) is implemented to evaluate the expected value of FS, $E(FS)$ and the variance of FS, $Var(FS)$.

Both the expected value and the variance of the factor of safety could be evaluated using a first order approximation as follows (Gilbert 1999):

$$E(FS) = E_Z(\mu_{FS|Z}) \quad (5-5)$$

$$Var(FS) = E_Z(\sigma_{FS|Z})^2 + Var_Z(\sigma_{FS|Z}) + Var_Z(E_{FS|Z}) \quad (5-6)$$

Where:

- $\mu_{FS|Z}$ and $\sigma_{FS|Z}$ are the mean value and standard deviation of FS (both are random variables since they are function of the uncertain model parameters Z (see Equation 5-3 and 5-4).
- $E(FS)$ and $Var(FS)$ are the expected mean and variance of FS as obtained from the first order approximation. It should be noted that

It is worthwhile, mentioning that Equation (5-6) indicates that the uncertainty in FS arises from two sources:

1. Random Variability that is modeled by the model parameters, $E_Z(\sigma_{FS|Z})^2$
2. Uncertainty in the model parameters themselves, $Var_Z(\sigma_{FS|Z})$ and $Var_Z(E_{FS|Z})$

The first and second moments for $\mu_{FS|Z}$ and $\sigma_{FS|Z}$ themselves can be approximated as functions of the first and second moments of the model parameters Z , using first order Taylor series expansion such that:

$$E_Z(\mu_{FS|Z}) = h_\mu(\bar{\mu}_Z) \quad (5-7)$$

$$Var_Z(E_{FS|Z}) = \left\{ \frac{\partial h_\mu}{\partial \delta_{Z_i}} \bigg|_{\mu_Z} \right\}^T C_Z \left\{ \frac{\partial h_\mu}{\partial \delta_Z} \bigg|_{\mu_Z} \right\} \quad (5-8)$$

$$E_Z(\sigma_{FS|Z}) = h_\sigma(\bar{\mu}_Z) \quad (5-9)$$

$$Var_Z(\sigma_{FS|Z}) = \left\{ \frac{\partial h_\sigma}{\partial \delta_{Z_i}} \bigg|_{\mu_Z} \right\}^T C_Z \left\{ \frac{\partial h_\sigma}{\partial \delta_{Z_i}} \bigg|_{\mu_Z} \right\} \quad (5-10)$$

Where:

- $\left\{ \frac{\partial h_\mu}{\partial \delta_{Z_i}} \bigg|_{\mu_Z} \right\}$ and $\left\{ \frac{\partial h_\sigma}{\partial \delta_{Z_i}} \bigg|_{\mu_Z} \right\}$ are vectors containing the partial derivatives of $h_\mu(Z)$ and $h_\sigma(Z)$, respectively, evaluated at the mean values of the model parameters

$h_\mu(Z)$ and $h_\sigma(Z)$ are the expressions of the probabilistic model of the μ_{FS} and σ_{FS} , respectively.

Equations 5-5 and 5-6 allow for estimating the mean and variance of FS given information about the spatial variability of the undrained shear strength as reflected by the coefficient of variation of the undrained shear strength (V) and the vertical and horizontal correlation distances (δ_z and δ_x). Other important input to these equations are the predicted factor of safety (FS_d) and the length of the failure surface (L_f).

CHAPTER 6

Combination of Both Model Uncertainty and Spatial Variability

6.1 Introduction

In this chapter, a mathematical framework is provided to study the reliability and evaluate the statistical parameters (mean and variance) of the factor of safety of undrained slopes. This framework models the factor of safety that combines both model uncertainty and spatial variability. Moreover, a practical approach for incorporating a lower-bound factor of safety in the reliability analysis is investigated and a probability distribution that can accommodate a lower-bound factor of safety is recommended.

6.2 Conventional Probability Distributions for Factor of Safety

Traditionally, normal and lognormal probability distributions have been used to model the uncertainty in the factor of safety. Parameters and mathematical forms of the normal and lognormal distributions in addition to the advantages and disadvantages of both distributions are described in the following sections.

6.2.1 Normal Distribution

The normal distribution is the most widely known and used distribution in engineering due to the simplicity of its mathematical form and to the physical

significance of the parameters describing it. The normal distribution which is also referred to as the Gaussian distribution has a probability density function (PDF) that is defined over a range of values that extend from $-\infty$ to $+\infty$. The normal distribution is symmetrical in shape and is defined by two parameters, the mean μ and the standard deviation σ . Because of symmetry, the mean of the normal distribution is equal to the median value (50th percentile value). The PDF of the normal distribution is shown in the following equation:

$$f_X(x) = \frac{1}{\sigma\sqrt{2\pi}} e^{-\frac{1}{2}\left(\frac{x-\mu}{\sigma}\right)^2} \quad -\infty < x < \infty \quad \text{Equation 6-1}$$

The probability density function (PDF) of examples of normal distributions are shown in Fig. 6.1.

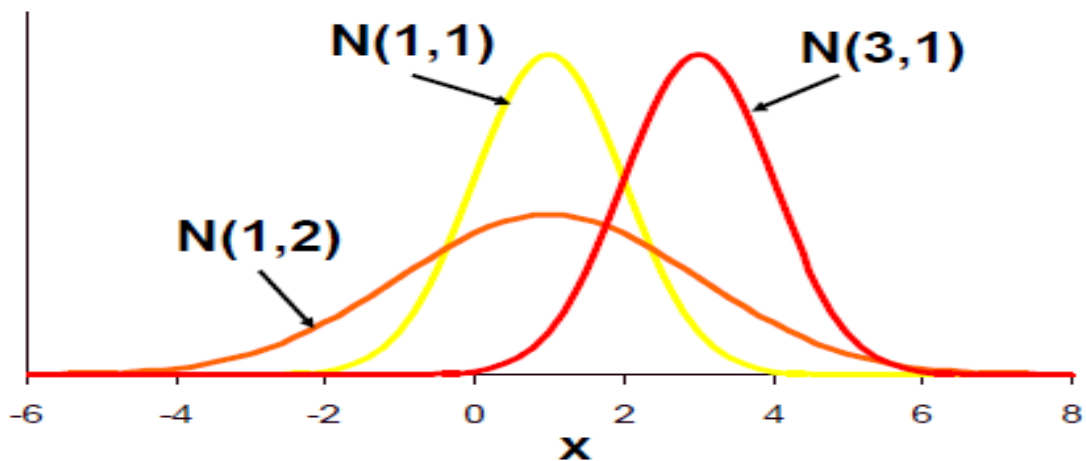


Figure 6. 1 Normal Probability Distribution

When the normal distribution is used to model uncertainty in the capacity or factor of safety of engineering systems, the distribution has a shortcoming in that the left-hand tail

of the distribution can extend to values that are less than zero (see Figure 6.1.). Negative values of capacity and factor of safety are not physically possible in engineering design.

6.2.2 Lognormal Distribution

The lognormal distribution has a probability density function (PDF) that is defined over a range of values that extends from zero to $+\infty$. The probability density function (PDF) of the lognormal distribution is given by the mathematical expression shown below:

$$f_X(x) = \frac{1}{x\zeta\sqrt{2\pi}} e^{-\frac{1}{2}\left(\frac{\ln(x)-\lambda}{\zeta}\right)^2} \quad 0 \leq x < \infty$$

Equation 6-2

The lognormal distribution is skewed to the right and is defined by two parameters, λ and ζ . These two parameters represent the mean and the standard deviation of the natural logarithm of the variable. λ and ζ can be evaluated using the following equations:

$$\lambda = E[\ln(X)] = \ln(\mu_X) - \frac{\zeta^2}{2}$$

Equation 6-3

$$\zeta^2 = \text{Var}[\ln(X)] = \ln(1 + \delta^2)$$

$$x_{median} = e^\lambda$$

Equation 6-4

Where δ is the coefficient of variation of the random variable x that is defined as the ratio of the standard deviation to the mean of random variable. The probability density function of examples of lognormal distributions are shown in Fig.6.2.

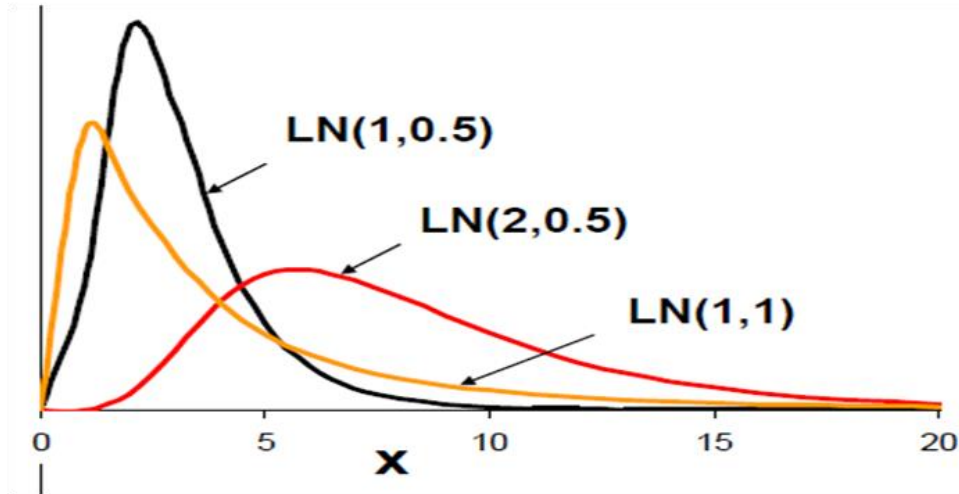


Figure 6. 2 Lognormal Probability distribution

The lognormal distribution has been used widely to model the uncertainty in the load and capacity in conventional reliability analyses in civil engineering in general and in geotechnical engineering in particular (Tang 1988 and 1990; Hamilton and Murff 1992; Tang and Gilbert 1993; API 1993; Hornsell and Toolan 1996; Bea et al. 1999; McVay 2000; 2002; and 2003; Kulhawy and Phoon 2002; Phoon et al. 2003; AASHTO 2004).

The main reasons for the wide-spread use of the lognormal distribution are related to the fact that it is skewed to the right and has a lower bound of zero. However, the lognormal distribution, with a lower tail that extends to zero, does not capture the realistic possibility that there is a physical minimum or lower bound for the capacity or factor of safety of geotechnical engineering systems. This lower-bound factor of safety could be greater than zero and is not modeled properly by conventional distributions.

6.3 Distribution Types Adopted in the Analysis

In this analysis, the lognormal distribution is assumed to model the uncertainty in the factor of safety. To incorporate the lower-bound factor of safety into reliability assessments, a simple approach is adopted through the use of a truncated lognormal probability distribution (Fjeld 1977, Rodriguez et al. 1988). A Lognormal distribution that is truncated at a lower-bound factor of safety (FS_{LB}) can be used to accomplish this purpose. The use of truncated lognormal distribution is convenient because the parameters describing the distribution are the same as those of the non-truncated distribution with the addition of one extra parameter, the lower-bound factor of safety (FS_{LB}). However, the mean and the coefficient of variation of truncated lognormal distribution can be quite different than the mean and the coefficient of variation of non-truncated distribution, especially as the lower-bound factor of safety increases and becomes close to the mean or median factor of safety. The probability density function of an example truncated lognormal distribution is illustrated on Fig.6.3.

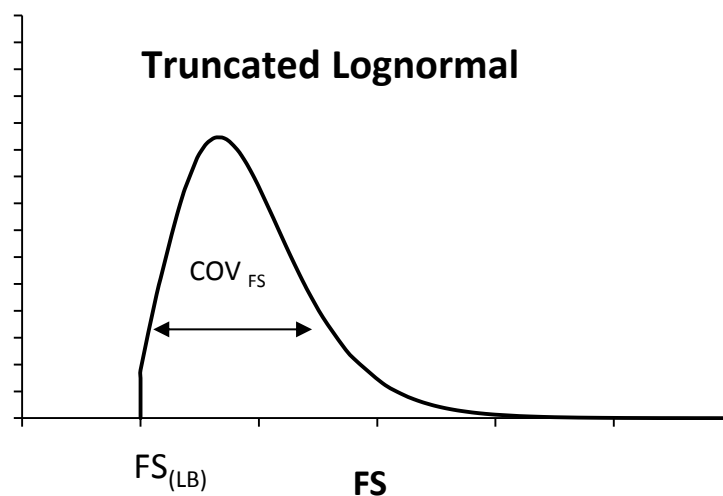


Figure 6. 3 Probability density function of truncated lognormal

6.4 Estimation of the Statistical Parameters of the Factor of Safety

The statistical parameters of the factor of safety are estimated by combining the uncertainties in the factor of safety (FS) due to model uncertainty and due to spatial variability. To accomplish this objective, the factor of safety is assumed to be equal to the product of two random variables as indicated in Equation 6-5.

$$FS = \lambda_{\text{model}} \cdot FS_{\text{spatial}} \quad \text{Equation 6-5}$$

The first random variable (FS_{spatial}) models the effect of spatial variability in the undrained shear strength on FS. The mean and the coefficient of variation of FS_{spatial} are estimated as indicated in chapter 5 using Equations 5-5 and 5-6. The second random variable (λ_{model}) represents the model uncertainty as reflected in the ratio of the measured to predicted factor of safety of the slope. The mean and coefficient of variation of (λ_{model}) are evaluated from the analysis of the database which includes the real case histories of failed slopes as illustrated in chapter 4.

The distributions of the two random variables are assumed lognormal. Thus, exact solutions that allow for combining the uncertainties in both parameters to calculate the parameters λ and ζ of the total factor of safety are available and result in a total factor of safety that is also lognormally distributed. The mathematical expressions shown in Table 6.1 can be used for this purpose.

Table 6. 1. Estimation of λ and ζ of the factor of safety

Function, $Y = g(\vec{X})$	Probability Distribution for X_i	Probability Distribution for Y
$Y = b \prod_{i=1}^n X_i^{a_i}$	<p>Lognormal($\lambda_{X_i}, \zeta_{X_i}$)</p> <p>$\text{COV}[\ln(X_i), \ln(X_j)] = \rho_{i,j} \zeta_{X_i} \zeta_{X_j}$</p>	<p>Lognormal(λ_Y, ζ_Y)</p> <p>$\lambda_Y = \sum_{i=1}^n a_i \lambda_{X_i} + \ln(b)$</p> <p>$\zeta_Y = \sqrt{\sum_{i=1}^n \sum_{j=1}^n a_i a_j \text{COV}[\ln(X_i), \ln(X_j)]}$</p>

6.5 Summary

Most reliability analyses focus on the mean, variance, and an assumed mathematically convenient distribution to model the left-hand tail of the factor of safety distribution. In this analysis, the lognormal distribution is assumed to model the uncertainty in the factor of safety and this is due to the fact that it is skewed to the right and has a lower-bound of zero (does not allow negative values). For analysis in which the effect of the lower-bound factor of safety is included in the analyses, a truncated lognormal distribution is used instead of the conventional lognormal distribution.

CHAPTER 7

Recommendations for design factors of safety for undrained slopes

7.1 Introduction

In this chapter, a reliability-based design framework is proposed to recommend design factors of safety that would result in target probabilities of failure for undrained slopes. As a first step, uncertainties due to spatial variability and model uncertainty are combined to evaluate the probability of failure of undrained slopes that are designed with different factors of safety. In the second step, the effect of incorporating a lower-bound factor of safety on the probability of failure is investigated. The third and final step consists of recommending factors of safety to be used for different design scenarios to achieve target levels of risk.

7.2 Reliability-based design of undrained slopes

The sensitivity of the probability of failure (P_f) to variations in the deterministic factor of safety, coefficient of variation of the undrained shear strength, vertical correlation distance, and lower-bound factor of safety is investigated in this section. A number of spatially variable clay slopes that cover the typical range of design slope conditions are considered. For each analyzed slope, a reliability analysis is conducted to quantify the probability of failure (P_f) of the slope with and without the inclusion of the estimated lower-bound factor of safety. For the two cases, the probability of failure (P_f) is defined as the probability that the factor of safety is less than one as is the convention.

Equation 7-1 is used to calculate the probability of failure (P_f) and the reliability index, β without the inclusion of the lower bound factor of safety:

$$p_f = \Phi\left(\frac{LN(1)-\lambda}{\zeta}\right) = \Phi(-\beta) \quad \text{Equation 7-1}$$

Where $\Phi()$ is the standard normal cumulative distribution function, λ and ζ are statistical parameters (lognormal distribution) that are related to the mean and coefficient of variation of the factor of safety, and β is the reliability index.

In the presence of the lower-bound factor of safety, the lognormal distribution, with a left tail that extends to zero, doesn't capture the realistic possibility that there is a physical minimum or lower-bound for the factor of safety of the slope. This lower-bound is expected to be greater than zero. Therefore, a truncated lognormal distribution is used to model the uncertainty in the factor of safety of the slope in the presence of the lower-bound factor of safety. The mathematical expression of the probability of failure (P_f) including the lower-bound is presented in Equation 7-2.

$$p_f = \left(\frac{\Phi\left(\frac{LN(1)-\lambda}{\zeta}\right) - \Phi\left(\frac{LN(LB)-\lambda}{\zeta}\right)}{1 - \Phi\left(\frac{LN(LB)-\lambda}{\zeta}\right)} \right) \quad \text{Equation 7-2}$$

Where LB is the lower-bound factor of safety of the slope.

7.2.1 Effect of coefficient of variation and scale of fluctuation of undrained shear strength on the probability of failure

As illustrated in chapter 5, both the ratio of δ_z/L_f and the coefficient of variation (V) of the undrained shear strength have a significant effect on the statistical parameters

of the factor of safety. To study the effect of δ_z/L_f and the coefficient of variation of the undrained shear strength (V) on the probability of failure (P_f) of slopes, a number of spatially variable slopes with different slope geometries and different soil properties were considered. The coefficient of variation (V) was varied between 0.1, 0.2, 0.3, 0.4, and 0.5 and δ_z/L_f was taken as 0.001, 0.005, 0.01, 0.05, 0.1, 0.15, 0.2, and 0.3. Due to the fact that δ_x doesn't have a significant effect on the probability of failure (P_f) of slopes, the ratio of δ_x/δ_z is taken to be 20 (Phoon and Kulhawy 1999). The probability of failure of each case is calculated using Equation 7-1 where the statistical parameters λ and ζ are estimated using the procedure shown in chapter 6 that takes into account both model uncertainty and spatial variability. In this analysis, the statistical parameters of the model uncertainty are those evaluated for Spencer's method knowing that there is no large difference in the statistical parameters between the four methods.

Figures 7.1., 7.2., and 7.3. show typical results for the variation of probability of failure (P_f) with the ratio of δ_z/L_f for different deterministic design factors of safety and different coefficients of variation. The deterministic factors of safety are estimated based on the mean of the undrained shear strength that is measured using Undrained Unconsolidated tests (UU) as an input. As a result, these design factors of safety could be different from actual design factors of safety that are conventionally used in slopes, whereby conservative estimates (rather than the mean) and other test methods (such as the unconfined compression tests) of the undrained shear strength are generally adopted. For such studies, the design factors of safety are expected to be lower than the values adopted in Figs. 7.1 to 7.3.

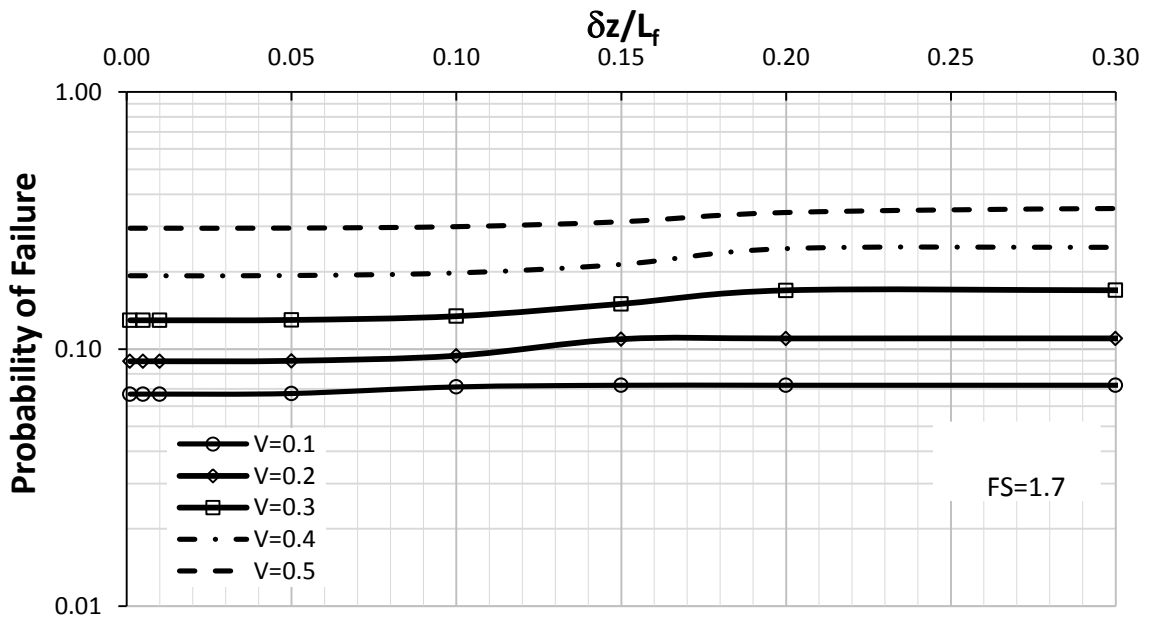
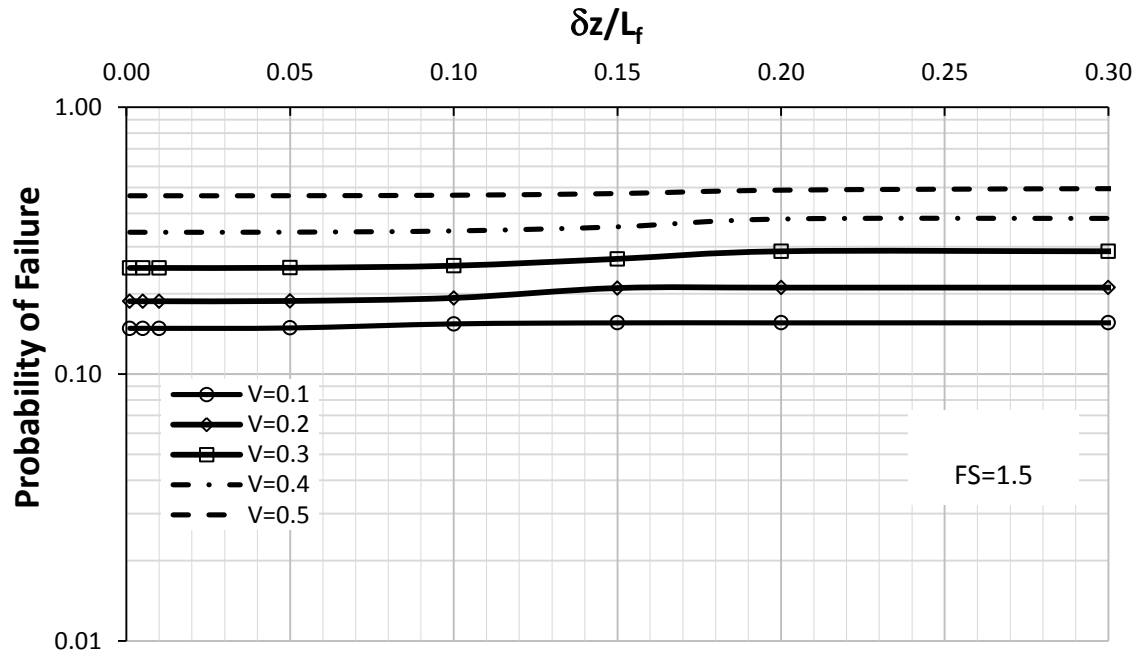


Figure 7. 1 Variation of P_f with V and $\delta z/L_f$ for $FS = 1.5$ & $FS = 1.7$

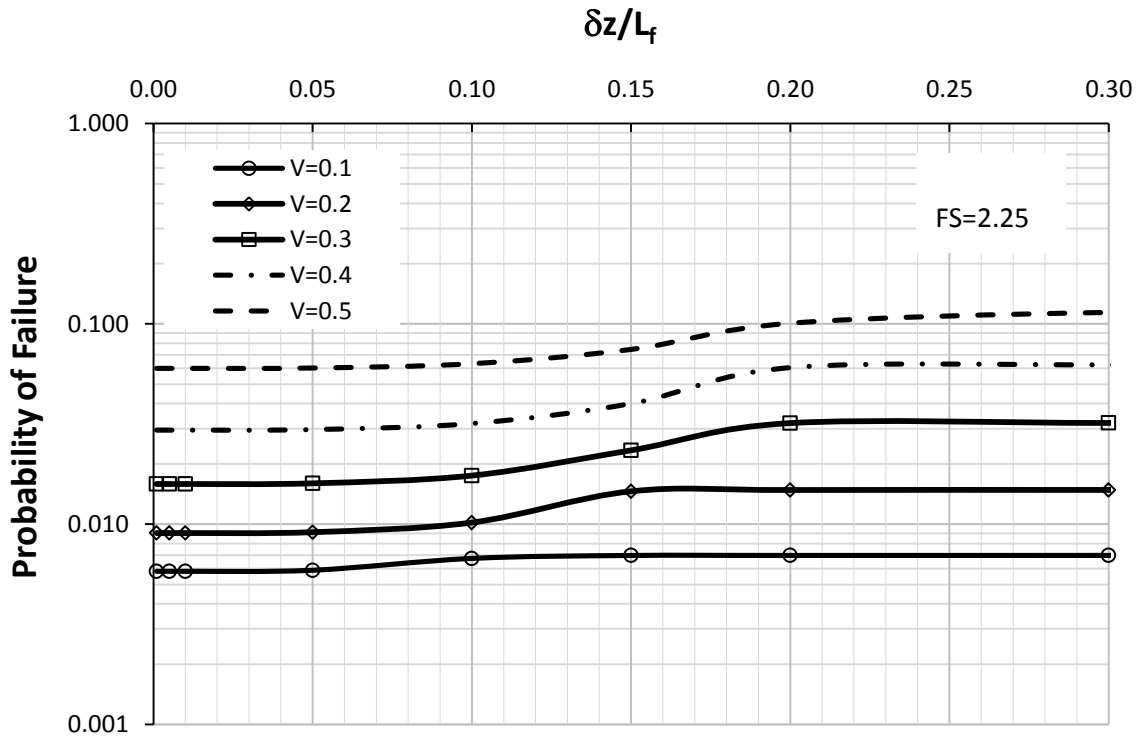
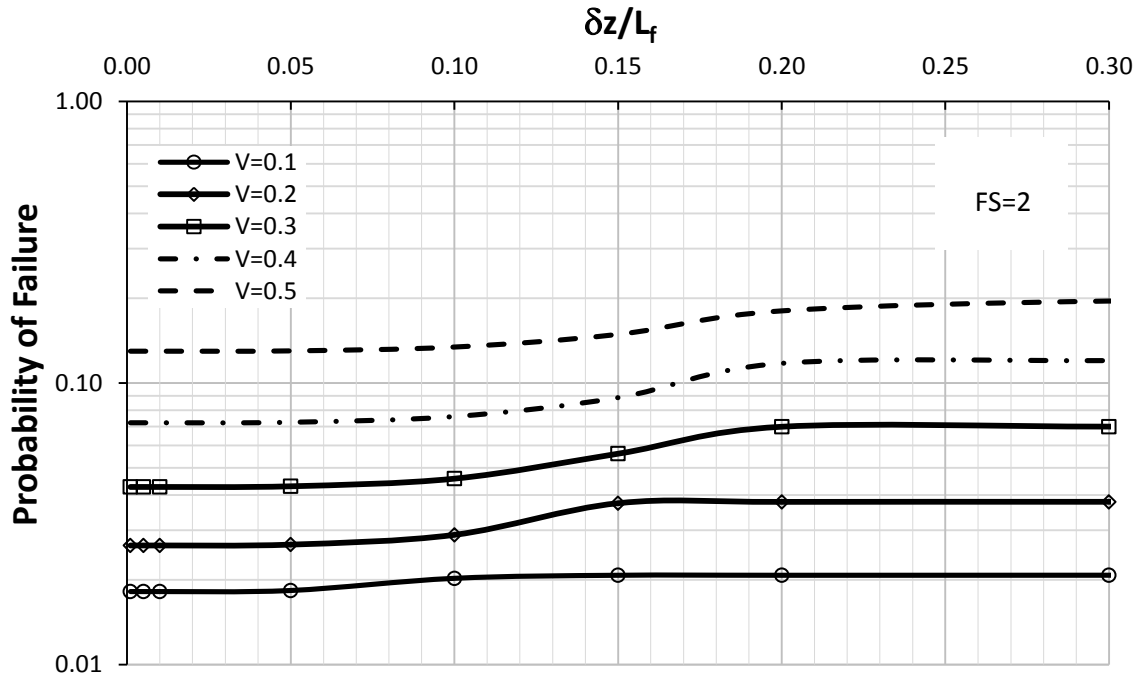


Figure 7.2 Variation of P_f with V and $\delta z / L_f$ for $FS = 2$ & $FS = 2.25$

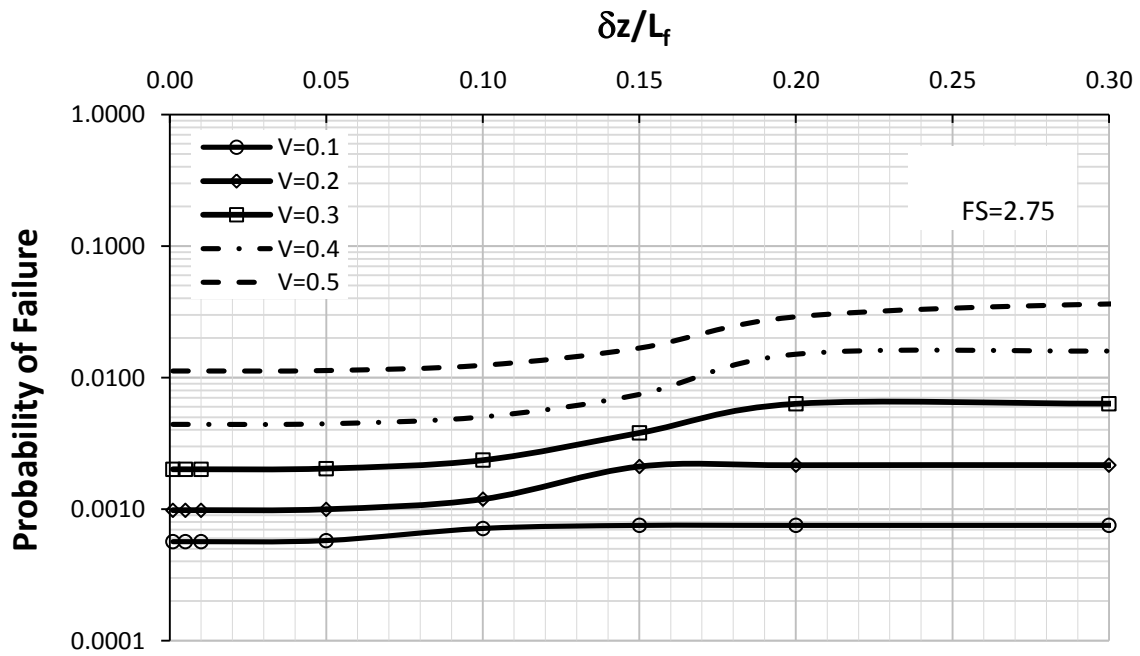
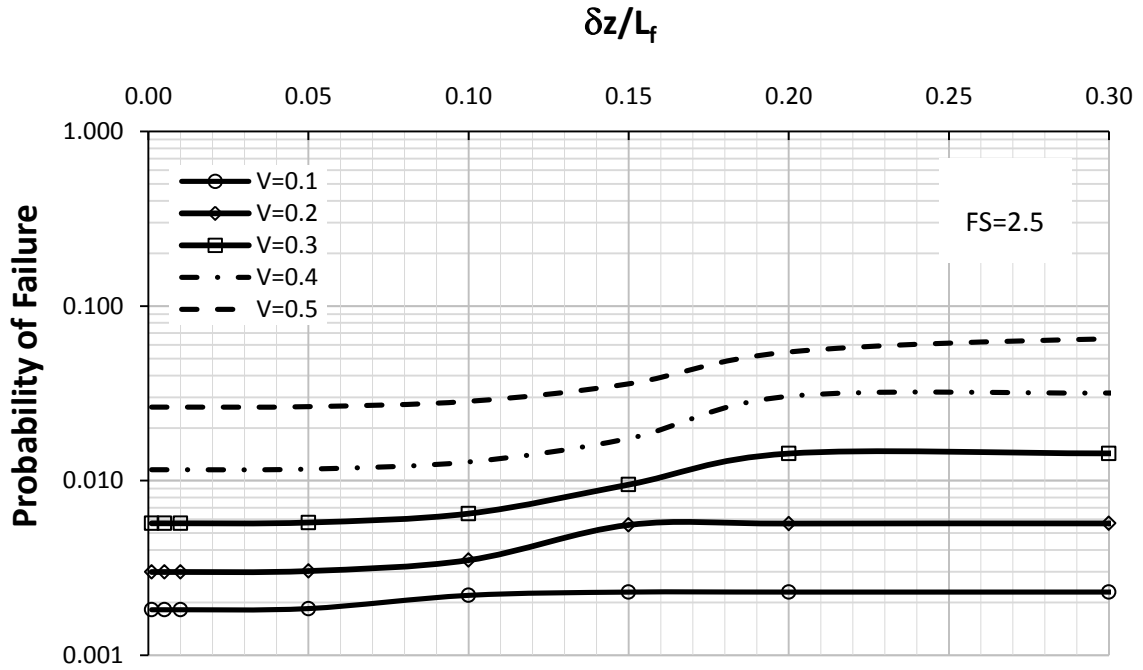


Figure 7.3 Variation of P_f with V and $\delta z/L_f$ for $FS = 2.5$ & $FS = 2.75$

The results show that the probability of failure (P_f) depends on the coefficient of variation, the factor of safety, and the scale of fluctuation. The primary conclusion from Figures 7.1.,7.2., and 7.3. is that the spatial variability has a significant effect on the probability of failure of slopes. The probability of failure increases significantly with the increase in the coefficient of variation. As an example, consider the case where the factor of safety is equal to 1.5 and $\delta_z/L_f = 0.15$. For this case, P_f is found to increase from 15% for the case where the undrained shear strength is the least variable ($V=0.1$) to 48% for the case where the undrained strength is highly variable ($V=0.5$). This increase in P_f diminishes with the increase in the factor of safety due to the fact that the magnitude of P_f decreases at any value of the ratio δ_z/L_f with the increase in the factor of safety. Along the same lines, it is worth noting that the calculated probabilities of failure for the case with $FS = 1.5$ (which is a common design case) are relatively high (range from 15% to 50% depending on the coefficient of variation of the undrained shear strength) compared to typical probabilities of failure that are considered as acceptable in engineering practice.

The second conclusion is that there is a significant decrease in (P_f) with the increase of FS. For example, consider the case where the ratio $\delta_z/L_f = 0.15$ and $V = 0.5$. For this case, the probability of failure (P_f) decreases from 48% for $FS = 1.5$ to 2% for $FS = 2.75$. For the case with the lowest spatial variability ($V = 0.1$) and $\delta_z/L_f = 0.15$, the probability of failure (P_f) decreases from 14% for $FS = 1.5$ to 0.07% for $FS = 2.75$.

The third conclusion from Figures 7.1.,7.2., and 7.3. is that there is a threshold value for the ratio of δ_z/L_f ($\delta_z/L_f = 0.1$), above which the probability of failure (P_f) slightly increases until it reaches another threshold ($\delta_z/L_f = 0.2$) beyond which the

probability of failure (P_f) remains constant with the increase of the ratio δ_z/L_f . This increase in the probability of failure between $\delta_z/L_f = 0.1$ and $\delta_z/L_f = 0.2$ is related to the variance reduction in the undrained shear strength due to averaging along the failure surface. As δ_z/L_f decreases (either due to small scale of fluctuation or long failure surface), there is more averaging in the undrained shear strength that occurs along the failure surface leading to variance reduction which ultimately translated into a reduction in the probability of failure. The effect of this averaging seems to be minor at lower factors of safety but increases slightly when the factor of safety increases. The reason why this effect is minor is related to the fact that model uncertainty masks the uncertainty due to spatial variability when the two sources of uncertainty are combined.

To portray the effect of δ_z/L_f on the calculated probability of failure, an analysis is conducted without including the model uncertainty in the analysis. The results of the analysis are presented in Fig.7.4 which shows the variation of the probability of failure (P_f) with δ_z/L_f for a design factor of safety of 1.5 and for different coefficients of variation of the undrained shear strength. Results on Fig.7.4 indicate that the effect of variance reduction in the undrained shear strength becomes visible at ratios of δ_z/L_f that around 0.2. This effect is shown as a decrease in the probability of failure. The maximum benefit from variance reduction is achieved at ratios of δ_z/L_f that are around 0.1, since no considerable further reduction in the variance occurs below that level. This significant effect of variance reduction on the probability of failure doesn't appear clearly in Figures 7.1, 7.2, and 7.3 since the model uncertainty dominates the probability of failure in the reliability analysis.

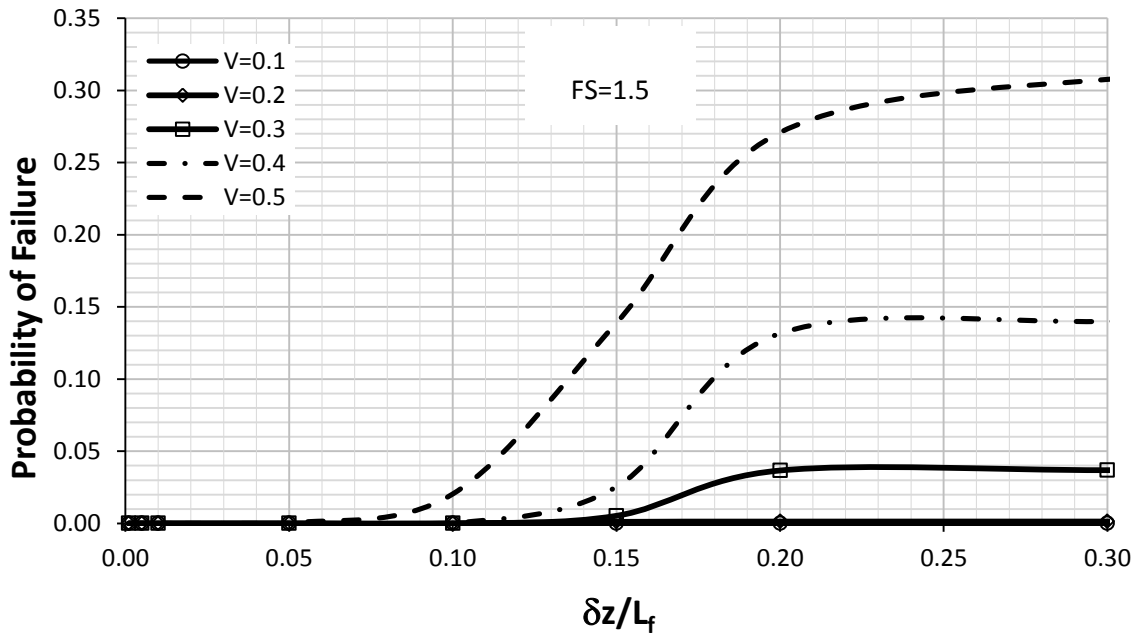


Figure 7.4 Variation of P_f with V and δ_z/L_f for $FS = 1.5$ by considering spatial variability only

Fig.7.4. shows the significant effect of spatial variability on the probability of failure of slopes. For instance, the probability of failure of a slope that has a ratio of $\delta_z/L_f = 0.2$ increases from about 0 when $V=0.1$ to a high P_f of about 27% when $V=0.5$. To explain this result, one should look at the increase in the coefficient of variation of the factor of safety (V_{FS}) that enters in the calculation of the probability of failure. V_{FS} is calculated using Equations 5-1 & 5-2 in chapter 5. It is found that V_{FS} increases from 0.061 for $V=0.1$ to 0.174 for $V=0.5$. This increase in V_{FS} doesn't explain the large increase in the probability of failure from 0 to 27%. There is another factor that leads to the increase in the probability of failure which is the mean of the factor of safety (μ_{FS}) which is found to decrease from 1.467 for $V=0.1$ to 1.129 for $V=0.5$. Hence, spatial variability has two effects on the probability of failure; (1) increasing the total uncertainty of the factor of safety, (2) decreasing the mean of the factor of safety.

7.2.2. Effect of lower-bound factor of safety on the probability of failure

To illustrate the effect of the lower-bound factor of safety on the probability of failure of slopes, a number of homogenous slopes with spatially variable undrained shear strength are considered. The probability of failure is evaluated using Equation 7-2 that takes into consideration the lower-bound factor of safety. This lower-bound factor of safety is calculated by replacing the undisturbed undrained shear strength with the remolded shear strength that is evaluated using the sensitivity equation. The sensitivity of clays is defined as the ratio of the undisturbed undrained shear strength to the remolded undrained shear strength of the clay. The analysis is conducted for different conditions for the lower-bound factor of safety (clays with different sensitivities). Sensitivities of 1.5, 1.75, 2, 2.25, 2.5, and 3 are considered in the analysis for the calculation of the lower-bound factor of safety, and for showing the effect of these lower-bound values on the probability of failure of slopes.

Curves showing the variation of the probability of failure as a function of the sensitivity of clays and the coefficient of variation of the undrained shear strength for slopes with ratio of $\delta_z/L_f = 0.1$ are shown in Figures 7.5, 7.6, and 7.7. The results are illustrated according to different values of deterministic factors of safety. The curves on Figures 7.5, 7.6, and 7.7. represent the cases where the uncertainty in the undrained shear strength takes different values ($V = 0.1, 0.2, 0.3, 0.4, \text{ and } 0.5$).

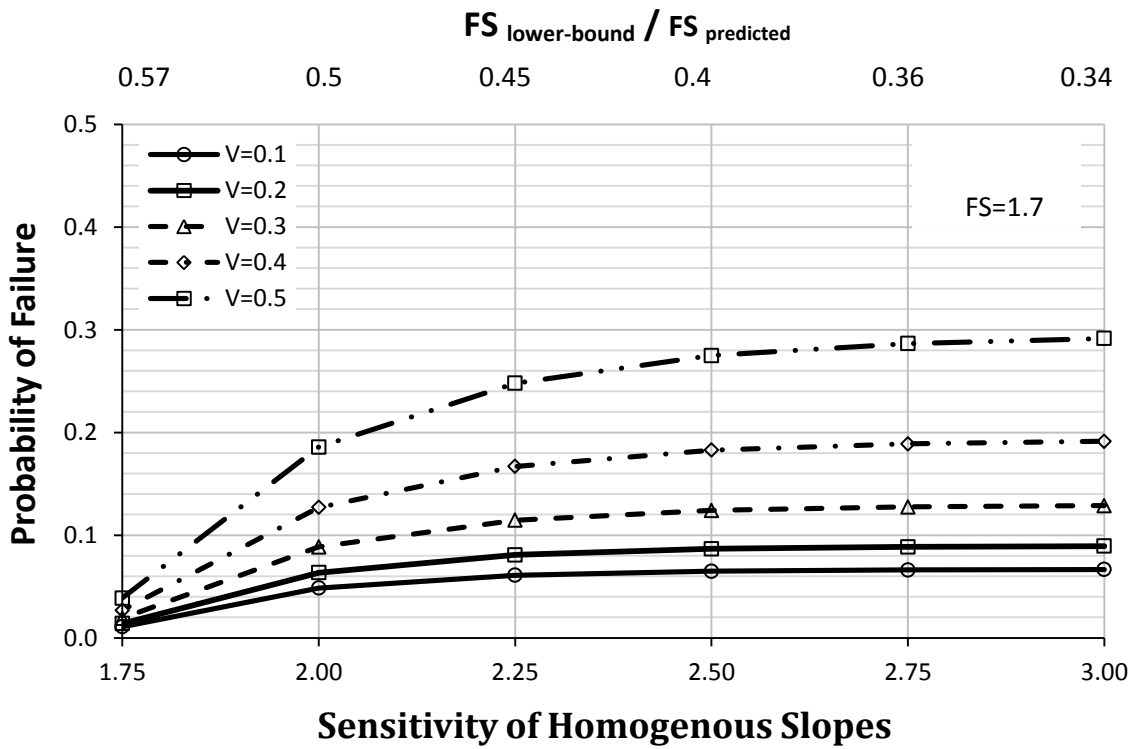
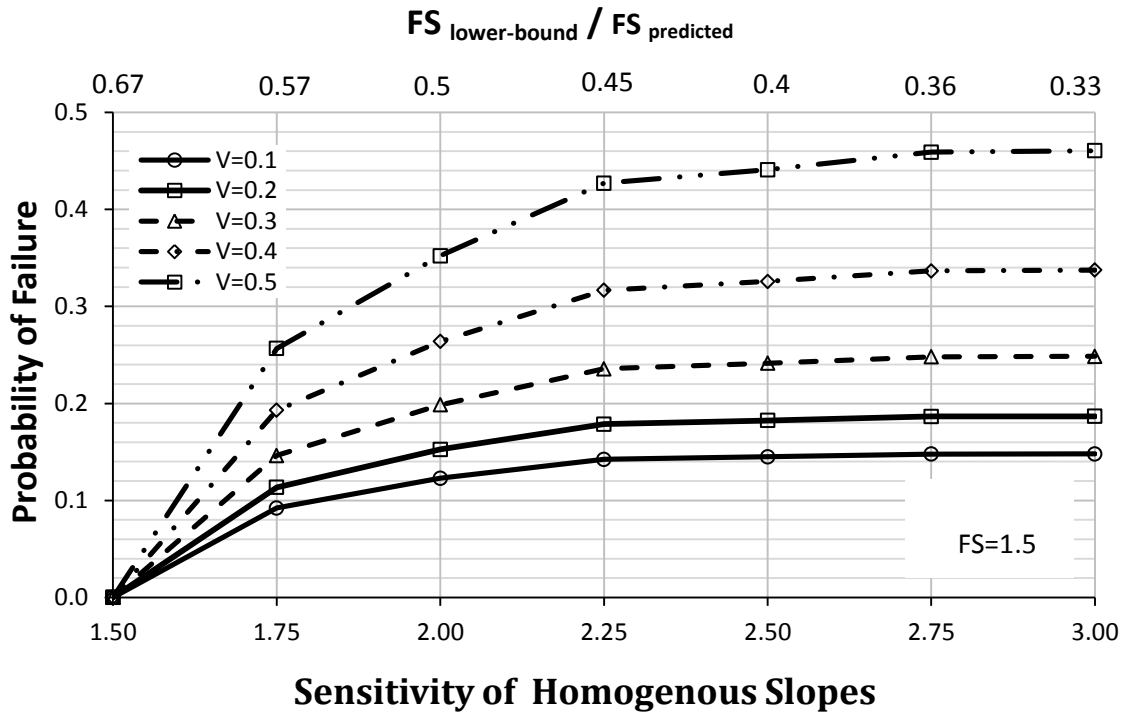


Figure 7.5 Variation of P_f with V and Sensitivity for $\delta_z/L_f = 0.1$, $FS = 1.5$ & $FS = 1.7$

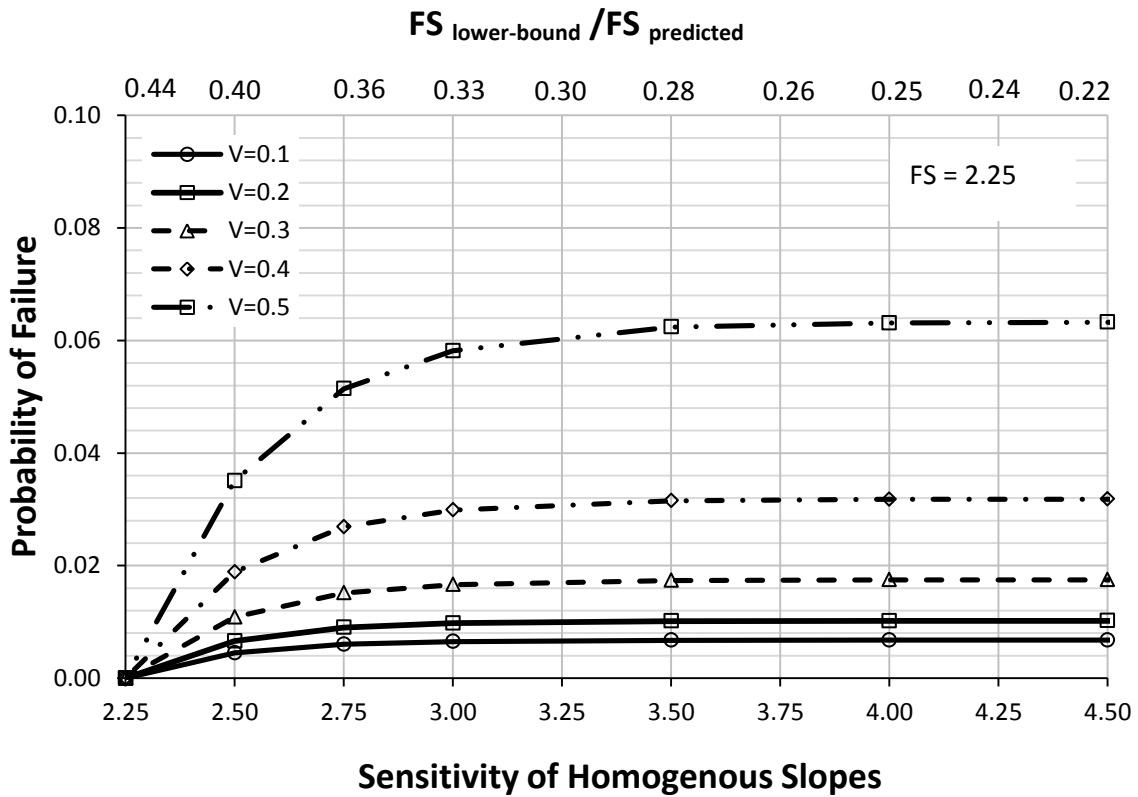
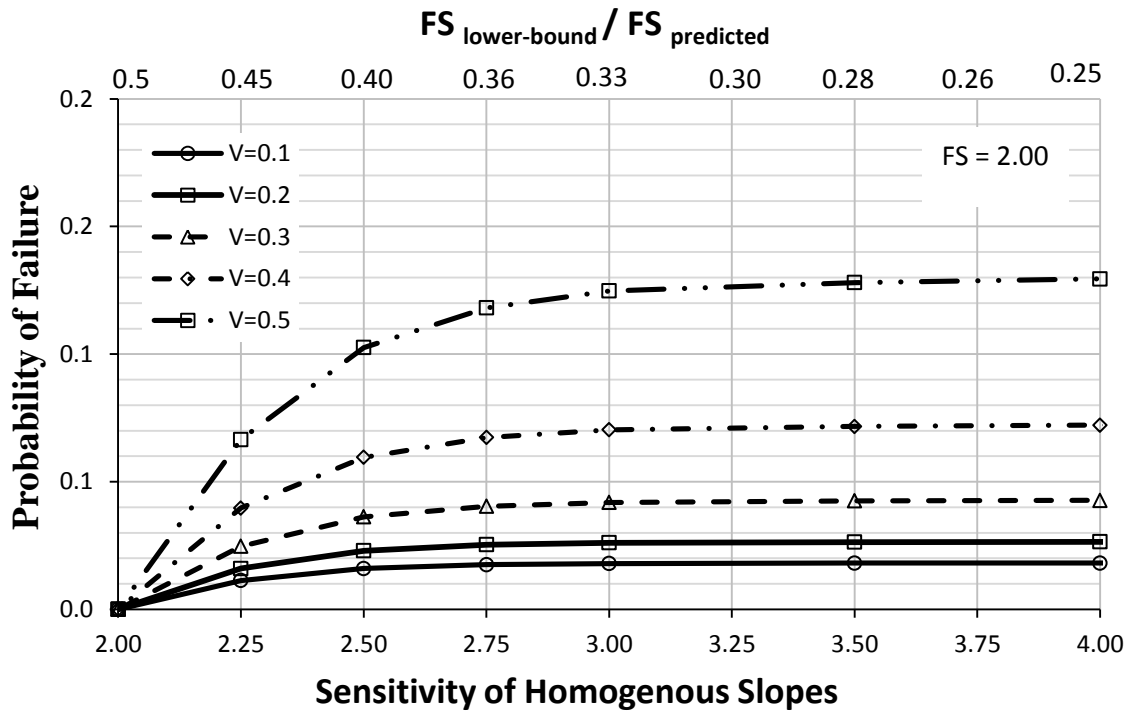


Figure 7. 6 Variation of P_f with V and Sensitivity for $\delta_z/L_f = 0.1$, $FS = 2.00$ & $FS = 2.25$

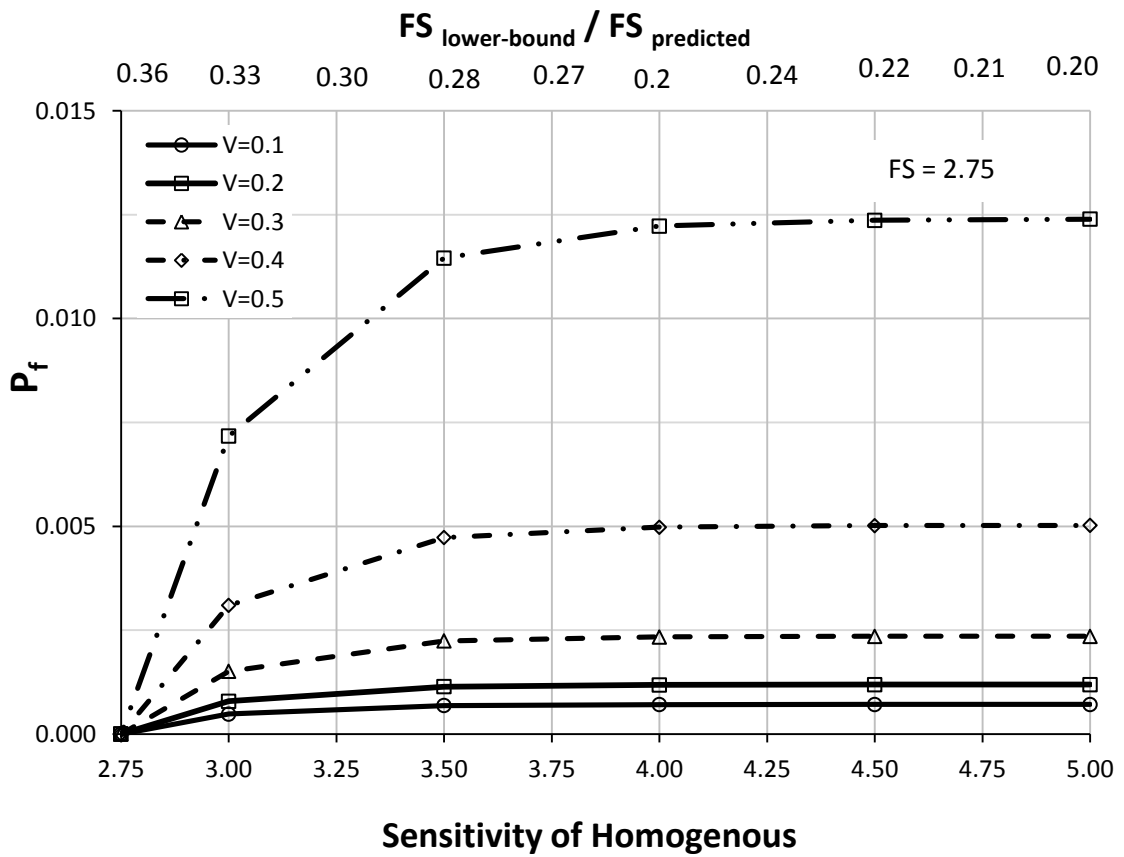
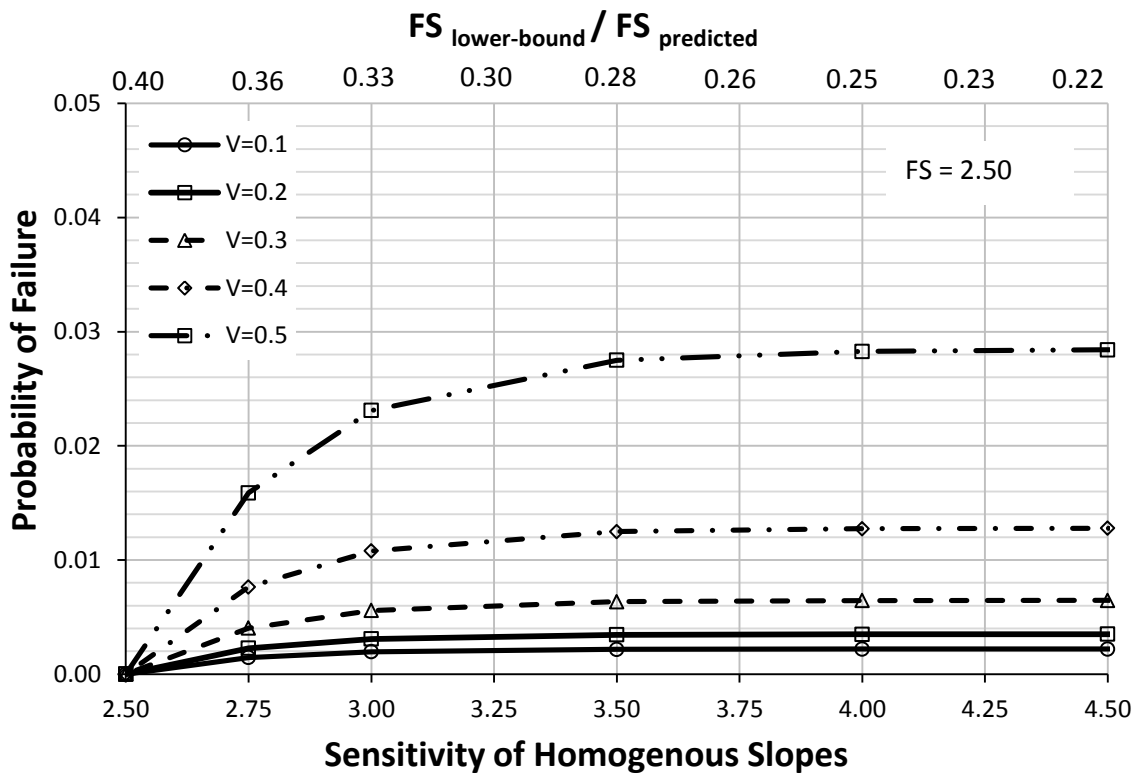


Figure 7. 7 Variation of P_f with V and Sensitivity for $\delta_z/L_f = 0.1$, $FS = 2.50$ & $FS = 2.75$

The results shown on Figs. 7.4 to 7.7 correspond to a ratio of $\delta_z/L_f = 0.1$ which is a ratio that is typical for undrained slopes. The primary conclusion from Figures 7.5, 7.6, and 7.7 is that a lower-bound factor of safety can have a significant effect on the calculated probability of failure. For example, consider a typical case where the factor of safety of the slope is 1.5. If the sensitivity of the soil is 1.75 (ratio of lower-bound to predicted factor of safety of about 0.57), the probability of failure decreases to half of its magnitude compared to the case where there is no lower-bound factor of safety (Fig.7.5).

The second conclusion from Figures 7.5, 7.6, and 7.7 is that there is a threshold value for the sensitivity (sensitivity of about 3), below which the lower-bound factor of safety affects the probability of failure. Above this threshold, the lower-bound factor of safety has essentially no effect on the probability of failure.

The effect of the lower-bound factor of safety on the probability of failure is influenced by the magnitude of the deterministic factor of safety and by the value of the coefficient of variation; as the deterministic factor of safety increases, the lower-bound becomes more effective in reducing the probability of failure. Also, as the uncertainty in the coefficient of variation (V) increases, the probability of failure becomes more sensitive to the lower-bound factor of safety where the importance of the lower-bound factor of safety increases more. This is related to the fact that as the coefficient of variation increases, the mean factor of safety decreases. Thus, the magnitude of the ratio of the lower-bound factor of safety to the mean factor of safety becomes larger making the probability of failure more sensitive to the lower-bound factor of safety. It should be noted that the same conclusions are applicable for a ratio of $\delta_z/L_f = 0.2$.

7.2.3 Recommendation for the factors of safety of undrained slopes

In this section, recommendations for the factor of safety of undrained slopes are presented to achieve target levels of acceptable risk. This analysis is conducted for different levels of the spatial variability of the undrained shear strength, and different conditions for the lower-bound factor of safety (clays with different sensitivities).

Relationships between the factor of safety and the probability of failure were established for cases with different lower-bound factors of safety (as indicated by the sensitivity) and different coefficients of variation of the undrained shear strength. Plots showing these relationships for coefficients of variation of 0.1, 0.2, 0.3, 0.4, and 0.5 are shown in Figures 7.8., 7.9., and 7.10 for the case with $\delta_z/L_f = 0.1$ while similar relationships are shown in Figures 7.11., 7.12., and 7.13 for the case with $\delta_z/L_f = 0.2$. The relationships between the factor of safety and the probability of failure illustrate the effect of the lower-bound factor of safety on the probability of failure by comparing the probability of failure of the slope without the inclusion of the lower-bound with that with the inclusion of the lower-bound factor of safety.

For the case with $\delta_z/L_f = 0.1$, the relationships shown in Figs. 7.8., 7.9., and 7.10 indicate that as the factor of safety increases, the probability of failure decreases as expected. For relatively small coefficients of variation of the undrained shear strength ($V = 0.1$ & 0.2), when the lower-bound is incorporated in the analysis, the relationship between FS and p_f seems to be unaffected by the lower-bound for cases with sensitivities ranging from 2 to 3. For sensitivities smaller than 2, the lower-bound factor of safety starts to play a role in decreasing the probability of failure for a given factor of safety. The importance of the

lower-bound becomes more significant for cases involving higher coefficients of variation of the undrained shear strengths ($V = 0.3, 0.4,$ and 0.5), where considerable effects of lower-bound on the probability of failure are noticed from sensitivities as high 2.5 and 2.75.

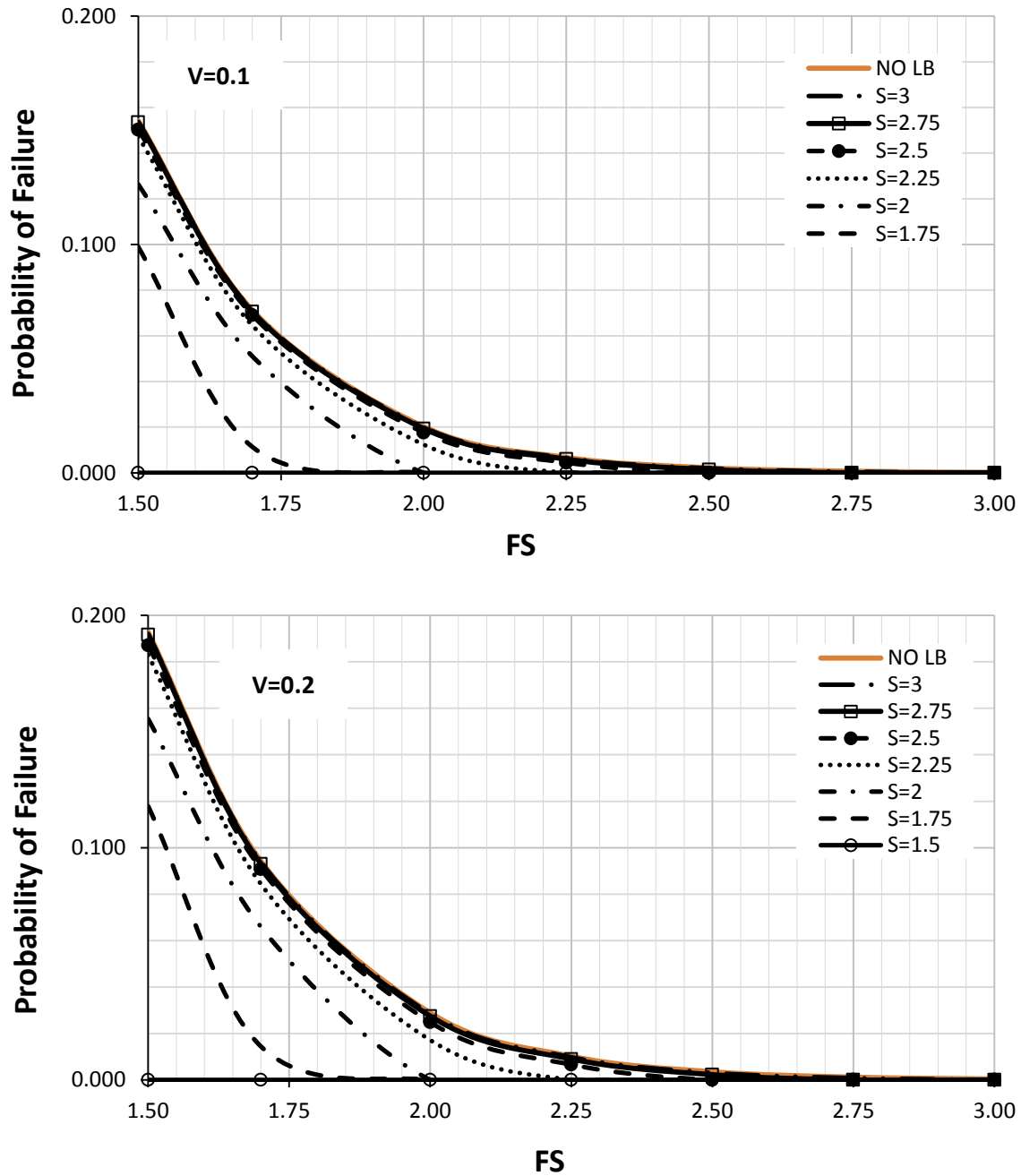


Figure 7. 8 Recommended factor of safety needed to accomplish a target P_f for different sensitivities for $V = 0.1$ & $V = 0.2$ and $\delta_z/L_f = 0.1$

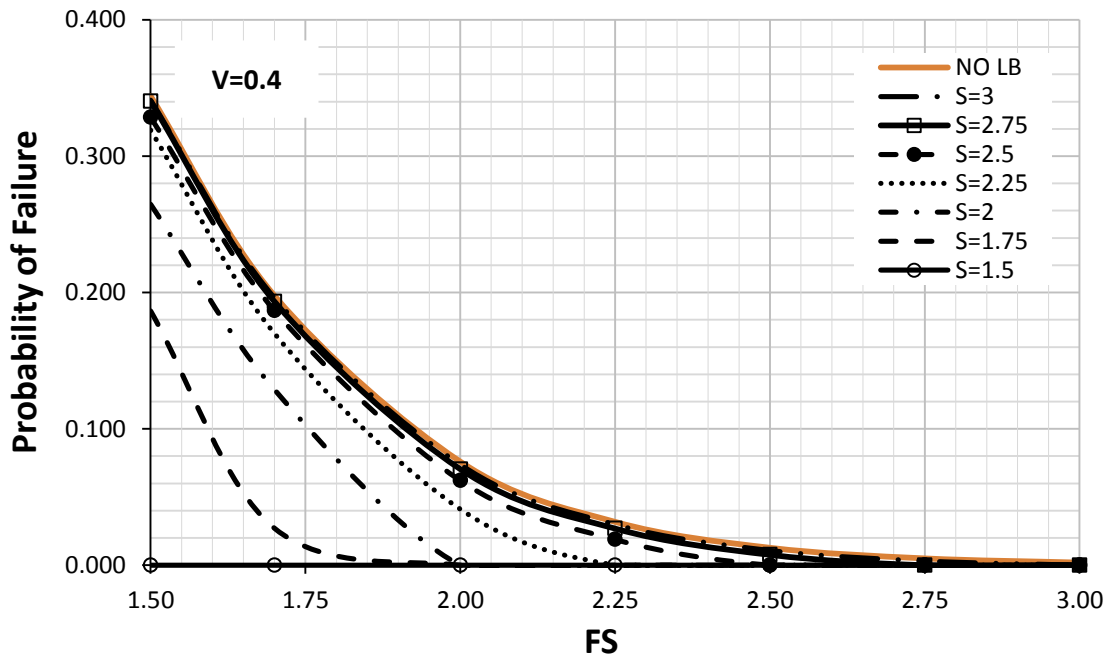
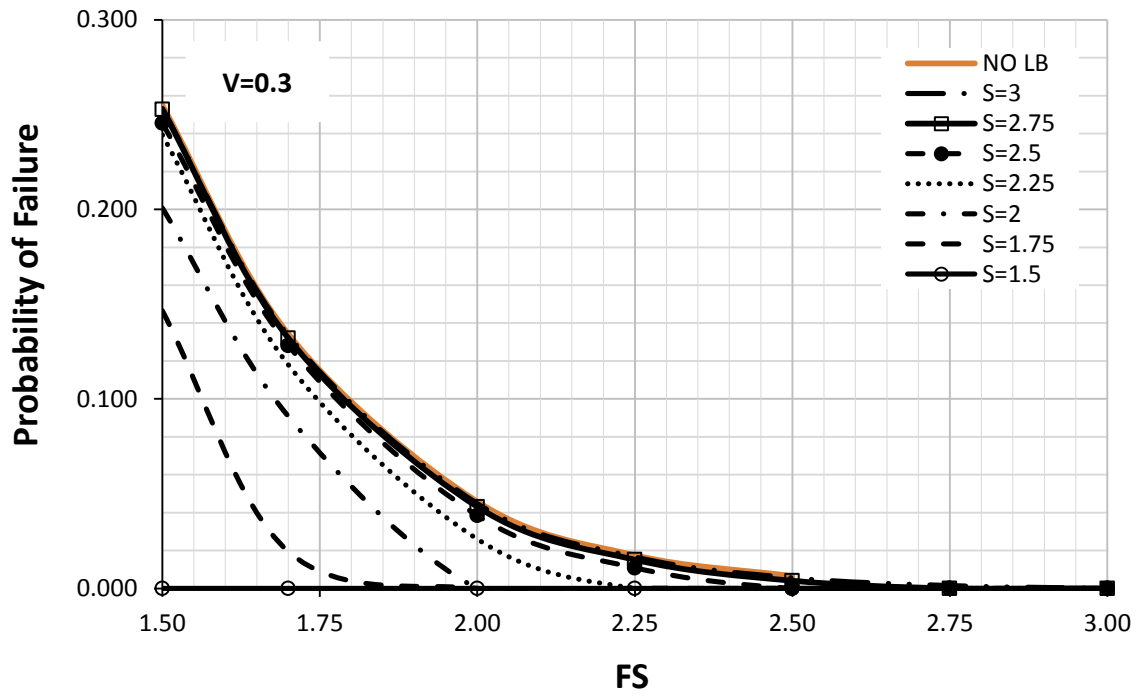


Figure 7.9 Recommended factor of safety needed to accomplish a target P_f for different sensitivities for $V=0.3$ & $V=0.4$ and $\delta_z/L_f = 0.1$

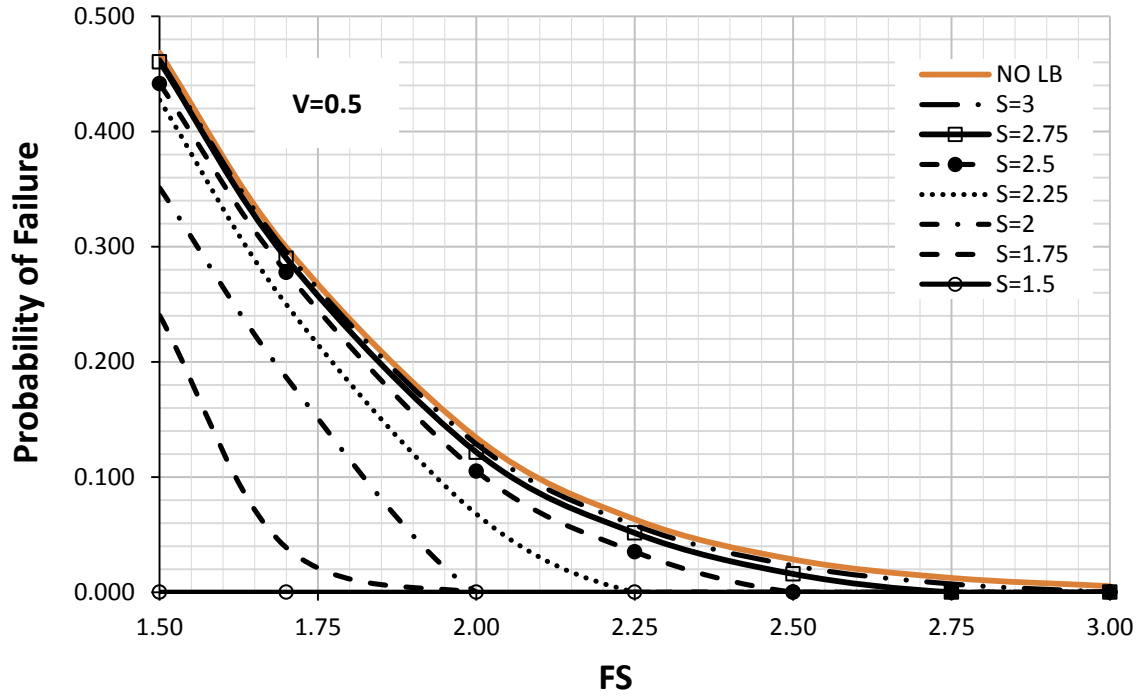


Figure 7. 10 Recommended factor of safety needed to accomplish a target P_f for different sensitivities for $V=0.5$ and $\delta_z/L_f = 0.1$

Similar results are obtained for the cases with a ratio $\delta_z/L_f = 0.2$ as indicated in Figures 7.11., 7.12., and 7.13., except that the calculated probabilities of failure for a given coefficient of variation, a given factor of safety, and a given lower-bound factor of safety (sensitivity) are slightly higher than the probabilities of failure of slopes with ratio $\delta_z/L_f = 0.1$. This is expected given that the effect of variance reduction diminishes for the case of $\delta_z/L_f = 0.2$.

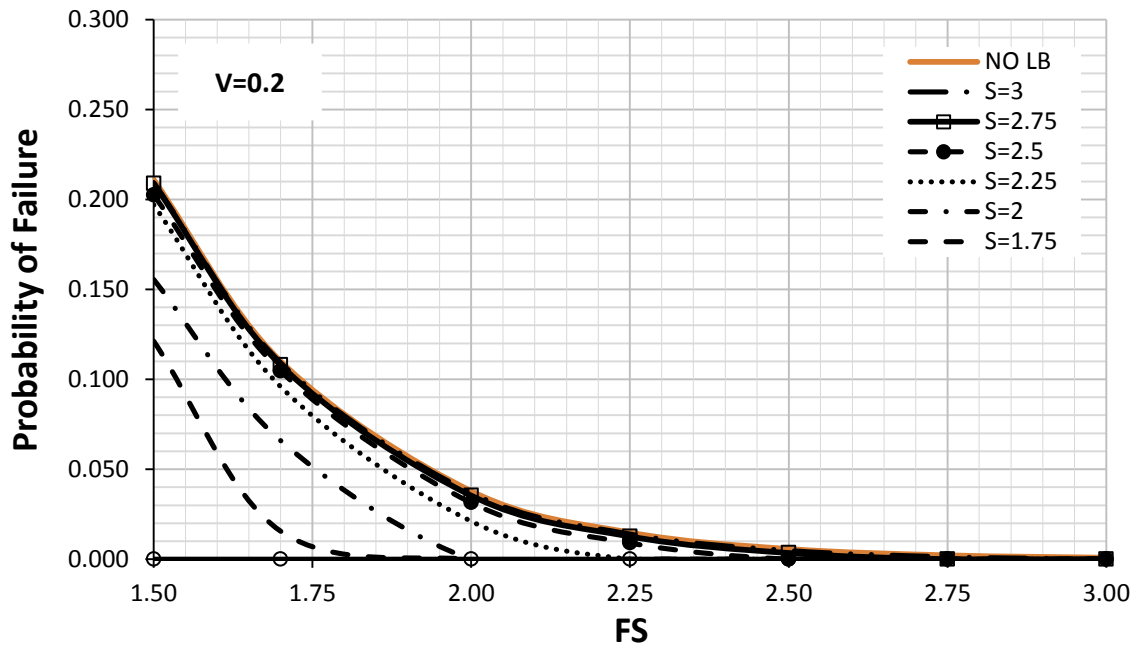
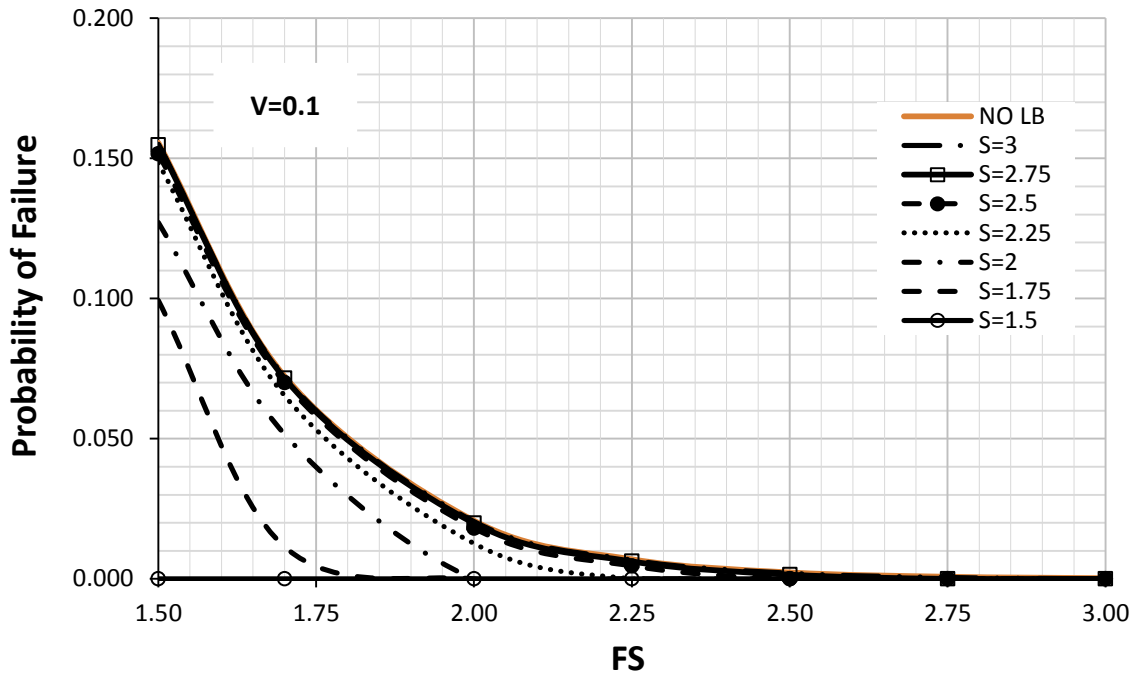


Figure 7. 11 Recommended factor of safety needed to accomplish a target P_f for different sensitivities for $V=0.1$ and $V=0.2$ and $\delta_z/L_f = 0.2$

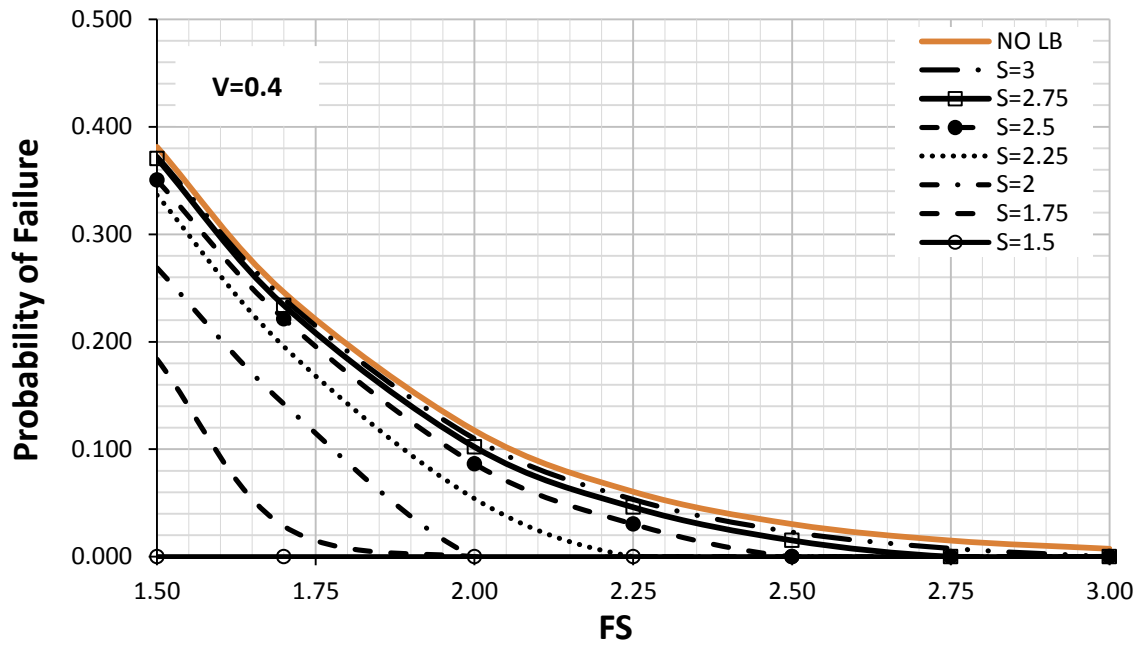
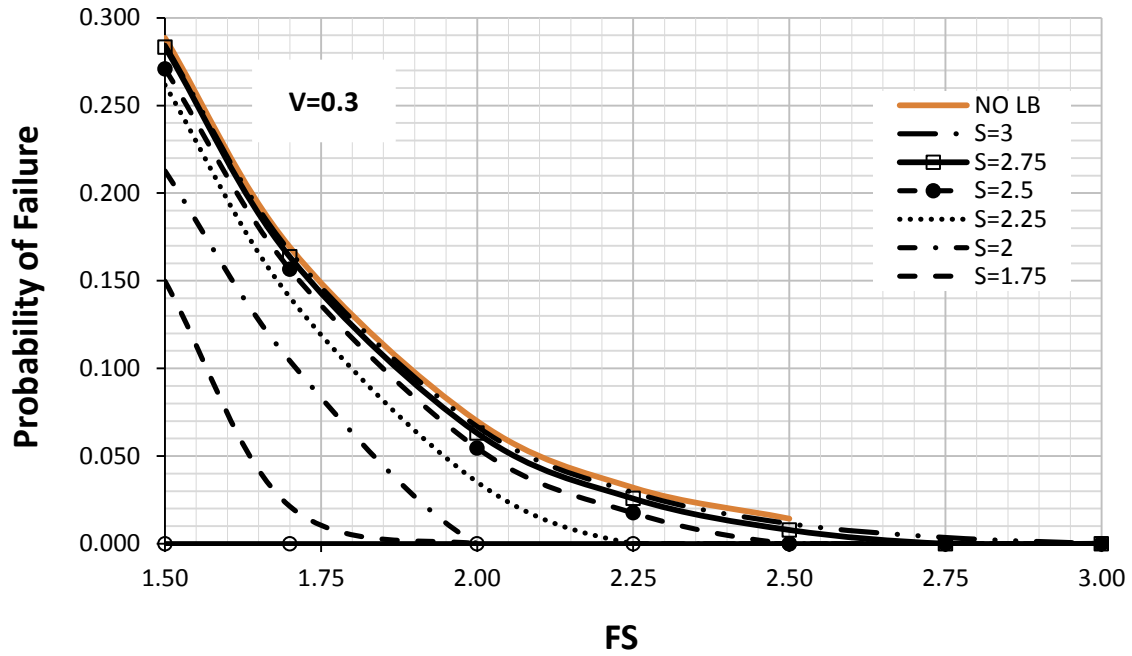


Figure 7. 12 Recommended factor of safety needed to accomplish a target P_f for different sensitivities for $V=0.3$ and $V=0.4$ and $\delta_z/L_f = 0.2$

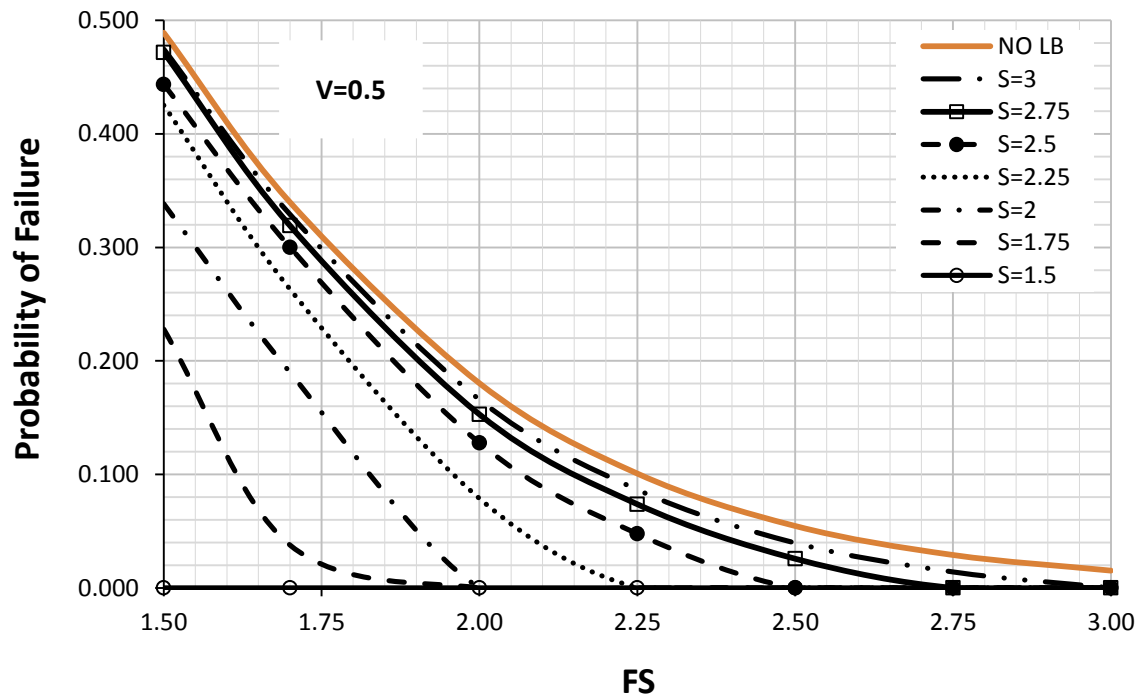


Figure 7.13 Recommended factor of safety needed to accomplish a target P_f for different sensitivities for $V=0.5$ and $\delta_c/L_f = 0.2$

7.2.3.1 Acceptable probability of failure

A reliability analysis calculates the probability of failure of a given system. In geotechnical engineering, acceptable probabilities of failure vary according to how important the structure is and how dangerous the consequences of failure are. Thus, the concept of risk may be understood in terms not only of the likelihood that certain events will occur but also of what these events consist of and what they would lead to in terms of environmental damage, casualties, financial losses, and other undesirable outcomes (Salgado et al. 2014). Chowdhury and Flentje (2003) suggested maximum values for the probability of failure of slopes that have different functions and which have different consequences of failure. The acceptable probabilities of failure range could be as low as

0.001 for cases involving slopes that might result in loss of lives upon failure to about 0.15 for slopes and temporary slopes where failure would not result in potential loss of lives. Christian et al. (1994) suggested that $P_f = 0.001$ would be a reasonable number to use in design. Loehr et al. (2005) set the range of P_f from 0.001 to 0.01 for slopes: 0.01 for relatively low potential risk and 0.001 for high potential risk. Santamarina et al. (1992) made an effort to determine an acceptable probability of failure of slopes. The results are summarized in Table 7.1.

Table 7. 1. Acceptable probability of failure of slopes (Santamarina et al. 1992)

Conditions	Acceptable probability of failure
Temporary structures: no potential life loss, low repair cost	0.1
Minimal consequences of failure: high cost to reduce the probability of failure (bench slope or open pit mine)	0.1-0.2
Minimal consequences of failure: repairs can be done when time permits (repair cost is less than cost of reducing probability of failure)	0.01
Existing large cut in interstate highway	0.01-0.02
Large cut on interstate highway to be constructed	< 0.01
Lives may be lost when slopes fail	0.001

The typical acceptable probabilities of failure range from as high as 20% for cases with minimal consequences of failure to values of 0.001 for extreme cases where lives may be lost when slopes fail. In this study, probabilities of 0.001, 0.005, 0.01, 0.05, and 0.1 are considered acceptable probabilities of failure for the recommendation of the factors of safety.

7.2.3.2 Design graphs for factors of safety of undrained slopes

In this section, required factors of safety are recommended to achieve different target probabilities of failure for different cases of spatial variability and soil sensitivity. The factors of safety recommended to achieve probabilities of 0.001, 0.005, 0.01, 0.05, and 0.10 according to different coefficients of variations ($V = 0.1, 0.3, \text{ and } 0.5$) for slopes with ratio $\delta_z/L_f = 0.1$ and $\delta_z/L_f = 0.2$ are presented in Figures 7.14, 7.15., 7.16., 7.17., 7.18., and 7.19.

For the case where the lower-bound factor of safety is not included in the analysis, results on Figs. 7.14 to 7.19 indicate that the required factor of safety decreases significantly as the target reliability level of the slope increases. For example, for the case of intermediate spatial variability ($V = 0.3$) in the undrained shear strength, the required factor of safety decreases from a high value of 2.8 for the case with a target probability of failure 0.001 (slopes that have loss of lives) to a low value of 1.76 for the case where the target probability of failure is 0.1. These required factors of safety decrease when the lower-bound factor of safety is incorporated in the analysis. For example, when a lower-bound factor of safety that is consistent with a sensitivity of 2 is incorporated, the required factor of safety decreases from 2.8 to 2.0 (for the case with a target probability of failure 0.001) and from 1.76 to 1.66 (for the case with a target probability of failure 0.1). These results are significant because they indicate that the lower-bound factor of safety could play a significant role in reducing conservatism in the design, particularly for slopes designed for a higher reliability level.

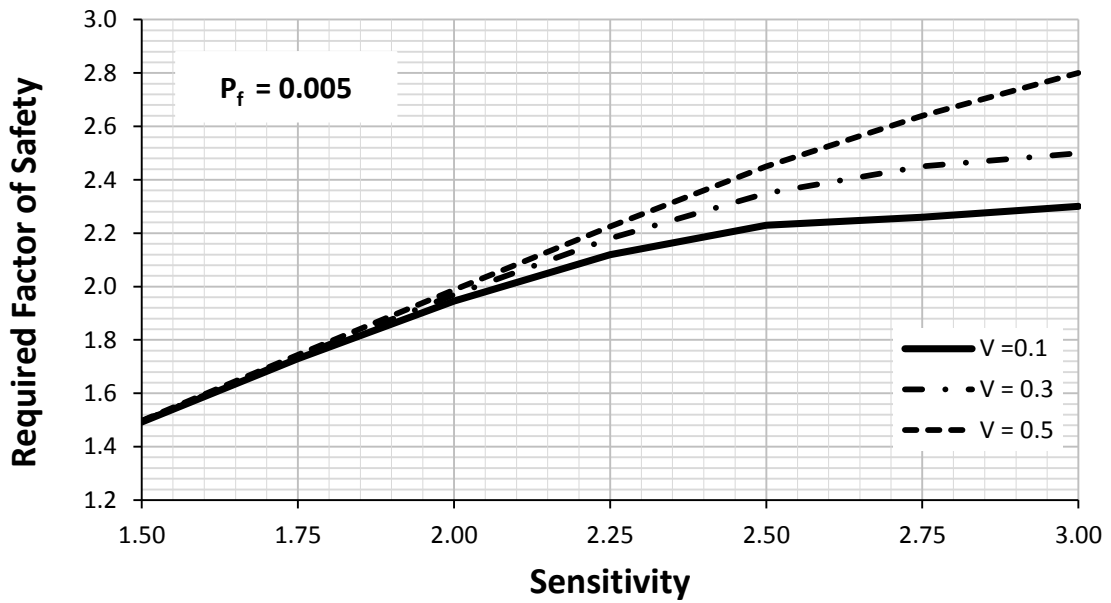
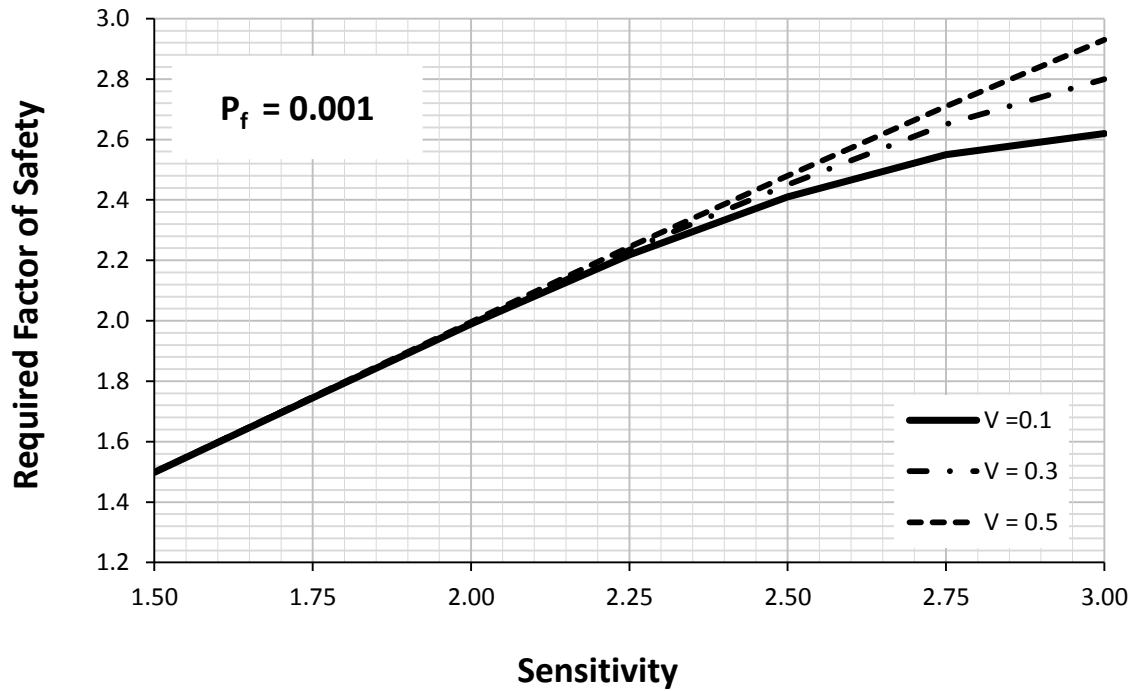


Figure 7. 14 Recommended factors of safety for different coefficients of variation for probabilities of failure of 0.001 & 0.005 for slopes with ratio $\delta_z / L_f = 0.1$

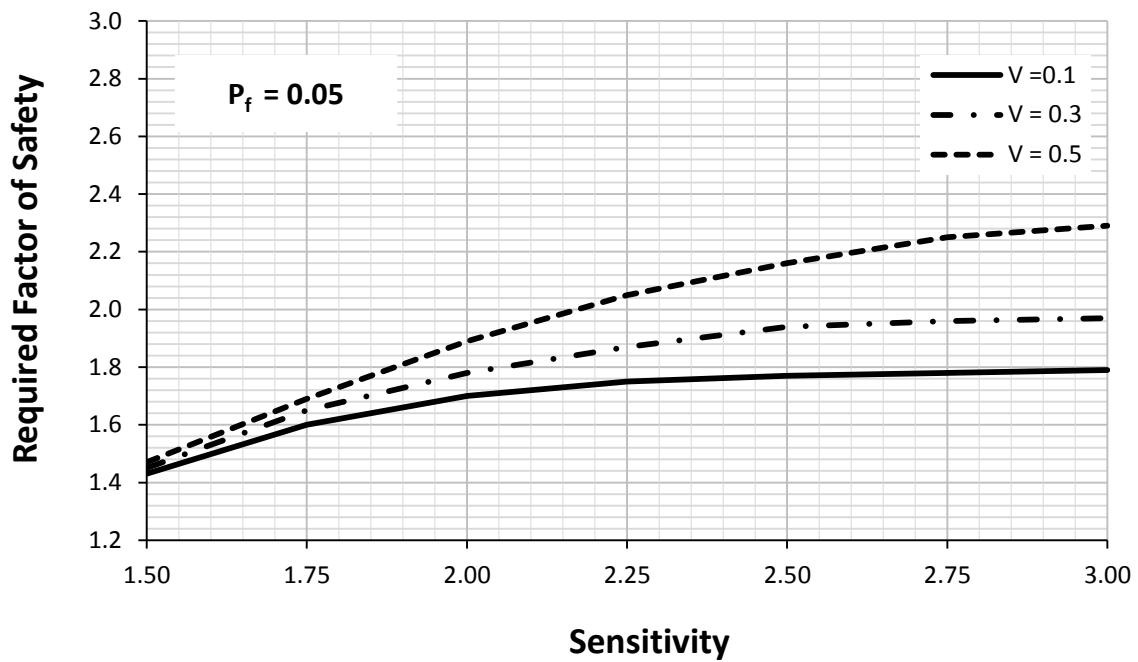
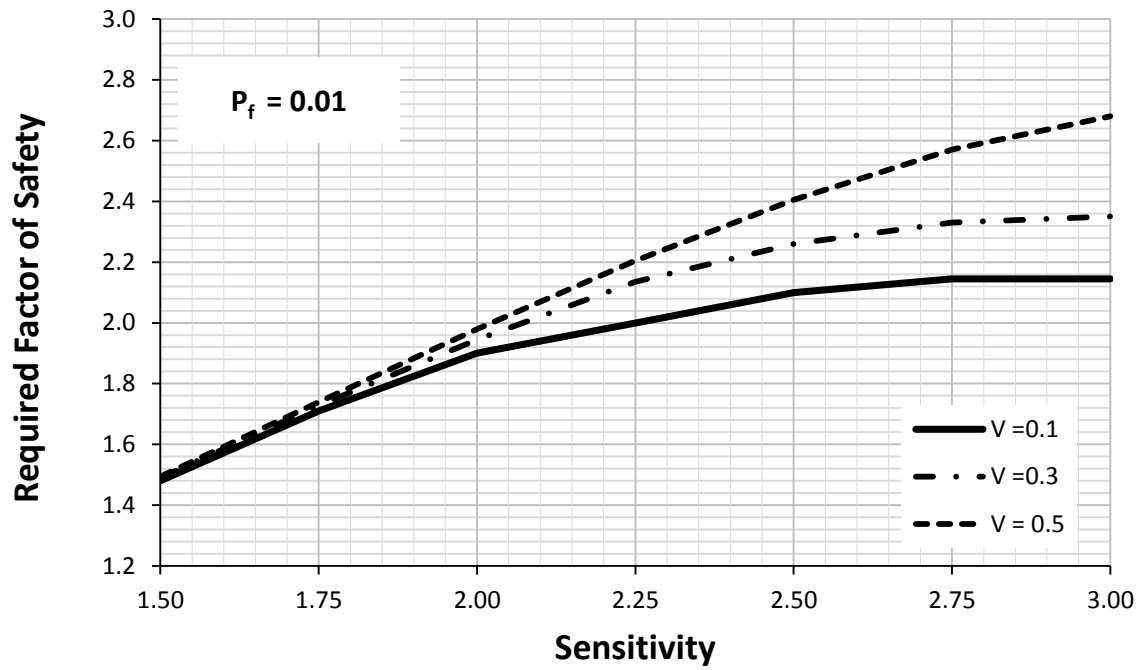


Figure 7. 15 Recommended factors of safety for different coefficients of variation to achieve probabilities of failure of 0.01 & 0.05 for slopes with ratio $\delta z / L_f = 0.1$

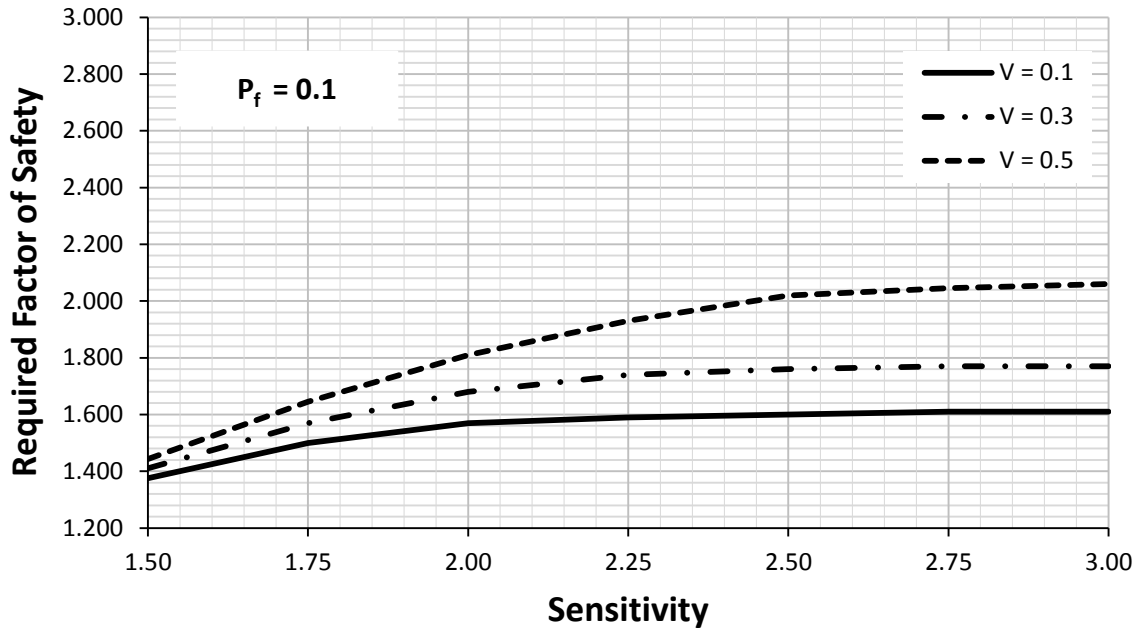


Figure 7. 16 Recommended factors of safety for different coefficients of variation to achieve probability of failure of 0.1 for slopes with ratio $\delta z / L_f = 0.1$

The cases that were analyzed above represent the case with a $\delta z / L_f = 0.1$. To check the sensitivity of the results to the ratio of $\delta z / L_f$, the analysis is repeated for a ratio of $\delta z / L_f = 0.2$ and the results are included in Figs. 7.17 to 7.19. For the case where the lower-bound factor of safety is not included in the analysis and for the case of intermediate spatial variability ($V = 0.3$) in the undrained shear strength, the required factor of safety decreases from a high value of 2.82 (instead of 2.8 for $\delta z / L_f = 0.1$) for the case with a target probability of failure 0.001 to a low value of 1.83 (instead of 1.76 for $\delta z / L_f = 0.1$) for the case where the target probability of failure is 0.1. These results indicate that the resulting required factor of safety is not highly sensitive to the ratio of $\delta z / L_f$.

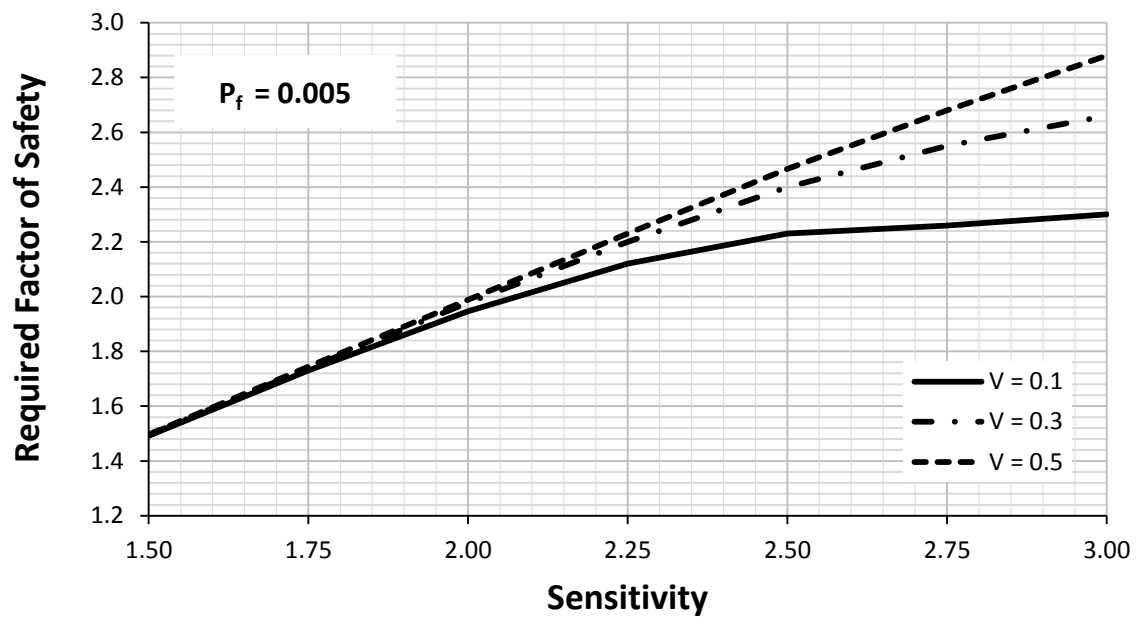
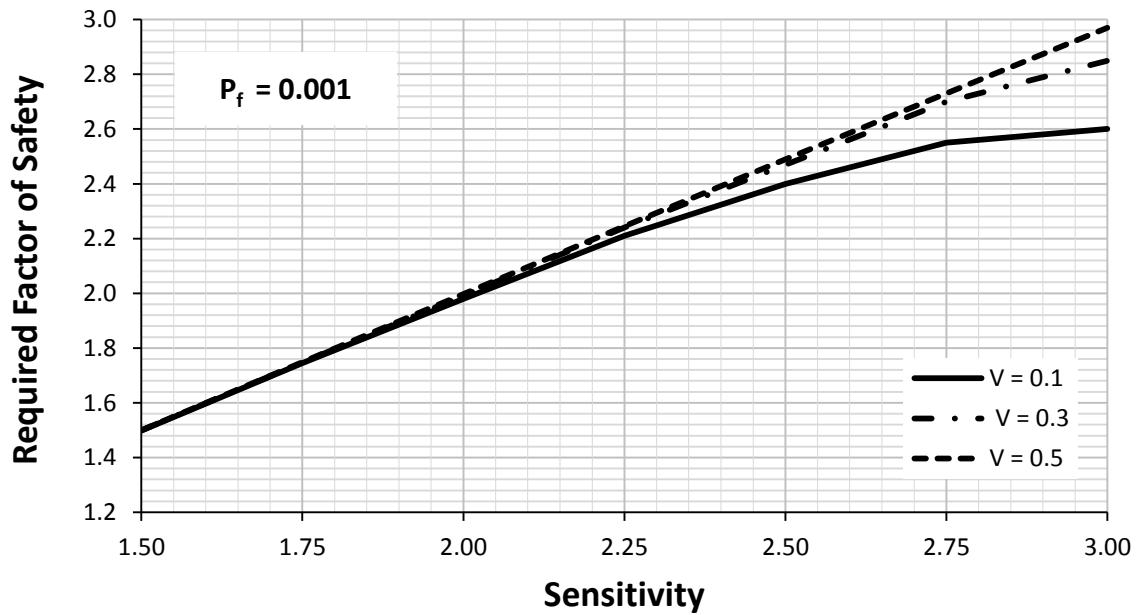


Figure 7. 17 Recommended factors of safety for different coefficients of variation to achieve probability of failure of 0.001 and 0.005 for slopes with ratio $\delta z/L_f = 0.2$

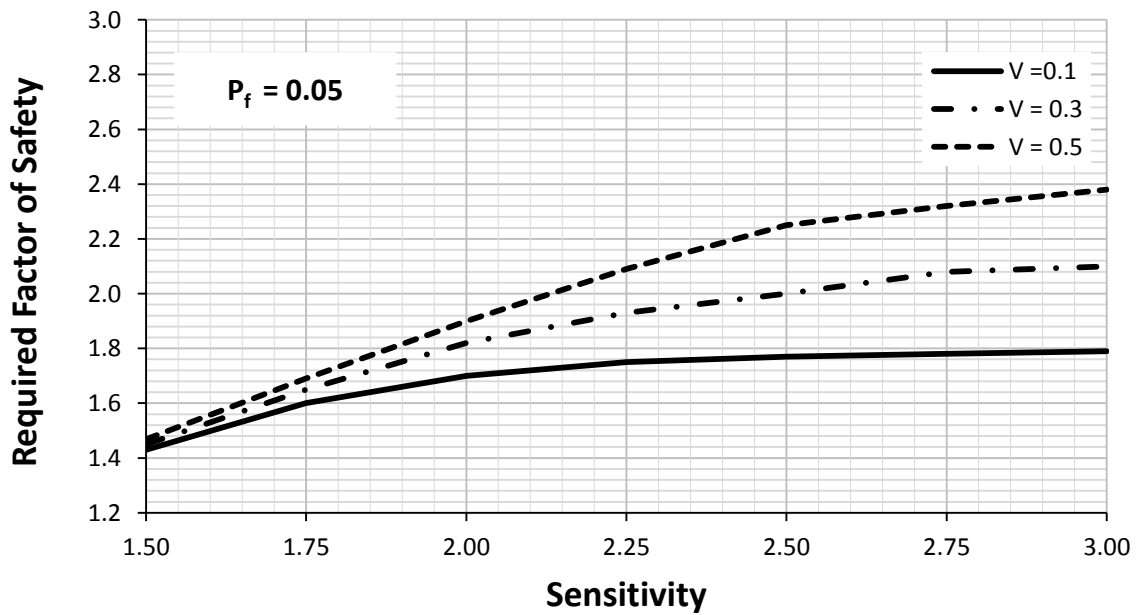
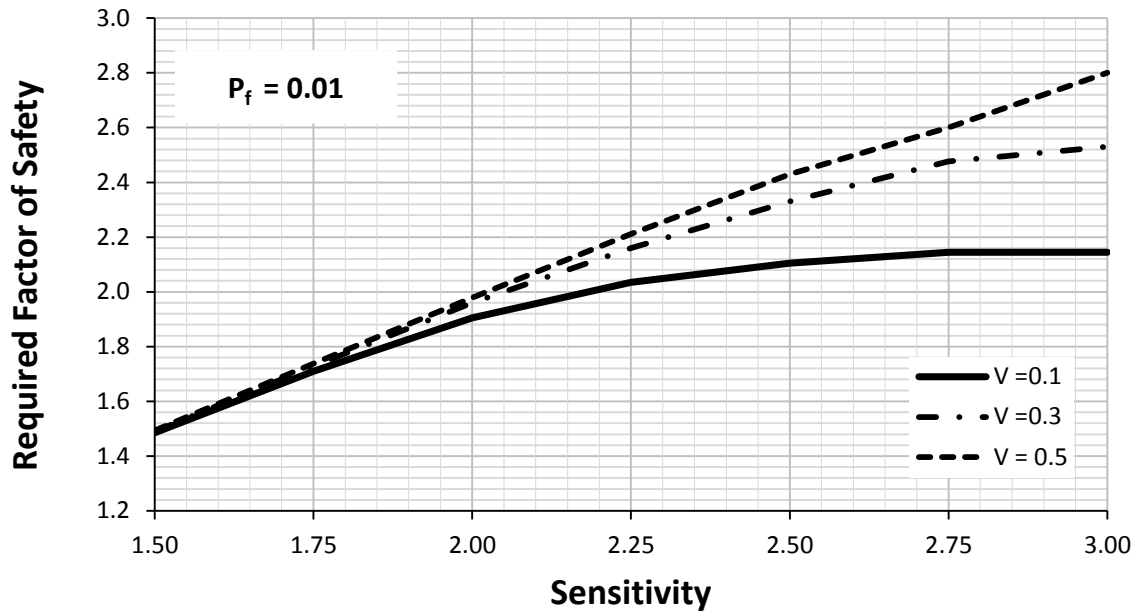


Figure 7. 18 Recommended factors of safety for different coefficients of variations to achieve probabilities of failure of 0.01 & 0.05 for slopes with ration of $\delta z/L_f = 0.2$

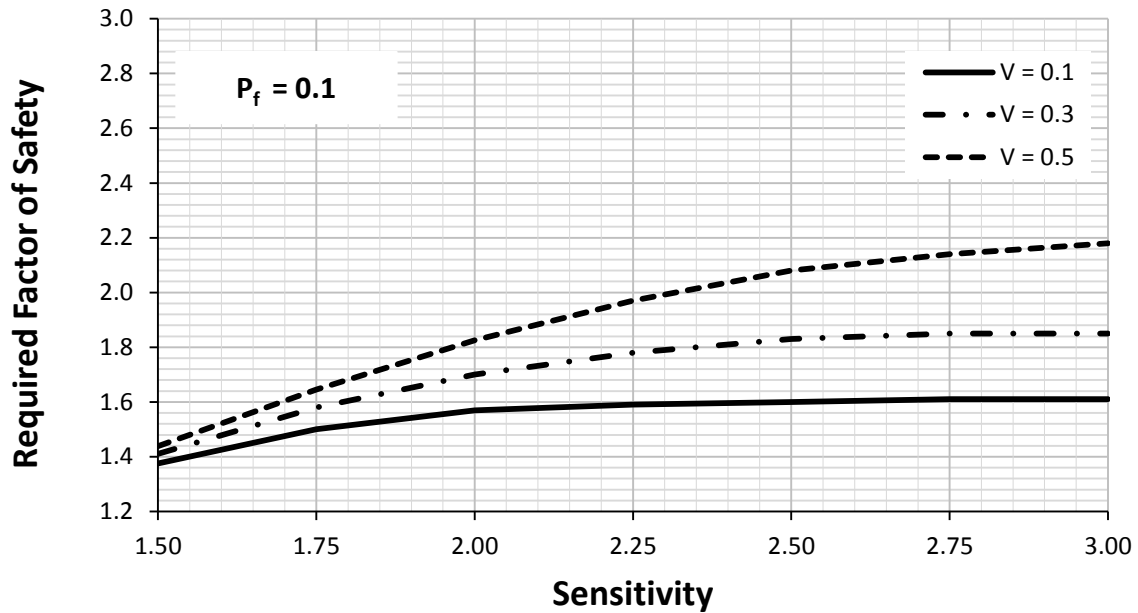


Figure 7. 19 Recommended factors of safety for different coefficients of variation to achieve probabilities of failure of 0.1 for slopes with ratio $\delta z / L_f = 0.2$

Design tables are also shown in the following section to illustrate the required factors of safety needed to achieve a target level of the probability of failure for the ratios of $\delta z / L_f = 0.1$ & 0.2 for different coefficients of variations.

Table 7.2 Recommended Factors of Safety needed to accomplish a target P_f for different sensitivities for $V = 0.1$ & $\delta z / L_f = 0.10$

P_f \ Sensitivity	1.5	1.75	2	2.25	2.5	2.75	3
0.001	1.498	1.745	1.989	2.218	2.41	2.55	2.62
0.005	1.492	1.73	1.946	2.12	2.23	2.26	2.3
0.01	1.48	1.71	1.9	2	2.1	2.145	2.145
0.05	1.43	1.6	1.7	1.75	1.77	1.78	1.79
0.1	1.375	1.5	1.57	1.59	1.6	1.61	1.61

Table 7.3 Recommended Factors of Safety needed to accomplish a target P_f for different sensitivities for $V=0.3$ & $\delta_z/L_f=0.10$

P_f \ Sensitivity	1.5	1.75	2	2.25	2.5	2.75	3
0.001	1.499	1.747	1.990	2.235	2.450	2.650	2.800
0.005	1.495	1.738	1.970	2.180	2.350	2.450	2.500
0.01	1.490	1.782	1.945	2.135	2.260	2.330	2.350
0.05	1.450	1.650	1.780	1.870	1.940	1.960	1.970
0.1	1.410	1.570	1.680	1.740	1.760	1.770	1.770

Table 7.4 Recommended Factors of Safety needed to accomplish a target P_f for different sensitivities for $V=0.5$ & $\delta_z/L_f=0.10$

P_f \ Sensitivity	1.5	1.75	2	2.25	2.5	2.75	3
0.001	1.499	1.748	1.996	2.245	2.48	2.71	2.93
0.005	1.497	1.744	1.987	2.225	2.45	2.64	2.8
0.01	1.494	1.739	1.979	2.205	2.405	2.57	2.68
0.05	1.47	1.69	1.89	2.05	2.16	2.25	2.29
0.1	1.443	1.645	1.81	1.93	2.02	2.045	2.06

Table 7.5 Recommended Factors of Safety needed to accomplish a target P_f for different sensitivities for $V=0.1$ & $\delta_z/L_f=0.20$

P_f \ Sensitivity	1.5	1.75	2	2.25	2.5	2.75	3
0.001	1.498	1.745	1.98	2.21	2.4	2.55	2.6
0.005	1.492	1.73	1.946	2.12	2.23	2.26	2.3
0.01	1.485	1.71	1.905	2.035	2.105	2.145	2.145
0.05	1.43	1.6	1.7	1.75	1.77	1.78	1.79
0.1	1.375	1.5	1.57	1.59	1.6	1.61	1.61

Table 7.6 Recommended Factors of Safety needed to accomplish a target P_f for different sensitivities for $V = 0.3$ & $\delta_z / L_f = 0.20$

P_f \ Sensitivity	1.5	1.75	2	2.25	2.5	2.75	3
0.001	1.499	1.747	1.992	2.24	2.47	2.7	2.85
0.005	1.495	1.738	1.978	2.2	2.4	2.55	2.66
0.01	1.49	1.728	1.916	2.16	2.33	2.476	2.53
0.05	1.45	1.65	1.82	1.93	2	2.08	2.1
0.1	1.41	1.58	1.7	1.78	1.83	1.85	1.85

Table 7.7 Recommended Factors of Safety needed to accomplish a target P_f for different sensitivities for $V = 0.5$ & $\delta_z / L_f = 0.20$

P_f \ Sensitivity	1.5	1.75	2	2.25	2.5	2.75	3
0.001	1.499	1.748	1.997	2.245	2.49	2.73	2.97
0.005	1.497	1.744	1.989	2.23	2.466	2.68	2.88
0.01	1.494	1.738	1.979	2.211	2.43	2.6	2.8
0.05	1.468	1.69	1.9	2.09	2.25	2.32	2.38
0.1	1.438	1.645	1.825	1.97	2.08	2.14	2.18

7.3 Summary

The major conclusion from this chapter is that a lower-bound factor of safety can cause a significant increase in the calculated reliability for slope design. The effect of the lower-bound factor of safety on the reliability is more pronounced when the uncertainty in the undrained shear strength is large. Moreover, reliability analyses will provide more robust, realistic, and useful information for decision making purposes if they include information about lower-bound factor of safety. Finally, it is found that the probability of failure of slopes is affected mostly by the ratio of the lower-bound to mean factor of safety.

CHAPTER 8

Conclusions and Recommendations

8.1 Introduction

In this Chapter the conclusions and recommendations that resulted from this research work besides the design steps that may be followed to evaluate the probability of failure and the design factors of safety of slopes are presented. The conclusions and recommendations are based on a reliability-based design analysis that was conducted for undrained slopes while incorporating the effects of both model uncertainty and uncertainty due to spatial variability. The model uncertainty was evaluated based on a database of 52 case histories of failure slopes, while the uncertainty due to spatial variability was evaluated from the findings of the study by Jha and Ching (2013) who used a random finite element analysis to characterize this uncertainty for undrained slopes.

8.2 Summary of Findings

The following findings, conclusions, and recommendations emerged from the study conducted in this thesis:

1. Based on the analysis of 52 case histories of failed slopes, it was concluded that the model uncertainty as reflected in the ratio of measured to predicted factor of safety, λ , for 4 commonly used Limit Equilibrium Methods (Bishop, Janbu, OMS, and Spencer) has a mean of about 1.0 and a coefficient of variation that is in the

- order of 0.27 to 0.29. The parameter λ was found to be properly modeled by a lognormal probability distribution.
2. Based on the same database, it was found that there is strong evidence of the existence of a lower-bound factor of safety for undrained slopes that could be estimated from information regarding the remolded undrained shear strength of the soil. The lower-bound factor of safety has a mean value of that ranges from 0.45 to 0.47 when cases of very high soil sensitivity were excluded from the analysis. For such values of lower-bound factors of safety, the lower-bound is expected to have a considerable effect on the design of a slope. This effect increases as the magnitude of the lower bound factor of safety increases.
 3. The spatial variability in the undrained shear strength of clays as reflected in the coefficient of variation and the scale of fluctuation has a direct effect on the mean of the factor of safety and its coefficient of variation. As the coefficient of variation in the undrained shear strength increases, the mean of the factor of safety decreases compared to its deterministic design value and the coefficient of variation in the factor of safety increases. The effect of the scale of fluctuation is in reducing the uncertainty in the factor of safety since it results in a variance reduction due to spatial averaging along the failure surface. The ratio of the scale of fluctuation to the length of the failure surface dictates the magnitude of the variance reduction due to averaging.
 4. The probability of failure that was calculated for the cases were the uncertainties in the spatial variability and model uncertainty are combined indicated that the probability of failure decreases as (1) the design factor of safety increases, (2) the

- coefficient of variation in the undrained shear strength decreases, (3) the ratio of $\delta z / L_f$ decreases below a threshold value of 0.2, and (4) the lower-bound factor of safety increases.
5. The effect of the lower-bound factor of safety on the reliability of the slope was found to be significant and depends on the magnitude of the lower-bound factor of safety relative to the design factor of safety, the coefficient of variation of the undrained shear strength, and on the magnitude of the design factor of safety. For relatively small values of the coefficient of variation of the undrained shear strength ($V = 0.1$ and 0.2), the lower-bound factor of safety was found to have an effect on the reliability only for cases with relatively small sensitivities (less than 2.0). For cases with higher coefficients of variation of the undrained shear strength ($V > 0.3$), the effect of the lower-bound factor of safety on the reliability is evident at higher sensitivities (2.75 to 3.0).
 6. The probability of failure could be reduced by more than half for cases where a lower bound factor of safety is included in the analysis. This reduction in the probability of failure due to the lower bound translates into a reduction in the required factor of safety that could be used in a design with a target level of reliability.
 7. Relationships between the target probability of failure and the required factor of safety were established and presented for cases with different conditions of spatial variability (different V and different $\delta z / L_f$) and different lower-bound factors of safety as reflected in the sensitivity of the soils. Based on these relationships, recommendations were made for the factors of safety to be used in the design of

undrained slopes for different target reliability levels. The range of the different reliability levels was chosen to be between a probability of failure of 10% (applicable for temporary slopes where no loss of lives is envisaged) and a probability of failure of 0.1% (applicable to slopes with potential loss of lives upon failure). As an example, for the case of intermediate spatial variability ($V = 0.3$), the required factor of safety decreases from a high value of 2.8 for the case with a target probability of failure 0.1% to a low value of 1.76 for the case where the target probability of failure is 10%. These required factors of safety decrease to 2.0 (for $p_f = 0.1\%$) and 1.66 (for $p_f = 10\%$) when the lower-bound factor of safety is incorporated in the analysis.

8.3 Design Steps

This section illustrates the steps that may be followed to evaluate the probability of failure and the design factors of safety of undrained slopes.

8.3.1 Estimation of the probability of failure of undrained slopes

1. A deterministic slope stability analysis should be adopted for the evaluation of the deterministic factor of safety of the undrained slope.
2. Using the results of the deterministic analysis, the length of the failure surface (L_f) should be measured.
3. Based on the undrained shear strength borehole, both the vertical scale of fluctuation (δz) and the coefficient of variation (V) can be evaluated. For

estimating δz , either equation 5-1 shown in chapter 5 can be used or an assumed value between 1-2.5m can be adopted as recommended by Phoon and Kulhawy (1999).

4. After estimating both δz and L_f , the ratio of $\delta z / L_f$ can be evaluated simply.
5. Suppose the ratio of $\delta z / L_f$, deterministic factor of safety, and the coefficient of variation of undrained shear strength are evaluated using the above steps; the probability of failure of the slope can be evaluated using graphs 7.1, 7.2, & 7.3.

8.3.2 Estimation of the design factor of safety of undrained slopes

The following steps are needed to investigate the required factor of safety needed to accomplish a target level of probability of failure.

1. The ratio of $\delta z / L_f$ is evaluated as illustrated before in section 8.3.1.
2. The sensitivity of the soil of each slope can be evaluated.
3. Using Tables 7.2, 7.3, 7.4, 7.5, 7.6, & 7.7 and by knowing the sensitivity of the soil the required factor of safety needed to achieve a target level of probability of failure can be estimated.

REFERENCES

- Alonso, E. E. 1976. "Risk analysis of slopes and its application to slopes in Canadian sensitive clays." *Geotechnique*, 26, 453–472.
- American Association of State Highway and Transportation Officials (AASHTO). (2004) *LRFD Bridge Design Specifications*, Washington, D.C.
- Bea, R.G., Jin, Z., Valle, C., and Ramos, R. (1999) "Evaluation of Reliability of Platform Pile Foundations", *Journal of Geotechnical and Geoenvironmental Engineering*, ASCE, Vol. 125, No.8, pp. 696-704.
- Bhattacharya, G., Jana, D., Ojha, S., and Chakraborty, S. 2003. "Direct search for minimum reliability index of earth slopes." *Comput. Geotech.*, 306, 455–462.
- Babu, G. L. S., and Mukesh, M. D. 2004. "Effect of soil variability on reliability of soil slopes." *Geotechnique*, 545, 335–337.
- Crooks, J.H.A., Been, K., and Mickleborough, B.W. 1986. "An Embankment Failure on Soft Fissured Clay." *Can. Geotech. J.*, Vol. 23, pp. 528-540.
- Chowdhury, R. N., and Tang, W. H. 1987. "Comparison of risk models for slopes." *Proc., 5th Int. Conf. on Applications of Statistics and Probability in Soil and Structural Engineering*, Vol. 2, Univ. of British Columbia, Vancouver, BC, Canada, 863–869.
- Chen, Z., and Shao, C. (1988). "Evaluation of minimum factor of safety inslope stability analysis." *Can. Geotech. J.*, 25(4), 735–748.
- Christian, J. T., Ladd, C. C., and Baecher, G. B. (1994). "Reliability applied to slope stability analysis." *J. Geotech. Eng.*, 120(12), 2180–2207.
- Chowdhury, R. N., and Xu, D. W. 1995. "Geotechnical system reliability of slopes." *Reliab. Eng. Syst. Saf.*, 47, 141–151.
- Christian, J. T. 1996. "Reliability methods for stability of existing slopes." *Proc., Uncertainty in the Geologic Environment: From Theory to Practice*, C. D. Shackelford, P. P. Nelson, and M. J. S. Rotheds., ASCE, Reston, Va., 409–419.
- Chai, J.-C., Miura, N., and Shen, S.-L. (2002). "Performance of embankments with and without reinforcement on soft subsoil." *Canadian Geotechnical Journal*, 39(4), 838–848.
- Cho, S. E. 2007. "Effects of spatial variability of soil properties on slope stability." *Eng. Geol.*, 923–4, 97–109.

- Dascal, O., Tournier, J. P., Tavenas, F., and La Rochelle, P. (1972). "Failure of a test embankment on sensitive clay." *Proceedings of the Specialty Conference on Performance of Earth and Earth-Supported Structures*, ASCE, Lafayette, IN, 129– 158.
- Dascal, O., and Rournier, J. P. (1975). "Embankment on soft and sensitive clay foundation." *J. Geotech. Eng.*, 101(3), 297–314.
- D'Andrea, R. A., and Sangrey, D. A. 1982. "Safety factors for probabilistic slope design." *J. Geotech. Engrg. Div.*, 1089, 1108–1118.
- Day, R. W. (1996). "Failure of Desert View Drive embankment." *J. Perform. Constr. Facil.*, 10(1), 11–1.
- Duncan, J. M. 2000. "Factors of safety and reliability in geotechnical engineering." *J. Geotech. Geoenviron. Eng.*, 1264, 307–316.
- Duncan, J. M., and Wright, S. G. (2005). *Soil strength and slope stability*, Wiley, Hoboken, NJ.
- Eide, O., and Holmberg, S. (1972). "Test fills to failure on the soft Bangkok Clay." *Proceedings of the Specialty Conference on Performance of Earth and Earth- Supported Structures*, ASCE, Lafayette, IN, 159–180.
- El-Ramly, H., Morgenstern, N. R., and Cruden, D. M. 2002. "Probabilistic slope stability analysis for practice." *Can. Geotech. J.*, 39, 665– 683.
- Flaate, K., and Preber, T. (1974). "Stability of road embankments in soft clay." *Canadian Geotechnical Journal*, 11(1), 72–88.
- Fjeld, S. (1977) "Reliability of Offshore Structures", Proceeings, 9th Offshore Technology Conference. OTC 3027, PP459-471.
- Ferkh, Z., and Fell, R. (1994). "Design of embankments on soft clay." *Proceedings of Thirteenth International Conference on Soil Mechanics and Foundation Engineering*, New Delhi, India, 733-738.
- Golder, H.Q., and Palmer, D.J. (1954). "Investigation of a Bank Failure at Scrapsgate, ISLE of Sheppey, Kent." *Géotechnique*, 5, 55-73.
- Griffiths, D. V., and Fenton, G. A. 2004. "Probabilistic slope stability analysis by finite elements." *J. Geotech. Geoenviron. Eng.*, 1305, 507–518.
- Griffiths, D. V., Fenton, G. A., and Denavit, M. D. 2007. "Traditional and advanced probabilistic slope stability analysis." *Proc., GeoDenver 2007 Symp.*, K. K. Phoon, G. A. Fenton, E. F. Glynn, C. H. Juang, D. V. Griffiths, T. F. Wolff, and L. Zhang, eds., ASCE, Reston, Va., 1–10.
- Griffiths, D. V., Huang, J., and Fenton, G., (2010). "Comparison of slope reliability methods of analysis." *GeoFlorida*, 1952-1961.

Haupt, R., and Olsen, J. (1972). "Case history—Embankment failure on soft varved silt." *Proc. Spec. Conf. Perf. of Earth and Earth Supported Structures*, 1(1), 1–28.

Hasofer, A. M., and Lind, N. C. 1974. "Exact and invariant second moment code format." *J. Engrg. Mech. Div.*, 1001, 111–121.

Hanzawa, H., Kishida, T., Fukusawa, T., and Hideyuki, A. (1994). "A case study of the application of direct shear and cone penetration tests to soil investigation: design and quality control for peaty soils." *Soils and Foundations*, 34(4), 13–22.

Hassan, A. M., and Wolff, T. F. 1999. "Search algorithm for minimum reliability index of earth slopes." *J. Geotech. Geoenviron. Eng.*, 1254, 301–308.

Hong, H. P., and Roh, G., (2008). "Reliability evaluation of earth slopes." *J. Geotech. Engrg.*, 134, 1700-1705.

Huang, J., Griffiths, D. V., and Fenton, G. A., (2013). "A benchmark slope for system reliability analysis." *Geo- Congress*, 962-971.

Indraratna, B., Balasubramaniam, A.S., and Balachandran, S. (1992). "Performance of Test Embankment Constructed to Failure on Soft Marine Clay." *J. Geotech. Engrg.*, 118(1), pp. 12-33.

Jha, S. and Ching, J. (2013). "Simplified reliability method for spatially variable undrained engineered slopes." *Soils and Foundations*, 53(5), 708-719.

Kjærnsli, B., and Simons, N. (1962). "Stability investigations of the North Bank of the Drammen River." *Géotechnique*, 12(2), 147–167.

Kulhawy, F. (1992). On Evaluation of Static Soil Properties. In R. Seed, & R. Boulanger, *In stability and Performance of Slopes and Embankments II* (pp. 95-115). New York: American Society of Civil Engineers.

Kulhawy, F. H. (1996). From Casagrande's "Calculated Risk" to Reliability Based Design in Foundation Engineering. *Civil Engineering Practice, Boston Society of Civil Engineers*, 43-56.

Kulhawy, F.H., and Phoon, K.K. (2002) "Observations on Geotechnical Reliability-Based Design Development in North America", *Proc. Int. Workshop on Foundation Design Codes and Soil Investigation in view of International Harmonization and Performance Based Design*, Tokyo, Japan, April, pp.31-48.

Lacasse, S. M., Ladd, C. C., and Barsvary, A. K. (1977). "Undrained behavior of embankments on New Liskeard varved clay." *Canadian Geotechnical Journal*, 14(3), 367–388.

Li, K. S., and Lumb, P. 1987. "Probabilistic design of slopes." *Can. Geotech. J.*, 24, 520–531.

- Lacasse, S. 1994. "Reliability and probabilistic methods." *Proc., 13th Int. Conf. Soil Mechanics and Foundation Engineering, New Delhi, India*, 225–227.
- Lacasse, S., and Nadim, F. 1996. "Uncertainties in characterizing soil properties." *Proc., Uncertainty 1996*, C. D. Shackelford, P. P. Nelson, and M. J. S. Roth, eds., ASCE, Reston, Va., 49–75.
- Low, B. K. 1996. "Practical probabilistic approach using spreadsheet." *Proc., Uncertainty in the Geologic Environment: From Theory to Practice, Vol. 2*, Reston, Va., 1284–1302.
- Low, B. K., and Tang, W. H. 1997a. "Reliability analysis of reinforced embankments on soft ground." *Can. Geotech. J.*, 345, 672–685.
- Low, B. K., and Tang, W. H. 1997b. "Efficient reliability evaluation using spreadsheet." *J. Geotech. Geoenviron. Eng.*, 1237, 749–752.
- Low, B. K., Gilbert, R. B., and Wright, S. G. 1998. "Slope reliability analysis using generalized method of slices." *J. Geotech. Geoenviron. Eng.*, 1244, 350–362.
- Low, B. K. 2003. "Practical probabilistic slope stability analysis." *Proc., Soil and Rock America 2003, 12th Panamerican Conf. on Soil Mechanics and Geotechnical Engineering*, and 39th U.S. Rock Mechanics Symp., MIT, Cambridge, Mass., Vol. 2, Verlag Glückauf GmbH, Essen, Germany, 2777–2784.
- Low, B. K., Lacasse, S., and Nadim, F. 2007. "Slope reliability analysis accounting for spatial variation." *Georisk, Vol. 1*, Taylor and Francis, London, 177–189.
- Matsuo, M., and Kuroda, K. 1974. "Probabilistic approach to the design of embankments." *Soils Found.*, 141, 1–17.
- Mostyn, G. R., and Li, K. S. 1993. "Probabilistic slope stability— State of play." *Proc., Conf. Probabilistic Meth. Geotech. Eng.*, K. S. Li and S.-C. R. Lo, eds., Balkema, Rotterdam, The Netherlands, 89– 110.
- Malkawi, A. I., Hassan, W. F., and Abdulla, F. A., (2000). "Uncertainty and reliability analysis applied to slope stability." *Structural Safety* 22, 161-187.
- McGinn, M., and O'Rourke, T.D., *Performance and Evaluation of Tunnels, Excavations, and Retaining Structures*, ASCE, pp. 480-495.
- Oka, Y., and Wu, T. H. 1990. "System reliability of slope stability." *J. Geotech. Engrg.*, 116, 1185–1189.
- Peterson, R., Iverson, N.L., and Rivard, P.J. 1957. "Studies of Several Dam Failures on Clay Foundations." *Proceedings of the 4th International Conference on Soil Mechanics and Foundation Engineering*, London, England, Vol. 11, pp. 348-352.

- Parry, R. (1968). "Field and laboratory behavior of a lightly overconsolidated clay." *Géotechnique*, 18, 151–171
- Pilot, G. (1972). "Study of five embankment failures on soft soils." *Proceedings of the Specialty Conference on Performance of Earth and Earth-Supported Structures*, ASCE, Lafayette, IN, 81–100.
- Pilot, G., Trak, B., and La Rochelle, P. (1982). "Effective stress analysis of the stability of embankments on soft soils." *Canadian Geotechnical Journal*, 19(4), 433–450.
- Rivard, P., and Lu, Y. (1978). "Shear strength of soft-fissured clays." *Can. Geotech. J.*, 15(3), 382–390.
- Ramalho-Ortigão, J. A., Werneck, M. L. G., and Lacerda, W. A. (1983). "Embankment failure on clay near Rio de Janeiro." *Journal of Geotechnical Engineering*, 109(11), 1460–1479.
- Rodriguez, S.G.H., Henriques, C.C.D., Ellwanger, G.B., and de Lima, E.C.P. (1998) "Structural Reliability with Truncated Probability Distributions", *Proceedings of the International Conference on Offshore Mechanics and Arctic Engineering*, OMAE, July, 5-9, 1998, Lisbon, Portugal, 6 pp.
- Skempton, A.W., and P. La Rocheelle (1965). "The Bradwell Slip: A Short-term Failure in London Clay." *Géotechnique*, 15, No.3, pp. 221-242.
- Skempton, A.W., and Coats, D. J. (1985). "Carsington dam failure." *Failures in Earthworks*, Thomas Telford, London, 203–220.
- Shinoda, M. 2007. "Quasi-Monte Carlo simulation with low discrepancy sequence for reinforced soil slopes." *J. Geotech. Geoenviron. Eng.*, 1334, 393–404.
- Shogaki, T., and Kumagai, N. (2008). "A slope Stability analysis Considering Undrained Strength Anisotropy of Natural Clay Deposits." *Soils and Foundations*, Vol.48, No.6, 805-819.
- Tang, W. H., Yucemen, M. S., and Ang, A. H. S. 1976. "Probability based short-term design of slopes." *Can. Geotech. J.*, 13, 201–215.
- Travis, Q.B., Schmeeckle, M.W., and Seibert, D.M. (2010). "Meta-analysis of 301 slope failure calculations. I: Database description." *Journal of Geotechnical and Geoenvironmental Engineering*, 1(1), 264.
- Vanmarcke, E. H. 1977. "Reliability of earth slopes." *J. Geotech. Engrg. Div.*, 10311, 1247–1265.
- Wolfskill, L. A., and Lambe, T. W (1967). "Slide in the Siburua Dam." *J. Soil Mech. and Found. Div.*, 93(SM4), 107–113.
- Wu, T. H., Thayer, W. B., and Lin, S. S. (1975). "Stability of embankment on clay." *J. Geotech. Engrg. Div.*, 101(9), 913–932.

Wolff, T. F. 1996. "Probabilistic slope stability in theory and practice." *Uncertainty in the geologic environment: From theory to practice*, C. D. Shackelford, P. P. Nelson, and M. J. S. Roth, eds., ASCE, Reston, Va., 419–433.

Whitman, R. V. 2000. "Organizing and evaluating in geotechnical engineering." *J. Geotech. Geoenviron. Eng.*, 1267, 583–593.

Wu, T.H. (2009). "Reliability of geotechnical predictions." *Geotechnical Risk and Safety, Proceedings of the 2nd International Symposium on Geotechnical Safety and Risk*, CRC Press, Taylor & Francis Group, Gifu, Japan, 3-10.

Xu, B., and Low, B. K. 2006. "Probabilistic stability analyses of embankments based on finite-element method." *J. Geotech. Geoenviron. Eng.*, 13211, 1444–1454

Zhang, Z., Tao, M., and Morvant, M. (2005). "Cohesive slope surface failure and evaluation." *J. Geotech. Geoenviron. Eng.*, 131(7), 898–906.

Zhang, J., Huang, H. W., Juang, C. H., and Li, D. Q., (2013). "Extension of Hassan and Wolff method for system reliability analysis of soil slopes." *Engineering Geology* 160, 81-88.

